Target Site Bioanalysis and Pharmacokinetics of Antileishmanial Drugs

Ignace C. Roseboom

Target Site Bioanalysis and Pharmacokinetics of Antileishmanial Drugs

Ignace C. Roseboom

Target site bioanalysis and pharmacokinetics of antileishmanial drugs

Lokale bioanalyse en farmacokinetiek van antileishmaniale middelen

(met een samenvatting in het Nederlands)

Proefschrift

ter verkrijging van de graad van doctor aan de Universiteit Utrecht

op gezag van de rector magnificus, prof.dr. H.R.B.M. Kummeling,

ingevolge het besluit van het college voor promoties

in het openbaar te verdedigen op

woensdag 22 februari 2023 des middags te 12.15 uur

door

Ignace Charles Roseboom

geboren op 11 juni 1992

te Almere

Promotor:

Prof. dr. J.H. Beijnen

Copromotor:

Dr. T.P.C. Dorlo

Contents

Preface

Leishmaniasis is one of the most important neglected tropical diseases worldwide and mainly affects low-income populations in low- and middle-income countries around the world with an estimation of 12 to 15 million people infected in over more than 90 countries, risking around 350 million people to acquire the disease [1]. There is an urgent shortage of drug development for this disease due to a lack of economic interest, which categorizes leishmaniasis as a neglected tropical disease [2]. Endemic regions include South America, East Africa, the Middle East, and South and Central Asia [3]. The disease is caused by over 20 different *Leishmania* parasite subspecies and is transmitted by a bite of *Leishmania*-infected sandflies mainly of the genera *Phlebotomus* and *Lutzomyia* [1]. Due to the phenotypical diversity of *Leishmania* parasites, different clinical manifestations exist. The most important clinical phenotypes include cutaneous leishmaniasis and visceral leishmaniasis where cutaneous leishmaniasis is the most common infection. Cutaneous leishmaniasis is characterized by formation of skin ulcers at the site of infection after weeks of incubation, creating a site for new possible infections by microbial agents. Visceral leishmaniasis (also known as kala-azar meaning black fever in Hindu) is the deadliest clinical phenotype and is the second largest parasitical killer in the world after malaria [3]. The disease is characterized by the swelling of spleen and liver and can be fatal within months if left untreated [4,5]. After successful treatment of visceral leishmaniasis, dependent on the geographical region and the *Leishmania* subspecies, between 5%-10% in India and 50%-60% in Sudan of the patients develop a dermatological condition called post-kala-azar dermal leishmaniasis [6,7]. This skin condition is characterized by macular, papular, or nodular lesions all around the body from parasites that reside and divide in the dermis of the skin and can take up to a few months incubation time for it to show.

The antileishmanial drugs that are available to patients suffering from leishmaniasis include some old and highly toxic medicines. Pentavalent antimonials are antimony compounds that are used as first-line treatment for leishmaniasis. Unfortunately, these compounds are associated with fatal cardiotoxicity and therefore there is an urgent need to develop new treatment regimens, preferably combinations regimens to limit the risk of emerging drug resistance and to further improve efficacy [8–13]. Currently, various alternative drug regimens have been investigated in clinical trials in combination with pharmacokinetic studies mainly focusing on (combinations of) three crucial drugs, amphotericin B, miltefosine, and paromomycin. Pharmacokinetic studies in leishmaniasis have typically been limited to plasma concentration data, while little was known about drug exposure at the site where the parasite is present and replicating. Little is known about the drug distribution and exposure-response relationships in skin tissue of patients suffering from dermal forms of leishmaniasis [14]. Bioanalytical assays supporting clinical trials in amphotericin B, miltefosine, and paromomycin regimens were limited to blood-based matrices, and target-site pharmacokinetic studies in human skin tissue were lacking so far. Skin tissue bioanalytical methods for the quantification of pharmaceutical compounds were scarce and not much was described and known about homogenization sample preparations of such a challenging biomatrix [15], therefore valuable data to investigate and improve treatment efficacy was limited. In this thesis we present the development and validation of antileishmanial drugs in human skin tissue, as well as a bioanalytical method in plasma to improve pharmacokinetic studies and provide target-site data from patients suffering from visceral leishmaniasis and post-kala-azar dermal leishmaniasis. Furthermore, skin pharmacokinetic and pharmacodynamic data from clinical studies were interpreted by advanced pharmacokinetic methods.

Thesis outline

Chapter 1 provides an overview of bioanalytical quantification methods of the most relevant antileishmanial used in human pharmacokinetic studies and clinical trials. It covers (liposomal) amphotericin B, miltefosine, paromomycin, pentamidine and pentavalent antimonials and summarizes sample preparation, calibration model, separation, and detection methods in various human matrices from identified published method validations and included future perspectives in the development of antileishmanial bioanalysis.

Chapter 2 presents the development and validation of a modern bioanalytical method for the quantification of paromomycin in human plasma using ion-pair ultra-high performance liquid chromatography tandem mass spectrometry. It was the first bioanalytical assay that employed a stable isotope labelled internal standard in the quantification of paromomycin. The relevance of developing a sensitive method for the quantification of paromomycin in human plasma is discussed, furthermore its supporting role in clinical pharmacokinetic studies in patients suffering from visceral leishmaniasis in Kenya.

Chapter 3 discusses and presents target-site bioanalytical methods for the quantification of antileishmanial drugs in human skin tissue. **Chapter 3.1** provides an overview of existing skin tissue sample pre-treatment and homogenization techniques for quantification of pharmaceutical compounds. It discusses the advantages and disadvantages of certain homogenization techniques relative to the accuracy and recovery from skin tissue of the bioanalytical method. In **chapter 3.2** the development and validation of a bioanalytical method for the quantification of miltefosine in human skin tissue is presented. It describes a detailed development of a homogenization method employing enzymatic digestion by collagenase A for human skin tissue sample processing. Furthermore, its clinical applicability to target-site pharmacokinetic studies in post-kala azar dermal leishmaniasis patients in

Bangladesh is demonstrated. **Chapter 3.3** focuses on the development and validation of a bioanalytical method for the quantification of amphotericin B in human skin tissue with a clinical application in post-kala azar dermal leishmaniasis patients in India. Finally, **chapter 3.4** provides the development and validation of a bioanalytical method for the quantification of paromomycin in human skin tissue and a clinical application in a pharmacokinetic study in post-kala-azar dermal leishmaniasis patients in Sudan.

Chapter 4 explores the pharmacokinetic outcomes of target-site pharmacokinetic studies employing human skin tissue data. **Chapter 4.1** evaluates miltefosine pharmacokinetic and pharmacodynamic outcomes and presents the first skin tissue model characterizing the distribution of miltefosine from blood-based matrices to skin tissue from patients suffering from post-kala azar dermal leishmaniasis in India and Bangladesh. **Chapter 4.2** presents a pharmacokinetic model for liposomal amphotericin B in both human plasma and skin tissue, exploring the target-site exposure and distribution of this antileishmanial drug based on clinical pharmacokinetic data of patients suffering from post-kala azar dermal leishmaniasis in India and Bangladesh.

Chapter 5 summarizes and concludes the thesis and furthermore presents the authors' views on future perspectives for the development of bioanalytical methods for antileishmanial drugs.

References

[1] E. Torres-Guerrero, M.R. Quintanilla-Cedillo, J. Ruiz-Esmenjaud, R. Arenas, Leishmaniasis: a review, F1000Research. 6 (2017) 750. https://doi.org/10.12688/f1000research.11120.1.

[2] P.J. Hotez, S. Aksoy, P.J. Brindley, S. Kamhawi, What constitutes a neglected tropical disease?, PLoS Negl. Trop. Dis. 14 (2020) e0008001. https://doi.org/10.1371/journal.pntd.0008001.

[3] World Health Organization, Leishmaniasis WHO Fact Sheet, 2022.

[4] B.C. Sen Gupta, History of kala-azar in India. 1947., Indian J. Med. Res. 123 (2006) 281–6. http://www.ncbi.nlm.nih.gov/pubmed/16789340.

[5] T.P.C. Dorlo, M. Balasegaram, J.H. Beijnen, P.J. de Vries, Miltefosine: a review of its pharmacology and therapeutic efficacy in the treatment of leishmaniasis, J. Antimicrob. Chemother. 67 (2012) 2576–2597. https://doi.org/10.1093/jac/dks275.

[6] E. Zijlstra, A. Musa, E. Khalil, I. El Hassan, A. El-Hassan, Post-kala-azar dermal leishmaniasis, Lancet Infect. Dis. 3 (2003) 87–98. https://doi.org/10.1016/S1473-3099(03)00517-6.

[7] S. Ganguly, N.K. Das, J.N. Barbhuiya, M. Chatterjee, Post-kala-azar dermal leishmaniasis - an overview, Int. J. Dermatol. 49 (2010) 921–931. https://doi.org/10.1111/j.1365-4632.2010.04558.x.

[8] H. Goto, Review of the current treatments for leishmaniases, Res. Rep. Trop. Med. 34 (2012) 69. https://doi.org/10.2147/RRTM.S24764.

[9] J. Alvar, S. Croft, P. Olliaro, Chemotherapy in the Treatment and Control of Leishmaniasis, in: Adv. Parasitol., 2006: pp. 223–274. https://doi.org/10.1016/S0065-308X(05)61006-8.

[10] S. Sundar, Drug resistance in Indian visceral leishmaniasis, Trop. Med. Int. Heal. 6 (2001) 849–854. https://doi.org/10.1046/j.1365-3156.2001.00778.x.

[11] R.T. Kenney, A.A. Gam, M. Ray, S. Sundar, K. Pai, R. Kumar, K. Pathak-Tripathi, Resistance to treatment in Kala-azar: speciation of isolates from northeast India, Am. J. Trop. Med. Hyg. 65 (2001) 193–196. https://doi.org/10.4269/ajtmh.2001.65.193.

[12] C.T.R. India, New treatment regimens for treatment of Post Kala Azar Dermal Leishmaniasis patients in India and Bangladesh region, New Delhi Database Publ. (India). Identifier CTRI/2017/04/008421. (2017) 7.

[13] NCT03399955, Short Course Regimens for Treatment of PKDL (Sudan), 2018.

[14] I.C. Roseboom, B. Thijssen, H. Rosing, F. Alves, D. Mondal, M.B.M. Teunissen, J.H. Beijnen, T.P.C. Dorlo, Development and validation of an HPLC-MS/MS method for the quantification of the anti-leishmanial drug miltefosine in human skin tissue, J. Pharm. Biomed. Anal. (2021) 114402. https://doi.org/10.1016/j.jpba.2021.114402.

[15] I.C. Roseboom, H. Rosing, J.H. Beijnen, T.P.C. Dorlo, Skin tissue sample collection, sample homogenization, and analyte extraction strategies for liquid chromatographic mass spectrometry quantification of pharmaceutical compounds, J. Pharm. Biomed. Anal. 191 (2020) 113590. https://doi.org/10.1016/j.jpba.2020.113590.

1

| Introduction

Bioanalytical methods for pharmacokinetic studies of antileishmanial drugs

Ignace C. Roseboom
Hilde Rosing
Jos H. Beijnen
Thomas P.C. Dorlo

1.1

Abstract

Bioanalytical method development and validation for the quantification of antileishmanial drugs are pivotal to support clinical trials and provide the data necessary to conduct PK analysis. This review provides a comprehensive overview of published validated bioanalytical assays for the quantification of antileishmanial drugs amphotericin B, miltefosine, paromomycin, pentamidine, and pentavalent antimonials in human matrices. Each antileishmanial drug was discussed regarding their applicability of the assay for leishmaniasis clinical trials as well as providing their relevance for PK studies with emphasis on the choice of matrix, calibration range, sample volume, sample preparation, choice of internal standards, separation, and detection. Given that no published bioanalytical methods included multiple antileishmanial drugs in a single assay while antileishmanial shortened combination regimens currently were under investigation, it was recommended to combine various drugs in a single bioanalytical method. Furthermore, bioanalytical method development regarding target site matrix as well as applying microsampling strategies was recommended to optimize future clinical PK studies in leishmaniasis.

1. Introduction

Leishmaniasis is a neglected parasitic tropical disease caused by protozoan *Leishmania* parasites with an estimated incidence of 700,000 to 1,000,000 annually. Low-income populations in resource-poor regions of the world are disproportionally suffering from neglected tropical diseases for which there is a shortage of new drugs being developed due to a lack of economic interest [1]. Non-profit organizations such as Drugs for Neglected Diseases initiative (DNDi) are driving the development of new treatment options for leishmaniasis in endemic regions. *Leishmania* is transmitted by the bite of a sandfly commonly of the genera *Phlebotomus* and *Lutzomyia* [2]. There are over 20 *Leishmania* species known and their respective habitats are across South-America, East-and West-Africa, the Mediterranean, the Middle East and South Asia with over 90 countries affected [3,4]. Main clinical phenotypes include cutaneous leishmaniasis (CL), mucocutaneous leishmaniasis (MCL) and visceral leishmaniasis (VL), also known as kala-azar, which is associated with a high burden of mortality. CL and MCL are characterized by skin ulcers at the site of infection that, dependent on *Leishmania* subspecies, may self-heal within 18 months, however are prone to lifelong scars and stigmatization due to disfigurement if available treatment options are not received [5]. Visceral leishmaniasis lead to a widespread infection in the reticuloendothelial system, corrupting the spleen and liver and is fatal if left untreated [6,7]. After successful treatment of visceral leishmaniasis, a new clinical skin-related phenotype may occur that is divined by the appearance of skin complications in the form of small *Leishmania* pockets all over the body and is known as post kala-azar dermal leishmaniasis (PKDL) [8]. Leishmaniasis patients often suffer from anemia and hypovolemia symptoms [9], as well as from co-infections, therefore it is of importance in pharmacokinetic (PK) studies that sampling volumes are low (≤ 50 µL) and sampling procedures are minimal invasive.

The most commonly administered chemotherapeutic options for leishmaniasis include liposomal amphotericin B, miltefosine, paromomycin, pentamidine and various pentavalent antimonials [10,11]. The oldest first-line treatment therapy still being used includes pentavalent antimonials, nowadays administered as methylglucamine antimoniate or sodium stibogluconate [12]. Pentavalent antimonials are administered through intralesional, intramuscular or intravenous injections, and are currently used in the treatment of VL and CL throughout Africa, South America, and the Indian subcontinent [11,12]. VL treatment failures were reported potentially due to acquired drug resistance of *Leishmania* parasites [13–16]. CL treatment failures were reported in Brazil, Bolivia, and Colombia due to drug resistance [17,18]. Other treatment options became available, most notably amphotericin B (in liposomal formulation) for VL [11], which is further being included in various shortened combination regimens currently under investigation. Liposomal amphotericin B is administered intravenously and was the first FDA approved antileishmanial drug

for the treatment of VL [19]. Miltefosine is the first and only oral FDA approved antileishmanial drug [20]. Miltefosine is available for the treatment of VL, CL and PKDL, and is also currently in clinical development as part of combination regimens [5,21–25]. Additionally, intramuscular administered paromomycin introduced as treatment for visceral leishmaniasis in 2006 [26] is in new clinical development as part of shortened combination regimens against PKDL [27], whereas it has been recommended for clinical use in combination with pentavalent antimonials for the treatment of VL in Eastern Africa [28–30]. Pentamidine, administered intramuscularly, was first used as treatment option for VL of antimony-resistant *Leishmania* and successively was used as treatment option for CL [31–33].

Recently, efforts in clinical drug development for leishmaniasis has mainly been focused on the development of shortened combination regimens to improve safety and efficacy, as well as shortening treatment duration and limiting the risk of emergence of drug resistance. Bioanalytical method development and validation for the quantification of antileishmanial drugs are pivotal to support clinical trials and provide the data necessary to conduct further PK analysis. Target site PK studies, are increasingly important to optimize drug dosing regimens and thereby bioanalytical assays for unconventional biological matrices need to be developed to enable this type of targeted PK analysis [34–36]. A wide range of target sites in clinical leishmaniasis phenotypes are present, which could provide tissue level expose-response relationships and distribution of antileishmanial drugs in PK studies [37]. For CL or PKDL studies, skin tissue is the target site matrix, and for VL the spleen, liver and bone marrow matrices are of importance for the determination of parasite and antileishmanial drug levels. Intracellular determination of antileishmanial drugs is of equal importance to target site analysis, because of the direct exposure of drugs to intracellular parasites, for example miltefosine in peripheral blood mononuclear cells (PBMCs) serving as a proxy target site matrix [38]. For this purpose, ultra-sensitive bioanalytical assays are required to quantify the drugs in small sample volumes in PK studies of antileishmanial drugs, which also applies to target site bioanalytical assays. The goal of this review is to provide an overview of published validated bioanalytical assays for the quantification of antileishmanial drugs in human matrices, and to discuss the applicability of the assay for leishmaniasis clinical trials as well as providing their relevance for PK studies in terms of choice of matrix, calibration range, sample volume, sample preparation, choice of internal standards, separation, and detection.

2. Methodology

Bioanalytical methods for the quantification of antileishmanial drugs were identified using a PubMed database search, restricted to the English language,

using the following search terms for title and abstract contents: (amphotericin B OR fungizone OR ambisome OR paromomycin OR aminosidine OR miltefosine OR impavido OR hexadecylphosphocholine OR antimony OR antimonial* OR stibo* OR sodium stibogluconate OR meglumine antimoniate OR pentamidine) AND (human) AND (chromatography OR atomic absorption spectroscopy OR inductively coupled plasma). If the title or abstract contained information suggesting that the contents of the publication included a bioanalytical method for the quantification of antileishmanial drugs in human matrices, the publication was included in this review. Animal studies were excluded from this review because the focus of the review was bioanalytical methods supporting clinical trials.

3. Results

The literature search resulted in 541 identified studies (search date 25-07-2022). Based on the specified inclusion and exclusion criteria, 90 studies were finally included in this review, with 52 studies for amphotericin B, 7 for miltefosine, 4 for paromomycin, 9 for pentamidine, and 18 for pentavalent antimonials. The results are summarized in Tables 2 through 6.

Table 1: Chemical properties of antileishmanial drugs.

Properties [39]	Amphotericin B	Miltefosine	Paromomycin	Pentamidine	Meglumine antimoniate	Sodium stibo-gluconate
Monoisotopic mass (Da)	923.4878	407.3164	615.2963	340.1899	365.0071	905.9186
Molar mass (Da)	924.1	407.6	615.6	340.4	365.98	907.88
Water solubility (mg/mL) [40]	Insoluble	81	100	100	39	20
Log P	0.8	2.68	-2.9	1.32	-2.4	-0.08
pKa Strongest Acid	3.58	1.88	12.23	–	12.65	2.29
pKa Strongest Base	9.11	–	9.68	12.13	9.11	-3

4.1. Amphotericin B
Amphotericin B is a naturally formed biosynthetical polyketide. Chemical characteristics of amphotericin B are described as a bulky small molecule with no charge in physiological conditions, exercising the property that it can act as either a base or acid (hence the name amphoteric compound), although poorly water soluble. Chemical properties are summarized in Table 1. Amphotericin B

was clinically used since 1957 [41], at first in the treatment of fungal infections. The majority bioanalytical assays of amphotericin B in various matrices used for human PK studies were detected using conventional ultraviolet (UV) detection [42–83] that were more prominent before mass spectrometry (MS) detection [44,79,81,84–90] was standardized. There are multiple formulations for amphotericin B, including amphotericin B lipid complex (ABLC), liposomal amphotericin B (L-AmB), amphotericin B colloidal dispersion (ABCD), and amphotericin B deoxycholate. ABLC and ABCD are two different lipid formulations of amphotericin B, either bonded to L-a-dimyristoyl phosphatidylcholine and L-a-dimyristoyl phosphatidylglycerol or cholesteryl sulphate, respectively [91]. Amphotericin B deoxycholate formulation, as opposed to amphotericin B, can be dissolved at physiological pH, and L-AmB is amphotericin B is an unimellar vesicle formulation [91]. L-AmB is administered intravenously in patients suffering from leishmaniasis due to lower renal toxicity then the deoxycholate formulation and the advantages of targeted therapy by the uptake preferences of liposomal formulations in macrophages. Only a few PK studies have looked into the separation of liposomal and free amphotericin B [54,76,81,84,85,87,89], whereas the majority of bioanalytical methods for amphotericin B have focused on total amphotericin B in biomatrices. Mass balance studies reported a 90% renal and fecal clearance of unchanged amphotericin B after amphotericin B deoxycholate administration [44]. No metabolites were observed using mass spectrometry in these mass balance studies [44,92], therefore bioanalytical methods have not looked further into metabolite quantification. An overview of bioanalytical methods for the quantification of amphotericin B is given in Table 2.

4.1.1. Matrix, calibration range and sampling volume
Bioanalytical methods are developed to generate data beneficial for the research question of the PK study. Therefore plasma, serum and urine assays ranged from 0.5-8 ng/mL, the most sensitive method used for poorly absorbed orally administered amphotericin B [71], to 0.05-200 µg/mL with the highest dynamic range in a toxicological study in cancer patients [42]. Also, tissue analysis of biliary, lung, liver, spleen, kidney, brain, and pancreas were performed in autopsy material [61,66,82]. In the interest of leishmaniasis target site PK studies, quantification of amphotericin B in skin tissue has recently been developed [90]. There were six identified studies with sampling volumes of ≤50 µL for serum or heparinized/K_2EDTA plasma samples recommended to be used in leishmaniasis patients because little blood is required from patients [47,68,79,84,85,88]

4.1.2. Sample preparation
Sample preparation consisted in most cases of protein precipitation because amphotericin B is soluble in organic solvents. For total and free fraction amphotericin B quantification in plasma, serum, urine or tissue analysis, most often simple protein precipitation was performed using methanol or acetonitrile, occasionally together

with acetic acid, dimethyl sulfoxide (DMSO), ethylenediaminetetraacetic acid (EDTA) or zinc as co-solvent for precipitation improvements [42–44,47–53,55–57,59–69,72,73,75,77–84,86–88,90]. Amphotericin B in the liposomal fraction samples were primarily prepared using solid-phase extraction (SPE) techniques to preserve the liposomal formulation of amphotericin B and separate the free fraction from the liposomal fraction for selective analysis [54,81,89]
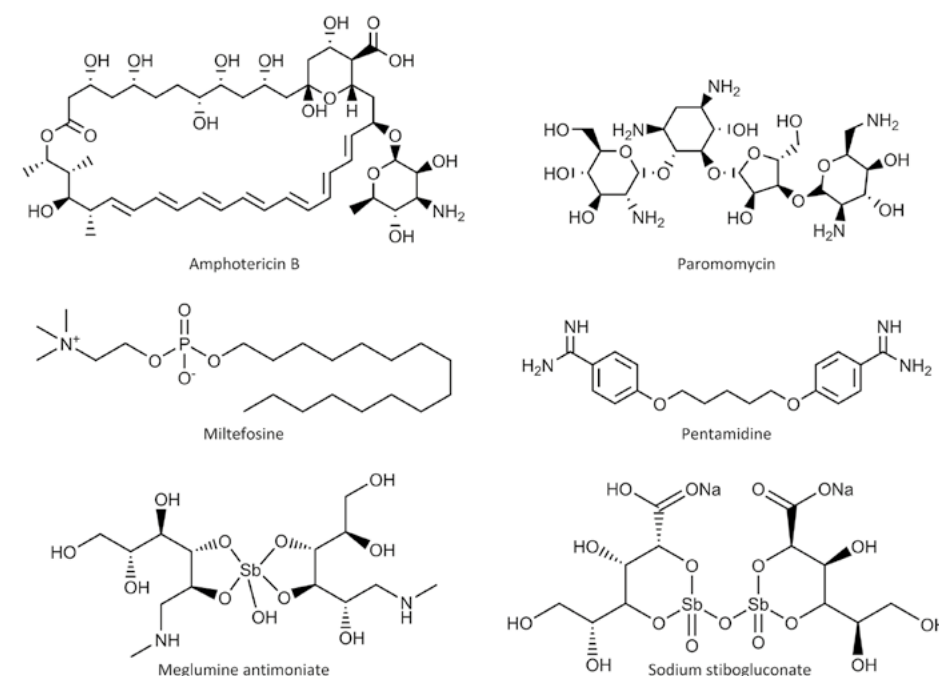
Figure 1: Chemical structures and names of antileishmanial drugs.

4.1.3. Internal standard, separation, and detection
The internal standards used for accurate quantification were diverse and a stable isotope labelled internal standard (SILIS) was not used because of two reasons. Liquid chromatography (LC)-UV employs internal standards that are chemical analogues, because UV detectors cannot discriminate between isotopes and isotope labelled amphotericin B, beneficial for liquid chromatography coupled to tandem mass spectrometry (LC-MS/MS) is not commercially available on the market yet. Natamycin is a chemical analogue that is mainly used as internal standard for the quantification of amphotericin B, however, 1-amino-4-nitronaphthalene, *p*-nitroaniline, carbamazepine, piroxicam, 3-nitrophenol, p-nitrobenzyloxyamine, fluconazole, clopidogrel and paclitaxel were also deployed. Only a single study used a SIL-IS for amphotericin B quantification employing D_3-amphotericin B,

however is also not commercially available hitherto [84]. Column separation was performed with little variability between studies, using reversed phase columns to employ hydrophobic interaction retention mechanisms with amphotericin B and the stationary phase of the columns. Mobile phase variations were made using different ionic additives, formic acid, monopotassium phosphate, ammonium acetate, or EDTA employing classic reversed phase mobile phases with water and methanol or acetonitrile organic phase preferences. Mobile phase ionic additives employed in LC-UV, LC-MS, or MS/MS posed variability. Additives monopotassium phosphate and EDTA are primarily used in UV detection environment, whereas formic acid and ammonium acetate are employed in all detection settings. Amphotericin B was detected using UV, MS or MS/MS detectors. UV settings employed in the detection of amphotericin B ranged from wavelengths of 340 nm - 410 nm, all dependent on the mobile phase detection interferences and the recovery of amphotericin B during sample preparation. For MS detection, a high-resolution mass spectrometer (Orbitrap) was used with transitions m/z 906.4815 or m/z 924.49517. For MS/MS detection, amphotericin B was detected in positive ion mode using the parent ion of around m/z 924, using triple quadrupole mass spectrometers. Tandem mass spectrometers were used with two different analyte transitions, m/z 924 → 906 or m/z 924 → 743. Preferably, no product ions are selected with a relative difference from their respective parent ion of 18 Da, which is presumably due to loss of a water molecule, because these transitions include non-unique characteristics of the MS spectra [93].

4.1.4. Clinical application

Bioanalytical assays for the quantification of amphotericin B described above were used in multiple PK studies. Because amphotericin B is a recommended drug for multiple fungal and virological diseases, variability in PK studies were observed. PK studies involving amphotericin B drug treatment regimens were mostly performed on paediatric children or adults suffering from malignant diseases [46,48,61,63,64,68,75,81]. Furthermore, neutropenic patients were also subject of PK studies as well as patients suffering from fungal diseases [44,57,65,79,80,82,86,94] and patients suffering from leishmaniasis [90,95]. PK studies and their drug treatment regimen contained various formulations of amphotericin B in the form of deoxycholate, liposomal, and dextrose addition. Patients were dosed with 0.5 – 2 mg/kg deoxycholate or dextrose amphotericin B with multiple dose administrations per day, commonly lasting for at least 7 days. Plasma or serum concentrations (C_{max}) ranging from 1.1 µg/mL – 22.9 µg/mL, liver concentrations of 12.1 – 208.8 µg/g, and spleen concentrations of 9.5 – 195.7 µg/g. There is limited data on the PK of liposomal amphotericin B in Ethiopian HIV-infected VL patients, which indicated a median C_{max} of 24.6 µg/mL after the first administration of a 5 mg/kg dose [95].

Table 2: An overview of bioanalytical methods for the quantification of amphotericin B.

Analytes	Matrix	Internal Standard	Sampling Volume	Sample prep	LC column	Mobile Phase	Range	Run time (min)	Detection and settings	Ref.
F-AmB	Serum (Human)	D_3–Amphotericin B	50 µL	Protein Precipitation (Precipitant P from RECIPE) followed by online mixed mode anion exchange-RP SPE	C_{18} Hypersil GOLD (50 x 2.1 mm, 1.9 µm Thermo Scientific)	loading phase: 0.2% FA in water A/B: Water/ACN/500 mM ammonium acetate/32% ammonia solution (5:92:1:2, v/v/v/v) Conditioning phase: Water/500 mM am-monium acetate/32% ammonia solution (98.9:0.1:1, v/v/v)	56–2590 ng/mL	4	HRMS (Orbitrap) 5ppm mass tolerance Analyte: m/z 906.4815 IS: m/z 923.5170	[84]
T-AmB	Plasma (Human)	Natamycin	200 µL	Protein Pre-cipitation (Zinc sulfate and ACN)	C_{18} Hypersil GOLD (50 x 2.1 mm, 1.9 µm Thermo Scientific)	A: 0.1 M KH_2PO_4 (mono-potassium phosphate pH 3.0) in water B: ACN	0.125–10 µg/mL	8	DAD Analyte: 384 and 407 nm IS: 304 nm	[43]
F-AmB	Plasma and CSF (Human)	Carbamazepine	20 µL	Hydrophilic-RP online SPE	Hydrophilic-RP online SPE Oasis HLB (20 x 2.1 mm, 15 µm Waters)	Washing: 10 mM ammonium formate (pH 3.0)/ACN (99:1, v/v) Conditioning: 10 mM ammonium formate (pH 5.0)/ACN (40:60, v/v) Elution: 10 mM ammo-nium formate (pH 4.0)/ACN (40:60, v/v)	40–2000 ng/mL	7	HRMS (Orbitrap) Analyte: m/z 924.49517 IS: m/z 237.10224	[85]

Analytes	Matrix	Internal Standard	Sampling Volume	Sample prep	LC column	Mobile Phase	Range	Run time (min)	Detection and settings	Ref.
F-AmB, L-AmB ABCD	Plasma (Human)	–	500 µL	Protein Precipitation (MeOH) followed by RP-SPE	LiChrosorb RP-8 (200 x 4.6 mm, 5 mm Agilent Technologies)	A/B: 10 mM NaH_2PO_4/MeOH/ACN (49:10:41, v/v/v)	5-5000 ng/mL	>6.7 (NS)	UV Detection 405 nm	[54]
T-AmB	Biliary tissue (Human)	NS	500 µL	Protein Precipitation (DMSO and MeOH)	Zorbax 300SB-C18 (12.5 x 4.6 mm, 5 µm Agilent Technologies)	A/B: 10 mM NaH_2PO_4/ACN (55:45, v/v)	10-NS ng/mL	>6.7 (NS)	UV Based on [54]: 405 nm	[65]
T-AmB	Plasma (Human)	NS	500 µL	RP-SPE						
L-AmB	Plasma (Human)	Piroxicam	N.A.	Protein Precipitation (MeOH)	C18 (50 x 2.0 mm, 5 µm Agilent Technologies)	A: 0.1% FA in water B: 0.1% FA in ACN	0.05-100 µg/mL	>7 (NS)	UV Detection Analyte/IS: 385 nm	[76]
	epithelial lining fluid (Human)		0.1-0.2 g	Protein Precipitation (acetic acid in MeOH)	µ-Bondapak RP-C18 (300 x 3.9 mm, 10 µm Waters)	A/B: 10 mM ammonium acetate (pH 4.0)/ACN (63:37, v/v)	0.03-6 µg/mL	>15 (NS)	UV based on [96] Analyte: 383 nm IS: 303 nm	
F-AmB	Plasma (Human)	Natamycin	50 µL	Hydrophilic-RP SPE	Chromolith Performance RP18e (100 × 4.6mm, 2µm Merck)	A: 5 mM ammonium acetate (pH 6.0) in ACN/MeOH (48:20:32, v/v/v) B: 5 mM ammonium acetate (pH 6.0) in ACN/MeOH (25:5:70, v/v/v)	1-100 ng/mL	6.5	Based on [88] Analyte: m/z 924 → 906.5 IS: m/z 666.2 → 503.3	[79]

Analytes	Matrix	Internal Standard	Sampling Volume	Sample prep	LC column	Mobile Phase	Range	Run time (min)	Detection and settings	Ref.
T-AmB	Lung tissue (Human)	1-amino-4-nitronaphthalene	0.15 g	Protein Precipitation (MeOH)	CAPCELL PAK C18 SG120 (250 x 4.6 mm, 5 µm Shisheido)	A/B: 2.5 mM EDTA (pH 5.0)/ACN (2:1, v/v)	0.1-NS µg/g	>20 (NS)	UV Detection Analyte/IS: 405 nm	[80]
	Plasma (Human)		100 µL				0.1-NS µg/mL			
T-AmB	Plasma (Human)	p-nitroaniline	100 µL	Protein Precipitation (MeOH)	Spherex C18 (150 x 4.6 mm, 5 µm Phenomenex)	A/B: 10 mM sodium acetate in 10 mM EDTA (pH 3.6)/ACN (65:35, v/v)	0.1-80 µg/mL	NS	UV Detection: Analyte/IS: 405 nm	[81]
L-AmB	Plasma lipoprotein fraction (Human)			RP-SPE			0.04-10.2 µg/mL			
L-AmB	Ultrafiltrate (Human)	Natamycin	200 µL	Ultrafiltration followed by RP-SPE	Synergi Max-RP (250 x 2.0 mm, 4 µm Phenomenex)	A/B: 10 mM ammonium acetate (pH 3.6)/ACN (62:38, v/v)	10-1050 ng/mL	6.5	Based on [88] Analyte: m/z 924 → 906.5 IS: m/z 666.2 → 503.3	[83]
	Plasma (Human)		250 µL	Protein Precipitation (MeOH)			0.15-20 µg/mL			
T-AmB	Lung tissue (Human)	NS	0.5 g	Protein Precipitation (MeOH)	Symmetry Shield RP8 (NS, Waters)	A/B: 2.5 mM EDTA/ACN (64:34, v/v)	0.5-50 µg/g	>7 (NS)	UV Detection 405 nm	[83]
T-AmB	Serum (Human)	3-nitrophenol	200 µL	Protein Precipitation (MeOH)	Alltima ODS (250 x 4.6 mm, 5 µm Alltech Associates)	A/B: 0.05 M sodium acetate/ACN (66:34, v/v)	0.05-200 µg/mL	>8.4 (NS)	UV Detection 405 nm	[42]
T-AmB	Plasma (Human)	NS	200 µL	Protein Precipitation (MeOH)	Supelcosil ABZ+ (150 x 4.6 mm, 5 µm Supelco)	A/B: 0.05 M sodium acetate/ACN (66:34, v/v)	0.1-15 µg/mL	NS	UV detection based on [42]: 405 nm	[44]

1.1

Analytes	Matrix	Internal Standard	Sampling Volume	Sample prep	LC column	Mobile Phase	Range	Run time (min)	Detection and settings	Ref.
T-AmB	Plasma (Human)	1-amino-4-Nitronaphthalene	1000 µL	RP-SPE	µ-Bondapak RP-C_{18} (300 x 4.6 mm, 5 µm Waters)	A/B: 20 mM EDTA/ACN (55:45, v/v)	0.01-2 µg/mL	>7 (NS)	UV detection 407 nm	[45]
T-AmB	Plasma (Human)	1-amino-4-Nitronaphthalene	1000 µL	RP-SPE	µ-Bondapak RP-C_{18} (300 x 4.6 mm, 5 µm Waters)	A/B: 20 mM EDTA/ACN (55:45, v/v)	0.01-2 µg/mL	NS	UV detection based on [45]: 407 nm	[46]
T-AmB	Plasma and serum (Human)	p-Nitrobenzyloxy-amine	25 µL	Protein Precipitation (ACN)	µ-Bondapak RP-C_{18} (300 x 4 mm, 10 µm Waters)	A/B: 10 mM sodium acetate (pH 7.0)/ACN (60:40, v/v)	0.5-2 µg/mL	>6 (NS)	UV detection 405 nm	[47]
T-AmB	Plasma (Human)	p-nitroaniline	100 µL	Protein Precipitation (ACN)	Spherex (150 x 4.3 mm, 5 µm Phenomenex)	A/B: 5.6 mM sodium acetate (pH 7.4)/ACN/EDTA (55.8:43.3:0.9, v/v/v)	0.1-6 µg/mL	>7 (NS)	UV detection based on [47]: 405 nm	[48]
T-AmB	Serum (Human)	3-nitrophenol	200 µL	Protein Precipitation (MeOH)	Alltima ODS (250 x 4.6 mm, 5 µm Alltech Associates)	A/B: 0.05 M sodium acetate/ACN (66:34, v/v)	0.05-200 µg/mL	>8.4 (NS)	UV Detection based on [42]: 405 nm	[49]
T-AmB	Serum (Human)	-	200 µL	Protein Precipitation (MeOH)	C_{18} (30 x 4.6 mm, 3 µm Perkin Elmer)	A/B: 2.5 mM EDTA/ACN (70:30, v/v)	0.05-25 µg/mL	>1.5 (NS)	UV detection 405 nm	[50]

Analytes	Matrix	Internal Standard	Sampling Volume	Sample prep	LC column	Mobile Phase	Range	Run time (min)	Detection and settings	Ref.
T-AmB	Bronchoaspiration (Human) bronchoalveolar lavage (Human)	-	N.A.	Protein Precipitation (MeOH) followed by RP-SPE	ODS (30 x 4.6 mm, 3 µm Perkin Elmer)	A/B: 2.5 mM EDTA/ACN (70:30, v/v)	0.1-5 µg/mL	>1.5 (NS)	UV detection based on [50]: 405 nm	[51]
T-AmB	Plasma (Human)	-	1000 µL	Protein Precipitation (ACN)	-	-	0.05-5 µg/mL	-	Second derivative spectroscopy detection 407.5 nm	[52]
T-AmB	Serum (Human)	-	N.A.	Protein Precipitation (EDTA in MeOH)	µ-Bondapak RP-C_{18} (300 x 3.9 mm, 10 µm Waters)	A/B: 5 mM EDTA in MeOH	0.05-NS µg/mL	>14 (NS)	UV detection 405 nm	[53]
T-AmB	Serum (Human)	1-amino-4-Nitronaphthalene	200 µL	Protein Precipitation (ACN)	µ-Bondapak RP-C_{18} (300 x 3.9 mm, 10 µm Waters) based on [97]	A/B: 0.01 EDTA (pH 4.2)/MeOH (60:40, v/v) based on [97]	0.3-19.5 µg/mL	NS	UV detection 408 nm	[55]
T-AmB	Serum (Human)	Fluconazole	100 µL	Protein Precipitation (ACN)	Nova-Pak RP-18 (100 x 8 mm, 4 µm Waters)	A/B: 0.5% EDTA in 10 mM ammonium acetate/ACN (70:30, v/v)	NS	>10 (NS)	UV detection 405 nm	[56]

Analytes	Matrix	Internal Standard	Sampling Volume	Sample prep	LC column	Mobile Phase	Range	Run time (min)	Detection and settings	Ref.
T-AmB	Serum (Human)	–	200 µL	Protein Precipitation (MeOH)	NS	A/B: 2.5 mM EDTA/ACN (70:30, v/v)	0.05–25 µg/mL	NS	UV detection based on [97]: 405 nm	[57]
T-AmB	CSF (Dogs and Human)	Nystatin	1000 µL	RP-SPE	Nova-Pak C$_{18}$ (150 × 3.9 mm, 4 µm Waters)	A/B: 0.01 M EDTA (pH 5)/ACN (65:35, v/v)	1–10 ng/mL	>9 (NS)	UV detection 410 nm	[58]
T-AmB	Serum (Human)	1-amino-4-Nitronaphthalene	200 µL	Protein Precipitation (MeOH)	Lichrospher 100 (250 x 4 mm, 5 µm Merck)	A/B: 5 mM EDTA in 10 mM KH$_2$PO$_4$ (pH 4.0)/ACN (55:45, v/v)	0.125–2 µg/mL	>12.5 (NS)	UV detection 405 nm	[59]
T-AmB	Serum (Human)	–	500 µL	Protein Precipitation (MeOH)	µ-Bondapak RP-C$_{18}$ (300 x 3.9 mm, 10 µm Waters)	A/B: 2.5 mM EDTA/MeOH/ACN (20:50:35, v/v/v)	0.1–10 µg/mL	6	UV detection 405 nm	[60]
T-AmB	Liver, spleen, kidney, lung, heart, pancreas, brain, adrenals, serum (Human)	–	75 mg 300 µL	Protein Precipitation (MeOH)	µ-Bondapak RP-C$_{18}$ (300 x 3.9 mm, 10 µm Waters) based on [60]	A/B: 2.5 mM EDTA/MeOH/ACN (20:50:35, v/v/v) based on [60]	0.1–10 µg/mL	6	UV detection based on [60]: 405 nm	[61]
T-AmB based on [98]	Serum (Human)	–	N.A.	Based on [98]	Based on [98]	Based on [98]	Based on [98]	Based on [98]	Based on [98]	[62]
T-AmB	Serum (Human)	1-amino-4-Nitronaphthalene	200 µL	Protein Precipitation (ACN)	µ-Bondapak RP-C$_{18}$ (300 x 3.9 mm, 10 µm Waters) based on [97]	A/B: 0.01 EDTA (pH 4.2)/MeOH (60:40, v/v) based on [97]	0.3–19.5 µg/mL	NS	UV detection based on [97]: 405 nm	[63]

Analytes	Matrix	Internal Standard	Sampling Volume	Sample prep	LC column	Mobile Phase	Range	Run time (min)	Detection and settings	Ref.
T-AmB based on [47]	Plasma and urine (Human)	p-Nitrobenzyloxy-amine	500 µL	Protein Precipitation (ACN) based on [47]	µ-Bondapak RP-C$_{18}$ (300 x 4 mm, 10 µm Waters) based on [47]	A/B: 10 mM sodium acetate (pH 7.0)/ACN (60:40, v/v) based on [47]	0.1–6 µg/mL	>7 (NS)	UV detection based on [47]: 405 nm	[64]
T-AmB based on [60]	Liver, spleen, kidney, lung, heart, pancreas, brain, adrenals, serum (Human)	–	75 mg 300 µL	Protein Precipitation (MeOH)	µ-Bondapak RP-C$_{18}$ (300 x 3.9 mm, 10 µm Waters) based on [60]	A/B: 2.5 mM EDTA/MeOH/ACN (20:50:35, v/v/v) based on [60]	0.1–10 µg/mL	6	UV detection based on [60]: 405 nm	[66]
T-AmB	Plasma and serum (Human)	p-nitroaniline	100 µL	Protein Precipitation (ACN)	CLC-C$_8$ (150 x 6 mm, 5 µm Shimadzu)	A/B: 0.1 M sodium acetate (pH 7.4)/ACN (60:40, V/V)	0.05–2 µg/mL	>6.6 (ns)	UV detection 405 nm	[67]
T-AmB	Serum (Human)	p-Nitrobenzyloxy-amine	25 µL	Protein Precipitation (ACN) based on [47]	µ-Bondapak RP-C$_{18}$ (300 x 4 mm, 10 µm Waters) based on [47]	A/B: 10 mM sodium acetate (pH 7.0)/ACN (60:40, v/v) based on [47]	0.1–6 µg/mL	>7 (NS)	UV detection based on [47]: 405 nm	[68]
T-AmB	Serum (Human)	–	200 µL	Protein Precipitation (ACN)	CLC-trimethylsilyl (150 x 6 mm, 5 µm Shimadzu)	A/B: 10 mM acetate buffer (pH 7.4)/ACN (60:40, v/v)	0.05–2 µg/mL	NS	UV detection 405 nm	[69]
T-AmB	Serum (Human)	–	200 µL	Protein Precipitation (ACN) followed by CN-SPE	–	–	0.5–5 µg/mL	NS	spectroscopy detection 408 nm	[70]

Analytes	Matrix	Internal Standard	Sampling Volume	Sample prep	LC column	Mobile Phase	Range	Run time (min)	Detection and settings	Ref.
T-AmB	Urine (Human)	–	25 mL 50 mL	RP-SPE	μ-Bondapak RP-C$_{18}$ (300 x 3.9 mm, 10 μm Waters)	A/B: 10 mM acetate buffer (pH 7.0)/ACN/MeOH/tetrahydrofuran (50:25:20:5, v/v/v/v)	0.5–8 ng/mL	>15 (NS)	UV detection 405 nm	[71]
T-AmB	Serum (Human)	–	1000 μL	Protein Precipitation (ACN)	μ-Bondapak RP-C$_{18}$ (300 x 3.9 mm, 10 μm Waters)	A/B: 50 mM sodium succinate buffer (pH 6.0)/MeOH/DMSO (20:75:5, v/v/v)	0.1–10 μg/mL	>6 (NS)	UV detection 405 nm	[72]
T-AmB	Serum (Human)	–	N.A.	Protein Precipitation (EDTA and MeOH)	Rad-Pak C$_{18}$ (100 x 8 mm, 10 μm Waters)	A/B: 5 mM EDTA (pH 7.8)/MeOH (20:80, v/v)	0.1–1.4 μg/mL	>6 (NS)	UV detection 340 nm and 405 nm	[73]
T-AmB	Serum (Human)	Disperse yellow 42 dye	1000 μL	RP-phenyl-SPE	ODS (150 x 4.6 mm, 5 μm Perkin Elmer)	A/B: 5 mM EDTA/ACN/MeOH (354:187:449, v/v/v)	0.05–5 μg/mL	>6.3 (NS)	UV detection 386 nm	[74]
T-AmB based on [98]	Plasma (Human)	–	N.A.	Protein Precipitation (ACN)	Based on [98]	Based on [98]	0.02–1.5 μg/mL	Based on [98]	Based on [98]	[75]
T-AmB	Plasma (Human)	p-Nitrophenol	1000 μL	Protein Precipitation (MeOH)	Ultrasphere ODS (150 x 4.6 mm, 5 μm Perkin Elmer)	A: 0.01 M EDTA in 50% MeOH B: 0.01 M EDTA in 50% ACN	0.08–10 μg/mL	19	UV detection 388 nm	[77]
T-AmB	Serum and CSF (Human)	–	1000 μL	Protein Precipitation (MeOH)	μ-Bondapak RP-C$_{18}$ (300 x 3.9 mm, 10 μm Waters)	A/B: 5 mM EDTA/MeOH (2:8, v/v)	0.03–5 μg/mL	>4 (NS)	UV detection 405 nm	[78]

Analytes	Matrix	Internal Standard	Sampling Volume	Sample prep	LC column	Mobile Phase	Range	Run time (min)	Detection and settings	Ref.
T-AmB	Plasma (Human)	clopidogrel	250 μL	Protein Precipitation (1:4 MeOH)	Acquity UPLC™ BEH Shield RP$_{18}$ (50 x 2.1 mm, 1.7 μm Waters)	A: 10 mM ammonium formate (pH 3.0) in 0.2% FA in 1% ACN B: 0.1% FA in MeOH/ACN (50:50, v/v)	200–4000 ng/mL	3.2	Analyte: m/z 925.1 → 742.3 IS: m/z 321.8 → 155	[86]
F-AmB	Plasma (Human or minipig)	Paclitaxel	150 μL	Protein Precipitation (1:3 MeOH/ACN (1:3, v/v)	Gemini C$_{18}$ column (100 x 4.6 mm, 5 μm Phenomenex)	A: 0.1% FA in water B: MeOH/ACN (2:3, v/v)	5–2500 ng/mL	7	Analyte: m/z 924.6 → 743.3 IS: m/z 854.3 → 286.1	[87]
	Plasma (Human)			Protein Precipitation (DMSO and MeOH)			2–150 μg/mL			
T-AmB	Ultrafiltrate (Human)	Natamycin	50 μL	Ultrafiltration, protein precipitation (MeOH) and RP-SPE	Symmetry C$_{18}$ (150 x 3.0 mm, 5 μm Waters)	A/B: MeOH/ water/acetic acid (68.6/29.4/1.96, v/v/v)	0.01–2 μg/mL	4	Analyte: m/z 924 → 906.5 IS: m/z 666.2 → 503.3	[88]
	Urine and Feces (Human)			Protein Precipitation (DMSO and MeOH) and RP-SPE			Urine: 0.05–30 μg/mL Feces: 0.4–40 μg/mL			

Analytes	Matrix	Internal Standard	Sampling Volume	Sample prep	LC column	Mobile Phase	Range	Run time (min)	Detection and settings	Ref.
	Plasma (Human)			Protein Precipitation (DMSO and MeOH)			2–150 µg/mL		Based on [88]	
T-AmB	Urine and Feces (Human)	Natamycin	200 µL	Protein Precipitation (DMSO and MeOH) and RP-SPE	Symmetry C18 (150 × 3.0 mm, 5 µm Waters)	A/B: MeOH/water/acetic acid (69/29/2, v/v/v)	Urine: 0.05–30 µg/mL Feces: 0.4–40 µg/mL	NS	Analyte: m/z 924 → 906 IS: m/z 666 → 503	[44]
L-AmB	Ultrafiltrate (Human)	Natamycin	200 µL	Ultrafiltration followed by RP-SPE	Synergi Max-RP (250 × 2.0 mm, 4 µm Phenomenex)	A/B: 10 mM ammonium acetate (pH 3.6)/ACN (62:38, v/v)	10–1050 ng/mL	6.5	Based on [88] Analyte: m/z 924 → 906.5 IS: m/z 666.2 → 503.3	[81]
F-AmB	Plasma (Human)	Natamycin	250 µL	Hydrophilic-RP SPE	Chromolith Performance RP18e (100 × 4.6mm, 2µm Merck)	A: 5 mM ammonium acetate (pH 6.0) in ACN/MeOH (48:20:32, v/v/v) B: 5 mM ammonium acetate (pH 6.0) in ACN/MeOH (25:5:70, v/v/v)	250–15,000 ng/mL	6.5	Analyte: m/z 924.5 → 906.6 IS: m/z 666.2 → 503.4	[89]
L-AmB	Plasma (Human)	Natamycin	250 µL	Hydrophilic-RP SPE followed by heating, LLE, and sonication	Chromolith Performance RP18e (100 × 4.6mm, 2µm Merck)	A: 5 mM ammonium acetate (pH 6.0) in ACN/MeOH (48:20:32, v/v/v) B: 5 mM ammonium acetate (pH 6.0) in ACN/MeOH (25:5:70, v/v/v)	1000–100,000 ng/mL	6.5	Analyte: m/z 924.5 → 906.6 IS: m/z 666.2 → 503.4	[89]

Analytes	Matrix	Internal Standard	Sampling Volume	Sample prep	LC column	Mobile Phase	Range	Run time (min)	Detection and settings	Ref.
T-AmB	Skin biopsy (Human)	Natamycin	50 µL	Enzymatic digestion followed by methanol protein precipitation, evaporation and reconstitution	Gemini C18 column (50 × 2.0 mm, 5 µm Phenomenex)	A: 0.1% FA in water B: 0.1% FA in MeOH	10 – 2000 ng/mL	4.5	Analyte: m/z 924.496 → 743.400 IS: m/z 666.340 → 503.200	[90]

Abbreviations: ABCD = amphotericin B colloidal dispersion; ACN = acetonitrile; CN = cyanopropyl; CSF = cerebrospinal fluid; DAD = diode array detection; DMSO = dimethyl sulfoxide; EDTA = ethylenediaminetetraacetic acid; FA = formic acid; F-AmB = free amphotericin B; HRMS = high resolution mass spectrometry; IS = internal standard; L-AmB = liposomal amphotericin B; LLE = liquid–liquid extraction; MeOH = methanol; NS = not specified; RP = reversed phase; SPE = solid phase extraction; T-AmB = total combined amphotericin B; UV = ultraviolet

4.2 Miltefosine

Miltefosine (hexadecylphosphocholine), see Figure 1, is an alkyl phosphocholine drug, a phospholipid-like molecule. The most notable molecule-specific chemical properties are the zwitterionic attribute of the cationic quaternary amine and the anionic phosphate and the high water-soluble property acting like soap. The administration route for miltefosine is orally. Chemical properties are summarized in Table 1. Published bioanalytical assays of miltefosine are scarce, seven in total, and were developed and validated in the tandem mass spectrometry era. Because miltefosine lacks chromophores, the analyte cannot be detected directly by UV. Drug metabolites were observed, possibly mediated by phospholipases, cleaving miltefosine into choline, phosphocholine, diacyl lecithin, and alcohol [7]. Little excretion (< 0.2% of the administered dose) was reported of unchanged miltefosine [99]. Miltefosine's metabolites are all endogenous compounds and are not clinically relevant. Table 3 summarizes the bioanalytical methods for quantification of miltefosine.

4.2.1. Matrix, calibration range and sampling volume

Modern methods utilize LC systems for the separation of miltefosine in biological matrices, like plasma, serum, cerebrospinal fluid, and skin tissue. Bioanalytical assays involving quantification of miltefosine in skin tissue combined with bioanalytical assays in human plasma are interesting assays for target site PK studies of antileishmanial drugs, especially for PKDL and cutaneous leishmaniasis. Also interesting for target site PK studies is a PBMC bioanalytical assay. Intracellular *Leishmania* parasites reside and survive in macrophages, therefore quantifying miltefosine intracellularly directly provides the exposure in concentration of *Leishmania* to miltefosine [38]. The validated calibration model ranges of the bioanalytical methods for miltefosine, included calibration ranges of 300-2500 ng/mL [100], 2.5-400 ng/mL [101], 4-1000 ng/mL [37], and 4-2000 ng/mL [38,102–105]. The range of 2.5-400 ng/mL was the most sensitive bioanalytical assay for miltefosine using tandem mass spectrometry, although showing a low sample preparation volume of 50 µL [101]. However, high maximum concentrations (C_{max}) of miltefosine in patients leads to the dilution of clinical samples to fit the calibration range, therefore a smaller portion of clinical blood samples could be used in the other assays. Bioanalytical assays in microsampling volumes like DBS [103] and VAMS [104] included the lowest sample preparation volumes together with the advantage of removing cold chain transportation and storage of the samples.

4.2.2. Sample preparation

Considering the sample preparation, two methods were used exclusively, i.e., methanol protein precipitation and phenyl-SPE. Both methods involve methanol since alkylphospholcholine amphophilic compounds are readily soluble in organic solvents as well as in water. Miltefosine is highly plasma protein bound, 96%-98% [7,106], by using organic solvents miltefosine detaches from proteins and dissolves readily in organic solvent. Multiple SPE stationary phases were investigated to increase the recovery of miltefosine from plasma, however miltefosine possessing both zwitterionic and polar/apolar properties was shown to interact with silica sorbents, leading to secondary interaction mechanisms [102]. The highest recovery (82.1%) using SPE was achieved using phenyl-SPE [102].

4.2.3. Internal standard, separation, and detection

The internal standards used for quantification in various bioanalytical assays were a deuterated form of miltefosine (D_4-miltefosine) and phenacetin. In some cases, no internal standard was used for the quantification. The absence of internal standard is an unreliable choice of setup in terms of compromising precision by the absence of analyte correction for matrix effects and extraction recoveries when running a patient sample batch. Admitting that phenacetin is not a chemical analogue in terms of chemical structure, the internal standard was described possessing comparable chemical properties and similar elution times as miltefosine using an amide column, which in turn are preferable characteristics for the selection of an internal standard. The disadvantage of using a non-chemical analogue as internal standard is the correction during stability issues because of differences in chemical structures and properties. Employing D_4-miltefosine as internal standard ensures precise and accurate measurements, because retention times, peak shape, and ionization patterns are similar. Finally, the assay using the lowest sampling volume of 50 µL [101] lowered detection noise, using an amide column with 0.2% FA compared to the other methods using ammonium derivatives combined with C8 or C18 stationary phases. Lowering detection noise was achieved using a more compatible stationary phase in combination with addition of low noise mobile phase ionic additions. Detection of miltefosine and IS were performed using triple quadrupole or quadrupole – linear ion trap mass spectrometers, using transition m/z 408.5 → 125.1 for miltefosine, m/z 412.6 → 129.2 for D_4-miltefosine, and m/z 180.1 → 138.2 for phenacetin in positive ion mode. Miltefosine and D_4-miltefosine fragment ions consisted of a positive charged ethylphosphate group, cleaving both the C_{16} chain and trimethylamine groups.

4.2.4. Clinical application

Miltefosine is mainly used in the treatment of leishmaniasis. Therefore, PK studies including miltefosine drug treatment regimens measured using above mentioned bioanalytical assays were performed on patients suffering from leishmaniasis [23,95,107–112]. Either monotherapy or combination therapies including amphotericin B were performed in the mentioned PK studies. Miltefosine was conventionally dosed at 2.5 mg/kg, but after failure of treatment due to low exposure of miltefosine in particularly children, an allometric dosing regimen was developed and recommended [111]. Allometric dosing based on fat free mass increased exposure and efficacy in children. The allometric dosing regimen led to a plasma C_{max} of around 21.0 µg/mL as compared to 19.9 µg/mL for the conventional linear dosing regimen in Eastern African pediatric VL patients, treated for 28 days in total [23].

Table 3: An overview of bioanalytical methods for the quantification of miltefosine.

Matrix	Internal Standard	Sampling Volume	Sample prep	LC column	Mobile Phase	Range	Run time (min)	Detection and settings	Ref.
Plasma (Human)	-	250 µL	Phenyl-RP SPE	Gemini C18, (150 × 2.0 mm, 5 µm Phenomenex)	A/B: 10 mM ammonium hydroxide in water/ 10 mM ammonium hydroxide in MeOH (5:95, v/v)	4 – 2000 ng/mL	7	m/z 408.4 → 124.8	[102]
DBS (Human)	D_4–Miltefosine	3-mm Punch	Protein Precipitation (MeOH)	Gemini C18, (150 × 2.0 mm, 5 µm Phenomenex)	A/B: 10 mM ammonium hydroxide in water/ 10 mM ammonium hydroxide in MeOH (5:95, v/v)	4 – 2000 ng/mL	5	Based on [102] Analyte: m/z 408.5 → 125.1 IS: m/z 412.6 → 129.2	[103]
VAMS (Human)	D_4–Miltefosine	1 VAMS Tip	Protein Precipitation (MeOH)	Gemini C18, (150 × 2.0 mm, 5 µm Phenomenex)	A/B: 10 mM ammonium hydroxide in water/ 10 mM ammonium hydroxide in MeOH (5:95, v/v)	4 – 2000 ng/mL	5	Based on [102] Analyte: m/z 408.5 → 125.1 IS: m/z 412.6 → 129.2	[104]
PBMCs (Human)	D_4–Miltefosine	250 µL	Phenyl-RP SPE	Gemini C18, (150 × 2.0 mm, 5 µm Phenomenex)	A/B: 10 mM ammonium hydroxide in water/ 10 mM ammonium hydroxide in MeOH (5:95, v/v)	4 – 2000 ng/mL	5	Based on [102] Analyte: m/z 408.5 → 125.1 IS: m/z 412.6 → 129.2	[38]
Plasma (Human and hamster)	Phenacetin	250 µL	Protein Precipitation (MeOH)	Unisol Amide column (100 × 4.6 mm, 3 µm Agela Technologies)	A/B: 0.2% FA in water/MeOH (1:9, v/v)	2.5 – 400 ng/mL	4.5	Analyte: m/z 408.1 → 125.1 IS: m/z 180.1 → 138.2	[101]
CSF and serum in plasma (Human)	-	50 µL	Phenyl-RP SPE	Gemini C18, (150 × 2.0 mm, 5 µm Phenomenex)	A/B: 10 mM ammonium hydroxide in water/ 10 mM ammonium hydroxide in MeOH (5:95, v/v)	4 – 2000 ng/mL	7	m/z 408.4 → 124.8	[105]
Skin (Human)	D_4–Miltefosine	250 µL	Phenyl-RP SPE	Gemini C18, (150 × 2.0 mm, 5 µm Phenomenex)	A/B: 10 mM ammonium hydroxide in water/ 10 mM ammonium hydroxide in MeOH (5:95, v/v)	4 – 1000 ng/mL	5	Based on [102] Analyte: m/z 408.5 → 125.1 IS: m/z 412.6 → 129.2	[37]

Abbreviations: CSF = cerebrospinal fluid; DBS = dried blood spots; FA = formic acid; IS = internal standard; MeOH = methanol; NS = not specified; PBMCs = peripheral blood mononuclear cells; RP = reversed phase; SPE = solid phase extraction; VAMS = volumetric absorptive microsampling

4.3. Paromomycin

Paromomycin (aminosidine), displayed in Figure 1, is an aminoglycoside derived from *Streptomyces* bacteria. Paromomycin and aminoglycosides in general are amino-sugar molecules, implicating that these types of molecules are alkaline compounds because of the amino bonds and are very water soluble. The chemical properties are summarized in Table 1. Paromomycin treatment is administered intramuscularly leading to high concentrations of paromomycin within the first hour, before being excreted relatively fast renally [113]. Because paromomycin is readily used as an antibiotic drug in animals, most published bioanalytical methods are in animal matrices, whereas published bioanalytical assay in human matrices were only four in total. Paromomycin does not have known drug metabolites and is secreted unchanged in the kidneys [114,115]. Paromomycin is stable under physiological conditions and can be heated op to at least 120°C for 24 hours in injectable doses formulation [116]. An overview of the bioanalytical methods is given in Table 4.

4.3.1. Matrix, calibration range and sampling volume

The human matrices for these bioanalytical assays include plasma, urine, and serum. No tissue assay was published in human matrices to date that could help in target site PK studies. Calibration curves vary for human blood matrices from 0.5-50 µg/ml [117,118], 100 – 5000 ng/mL [119] to 5 – 1000 ng/mL [120], whereas the only published urine method exhibited a calibration range of 1-50 µg/mL [117]. Three out of four published bioanalytical assays used large volumes of blood-based matrices, 300 µL [117,118] and 500 µL [119], while the other bioanalytical method used 50 µL combined with the highest sensitivity [120], accomplishing a fitting bioanalytical assay for anemic patients.

4.3.2. Sample preparation

Sample preparation methods were diverse, employing conventional sample preparation methods such as protein precipitation, liquid-liquid extraction (LLE) and SPE. Protein precipitation was performed using acidic solvents (perchloric acid or trichloroacetic acid) instead of the conventional organic solvents like methanol or acetonitrile. Paromomycin is stable for at least 44 days at 2-8°C in trichloroacetic acid and was assessed in plasma final extracts [120]. Paromomycin is poorly soluble in organic solvents and can therefore be unfavourable for extraction recovery, whereas a highly acidic aqueous solvent is favourable for the solubility and recovery of such alkaline compound and highly polar compounds while at the same is an effective precipitant for proteins. Sample preparation methods that included LLE were established after a derivatization step to covalently bind paromomycin to an organic solvable chromophore (benzene ring), to transfer paromomycin to the organic layer of the immiscible solvent. Extraction of paromomycin using cation-exchange SPE was also used in serum, employing an effective stationary phase for the extraction of basic molecules because of its negative charge.

4.3.3. Internal standard, separation, and detection

Internal standards used in the separation and quantification of paromomycin include kanamycin B, deuterated paromomycin and in some methods no internal standard was used. Selection of an aminoglycoside chemical analogue, kanamycin B, as internal standard provides sufficient correction for the sample preparation and detection of paromomycin because they are chemically structural and property similar. A SIL-IS is recommended in the use of (LC-MS/MS), however, the internal standard recovery of the analyte should be assessed [121]. A multiple deuterated internal standard was used for the quantification of paromomycin, that could introduce interference resulting in a bias in the quantification [120]. The internal standard included 0.13% D_0 that could lead to potential cross-over of internal standard to the analyte transition but was eventually solved by addition of a small volume to plasma (20 µL IS against 50 µL plasma sample) at a low concentration to decrease the selectivity risk of the assay [120]. Paromomycin does not have chromophores, however derivatization of 2,4-dinitrofluorobenzene chromophores to paromomycin and IS facilitated the use of UV methods at 350 nm [117,118]. The recovery of paromomycin is dependent on the yield from the derivatization step, however the extraction recovery is relatively high (87%). The derivatization method included an advantage for separation using an analytical reversed phase column, because paromomycin does not retain on classic C_{18} columns without addition of ion-pair in mobile phase or pre-column derivatization [122]. For this reason, published LC-MS/MS methods used either a ZIC-HILIC column [119] for separation, ion-exchange based on stationary phase, or an ion-pair reagent (heptafluorobutyric acid) as mobile phase in combination with an UHPLC C_{18} column [120], ion-exchange based on mobile phase addition. The detection of paromomycin with mass spectrometry was performed using a triple quadrupole or quadrupole – linear ion trap mass spectrometers in ion positive mode, exerting transitions m/z 616.6 → 163.1.

4.3.4. Clinical application

Despite being an old drug, PK studies of intramuscular administered paromomycin are scarce. Studies were performed in healthy volunteers [118] or in patients suffering from VL [123–126]. Paromomycin has been administered intramuscularly at different dosing regimen schedules. Healthy volunteers received a single dose of 12 – 15 mg/kg. VL patients treated with paromomycin in India were dosed intramuscularly 15 mg/kg/day for 21 days, displaying a high efficacy (94.6% cure rate) [123]. In Eastern Africa, efficacy with the same regimen was generally lower, displaying a high geographical variability in efficacy. [126]. Eventually, PK studies were conducted in India and Eastern Africa using various treatment dosing regimens to assess differences in geographical exposure and efficacy [125]. Paromomycin plasma concentrations were highly variable, with a C_{max} around 22 µg/mL within the first few hours of administration and is excreted renally with a $t_{1/2}$ between 2-3 hours [118,124]. Exposure differences could not explain the observed geographical differences in efficacy [125].

Table 4: An overview of bioanalytical methods for the quantification of paromomycin.

Matrix	Internal Standard	Sampling Volume	Sample prep	LC column	Mobile Phase	Range	Run time (min)	Detection and settings	Ref.
Plasma (Human)	Kanamycin B	300 µL	Protein precipitation (perchloric acid) followed by LLE after 2,4-dinitrofluorobenzene derivatization	Zorbax SB-C18 (50 x 4.6 mm, 5 µm Agilent Technologies)	A/B: phosphoric acid (pH 3.0) in MeOH (36:64, v/v)	0.5-50 µg/ml	>24 (NS)	UV detection 350 nm	[117]
Urine (Human)						1-50 µg/mL			
Plasma (Human)	Kanamycin B	300 µL	Protein precipitation (perchloric acid) followed by LLE after 2,4-dinitrofluorobenzene derivatization	Zorbax SB-C18 (50 x 4.6 mm, 5 µm Agilent Technologies)	A/B: phosphoric acid (pH 3.0) in MeOH (36:64, v/v)	0.5-50 µg/ml	>24 (NS)	UV detection 350 nm based on [117]	[118]
Serum (Human)	–	500 µL	Cation-exchange SPE	ZIC-HILIC (100 x 2.1 mm, 5 µm SeQuant)	A: 0.2% FA in 2mM ammonium acetate/ ACN (95:5, v/v) B: 0.2% FA in 2mM ammonium acetate/ ACN (5:95, v/v)	100 – 5000 ng/mL	10.8	m/z 616.1 → 163.1	[119]
Plasma (Human)	D_5-Paromomycin	50 µL	Protein Precipitation (TCA)	Acquity UPLC HSS T3 (150 x 2.1 mm, 1.8 µm Waters)	A/B: 5 mM HFBA in water/ACN (7:3, v/v)	5 – 1000 ng/mL	3	Analyte: m/z 616.6 → 163.1 IS: m/z 621.6 → 165.1	[120]

Abbreviations: ACN = acetonitrile; FA = formic acid; HFBA = heptafluorobutyric acid; IS = internal standard; LLE = liquid-liquid extraction; MeOH = methanol; NS = not specified; SPE = solid phase extraction; TCA = trichloroacetic acid; UV = ultraviolet; ZIC-HILIC = zwitterionic hydrophilic interaction liquid chromatography

4.4. Pentamidine

Pentamidine, shown in Figure 1, is an aromatic diamidine compound. This class of molecules is characterized by amidine groups at both ends of the molecule and possessing stereoisomeric traits if the molecule is divided in half. No information was available about the efficacy of the variability of isomers hitherto. Stereoisomers would not pose problems for LC separation because the hydrophobic section in the molecule is dominantly present. Pentamidine isethionate (salt formulation) is water soluble [127] whereas pentamidine itself is poorly water soluble [128]. It is an alkaline molecule, but due to the high pKa of the amidine groups and poor bioavailability, it is administered by intramuscular or intravenous injection only [129], however with variable treatment outcomes per administration route for various *Leishmania* subspecies reported [130]. Pentamidine is metabolized by cytochrome p450 enzymes in the liver, however no data were found on the drug metabolites [131]. Chemical properties of pentamidine are summarized in Table 1.

4.4.1. Matrix, calibration range and sample volume

Bioanalytical assays for the quantification of pentamidine in human matrices were performed in blood (whole blood, serum, or plasma), urine or bronchoalveolar lavage, however no assay included determination in tissue material. Calibration models were diverse, varying in sensitivity and dynamic range. The calibration curve with the highest ULOQ ranged from 5-200 µg/mL [132], whereas the largest dynamic range included a calibration curve of 0.229-20.1 µg/mL [133] and the most sensitive calibration curve was 2.29-573 ng/mL [133]. Pentamidine bioanalytical assays were published between 1985 to 2004, with relatively high sample volumes, between 120 µL and 1000 µL of serum, plasma, whole blood, and urine.

4.4.2. Sample preparation

Extraction of pentamidine was performed using various methods, including protein precipitation using acetonitrile or sodium hydroxide, SPE with a reversed phase stationary phase, ultrafiltration, or LLE using chloroform. Pentamidine is soluble in organic solvents and is highly plasma protein bound [134]. Because of this protein binding, LLE has been performed after protein precipitation, to improve extraction of unbound pentamidine to the immiscible organic phase (chloroform). A similar strategy was included during SPE sample preparation for the same reason, other than unbound pentamidine binding to the reversed phase stationary phase of the SPE cartridge, that binds the hydrophobic structures of pentamidine. Ultrafiltration with a 30 kDa cut-off was also employed as a sample preparation method and was successful in extracting pentamidine, differentiating free from protein bound fraction.

4.4.3. Internal standard, separation, and detection

Pentamidine bioanalytical assays either used hexamidine or disopyramidine as internal standard or used no internal standard at all. Disopyramidine is not a chemical analogue

but shares a common property with pentamidine, being a highly alkaline compound. Therefore, disopyramidine corrects for the LLE sample preparation method only in the form of deprotonation of pentamidine and the transfer to the organic layer. The use of hexamidine is probably more appropriate, given that hexamidine is a chemical analogue, differing by only one additional methyl group. Separation of pentamidine was performed using HPLC reversed phase columns or high-performance capillary electrophoresis (HPCE). Performing electrophoresis for separation of pentamidine allowed a more simple and rapid sample preparation and excludes organic solvent waste, however, is limited to on-column detection methods, mostly spectroscopic (UV, Raman) and fluorescent detection. HPLC columns used were either C_8 or C_{18} columns, with the stationary phase binding the hydrophobic groups of pentamidine. Mobile phase ion additives exerted variability among different separation systems and detection settings. Borate buffer and sodium dodecyl sulphate (SDS) were used in combination with HPCE. Both phosphoric acid and tetramethylammonium chloride were included in fluorescent excitation detection. Ammonium acetate and ion-pair additive heptane sulfonic acid were employed in combination with UV detection, allowing pentamidine to bind to the stationary phase with an adduct to neutralize the cationic pentamidine. The methods of choice for the detection of pentamidine were fluorescence, using excitation wavelengths of 265 or 275 nm and emission wavelengths of 330 or 340 nm, or UV detection using 214 nm, 262 nm, or 280 nm. Pentamidine has two chromophores and therefore allows for UV detection, whereas could also be emitted to an excited state and transmit in UV wavelength ranges. No mass spectrometry detection has been applied. Table 5 summarizes the bioanalytical methods for pentamidine.

4.4.4. Clinical application

Pentamidine PK studies supported by the previously described bioanalytical methods were limited. Most pentamidine PK studies were performed between 1980 and 1990, with limited use of chromatographic bioanalytical methods. PK studies were performed on AIDS patients suffering from pneumonia [133,135] or patients receiving aerosol therapy [136]. Patients that underwent aerosol therapy received 600 mg of pentamidine by a nebulizer for a total of 21 days. Bronchoalveolar lavage and urine pentamidine concentrations were compared to investigate urine as an accurate clinical indicator for lung exposure in aerosol therapy based pentamidine treatment [136]. AIDS patients suffering from pneumonia PK studies administered pentamidine either intravenously or intramuscularly with a dose of 4 mg/kg/day. Patients suffering from *Pneumocystis carinii* received treatment for 12 – 21 days, dependent on their treatment outcomes [135]. Serum concentrations were measured to identify a threshold of >100 ng/mL in serum related to improved efficacy. Mean plasma concentrations in AIDS patients receiving intramuscular administered pentamidine (209 ± 48 ng/mL) were lower than for intravenous administered pentamidine (612 ± 371 ng/mL). Low pentamidine plasma concentrations (< 25 ng/mL) were discovered after 8 hours of administered pentamidine, indicating fast elimination of pentamidine [133].

Table 5: An overview of bioanalytical methods for the quantification of pentamidine.

Matrix	Internal Standard	Sampling Volume	Sample prep	LC column	Mobile Phase	Range	Run time (min)	Detection and settings	Ref.
Serum (Human)	Hexamidine isethionate	500 µL	Protein precipitation (ACN) followed by RP-SPE	Suplex pKb-100 (250 x 4.6 mm, 5 µm Sigma Aldrich)	A/B: 0.025 mol/L heptanesulfonic acid (pH 3.0) in water/MeOH (40:60, v/v)	15–600 ng/mL	>3.2 (NS)	Fluorescence excitation 265 nm, emission 330 nm	[135]
Serum (Human)	-	120 µL	Ultrafiltration (30 kDa cut-off)	High Performance Capillary Electrophoresis (HPCE) (570 mm x 75 µm I.D.; 500 mm length Beckman Instruments)	100 mM borate buffer (pH 8.35), 50 mM SDS at 25 kV	1–30 µg/mL	<10	UV Detection 214 nm	[137]
Placenta (Human)	-	500 µL	Protein precipitation (ACN)	µ-Bondapak RP-C$_{18}$	0.1 M acetate buffer (pH 4.0)/ACN (82:18, v/v)	0.05–24 µg/mL	>6 (NS)	UV detection 254 nm	[138]
Whole blood, plasma (Human)	Hexamidine isethionate	1000 µL	LLE using ACN, chloroform and 0.1 M phosphate buffer (pH 2.8)	Ultrasphere C$_8$ (150 x 4.6 mm, 5 µm Beckman)	1.8 mM tetramethylammonium chloride in 0.1% H$_3$PO$_4$ water/ACN (6:4, v/v)	5–200 µg/mL	>6.5 (NS)	Fluorescence excitation 275 nm, emission 340 nm	[132]
Urine (Human)		250 µL							
Plasma (Human)	Disopyramide	1000 µL	LLE using ACN, chloroform and 1 M sodium hydroxide	µ-Bondapak RP-C$_{18}$ (300 x 4 mm, 10 µm Waters)	0.1% H$_3$PO$_4$ in water/ACN (8:2, v/v)	5–408 µg/mL	>9.1 (NS)	UV detection 262 nm	[139]
Serum (Human)	Hexamidine isethionate	1000 µL	Protein precipitation (sodium hydroxide) followed by LLE using chloroform	C$_{18}$ (150 x 2.1, 5 µm Alltech)	0.05 M sodium heptanesulfonate in 0.014 M TEA/MeOH (2:3, v/v)	63.3–254 ng/mL	>8.2 (NS)	UV detection 280 nm	[140]

Matrix	Internal Standard	Sampling Volume	Sample prep	LC column	Mobile Phase	Range	Run time (min)	Detection and settings	Ref.
Plasma (Human)	Hexamidine isethionate	500 µL	Protein precipitation using ACN followed by RP-SPE	Ultrasphere Octyl (250 x 4.6 mm, 5 µm Altex)	0.1% H$_3$PO$_4$ in 0.02% tetramethylammonium chloride/ACN (55:45, v/v)	2.29–573 ng/mL	NS	Fluorescence excitation 275 nm, emission 340 nm	[133]
Urine (Human)			Protein precipitation (ACN)			0.229–20.1 µg/mL			
Serum (Human)	Based on [133]	500 µL	Based on [133]	Based on [133]	Based on [133]	Based on [133]	Based on [133]	Based on [133]	[141]
BAL and urine (Human)	Based on [133]	500 µL	Based on [133]	Based on [133]	Based on [133]	Based on [133]	Based on [133]	Based on [133]	[136]

Abbreviations: ACN = acetonitrile; BAL = bronchoalveolar lavage; LLE = liquid-liquid extraction; MeOH = methanol; NS = not specified; RP = reversed phase; SDS = sodium dodecyl sulphate; SPE = solid phase extraction; TEA = triethylamine; UV = ultraviolet

4.5. Pentavalent antimonials

Sodium stibogluconate and meglumine antimoniate, shown in Figure 1, are used against leishmaniasis under the collective name pentavalent antimonials and are in essence metallodrugs. The compounds can be characterized by their covalently bonded antimony (Sb^{3+} or Sb^{5+}) (meglumine antimoniate) or by the presence of two covalently bonded antimonies (sodium stibogluconate), see Figure 1. Pentavalent antimonials are poorly soluble in water and are administered by intravenous or intralesional injections. Drug metabolites discovered in urine were antimony isotopes (^{121}Sb and ^{123}Sb; $Sb3^+$ and Sb^{5+}) originating from the pentavalent antimonials, yet the other degradation products are still unknown [142]. From toxicological and drug efficacy point of view, these drug metabolites could provide valuable information about the consistency and potency of antimony ions present in the pentavalent antimonials due to the variability of ionic strength. The present paradigm is that Sb^{5+} is either directly responsible for the efficacy of antileishmanial activity [143] or Sb^{5+} is reduced to Sb^{3+} as a pro-drug to activate its antileishmanial activity [144].

4.5.1. Matrix, calibration range, sample preparation, separation, and detection

Bioanalytical methods for the quantification of antimonies were performed in blood matrices, liver, urine, breast milk, skin, and placenta. There was variability among the calibration ranges and, nevertheless, were sensitive overall, with 0.002-9.5 ng/L as the most sensitive calibration range [145]. Sample preparation for inductively coupled plasma mass spectrometry (ICP-MS) measurement was performed using nitric acid (HNO_3) digestion and dilution, assisted with microwave or heating incubations, to fully digest the biological matrix before detection. Gamma spectrometry separation and detection, irradiation was performed as sample preparation using a thermal flux set at 2.6×10^{12} n/cm² s¹ to 5.0×10^{13} n/cm² s¹ [146,147], using incubation times of approximately 1 hour to 2 days. In case of ICP-MS or gamma spectrometry detection, no specific sample separation was required, however, gas chromatography (GC) and LC were implemented in two publications before ICP-MS detection [142,145], with LC using anion exchange to separate Sb^{3+} from Sb^{5+} before detection. Sodium stibogluconate and meglumine antimoniate were quantified based on the elemental information of the covalently bonded antimonies, excluding further structural information of the antileishmanial drugs. Internal standards included various other metals, like Tb (terbium), Ge (germanium), Ir (iridium), Sc (scandium), Rh (rhodium), In (Indium) or Sb with isotopic number 123 (Sb^{5+}).

4.5.2. Clinical application

Pentavalent antimonials meglumine antimoniate and sodium stibogluconate were described in patients suffering from leishmaniasis using PK studies [148–150]. In each of the conducted PK studies, total antimony concentrations were measured. Patients suffering from VL or CL were treated with intramuscular administered pentavalent antimonials dosed at 10 mg/kg antimony daily for 30 days [150]. A plasma C_{max} of

9 – 12 µg/mL was reached 2 hours after administration. PK studies were performed to investigate the differences in efficacy in CL patients between children and adults following 20 mg/kg/day of meglumine antimoniate for 20 days [148]. Differences in C_{max} between children (32.7 ± 0.9) and adults (38.8 ± 2.1 µg/mL) were identified. After increasing the dose at day 20 to 30 mg/kg after 19 days 20 mg/kg/day, peak concentrations were much higher (43.8 ± 2.3 µg/mL). To conclude, lower exposure appears to result primarily from body weight-depending antimony clearance.

5. Discussion & conclusion

A comprehensive overview of the bioanalytical methods for the quantification of antileishmanial drugs amphotericin B, miltefosine, paromomycin, pentamidine, and pentavalent antimonials in human matrices is provided in this review. Publications were summarized and compared in terms of sampling matrices, calibration ranges, sample volumes, sample preparation methods, internal standards, separation, and detection methods for each antileishmanial separately, with respect to their respective chemical properties.

All published bioanalytical methods of antileishmanial drugs focused on quantification of one drug, no bioanalytical methods including multiple antileishmanial drugs in a single assay could be identified. Present clinical PK studies in leishmaniasis focus very much on novel combination treatments, for example miltefosine-paromomycin or miltefosine-liposomal amphotericin B regimens under investigation in Eastern Africa [27] and the Indian subcontinent [165]. Combination therapies are aimed at preventing drug resistance, as well as increasing efficacy and safety by decreasing dosing and/or treatment duration of the potentially toxic antileishmanial drugs [166]. An advantage of multiplex assays establishing simultaneous quantification of multiple antileishmanial drugs would be the increase in speed and efficiency and a lower sample volume required for the quantification of drug concentrations in patients treated combination therapies. The diverse chemical properties of amphotericin B/ miltefosine or miltefosine/paromomycin (Table 1) are a challenge to combine these compounds into a collective bioanalytical method, but still achievable. Amphotericin B is poor water-soluble however has good organic solubility that could theoretically be combined through organic solvent protein precipitation followed by reversed phase solid phase extraction (RP-SPE). RP-SPE using phenyl stationary phase was the only successful SPE method combined with a reversed phase property to extract miltefosine [102]. Amphotericin B and miltefosine are separated through classic reverse phase LC. However, miltefosine was separated on a C18 column using triethylamine (TEA) alkaline additives, thereby miltefosine was eluted using 100% organic phase, while amphotericin B is separated using acidic mobile phase. This could pose a challenge as chromatographic parameters like peak shape and elution

Table 6: An overview of bioanalytical methods for the quantification of antimonial drugs.

Pentavalent antimonials/ antimony	Matrix	Internal Standard	Sampling Volume	Sample prep	LC column	Mobile Phase	Range	Detection and settings	Ref.
Antimony	Liver (Human)	-	-	Microwave digestion using HNO$_3$	-	-	0.2-102 ng/g	ICP-MS	[151]
Antimony	Urine (Human)	-	1 mL	Sample digestion using HNO$_3$	-	-	LOQ 0.021 µg/L	ICP-MS	[152]
Antimony	Urine (Human)	Tb (terbium)	1 mL	Sample digestion using HNO$_3$	-	-	0.09-2 µg/L	ICP-MS	[153]
Antimony	Plasma (Human)	-	-	Deionized water dilution	-	-	0.01-2.67 µg/L	ICP-MS	[154]
Antimony	Whole Blood (Human)	In (Indium)	1 mL	Sample digestion using HNO$_3$ followed by addition of H$_2$O$_2$	-	-	0.03-25 µg/L	ICP-MS	[155]
Antimony	Liver (Human)	^{123}Sb (antimony)	0.2 g	Tissue freeze-dried followed by microwave digestion using HNO$_3$	-	-	0.375-1.5 µg/L	ICP-MS	[156]
Antimony	Plasma (Human)	-	-	Sample digestion using HNO$_3$	-	-	0.02-13.5 µg/L	ICP-MS	[157]
Antimony	Whole blood, placenta (Human)	-	0.5 mL blood 0.2 g placenta	Microwave digestion using HNO$_3$	-	-	0.06-7.99 µg/L 0.1-33.43 ng/g	ICP-MS	[158]
Antimony	Urine (Human)	-	4 mL	NaBH$_4$ reduction followed by water dilution and adjust pH using HCl	hydride generation (HG), low-temperature gas chromatography (LTGC)	-	0.002-9.5 ng/L	ICP-MS	[145]
Antimony	Serum (Human)	Rh (rhodium)	1 mL	Sample digestion using HNO$_3$	-	-	25-250 ng/mL	ICP-MS	[159]
Meglumine antimoniate	whole blood, blood plasma, urine, and hair (Human)	In (Indium)	0.5 – 2 cm hair	NaBH$_4$ microwave digestion HG followed by reduction using H$_2$SO$_4$, KI and ascorbic acid. Afterwards, samples were diluted in 2 mM or 20 mM EDTA	PRP-X100 (150 mm × 4.1 mm i.d., Hamilton, USA)	2 mM or 20 mM EDTA (pH 4.7) in water	^{121}Sb 0-100 µg/mL ^{123}Sb 0-100 µg/L	ICP-MS	[142]
Antimony	Whole blood (Human)	Ge (germanium); Ir (iridium); Sc (scandium) and Rh (rhodium)	130 µL	Dilution in ammonia solution (0.05% of EDTA, 0.05% of Triton X-100, and 1% of NH4OH	-	-	0.005 – 20 ng/mL	ICP-MS	[160]
Antimony	Serum (Human)	In (Indium)	2 mL	Sample digestion using HNO$_3$ and H$_2$O$_2$	-	-	-	ICP-MS	[161]
Antimony	Breast milk (Human)	-	-	Irradiation for 1h – 14h in a thermal flux (2.6 × 10^{12} n/cm^2 s^1)	-	-	-	Gamma spectrometry	[146]
Antimony	Plasma, PBMC (Human	In (Indium)	100 µL	Samples were added to indium internal standard solution, containing 1% TMAH/1% EDTA before 30 mixing.	-	-	25 – 10,000 ng/mL	ICP-MS	[162]

1.1

Pentavalent antimonials/antimony	Matrix	Internal Standard	Sampling Volume	Sample prep	LC column	Mobile Phase	Range	Detection and settings	Ref.
	Plasma (Human)	In (Indium)	-	Addition of internal standard followed by dilution with 0.5% nitric acid and 0.01% Triton X-100	-	-	LOD 0.020 µg/L	ICP-MS	[163]
Antimony	Skin (Human)		-	Digestion in a Start D Micro-wave Digestion System using using 10% nitric acid and hydrogen peroxide	-	-	LOD 0.008 µg/L		
	Plasma (Human)	-	10 mL	Protein precipitation using ACN. KI and ascorbic acid were used as reducing agents	-	-			
Antimony	Urine (Human)	-	25 mL	Sample digestion using HNO₃. KI and ascorbic acid were used as reducing agents	-	-	0.2-20 ng/ml	ICP-MS	[164]

Abbreviations: EDTA = ethylenediaminetetraacetic acid; TMAH = tetramethylammonium hydroxide

time can probably not be optimized under the same circumstances. Thereby, paromomycin samples were prepared by acidic non-organic solvent protein precipitation and separated through ion-exchange chromatography. Combination drug treatment regimen including pentavalent antimonials and other antileishmanial drugs, should be measured separately, because antimonials were measured through ICP-MS and gamma spectroscopy, requiring a very different sample preparation and detection setups.

The variability of human tissue matrices towards blood-based matrices is scarce in the publications of bioanalytical methods for the quantification of antileishmanial drugs, however the most important PK parameters rely often on blood-based matrices i.e., whole blood, serum, or plasma. Blood-based matrices formed the bulk matrix of published bioanalytical methods, with 46/52 amphotericin B, 6/7 miltefosine, 4/4 paromomycin, 8/9 pentamidine, and 11/18 antimonials blood-based publications (Tables 2- 6). Low sampling volumes are important for future human PK studies, because of the vulnerable and often anemic state of (visceral) leishmaniasis as well as removing cold chain transportation and storage by sampling using DBS or VAMS. Consequently, amphotericin B, miltefosine, and paromomycin already include methods with low sampling volumes (≤ 50 µL) whereas pentamidine lowest sampling volume was 120 µL of blood serum. There were two methods described, only for miltefosine, that used microsampling methods DBS and VAMS. PK studies conducted for antileishmanial drugs in patients suffering from leishmaniasis or other diseases investigated PK parameters in blood matrices, as shown in the clinical applications of the drugs. These PK studies improved formulation strategies for amphotericin B and improved therapeutic dosing regimens for all antileishmanial drugs by characterizing exposure and exposure-response relationships of the treatments. There is an increased interest to involve target site PK data coupled to classical blood matrices to gain more information about exposure-response relationships and distribution of drugs to their respective site of target [34−37]. Considering future target site antileishmanial PK studies the development and validation of bioanalytical methods for the quantification of antileishmanial drugs in human skin tissue (CL and PKDL), spleen, liver, and bone marrow (VL), and PMBCs (leishmaniasis in general) will gain prominence. Quantification in skin tissue was to date only published for amphotericin B [90], miltefosine [37], and pentavalent antimonials [163] and is expected to contribute to future antileishmanial target site PK studies in CL and PKDL patients. Quantification in liver was described for pentavalent antimonials [151,156]. Furthermore, bioanalytical measurements in PBMCs were described for both miltefosine [38] and pentavalent antimonials [162]. Paromomycin in skin tissue manuscript is in preparation of submitting.

In conclusion, various bioanalytical methods for the quantification of antileishmanial require different approaches dependent on the chemical properties of the analyte, as well as the goal of the PK study including sampling time-points that require sensitivity of the

assay or the use of different human matrices for target site studies, which in case of CL and PKDL would be human skin tissue, for VL patients would be liver, spleen and bone marrow, whereas all leishmaniasis would be intracellularly in PBMCs. Considering all aspects discussed above, the favored bioanalytical assay aspects for the quantification of antileishmanial drugs in multiple matrices are explained for each antileishmanial drug. Amphotericin B in blood or tissue matrices were extracted using protein precipitation as the main sample preparation method, shown in Table 2. Low sampling volumes are preferred, therefore as low as 50 µL of human plasma is satisfactory [88]. Simple RP separation combined with methanol organic phase was the preferred method of choice for amphotericin B, therefore methanol precipitation is most compatible. Tandem mass spectrometry for selectivity in combination with SIL-IS is ideal for bioanalytical assays. D_8-amphotericin B was used in combination with high-resolution mass spectrometry (HR-MS) [84], although in combination with tandem mass spectrometry using a high dynamic range (2 – 150 µg/mL in plasma) and sensitivity (0.01 – 2 µg/mL in ultrafiltrate) is advantageous [88]. Miltefosine in blood matrices (either 50 µL of 250 µL) was extracted by protein precipitation or phenyl-SPE. Protein precipitation methods are preferred because of their speed and low costs, however, miltefosine readily adsorbs to surfaces. Therefore, phenyl-SPE is the preferred sample preparation method of choice [37,38,102,105]. D_4-miltefosine was used as SIL-IS in multiple bioanalytical assays in combination with tandem mass spectrometry and offered a high dynamic range (4 – 2000 ng/mL) and satisfactory sensitivity [102–104]. Separation of miltefosine was performed with either high alkaline high organic phase RP separation or using slightly acidic mobile phase combined with an amide column. Less addition of ionic additives to mobile phase lowers the baseline (offset), therefore the amide column with less ionic mobile phase additives is preferred [101]. Paromomycin sampling volumes of 50 µL are preferred, together with simple protein precipitation using TCA [120]. A SIL-IS combined with tandem mass spectrometry displayed a sensitive method (5 – 1000 ng/mL). Separation using ion-pairing was mandatory to bind paromomycin to the stationary phase of a RP column, with the risk of contaminating the LC-MS/MS system. Therefore, using a ZIC-HILIC column with little ionic mobile phase addition was selected as method of choice [119]. For pentamidine, protein precipitation using ACN was preferred as extraction method [133,136,138,141]. Chemical analogue hexamidine isethionate closely resembles pentamidine and was used in UV or fluorescence detection, with fluorescence detection more selective than UV detection. Additionally, fluorescent detection (2.29 – 573 ng/mL [133]) was more sensitive compared to UV detection (5 – 408 ng/mL [139]). Pentavalent antimonials extraction was uniform, using sample dilution or sample digestion. Digestion degradation methods are preferred because of uniform homogenization of analytes in the samples [151–153,155–159,161,163]. Future bioanalytical studies for antileishmanial drugs are recommended to aim to combine various drugs in a single bioanalytical method together with their application in target site matrix as well as to consider developing and apply microsampling strategies, for optimized use in clinical PK studies in leishmaniasis.

References

[1]   P.J. Hotez, S. Aksoy, P.J. Brindley, S. Kamhawi, What constitutes a neglected tropical disease?, PLoS Negl. Trop. Dis. 14 (2020) e0008001. https://doi.org/10.1371/journal.pntd.0008001.

[2]   E. Torres-Guerrero, M.R. Quintanilla-Cedillo, J. Ruiz-Esmenjaud, R. Arenas, Leishmaniasis: a review, F1000Research. 6 (2017) 750. https://doi.org/10.12688/f1000research.11120.1.

[3]   World Health Organization, Leishmaniasis WHO Fact Sheet, 2022.

[4]   S. Mann, K. Frasca, S. Scherrer, A.F. Henao-Martínez, S. Newman, P. Ramanan, J.A. Suarez, A Review of Leishmaniasis: Current Knowledge and Future Directions, Curr. Trop. Med. Reports. 8 (2021) 121–132. https://doi.org/10.1007/s40475-021-00232-7.

[5]   S. Burza, S.L. Croft, M. Boelaert, Leishmaniasis., Lancet. 392 (2018) 951–970. https://doi.org/10.1016/S0140-6736(18)31204-2.

[6]   B.C. Sen Gupta, History of kala-azar in India. 1947., Indian J. Med. Res. 123 (2006) 281–6. http://www.ncbi.nlm.nih.gov/pubmed/16789340.

[7]   T.P.C. Dorlo, M. Balasegaram, J.H. Beijnen, P.J. de Vries, Miltefosine: a review of its pharmacology and therapeutic efficacy in the treatment of leishmaniasis, J. Antimicrob. Chemother. 67 (2012) 2576–2597. https://doi.org/10.1093/jac/dks275.

[8]   D. Mukhopadhyay, J.E. Dalton, P.M. Kaye, M. Chatterjee, Post kala-azar dermal leishmaniasis: an unresolved mystery, Trends Parasitol. 30 (2014) 65–74. https://doi.org/10.1016/j.pt.2013.12.004.

[9]   N. Varma, S. Naseem, Hematologic Changes in Visceral Leishmaniasis/Kala Azar, Indian J. Hematol. Blood Transfus. 26 (2010) 78–82. https://doi.org/10.1007/s12288-010-0027-1.

[10]   CDC - Leishmaniasis - Resources for Health Professionals, (n.d.). https://www.cdc.gov/parasites/leishmaniasis/health_professionals/index.html (accessed May 6, 2022).

[11]   S. Pradhan, R.A. Schwartz, A. Patil, S. Grabbe, M. Goldust, Treatment options for leishmaniasis, Clin. Exp. Dermatol. 47 (2022) 516–521. https://doi.org/10.1111/ced.14919.

[12]   A.K. Haldar, P. Sen, S. Roy, Use of Antimony in the Treatment of Leishmaniasis: Current Status and Future Directions, Mol. Biol. Int. 2011 (2011) 1–23. https://doi.org/10.4061/2011/571242.

[13]   H. Goto, Review of the current treatments for leishmaniases, Res. Rep. Trop. Med. 34 (2012) 69. https://doi.org/10.2147/RRTM.S24764.

[14]   J. Alvar, S. Croft, P. Olliaro, Chemotherapy in the Treatment and Control of Leishmaniasis, in: Adv. Parasitol., 2006: pp. 223–274. https://doi.org/10.1016/S0065-308X(05)61006-8.

[15]   S. Sundar, Drug resistance in Indian visceral leishmaniasis, Trop. Med. Int. Heal. 6 (2001) 849–854. https://doi.org/10.1046/j.1365-3156.2001.00778.x.

[16]   R.T. Kenney, A.A. Gam, M. Ray, S. Sundar, K. Pai, R. Kumar, K. Pathak-Tripathi, Resistance to treatment in Kala-azar: speciation of isolates from northeast India, Am. J. Trop. Med. Hyg. 65 (2001) 193–196. https://doi.org/10.4269/ajtmh.2001.65.193.

[17]   L.F. Grajalew, M.T. Ochoa, R. Palacios, L.E. Osorio, Treatment failure in children in a randomized clinical trial with 10 and 20 days of meglumine antimonate for cutaneous leishmaniasis due to Leishmania viannia species, Am. J. Trop. Med. Hyg. 64 (2001) 187–193. https://doi.org/10.4269/ajtmh.2001.64.187.

[18]   M.P. Oliveira-Neto, A. Schubach, C. Pirmez, M. Mattos, S.C. Goncalves-Costa, A Low-Dose Antimony Treatment in 159 Patients with American Cutaneous Leishmaniasis: Extensive Follow-up Studies (Up to 10 Years), Am. J. Trop. Med. Hyg. 57 (1997) 651–655. https://doi.org/10.4269/ajtmh.1997.57.651.

[19]   A. Meyerhoff, U.S. Food and Drug Administration approval of AmBisome (liposomal amphotericin B) for treatment of visceral leishmaniasis., Clin. Infect. Dis. 28 (1999) 42–8; discussion 49-51. https://doi.org/10.1086/515085.

[20]   Paladin Therapeutics, Impavido Package, Reference ID: 3473184, US Food Drug Adm. (2014).

[21] S. Sundar, T.K. Jha, H. Sindermann, K. Junge, P. Bachmann, J. Berman, Oral miltefosine treatment in children with mild to moderate Indian visceral leishmaniasis, Pediatr. Infect. Dis. J. 22 (2003) 434–438. https://doi.org/10.1097/01.inf.0000066877.72624.cb.

[22] S. SUNDAR, T.K. Jha, C.P. Thakur, J. Engel, H. SINDERMANN, C. FISCHER, K. JUNGE, A. BRYCESON, J. Berman, ORAL MILTEFOSINE FOR INDIAN VISCERAL LEISHMANIASIS, New J. Med. ©. 347 (2002) 897–904. https://doi.org/10.1056/NEJMoa012295.

[23] J. Mbui, J. Olobo, R. Omollo, A. Solomos, A.E. Kip, G. Kirigi, P. Sagaki, R. Kimutai, L. Were, T. Omollo, T.W. Egondi, M. Wasunna, J. Alvar, T.P.C.C. Dorlo, F. Alves, Pharmacokinetics, safety, and efficacy of an allometric miltefosine regimen for the treatment of visceral leishmaniasis in eastern African children: An open-label, phase II clinical trial, Clin. Infect. Dis. 68 (2019) 1530–1538. https://doi.org/10.1093/cid/ciy747.

[24] J. Soto, J. Toledo, P. Gutierrez, R.S. Nicholls, J. Padilla, J. Engel, C. Fischer, A. Voss, J. Berman, Treatment of American Cutaneous Leishmaniasis with Miltefosine, an Oral Agent, Clin. Infect. Dis. 33 (2001) e57–e61. https://doi.org/10.1086/322689.

[25] S.L. Croft, G.H. Coombs, Leishmaniasis– current chemotherapy and recent advances in the search for novel drugs, Trends Parasitol. 19 (2003) 502–508. https://doi.org/10.1016/j.pt.2003.09.008.

[26] V. Wiwanitkit, Interest in paromomycin for the treatment of visceral leishmaniasis (kala-azar), Ther. Clin. Risk Manag. 8 (2012) 323. https://doi.org/10.2147/TCRM.S30139.

[27] NCT03399955, Short Course Regimens for Treatment of PKDL (Sudan), 2018.

[28] C.N. Chunge, J. Owate, H.O. Pamba, L. Donno, Treatment of visceral leishmaniasis in Kenya by aminosidine alone or combined with sodium stibogluconate, Trans. R. Soc. Trop. Med. Hyg. 84 (1990) 221–225. https://doi.org/10.1016/0035-9203(90)90263-E.

[29] R.N. Davidson, J. Seaman, D. Pryce, H.E. Sondorp, A. Moody, A.D.M. Bryceson, R.N. Davidson, J. Seaman, D. Pryce, H.E. Sondorp, A. Moody, A.D.M. Bryceson, R.N. Davidson, J. Seaman, D. Pryce, H.E. Sondorp, A. Moody, A.D.M. Bryceson, Epidemic Visceral Leishmaniasis in Sudan: A Randomized Trial of Aminosidine plus Sodium Stibogluconate versus Sodium Stibogluconate Alone, J. Infect. Dis. 168 (1993) 715–720. https://doi.org/10.1093/infdis/168.3.715.

[30] C.P. Thakur, T.P. Kanyok, A.K. Pandey, G.P. Sinha, A.E. Zaniewski, H.H. Houlihan, P. Olliaro, A prospective randomized, comparative, open-label trial of the safety and efficacy of paromomycin (aminosidine) plus sodium stibogluconate versus sodium stibogluconate alone for the treatment of visceral leishmaniasis, Trans. R. Soc. Trop. Med. Hyg. 94 (2000) 429–431. https://doi.org/10.1016/S0035-9203(00)90130-5.

[31] A.N. Hazarika, Treatment of kala-azar with pentamidine isothionate; a study of 55, Ind. Med. Gaz. 84 (1949).

[32] T.K. Jha, Evaluation of diamidine compound (pentamidine isethionate) in the treatment of resistant cases of kala-azar occurring in North Bihar, India, Trans. R. Soc. Trop. Med. Hyg. 77 (1983) 167–170. https://doi.org/10.1016/0035-9203(83)90058-5.

[33] M. Piccica, F. Lagi, A. Bartoloni, L. Zammarchi, Efficacy and safety of pentamidine isethionate for tegumentary and visceral human leishmaniasis: a systematic review, J. Travel Med. 28 (2021) 1–13. https://doi.org/10.1093/jtm/taab065.

[34] I.C. Roseboom, H. Rosing, J.H. Beijnen, T.P.C. Dorlo, Skin tissue sample collection, sample homogenization, and analyte extraction strategies for liquid chromatographic mass spectrometry quantification of pharmaceutical compounds, J. Pharm. Biomed. Anal. 191 (2020) 113590. https://doi.org/10.1016/j.jpba.2020.113590.

[35] M. Rizk, L. Zou, R. Savic, K. Dooley, Importance of Drug Pharmacokinetics at the Site of Action, Clin. Transl. Sci. 10 (2017) 133–142. https://doi.org/10.1111/cts.12448.

[36] Y.-J. Xue, H. Gao, Q.C. Ji, Z. Lam, X. Fang, Z. Lin, M. Hoffman, D. Schulz-Jander, N. Weng, Bioanalysis of drug in tissue: current status and challenges, Bioanalysis. 4 (2012) 2637–2653. https://doi.org/10.4155/bio.12.252.

[37] I.C. Roseboom, B. Thijssen, H. Rosing, F. Alves, D. Mondal, M.B.M. Teunissen, J.H.

Beijnen, T.P.C. Dorlo, Development and validation of an HPLC-MS/MS method for the quantification of the anti-leishmanial drug miltefosine in human skin tissue, J. Pharm. Biomed. Anal. (2021) 114402. https://doi.org/10.1016/j.jpba.2021.114402.

[38] A.E. Kip, H. Rosing, M.J.X. Hillebrand, M.M. Castro, M.A. Gomez, J.H.M. Schellens, J.H. Beijnen, T.P.C. Dorlo, Quantification of miltefosine in peripheral blood mononuclear cells by high-performance liquid chromatography-tandem mass spectrometry, J. Chromatogr. B. 998–999 (2015) 57–62. https://doi.org/10.1016/j.jchromb.2015.06.017.

[39] DrugBank Online | Database for Drug and Drug Target Info, (n.d.). https://go.drugbank.com/ (accessed May 16, 2022).

[40] selleckchem, Datasheets Antileishmanials, (n.d.). https://www.selleckchem.com/ (accessed June 3, 2022).

[41] B.C. Walker, S.R. Walker, eds., Trends and Changes in Drug Research and Development, in: Trends Chang. Drug Res. Dev., Springer Netherlands, Dordrecht, 1988: p. 109. https://doi.org/10.1007/978-94-009-2659-2.

[42] A. Alak, S. Moy, I. Bekersky, A High-Performance Liquid Chromatographic Assay for the Determination of Amphotericin B Serum Concentrations After the Administration of AmBisome, a Liposomal Amphotericin B Formulation, Ther. Drug Monit. 18 (1996) 604–609. https://doi.org/10.1097/00007691-199610000-00014.

[43] S. Barco, A. Zunino, A. D'Avolio, L. Barbagallo, A. Maffia, G. Tripodi, E. Castagnola, G. Cangemi, A rapid and robust UHPLC-DAD method for the quantification of amphotericin B in human plasma, J. Pharm. Biomed. Anal. 138 (2017) 142–145. https://doi.org/10.1016/j.jpba.2017.01.048.

[44] I. Bekersky, R.M. Fielding, D.E. Dressler, J.W. Lee, D.N. Buell, T.J. Walsh, Pharmacokinetics, Excretion, and Mass Balance of Liposomal Amphotericin B (AmBisome) and Amphotericin B Deoxycholate in Humans, Antimicrob. Agents Chemother. 46 (2002) 828–833. https://doi.org/10.1128/AAC.46.3.828-833.2002.

[45] T. Eldem, N. Arican-Cellat, Determination of amphotericin B in human plasma using solid-phase extraction and high-performance liquid chromatography, J. Pharm. Biomed. Anal. 25 (2001) 53–64. https://doi.org/10.1016/S0731-7085(00)00499-4.

[46] T. Eldem, N. Arican-Cellat, I. Agabeyoglu, M. Akova, E. Kansu, Pharmacokinetics of liposomal amphotericin B in neutropenic cancer patients, Int. J. Pharm. 213 (2001) 153–161. https://doi.org/10.1016/S0378-5173(00)00663-3.

[47] C.L. Golas, C.G. Prober, S.M. MacLeod, S.J. Soldin, Measurement of amphotericin b in serum or plasma by high-performance liquid chromatography, J. Chromatogr. B Biomed. Sci. Appl. 278 (1983) 387–395. https://doi.org/10.1016/S0378-4347(00)84798-2.

[48] C.E. Nath, P.J. Shaw, R. Gunning, A.J. McLachlan, J.W. Earl, Amphotericin B in Children with Malignant Disease: a Comparison of the Toxicities and Pharmacokinetics of Amphotericin B Administered in Dextrose versus Lipid Emulsion, Antimicrob. Agents Chemother. 43 (1999) 1417–1423. https://doi.org/10.1128/AAC.43.6.1417.

[49] T.J. Walsh, V. Yeldandi, M. McEvoy, C. Gonzalez, S. Chanock, A. Freifeld, N.I. Seibel, P.O. Whitcomb, P. Jarosinski, G. Boswell, I. Bekersky, A. Alak, D. Buell, J. Barret, W. Wilson, Safety, Tolerance, and Pharmacokinetics of a Small Unilamellar Liposomal Formulation of Amphotericin B (AmBisome) in Neutropenic Patients, Antimicrob. Agents Chemother. 42 (1998) 2391–2398. https://doi.org/10.1128/AAC.42.9.2391.

[50] R. Lopez-Galera, L. Pou-Clave, C. Pascual-Mostaza, Determination of amphotericin B in human serum by liquid chromatography, J. Chromatogr. B Biomed. Sci. Appl. 674 (1995) 298–300. https://doi.org/10.1016/0378-4347(95)00322-3.

[51] R. Lopez, L. Pou, I. Andres, V. Monforte, A. Roman, C. Pascual, Amphotericin B determination in respiratory secretions by reversed- phase liquid chromatography, J. Chromatogr. A. 812 (1998) 135–139. https://doi.org/10.1016/S0021-9673(98)00205-2.

[52] C. Ganière Monteil, M.-F. Kergueris, P. Iooss, L. Thomas, C. Larousse, Quantitation of amphotericin B in plasma by second-derivative spectrophotometry, J. Pharm. Biomed.

Anal. 17 (1998) 481–485. https://doi.org/10.1016/S0731-7085(97)00215-X.

[53] V. Heinemann, B. Kähny, U. Jehn, D. Mühlbayer, A. Debus, K. Wachholz, D. Bosse, H.J. Kolb, W. Wilmanns, Serum pharmacology of amphotericin B applied in lipid emulsions., Antimicrob. Agents Chemother. 41 (1997) 728–732. https://doi.org/10.1128/AAC.41.4.728.

[54] P. Egger, R. Bellmann, C.J. Wiedermann, Determination of amphotericin B, liposomal amphotericin B, and amphotericin B colloidal dispersion in plasma by high-performance liquid chromatography, J. Chromatogr. B Biomed. Sci. Appl. 760 (2001) 307–313. https://doi.org/10.1016/S0378-4347(01)00292-4.

[55] J.D. Cleary, S.W. Chapman, T.C. Hardin, M.G. Rinaldi, J. Lee Spencer, J. Deng, G.J. Pennick, C.J. Lobb, Amphotericin B Enzyme-Linked Immunoassay for Clinical Use: Comparison with Bioassay and HPLC, Ann. Pharmacother. 31 (1997) 39–44. https://doi.org/10.1177/106002809703100105.

[56] T.K.C. Ng, R.C.Y. Chan, F.A.B. Adeyemi-Doro, S.W. Cheung, A.F.B. Cheng, Rapid high performance liquid chromatographic assay for antifungal agents in human sera, J. Antimicrob. Chemother. 37 (1996) 465–472. https://doi.org/10.1093/jac/37.3.465.

[57] A. Ayestarán, R.M. López, J.B. Montoro, A. Estíbalez, L. Pou, A. Julià, A. López, B. Pascual, Pharmacokinetics of conventional formulation versus fat emulsion formulation of amphotericin B in a group of patients with neutropenia., Antimicrob. Agents Chemother. 40 (1996) 609–612. https://doi.org/10.1128/AAC.40.3.609.

[58] H. Liu, H. Davoudi, T. Last, Determination of Amphotericin B in cerebrospinal fluid by solid-phase extraction and liquid chromatography, J. Pharm. Biomed. Anal. 13 (1995) 1395–1400. https://doi.org/10.1016/0731-7085(95)01566-4.

[59] J.W. Hülsewede, H. Dermoumi, Comparison of high-performance liquid chromatography and bioassay of amphotericin B in serum, Mycoses. 37 (1994) 17–21. https://doi.org/10.1111/j.1439-0507.1994.tb00279.x.

[60] H. Hosotsubo, K. Hosotsubo, C. Brassinne, C. Laduron, A. Coune, J.P. Sculier, C. Hollaert, N. Collette, F. Meunier, High-performance liquid chromatographic determination of amphotericin B in human serum, J. Chromatogr. B Biomed. Sci. Appl. 7 (1987) 975–979. https://doi.org/10.1016/0378-4347(87)80307-9.

[61] N. Collette, P. Van der Auwera, F. Meunier, C. Lambert, J.P. Sculier, A. Coune, Tissue distribution and bioactivity of amphotericin B administered in liposomes to cancer patients, J. Antimicrob. Chemother. 27 (1991) 535–548. https://doi.org/10.1093/jac/27.4.535.

[62] J.E. Baley, C. Meyers, R.M. Kliegman, M.R. Jacobs, J.L. Blumer, Pharmacokinetics, outcome of treatment, and toxic effects of amphotericin B and 5-fluorocytosine in neonates, J. Pediatr. 116 (1990) 791–797. https://doi.org/10.1016/S0022-3476(05)82674-5.

[63] J.M. Benson, M.C. Nahata, Pharmacokinetics of amphotericin B in children., Antimicrob. Agents Chemother. 33 (1989) 1989–1993. https://doi.org/10.1128/AAC.33.11.1989.

[64] G.G. Chabot, R. Pazdur, F.A. Valeriote, L.H. Baker, Pharmacokinetics and Toxicity of Continuous Infusion Amphotericin B in Cancer Patients, J. Pharm. Sci. 78 (1989) 307–310. https://doi.org/10.1002/jps.2600780409.

[65] R. Welte, S. Eschertzhuber, S. Weiler, S. Leitner-Rupprich, M. Aigner, C. Lass-Flörl, E. Stienecke, R. Bellmann-Weiler, M. Joannidis, R. Bellmann, Biliary amphotericin B pharmacokinetics and pharmacodynamics in critically ill liver transplant recipients receiving treatment with amphotericin B lipid formulations, Int. J. Antimicrob. Agents. 46 (2015) 325–331. https://doi.org/10.1016/j.ijantimicag.2015.04.009.

[66] N. Collette, P. van der Auwera, A.P. Lopez, C. Heymans, F. Meunier, Tissue concentrations and bioactivity of amphotericin B in cancer patients treated with amphotericin B-deoxycholate., Antimicrob. Agents Chemother. 33 (1989) 362–368. https://doi.org/10.1128/AAC.33.3.362.

[67] H. Hosotsubo, K. Hosotsubo, Improved high-performance liquid chromatographic determination of Amphotericin B in human serum and plasma, J. Pharm. Biomed. Anal. 7 (1989) 975–979. https://doi.org/10.1016/0731-7085(89)80022-6.

[68] G. Koren, A. Lau, J. Klein, C. Golas, M. Bologa-Campeanu, S. Soldin, S.M. MacLeod, C. Prober, Pharmacokinetics and adverse effects of amphotericin B in infants and children, J. Pediatr. 113 (1988) 559–563. https://doi.org/10.1016/S0022-3476(88)80653-X.

[69] H. Hosotsubo, J. Takezawa, N. Taenaka, K. Hosotsubo, I. Yoshiya, Rapid determination of amphotericin B levels in serum by high-performance liquid chromatography without interference by bilirubin., Antimicrob. Agents Chemother. 32 (1988) 1103–1105. https://doi.org/10.1128/AAC.32.7.1103.

[70] Z.K. Shihabi, B.L. Wasilauskas, J.E. Peacock, Serum Amphotericin-B Assay by Scanning Spectrophotometer, Ther. Drug Monit. 10 (1988) 486–489. https://doi.org/10.1097/00007691-198804000-00020.

[71] K. Kobayashi, T. Sakoguchi, K. Fujiwara, K. Taniuchi, K. Kohri, A. Matsuoka, High-performance liquid chromatographic determination of amphotericin B in human urine, J. Chromatogr. B Biomed. Sci. Appl. 417 (1987) 439–446. https://doi.org/10.1016/0378-4347(87)80142-1.

[72] F. Persat, M.-F. Monier, M.-A. Piens, M. Mojon, Determination of Amphotericin B in Human Serum by High-Performance Liquid Chromatography*, Mycoses. 28 (2009) 501–506. https://doi.org/10.1111/j.1439-0507.1985.tb02077.x.

[73] M. Leclercq, M. Fouillit, G. Panteix, R. Guinet, Reproducible measurement of amphotericin B in serum by high-performance liquid chromatography in alkaline buffer, J. Chromatogr. B Biomed. Sci. Appl. 337 (1985) 423–428. https://doi.org/10.1016/0378-4347(85)80058-X.

[74] P.R. Bach, Quantitative extraction of amphotericin B from serum and its determination by high-pressure liquid chromatography., Antimicrob. Agents Chemother. 26 (1984) 314–317. https://doi.org/10.1128/AAC.26.3.314.

[75] M. Ching, K. Raymond, R. Bury, M. Mashford, D. Morgan, Absorption of orally administered amphotericin B lozenges., Br. J. Clin. Pharmacol. 16 (1983) 106–108. https://doi.org/10.1111/j.1365-2125.1983.tb02152.x.

[76] W.W. Hope, J. Goodwin, T.W. Felton, M. Ellis, D.A. Stevens, Population Pharmacokinetics of Conventional and Intermittent Dosing of Liposomal Amphotericin B in Adults: a First Critical Step for Rational Design of Innovative Regimens, Antimicrob. Agents Chemother. 56 (2012) 5303–5308. https://doi.org/10.1128/AAC.00933-12.

[77] J.W. Mayhew, C. Fiore, T. Murray, M. Barza, An internally-standardized assay for amphotericin B in tissues and plasma, J. Chromatogr. B Biomed. Sci. Appl. 274 (1983) 271–279. https://doi.org/10.1016/S0378-4347(00)84430-8.

[78] I. Nilsson-Ehle, T.T. Yoshikawa, J.E. Edwards, M.C. Schotz, L.B. Guze, Quantitation of Amphotericin B with Use of High-Pressure Liquid Chromatography, J. Infect. Dis. 135 (1977) 414–422. https://doi.org/10.1093/infdis/135.3.414.

[79] S. Husain, B. Capitano, T. Corcoran, S.M. Studer, M. Crespo, B. Johnson, J.M. Pilewski, K. Shutt, D.L. Pakstis, S. Zhang, M.E. Carey, D.L. Paterson, K.R. McCurry, R. Venkataramanan, Intrapulmonary Disposition of Amphotericin B After Aerosolized Delivery of Amphotericin B Lipid Complex (Abelcet; ABLC) in Lung Transplant Recipients, Transplantation. 90 (2010) 1215–1219. https://doi.org/10.1097/TP.0b013e3181f995ea.

[80] A. Watanabe, K. Matsumoto, H. Igari, M. Uesato, S. Yoshida, Y. Nakamura, K. Morita, K. Shibuya, H. Matsubara, I. Yoshino, K. Kamei, Comparison between concentrations of amphotericin B in infected lung lesion and in uninfected lung tissue in a patient treated with liposomal amphotericin B (AmBisome), Int. J. Infect. Dis. 14 (2010) e220–e223. https://doi.org/10.1016/j.ijid.2009.07.020.

[81] Y. Hong, P.J. Shaw, B.N. Tattam, C.E. Nath, J.W. Earl, K.R. Stephen, A.J. McLachlan, Plasma protein distribution and its impact on pharmacokinetics of liposomal amphotericin B in paediatric patients with malignant diseases, Eur. J. Clin. Pharmacol. 63 (2007) 165–172. https://doi.org/10.1007/s00228-006-0240-x.

[82] H. Vogelsinger, Amphotericin B tissue distribution in autopsy material after treatment with liposomal amphotericin B and amphotericin B colloidal dispersion, J. Antimicrob.

Chemother. 57 (2006) 1153–1160. https://doi.org/10.1093/jac/dkl141.

[83] G. Demartini, C. Lequaglie, P.P. Brega massone, F. Scaglione, F. Fraschini, Penetration of Amphotericin B in Human Lung Tissue after Single Liposomal Amphotericin B (AmBisome) Infusion, J. Chemother. 17 (2005) 82–85. https://doi.org/10.1179/joc.2005.17.1.82.

[84] C. Schuster, M. Paal, J. Lindner, M. Zoller, U. Liebchen, C. Scharf, M. Vogeser, Isotope dilution LC-orbitrap-HRMS with automated sample preparation for the simultaneous quantification of 11 antimycotics in human serum, J. Pharm. Biomed. Anal. 166 (2019) 398–405. https://doi.org/10.1016/j.jpba.2019.01.038.

[85] L. Qu, J. Qian, P. Ma, Z. Yin, Utilizing online-dual-SPE-LC with HRMS for the simultaneous quantification of amphotericin B, fluconazole, and fluorocytosine in human plasma and cerebrospinal fluid, Talanta. 165 (2017) 449–457. https://doi.org/10.1016/j.talanta.2016.12.052.

[86] B.T. Al-Quadeib, M.A. Radwan, L. Siller, E. Mutch, B. Horrocks, M. Wright, A. Alshaer, Therapeutic monitoring of amphotericin B in Saudi ICU patients using UPLC MS/MS assay, Biomed. Chromatogr. 28 (2014) 1652–1659. https://doi.org/10.1002/bmc.3198.

[87] W. Qin, H. Tao, Y. Chen, Z. Chen, N. Wu, Sensitive, Accurate and Simple Liquid Chromatography-Tandem Mass Spectrometric Method for the Quantitation of Amphotericin B in Human or Minipig Plasma, J. Chromatogr. Sci. 50 (2012) 636–643. https://doi.org/10.1093/chromsci/bms049.

[88] J.W. Lee, M.E. Petersen, P. Lin, D. Dressler, I. Bekersky, Quantitation of Free and Total Amphotericin B in Human Biologic Matrices by a Liquid Chromatography Tandem Mass Spectrometric Method, Ther. Drug Monit. 23 (2001) 268–276. https://doi.org/10.1097/00007691-200106000-00015.

[89] N.M. Deshpande, M.G. Gangrade, M.B. Kekare, V. V. Vaidya, Determination of free and liposomal Amphotericin B in human plasma by liquid chromatography–mass spectroscopy with solid phase extraction and protein precipitation techniques, J. Chromatogr. B. 878 (2010) 315–326. https://doi.org/10.1016/j.jchromb.2009.11.036.

[90] I.C. Roseboom, B. Thijssen, H. Rosing, F. Alves, S. Sundar, J.H. Beijnen, T.P.C. Dorlo, Development and validation of a high-performance liquid chromatography tandem mass spectrometry method for the quantification of the antiparasitic and antifungal drug amphotericin B in human skin tissue, J. Chromatogr. B. 1206 (2022) 123354. https://doi.org/10.1016/j.jchromb.2022.123354.

[91] R.J. Hamill, Amphotericin B Formulations: A Comparative Review of Efficacy and Toxicity, Drugs. 73 (2013) 919–934. https://doi.org/10.1007/s40265-013-0069-4.

[92] I. Bekersky, R.M. Fielding, D.E. Dressler, J.W. Lee, D.N. Buell, T.J. Walsh, Plasma Protein Binding of Amphotericin B and Pharmacokinetics of Bound versus Unbound Amphotericin B after Administration of Intravenous Liposomal Amphotericin B (AmBisome) and Amphotericin B Deoxycholate, Antimicrob. Agents Chemother. 46 (2002) 834–840. https://doi.org/10.1128/AAC.46.3.834-840.2002.

[93] A.R. Johnson, E.E. Carlson, Collision-Induced Dissociation Mass Spectrometry: A Powerful Tool for Natural Product Structure Elucidation, Anal. Chem. 87 (2015) 10668–10678. https://doi.org/10.1021/acs.analchem.5b01543.

[94] L.F. Pippa, M.P. Marques, A.C.T. da Silva, F.C. Vilar, T.M. de Haes, B.A.L. da Fonseca, R. Martinez, E.B. Coelho, L. Wichert-Ana, V.L. Lanchote, Sensitive LC-MS/MS Methods for Amphotericin B Analysis in Cerebrospinal Fluid, Plasma, Plasma Ultrafiltrate, and Urine: Application to Clinical Pharmacokinetics, Front. Chem. 9 (2021) 1–14. https://doi.org/10.3389/fchem.2021.782131.

[95] A.E. Kip, S. Blesson, F. Alves, M. Wasunna, R. Kimutai, P. Menza, B. Mengesha, J.H. Beijnen, A. Hailu, E. Diro, T.P.C.C. Dorlo, Low antileishmanial drug exposure in HIV-positive visceral leishmaniasis patients on antiretrovirals: An Ethiopian cohort study, J. Antimicrob. Chemother. 76 (2021) 1258–1268. https://doi.org/10.1093/jac/dkab013.

[96] M. Polikandritou Lambros, S. Ali Abbas, D.W.A. Bourne, New high-performance liquid chromatographic method for amphotericin B analysis using an internal standard, J. Chromatogr. B Biomed. Sci. Appl. 685 (1996) 135–140. https://doi.org/10.1016/0378-4347(96)00162-4.

[97] G.G. Granich, G.S. Kobayashi, D.J. Krogstad, Sensitive high-pressure liquid chromatographic assay for amphotericin B which incorporates an internal standard., Antimicrob. Agents Chemother. 29 (1986) 584–588. https://doi.org/10.1128/AAC.29.4.584.

[98] I. Nilsson-Ehle, High-pressure liquid chromatography as a tool for determination of antibiotics in biological fluids., Acta Pathol. Microbiol. Scand. Suppl. (1977) 61–6. http://www.ncbi.nlm.nih.gov/pubmed/269648.

[99] German Drug Registration Authorities Impavido 10/50 mg Kapseln— Fachinformation, (2008). https://www.pharmnet-bund.de/static/de/index.html (accessed June 27, 2022).

[100] A. Lemke, O. Kayser, HPLC detection of miltefosine using an evaporative light scattering detector, Pharmazie. 61 (2006) 406–8. http://www.ncbi.nlm.nih.gov/pubmed/16724535.

[101] S. Jaiswal, A. Sharma, M. Shukla, J. Lal, LC-coupled ESI MS for quantification of miltefosine in human and hamster plasma, Bioanalysis. 8 (2016) 533–545. https://doi.org/10.4155/bio.16.7.

[102] T.P.C. Dorlo, M.J.X. Hillebrand, H. Rosing, T.A. Eggelte, P.J. de Vries, J.H. Beijnen, Development and validation of a quantitative assay for the measurement of miltefosine in human plasma by liquid chromatography–tandem mass spectrometry, J. Chromatogr. B. 865 (2008) 55–62. https://doi.org/10.1016/j.jchromb.2008.02.005.

[103] A.E. Kip, H. Rosing, M.J.X. Hillebrand, S. Blesson, B. Mengesha, E. Diro, A. Hailu, J.H.M. Schellens, J.H. Beijnen, T.P.C. Dorlo, Validation and Clinical Evaluation of a Novel Method To Measure Miltefosine in Leishmaniasis Patients Using Dried Blood Spot Sample Collection, Antimicrob. Agents Chemother. 60 (2016) 2081–2089. https://doi.org/10.1128/AAC.02976-15.

[104] A.E. Kip, K.C. Kiers, H. Rosing, J.H.M. Schellens, J.H. Beijnen, T.P.C. Dorlo, Volumetric absorptive microsampling (VAMS) as an alternative to conventional dried blood spots in the quantification of miltefosine in dried blood samples, J. Pharm. Biomed. Anal. 135 (2017) 160–166. https://doi.org/10.1016/j.jpba.2016.12.012.

[105] S.L. Roy, J.T. Atkins, R. Gennuso, D. Kofos, R.R. Sriram, T.P.C. Dorlo, T. Hayes, Y. Qvarnstrom, Z. Kucerova, B.J. Guglielmo, G.S. Visvesvara, Assessment of blood–brain barrier penetration of miltefosine used to treat a fatal case of granulomatous amebic encephalitis possibly caused by an unusual Balamuthia mandrillaris strain, Parasitol. Res. 114 (2015) 4431–4439. https://doi.org/10.1007/s00436-015-4684-8.

[106] J. Kötting, N.W. Marschner, W. Neumüller, C. Unger, H. Eibl, Hexadecylphosphocholine and octadecyl-methyl-glycero-3-phosphocholine: a comparison of hemolytic activity, serum binding and tissue distribution., Prog. Exp. Tumor Res. 34 (1992) 131–42. https://doi.org/10.1159/000420838.

[107] J. Berman, Miltefosine to treat leishmaniasis, Expert Opin. Pharmacother. 6 (2005) 1381–1388. https://doi.org/10.1517/14656566.6.8.1381.

[108] M. Del Mar Castro, M.A. Gomez, A.E. Kip, A. Cossio, E. Ortiz, A. Navas, T.P.C. Dorlo, N.G. Saravia, Pharmacokinetics of miltefosine in children and adults with Cutaneous leishmaniasis, Antimicrob. Agents Chemother. 61 (2017) 1–11. https://doi.org/10.1128/AAC.02198-16.

[109] T.P.C. Dorlo, P.P.A.M. Van Thiel, A.D.R. Huitema, R.J. Keizer, H.J.C. De Vries, J.H. Beijnen, P.J. De Vries, Pharmacokinetics of miltefosine in old world cutaneous leishmaniasis patients, Antimicrob. Agents Chemother. 52 (2008) 2855–2860. https://doi.org/10.1128/AAC.00014-08.

[110] T.P.C. Dorlo, A.D.R. Huitema, J.H. Beijnen, P.J. De Vries, Optimal dosing of miltefosine in children and adults with visceral leishmaniasis, Antimicrob. Agents Chemother. 56 (2012) 3864–3872. https://doi.org/10.1128/AAC.00292-12.

[111] T.P.C. Dorlo, S. Rijal, B. Ostyn, P.J. De Vries, R. Singh, N. Bhattarai, S. Uranw, J.C. Dujardin, M. Boelaert, J.H. Beijnen, A.D.R. Huitema, Failure of miltefosine in visceral leishmaniasis is

associated with low drug exposure, J. Infect. Dis. 210 (2014) 146–153. https://doi.org/10.1093/infdis/jiu039.

[112] S. Palic, A.E. Kip, J.H. Beijnen, J. Mbui, A. Musa, A. Solomos, M. Wasunna, J. Olobo, F. Alves, T.P.C. Dorlo, Characterizing the non-linear pharmacokinetics of miltefosine in paediatric visceral leishmaniasis patients from Eastern Africa, J. Antimicrob. Chemother. 75 (2020) 3260–3268. https://doi.org/10.1093/jac/dkaa314.

[113] A.S. of H.-S. Pharmacists, Paromomycin Monograph for Professionals - Drugs.com, (n.d.). https://www.drugs.com/monograph/paromomycin.html (accessed February 21, 2022).

[114] W.M.M. Kirby, J.T. Clarke, R.D. Libke, C. Regamey, Clinical Pharmacology of Amikacin and Kanamycin, J. Infect. Dis. 134 (1976) S312–S315. https://doi.org/10.1093/infdis/135.Supplement_2.S312.

[115] A.E. Kip, J.H.M. Schellens, J.H. Beijnen, T.P.C. Dorlo, Clinical Pharmacokinetics of Systemically Administered Antileishmanial Drugs, Clin. Pharmacokinet. 57 (2018) 151–176. https://doi.org/10.1007/s40262-017-0570-0.

[116] W. Khan, N. Kumar, Characterization, thermal stability studies, and analytical method development of Paromomycin for formulation development, Drug Test. Anal. 3 (2011) 363–372. https://doi.org/10.1002/dta.229.

[117] J. Lu, M. Cwik, T. Kanyok, Determination of paromomycin in human plasma and urine by reversed-phase high-performance liquid chromatography using 2,4-dinitrofluorobenzene derivatization, J. Chromatogr. B Biomed. Sci. Appl. 695 (1997) 329–335. https://doi.org/10.1016/S0378-4347(97)00192-8.

[118] T.P. Kanyok, A.D. Killian, K.A. Rodvold, L.H. Danziger, Pharmacokinetics of intramuscularly administered aminosidine in healthy subjects, Antimicrob. Agents Chemother. 41 (1997) 982–986. https://doi.org/10.1128/aac.41.5.982.

[119] R. Oertel, V. Neumeister, W. Kirch, Hydrophilic interaction chromatography combined with tandem-mass spectrometry to determine six aminoglycosides in serum, J. Chromatogr. A. 1058 (2004) 197–201. https://doi.org/10.1016/j.chroma.2004.08.158.

[120] I.C. Roseboom, B. Thijssen, H. Rosing, J. Mbui, J.H. Beijnen, T.P.C. Dorlo, Highly sensitive UPLC-MS/MS method for the quantification of paromomycin in human plasma, J. Pharm. Biomed. Anal. 185 (2020). https://doi.org/10.1016/j.jpba.2020.113245.

[121] E. Stokvis, H. Rosing, J.H. Beijnen, Stable isotopically labeled internal standards in quantitative bioanalysis using liquid chromatography/mass spectrometry: necessity or not?, Rapid Commun. Mass Spectrom. 19 (2005) 401–407. https://doi.org/10.1002/rcm.1790.

[122] F. Farouk, H.M.E. Azzazy, W.M.A. Niessen, Challenges in the determination of aminoglycoside antibiotics, a review, Anal. Chim. Acta. 890 (2015) 21–43. https://doi.org/10.1016/j.aca.2015.06.038.

[123] S. Sundar, T.K. Jha, C.P. Thakur, P.K. Sinha, S.K. Bhattacharya, Injectable Paromomycin for Visceral Leishmaniasis in India, N. Engl. J. Med. 356 (2007) 2571–2581. https://doi.org/10.1056/NEJMoa066536.

[124] A.M. Musa, B. Younis, A. Fadlalla, C. Royce, M. Balasegaram, M. Wasunna, A. Hailu, T. Edwards, R. Omollo, M. Mudawi, G. Kokwaro, A. El-Hassan, E. Khalil, Paromomycin for the Treatment of Visceral Leishmaniasis in Sudan: A Randomized, Open-Label, Dose-Finding Study, PLoS Negl. Trop. Dis. 4 (2010) e855. https://doi.org/10.1371/journal.pntd.0000855.

[125] L. Verrest, M. Wasunna, G. Kokwaro, R. Aman, A.M. Musa, E.A.G. Khalil, M. Mudawi, B.M. Younis, A. Hailu, Z. Hurissa, W. Hailu, S. Tesfaye, E. Makonnen, Y. Mekonnen, A.D.R. Huitema, J.H. Beijnen, S.A. Kshirsagar, J. Chakravarty, M. Rai, S. Sundar, F. Alves, T.P.C. Dorlo, Geographical Variability in Paromomycin Pharmacokinetics Does Not Explain Efficacy Differences between Eastern African and Indian Visceral Leishmaniasis Patients, Clin. Pharmacokinet. 60 (2021) 1463–1473. https://doi.org/10.1007/s40262-021-01036-8.

[126] A. Hailu, A. Musa, M. Wasunna, M. Balasegaram, S. Yifru, G. Mengistu, Z. Hurissa, W. Hailu, T. Weldegebreal, S. Tesfaye, E. Makonnen, E. Khalil, O. Ahmed, A. Fadlalla, A. El-Hassan, M. Raheem, M. Mueller, Y. Koummuki, J. Rashid, J. Mbui, G. Mucee, S. Njoroge, V.

Manduku, A. Musibi, G. Mutuma, F. Kirui, H. Lodenyo, D. Mutea, G. Kirigi, T. Edwards, P. Smith, L. Muthami, C. Royce, S. Ellis, M. Alobo, R. Omollo, J. Kesusu, R. Owiti, J. Kinuthia, Geographical Variation in the Response of Visceral Leishmaniasis to Paromomycin in East Africa: A Multicentre, Open-Label, Randomized Trial, PLoS Negl. Trop. Dis. 4 (2010) e709. https://doi.org/10.1371/journal.pntd.0000709.

[127] Pentamidine isethionate, Cas No. 140-64-7. (2022). www.chemicalbook.com (accessed June 2, 2022).

[128] Pentamidine Product Information Cayman Chemical, Item No. 20679. (2022). www.caymanchemical.com.

[129] M.N.C. Soeiro, K. Werbovetz, D.W. Boykin, W.D. Wilson, M.Z. Wang, A. Hemphill, Novel amidines and analogues as promising agents against intracellular parasites: a systematic review., Parasitology. 140 (2013) 929–51. https://doi.org/10.1017/S0031182013000292.

[130] J.-R. Christen, E. Bourreau, M. Demar, E. Lightburn, P. Couppié, M. Ginouvès, G. Prévot, J.-P. Gangneux, H. Savini, F. de Laval, V. Pommier de Santi, S. Briolant, Use of the intramuscular route to administer pentamidine isethionate in Leishmania guyanensis cutaneous leishmaniasis increases the risk of treatment failure, Travel Med. Infect. Dis. 24 (2018) 31–36. https://doi.org/10.1016/j.tmaid.2018.02.010.

[131] X.-Q. Li, A. Björkman, T.B. Andersson, L.L. Gustafsson, C.M. Masimirembwa, Identification of human cytochrome P 450 s that metabolise anti-parasitic drugs and predictions of in vivo drug hepatic clearance from in vitro data, Eur. J. Clin. Pharmacol. 59 (2003) 429–442. https://doi.org/10.1007/s00228-003-0636-9.

[132] Ö. Ericsson, M. Rais, Determination of Pentamidine in Whole Blood, Plasma, and Urine by High-Performance Liquid Chromatography, Ther. Drug Monit. 12 (1990) 362–365. https://doi.org/10.1097/00007691-199007000-00011.

[133] J.E. Conte, R.A. Upton, R.T. Phelps, C.B. Wofsy, E. Zurlinden, E.T. Lin, Use of a Specific and Sensitive Assay to Determine Pentamidine Pharmacokinetics in Patients with AIDS, J. Infect. Dis. 154 (1986) 923–929. https://doi.org/10.1093/infdis/154.6.923.

[134] M. Sands, M.A. Kron, R.B. Brown, Pentamidine: A Review, Clin. Infect. Dis. 7 (1985) 625–6344. https://doi.org/10.1093/clinids/7.5.625.

[135] B. Vinet, R. Comtois, A. Gervais, C. Lemieux, Clinical usefulness of high-pressure liquid chromatographic determination of serum pentamidine in AIDS patients, Clin. Biochem. 25 (1992) 93–97. https://doi.org/10.1016/0009-9120(92)80050-Q.

[136] G.C. Smaldone, V. Colleen, M. Lorraine, Urine Pentamidine as an Indicator of Lung Pentamidine in Patients Receiving Aerosol Therapy, Chest. 100 (1991) 1219–1223. https://doi.org/10.1378/chest.100.5.1219.

[137] M.J. Garzón, B. Rabanal, A.I. Ortiz, A. Negro, Determination of pentamidine in serum and urine by micellar electrokinetic chromatography, J. Chromatogr. B Biomed. Sci. Appl. 688 (1997) 135–142. https://doi.org/10.1016/S0378-4347(97)88065-6.

[138] S.J. Fortunato, R.E. Bawdon, Determination of pentamidine transfer in the in vitro perfused human cotyledon with high-performance liquid chromatography, Am. J. Obstet. Gynecol. 160 (1989) 759–761. https://doi.org/10.1016/S0002-9378(89)80076-6.

[139] L.J. Dusci, L.P. Hackett, A.M. Forbes, K.F. Ilett, High-Performance Liquid Chromatographic Method for Measurement of Pentamidine in Plasma and Its Application in an Immunosuppressed Patient with Renal Dysfunction, Ther. Drug Monit. 9 (1987) 422–425. https://doi.org/10.1097/00007691-198712000-00010.

[140] C.M. Dickinson, T.R. Navin, F.C. Churchill, High-performance liquid chromatographic method for quantitation of pentamidine in blood serum, J. Chromatogr. B Biomed. Sci. Appl. 345 (1985) 91–97. https://doi.org/10.1016/0378-4347(85)80138-9.

[141] M. Shen, E.S. Orwoll, J.E. Conte, M.J. Prince, Pentamidine-induced pancreatic beta-cell dysfunction, Am. J. Med. 86 (1989) 726–728. https://doi.org/10.1016/0002-9343(89)90457-9.

[142] N. Miekeley, S. Mortari, A. Schubach, Monitoring of total antimony and its species by ICP-MS and on-line ion chromatography in biological samples from patients treated for

leishmaniasis, Anal. Bioanal. Chem. 372 (2002) 495–502. https://doi.org/10.1007/s00216-001-1213-7.

[143] F. Frézard, C. Demicheli, R. Ribeiro, Pentavalent Antimonials: New Perspectives for Old Drugs, Molecules. 14 (2009) 2317–2336. https://doi.org/10.3390/molecules14072317.

[144] P. Baiocco, G. Colotti, S. Franceschini, A. Ilari, Molecular Basis of Antimony Treatment in Leishmaniasis, J. Med. Chem. 52 (2009) 2603–2612. https://doi.org/10.1021/jm900185q.

[145] J. Kresimon, U. Grüter, A. Hirner, HG/LT–GC/ICP–MS coupling for identification of metal(loid) species in human urine after fish consumption, Fresenius. J. Anal. Chem. 371 (2001) 586–590. https://doi.org/10.1007/s002160101087.

[146] G.F. Clemente, G. Ingrao, G.P. Santaroni, The concentration of some trace elements in human milk from Italy, Sci. Total Environ. 24 (1982) 255–265. https://doi.org/10.1016/0048-9697(82)90004-3.

[147] U. Demmel, A. Höck, K. Kasperek, L.E. Feinendegen, Trace element concentration in the human pineal body activation analysis of cobalt, iron, rubidium, selenium, zinc, antimony and cesium, Sci. Total Environ. 24 (1982) 135–146. https://doi.org/10.1016/0048-9697(82)90106-1.

[148] A. Cruz, P.M. Rainey, B.L. Herwaldt, G. Stagni, R. Palacios, R. Trujillo, N.G. Saravia, Pharmacokinetics of Antimony in Children Treated for Leishmaniasis with Meglumine Antimoniate, J. Infect. Dis. 195 (2007) 602–608. https://doi.org/10.1086/510860.

[149] I.Y. Zaghloul, M.A. Radwan, M.H. Al Jaser, R. Al Issa, Clinical Efficacy and Pharmacokinetics of Antimony in Cutaneous Leishmaniasis Patients Treated With Sodium Stibogluconate, J. Clin. Pharmacol. 50 (2010) 1230–1237. https://doi.org/10.1177/0091270009347674.

[150] J.D. Chulay, L. Fleckenstein, D.H. Smith, Pharmacokinetics of antimony during treatment of visceral leishmaniasis with sodium stibogluconate or meglumine antimoniate, Trans. R. Soc. Trop. Med. Hyg. 82 (1988) 69–72. https://doi.org/10.1016/0035-9203(88)90267-2.

[151] T.D.B. Lyon, M. Patriarca, A.G. Howatson, P.J. Fleming, P.S. Blair, G.S. Fell, Age dependence of potentially toxic elements (Sb, Cd, Pb, Ag) in human liver tissue from paediatric subjects, J. Environ. Monit. 4 (2002) 1034–1039. https://doi.org/10.1039/b205972j.

[152] W. Feng, X. Cui, B. Liu, C. Liu, Y. Xiao, W. Lu, H. Guo, M. He, X. Zhang, J. Yuan, W. Chen, T. Wu, Association of Urinary Metal Profiles with Altered Glucose Levels and Diabetes Risk: A Population-Based Study in China, PLoS One. 10 (2015) e0123742. https://doi.org/10.1371/journal.pone.0123742.

[153] P. Heitland, H.D. Köster, Biomonitoring of 30 trace elements in urine of children and adults by ICP-MS, Clin. Chim. Acta. 365 (2006) 310–318. https://doi.org/10.1016/j.cca.2005.09.013.

[154] M. Tonelli, N. Wiebe, A. Bello, C.J. Field, J.S. Gill, B.R. Hemmelgarn, D.T. Holmes, K. Jindal, S.W. Klarenbach, B.J. Manns, R. Thadhani, D. Kinniburgh, Concentrations of Trace Elements in Hemodialysis Patients: A Prospective Cohort Study, Am. J. Kidney Dis. 70 (2017) 696–704. https://doi.org/10.1053/j.ajkd.2017.06.029.

[155] A. Bazzi, J.O. Nriagu, M.C. Inhorn, A.M. Linder, Determination of antimony in human blood with inductively coupled plasma-mass spectrometry, J. Environ. Monit. 7 (2005) 1251. https://doi.org/10.1039/b510088g.

[156] M. Patriarca, T.D.B. Lyon, G.S. Fell, H.T. Delves, A.G. Howatson, Determination of low concentrations of potentially toxic elements in human liver from newborns and infants, Analyst. 124 (1999) 1337–1343. https://doi.org/10.1039/a904251b.

[157] M.K. Silver, A.L. Arain, J. Shao, M. Chen, Y. Xia, B. Lozoff, J.D. Meeker, Distribution and predictors of 20 toxic and essential metals in the umbilical cord blood of Chinese newborns, Chemosphere. 210 (2018) 1167–1175. https://doi.org/10.1016/j.chemosphere.2018.07.124.

[158] M. Iwai-Shimada, S. Kameo, K. Nakai, K. Yaginuma-Sakurai, N. Tatsuta, N. Kurokawa, S.F. Nakayama, H. Satoh, Exposure profile of mercury, lead, cadmium, arsenic, antimony, copper, selenium and zinc in maternal blood, cord blood and placenta: the Tohoku Study of Child Development in Japan, Environ. Health Prev. Med. 24 (2019) 35. https://doi.org/10.1186/s12199-019-0783-y.

[159] G. Zheng, H. Zhong, Z. Guo, Z. Wu, H. Zhang, C. Wang, Y. Zhou, Z. Zuo, Levels of Heavy Metals and Trace Elements in Umbilical Cord Blood and the Risk of Adverse Pregnancy Outcomes: a Population-Based Study, Biol. Trace Elem. Res. 160 (2014) 437–444. https://doi.org/10.1007/s12011-014-0057-x.

[160] R. Cabrera-Rodríguez, O.P. Luzardo, A. González-Antuña, L.D. Boada, M. Almeida-González, M. Camacho, M. Zumbado, A.C. Acosta-Dacal, C. Rial-Berriel, L.A. Henríquez-Hernández, Occurrence of 44 elements in human cord blood and their association with growth indicators in newborns, Environ. Int. 116 (2018) 43–51. https://doi.org/10.1016/j.envint.2018.03.048.

[161] M. Maynar, F. Llerena, F.J. Grijota, J. Alves, M.C. Robles, I. Bartolomé, D. Muñoz, Serum concentration of several trace metals and physical training, J. Int. Soc. Sports Nutr. 14 (2017) 1–5. https://doi.org/10.1186/s12970-017-0178-7.

[162] D.J. Garay-Baquero, D.E. Rebellón-Sánchez, M.D. Prieto, L. Giraldo-Parra, A. Navas, S. Atkinson, S. McDougall, M.A. Gómez, Inductively coupled plasma mass spectrometry method for plasma and intracellular antimony quantification applied to pharmacokinetics of meglumine antimoniate, Bioanalysis. 13 (2021) bio-2021-0013. https://doi.org/10.4155/bio-2021-0013.

[163] D.B. da J. Neves, E.D. Caldas, R.N.R. Sampaio, Antimony in plasma and skin of patients with cutaneous leishmaniasis--relationship with side effects after treatment with meglumine antimoniate., Trop. Med. Int. Health. 14 (2009) 1515–22. https://doi.org/10.1111/j.1365-3156.2009.02408.x.

[164] A.-A.M. El-Sharjawy, A.S. Amin, Use of cloud-point preconcentration for spectrophotometric determination of trace amounts of antimony in biological and environmental samples, Anal. Biochem. 492 (2016) 1–7. https://doi.org/10.1016/j.ab.2015.08.008.

[165] C.T.R. India, New treatment regimens for treatment of Post Kala Azar Dermal Leishmaniasis patients in India and Bangladesh region, New Delhi Database Publ. (India). Identifier CTRI/2017/04/008421. (2017) 7.

[166] J. van Griensven, M. Balasegaram, F. Meheus, J. Alvar, L. Lynen, M. Boelaert, Combination therapy for visceral leishmaniasis, Lancet Infect. Dis. 10 (2010) 184–194. https://doi.org/10.1016/S1473-3099(10)70011-6.

Bioanalysis in Human Plasma

2

Highly sensitive UPLC-MS/MS method for the quantification of paromomycin in human plasma

Ignace C. Roseboom
Bas Thijssen
Hilde Rosing
Jane Mbui
Jos H. Beijnen
Thomas P.C. Dorlo

2.1

Abstract

A highly sensitive method was developed to quantitate the antileishmanial agent paromomycin in human plasma, with a lower limit of quantification of 5 ng/mL. Separation was achieved using an isocratic ion-pair ultra-high performance liquid chromatographic (UPLC) method with a minimal concentration of heptafluorobutyric acid , which was coupled through an electrospray ionization interface to a triple quadrupole - linear ion trap mass spectrometer for detection. The method was validated over a linear calibration range of 5 to 1,000 ng/mL (r²≥0.997) with inter-assay accuracies and precisions within the internationally accepted criteria. Volumes of 50 µL of human K_2EDTA plasma were processed by using a simple protein precipitation method with 40 µL 20% trichloroacetic acid. A good performance was shown in terms of recovery (100%), matrix effect (C.V. ≤12.0%) and carry-over (≤17.5% of the lower limit of quantitation). Paromomycin spiked to human plasma samples was stable for at least 24 hours at room temperature, 6 hours at 35°C, and 104 days at -20°C. Paromomycin adsorbs to glass containers at low concentrations, and therefore acidic conditions were used throughout the assay, in combination with polypropylene tubes and autosampler vials. The assay was successfully applied in a pharmacokinetic study in visceral leishmaniasis patients from Eastern Africa.

1.   Introduction

Paromomycin (aminosidine) is an antimicrobial drug from the aminoglycoside branch. It is the only aminoglycoside with a clinically important anti-leishmanial activity and was discovered in 1963 in the USSR [1]. Paromomycin was primarily used as an antibiotic against gram-negative bacteria in humans before modern-day antibiotics were discovered and is still being used as a veterinary drug [2]. Since 2006, intramuscular paromomycin has been licensed for the treatment of the neglected tropical disease visceral leishmaniasis in India. High efficacy rates in a series of clinical trials in India and Eastern Africa, also in combination with sodium stibogluconate, combined with a good cost-effectiveness led to widespread implementation of this drug to treat visceral leishmaniasis [3–5].

Chemical characteristics of aminoglycosides include a high polarity, absence of hydrophobic side chains and poly-ionic charge in aqueous environments, which lack interaction with traditional reversed-phase (RP) liquid chromatography (LC) [6]. Hydrophilic interaction liquid chromatography (HILIC) [7,8], zwitterionic-HILIC (ZIC-HILIC) [9–11], derivatization of paromomycin [12] or ion-pairing (IP) combined with an RP stationary phase chromatographic system [13–16] have been reported in the analysis of paromomycin. Internal standards used in these bioanalytical assays were synthesized permethylated aminoglycosides (spectinomycin, dihydrostreptomycin and kanamycin A) or chemical analogues (various other aminoglycosides).

Published bioanalytical assays of paromomycin in human plasma have relatively high lower limits of quantification (LLOQ) of 50 [17], 100 [9] and 500 ng/mL [12], require larger sample volumes and involve labour-intensive analyte extraction (e.g. solid phase extraction (SPE) and liquid-liquid extraction (LLE)). Using these existing methods, trough concentrations and the terminal elimination rate could not be quantified previously due to a lack of sensitivity. A sensitive method to quantitate paromomycin in human plasma is therefore required to adequately perform pharmacokinetic studies to improve paromomycin-based dosing regimens, particularly in combination therapies. Other liquid chromatography coupled to tandem mass spectrometry (LC-MS/MS) bioanalytical assays quantifying paromomycin have been reported for use in residue analysis in food such as meat [7,11,13–16,18,19], milk [7,10,11,14,19], and honey [10,19] samples or pre-clinical in mice plasma [8].

The aim of the current investigation was to develop a sensitive and simple method for the quantification of paromomycin in human plasma using a small volume of human plasma and validate it according to current EMA and FDA guidelines [20,21]. To our knowledge, this is the first paromomycin bioanalytical assay fulfilling these requirements and using a stable isotopically labelled internal standard (IS) instead of a chemical analogue. The LLOQ of the assay is 5 ng/mL using only 50 µL of human plasma.

2. Materials and methods

2.1. Chemicals
Paromomycin sulfate and internal standard (multiple deuterated paromomycin acetic acid) were both purchased from Toronto Research Chemicals (North York, Ontario, Canada). The deuterium-label in the deuterated paromomycin IS varied between 0 (D_0) and 7 (D_7) deuterium atoms, with the following distribution: D_0 0.13%; D_1 0.53%; D_2 2.47%; D_3 8.77%; D_4 18.13%; D_5 22.23%; D_6 20.60%; D_7 13.62% according to the certificate of analysis. Methanol, formic acid, acetonitrile (ACN) and water (ULC grade) were bought from Biosolve Ltd (Valkenswaard, The Netherlands). Trichloroacetic acid (TCA) (99.5%) was supplied by Merck Chemicals B.V. (Amsterdam, the Netherlands), heptafluorobutyric acid (HFBA) solution (0.5 M) was from Sigma-Aldrich (Zwijndrecht, the Netherlands). Distilled water used for sample preparation came from B. Braun Medical (Melsungen, Germany). Blank human dipotassium ethylenediaminetetraacetic acid (K_2EDTA) plasma was obtained from BioIVT (West Sussex, United Kingdom).

2.2. Stock solutions and working solutions
Paromomycin stock solutions with a concentration of 0.1 mg/mL (free base) were made in water. Paromomycin stock solutions were separately made for calibration standards and quality control (QC) samples. The stock solutions were diluted in water to obtain working solutions. A stock solution of internal standard was prepared in water with a concentration of 1 mg/mL for the sum of all deuterated paromomycin. The working solution of IS (WIS) was made from dilution of IS stock solution in water to a concentration of 111 ng/mL D_5-paromomycin. The certificate of analysis of deuterated paromomycin estimated the amount of D_5-paromomycin in the sum of total deuterated paromomycin at 22.23%. D_5-paromomycin is the most abundant isotope form in the deuterated paromomycin mixture. Stock and working solutions were stored at -20°C.

2.3. Calibration standards, quality control samples
Calibration samples were prepared in a batch prior to validation. The stability of the samples was determined afterwards. Forty µL of working solution is spiked to 760 µL blank human plasma and aliquots of 50 µL were made. QC samples were prepared in batches before storing at -20°C in aliquots of 50 µL. The stability of these QC samples was tested afterwards with freshly prepared QC samples. Seven non-zero calibration standards were used in the development of this assay. Calibration standards were prepared in concentrations of 5, 10, 25, 50, 100, 500 and 1,000 ng/mL with QC samples at concentrations of 5, 15, 300 and 800 ng/mL for QC-LLOQ, QC-LOW, QC-MID, and QC-HIGH, respectively.

2.4. Sample preparation
Human plasma samples (calibration, QC or unknown) were thawed prior to preparing the samples for analysis, aliquots (50 µL) were transferred into 1.5 mL polypropylene reaction tubes. Ten µL of IS working solution was spiked to the aliquots except to the double blank before vortex mixing. Plasma proteins were precipitated by the addition of 40 µL of 20% (w/v) TCA in water. The samples were vortex mixed and centrifuged at 23,100 g for 5 minutes in a cooled down environment set at 5°C. 50 µL of clear supernatant was then transferred to a 1.5 mL polypropylene reaction tube and 50 µL distilled water was added to the samples to dilute 1:1 (v/v) yielding a TCA concentration of 4% (w/v) in the final extract. The final extracts were vortex mixed and transferred to polypropylene autosampler vials prior to analysis.

2.5. LC equipment and conditions
The chromatographic system used was a UPLC LC-30AD pump with an inline degasser connected to a UPLC LC-30AMCP autosampler, set at 4°C and CTO-20AC column oven (Nexera X2 series, Shimadzu Corporation, Kyoto, Japan). Chromatographic separation was achieved using an Acquity UPLC HSS T3 analytical column (Waters, Milford, MA, USA; 150 mm x 2.1 mm ID, 1.8 µm particles). The column temperature was kept at 40°C. The purge and strong wash solvent used was 0.1% formic acid in water/methanol (50:50, v/v). The eluent consisted of 5 mM HFBA in water/ACN (7:3, v/v) mixture (3.5 mM HFBA in the mixture), at an isocratic flow rate of 0.4 mL/min.

2.6. MS equipment and conditions
Detection of paromomycin was performed using a QTRAP 6500 (Sciex, Framingham, MA, USA) quadrupole - linear ion trap MS equipped with a turbo ionspray interface operating in positive ion mode. The mass spectrometer and ionization conditions were optimized to obtain maximal sensitivity for the analyte. The following settings were used: ion source voltage at 5500 V, ion source temperature at 500°C; ion source gas 1 at 60 psi (4.1 bar); ion source gas 2 at 40 psi (2.8 bar), curtain gas at 25 psi (1.7 bar) and collision gas at 10 psi (0.69 bar). Multiple reaction monitoring (MRM) mode was performed to quantify paromomycin [M+H]$^+$ using the transition of m/z 616.6 → 163.1 and the deuterated paromomycin (IS) with m/z 621.6 → 165.1 (Figure 1). Data acquisition and processing were performed with Analyst™ software (Sciex, version 1.6.2).
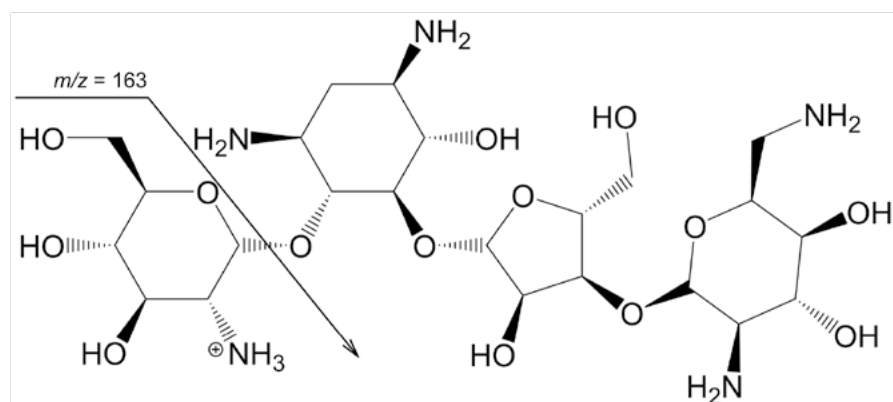
Figure 1: The chemical structure of paromomycin, including the proposed fragmentation pattern and the mass-over-charge (m/z) of the monitored product ion. The fragmentation pattern is indicated by an arrow.

2.7. Validation procedures

The validation of the assay was performed using the current EMA and FDA guidelines for the validation of bioanalytical assays in plasma [20,21]. The assay was validated for linearity, LLOQ, accuracy and precision, dilution integrity, carry-over, selectivity, matrix effect, recovery, and stability under various conditions.

2.7.1. Calibration model and lower limit of quantitation

Seven non-zero calibration standards ranging from 5-1000 ng/mL were prepared in duplicate for each run in three separate validation runs. Linear regression was performed on the analyte peak area/IS peak area ratio versus nominal analyte concentration (x), weighted by a weighting factor of $1/x^2$. The deviations from the mean for each non-zero calibration standard should be within ±15% (±20% for the LLOQ) for a minimum of 75% of the non-zero standards.

2.7.2. Accuracy and precision

Intra-and inter-assay accuracy and precision were determined by analyzing five replicates of QC samples in three separate validation runs at the LLOQ (5 ng/mL), low (15 ng/mL), mid (300 ng/mL) and high (800 ng/mL) levels. The concentration of each sample was determined using the calibration standards prepared and analyzed in the same batch. The accuracies were expressed as the bias from the nominal concentration and precision was calculated as the coefficient of variation (CV%). The intra-assay bias (%) is the bias of the mean measured concentration per analytical run as compared to the nominal concentration. The inter-assay bias (%) is the bias of the mean measured concentration in three analytical runs compared to the nominal concentration. The inter-run precision was calculated by performing a one-way ANOVA. The accuracy values should be within ±15% (±20% at the LLOQ) and precision ≤15% (≤20% for the LLOQ).

2.7.3. Carry-over

Carry-over was assessed by injecting two double blank samples after the upper limit of quantification (ULOQ, 1000 ng/mL) of the calibration standards. The peak areas at the retention times of the analyte and its internal standard detected in the double blank samples were compared to the mean area of the analyte and the IS in five QC-LLOQ samples. The carry-over was assessed in three separate validation runs. The peak areas in the double blank samples compared to the QC-LLOQ samples should be ≤20% for paromomycin and ≤5% for the IS.

2.7.4. Specificity and selectivity

Specificity and selectivity were evaluated in blank K_2EDTA human plasma batches from six different individuals. Co-eluting peaks at the retention time of the analyte and IS from endogenous interferences were assessed in double blanks and compared to the LLOQ samples from each individual batch. The peak areas in the double blank samples should be ≤20% compared to the peak areas of the LLOQ samples in each batch and ≤5% for the IS. The bias of the LLOQ samples should be ±20% in at least 4 of the 6 human plasma batches. Cross analyte/IS interferences were determined by spiking the analyte at the ULOQ concentration and separately the IS at the IS level. Interference of paromomycin with the IS should be ≤5% (peak area) and the interference of the IS with paromomycin should be ≤20% of the analyte peak area compared to the LLOQ samples.

2.7.5. Matrix effect and recovery

Matrix effect and recovery of the assay were determined using blank K_2EDTA human plasma batches from six individuals at two QC levels (QC-LOW and QC-HIGH). The absolute matrix effect factor was calculated as the analyte or IS peak area ratio between these QC samples (matrix present) and matrix absent samples at similar concentration levels. Furthermore, the IS-normalized matrix effect factor was calculated as the ratio between the absolute matrix effect factor of paromomycin and IS. The IS-normalized matrix factor value is accepted ≤15%. Matrix present samples were prepared by spiking QC working solutions to extracted blank plasma samples. The sample preparation recovery was calculated as the ratio between peak areas of the processed QC samples and spiked matrix samples.

2.7.6. Dilution integrity

Dilution integrity was determined in five-fold by applying a ten-fold, fifty-fold, and hundred-fold dilution of spiked human plasma samples at a concentration of 5,000 ng/mL (5 times the ULOQ). Dilution was performed using blank human K_2EDTA plasma. The accuracy and precision were determined with acceptance criteria of ±15% bias and ≤15% CV%, respectively.

2.7.8. Stability

Short-term stability in human plasma at QC-LOW and QC-HIGH concentrations was evaluated for 6 and 24 hours at 2-8°C, room temperature and 35°C (simulated room temperature in tropical regions, in view of future pharmacokinetic studies). Additionally, stability was evaluated in final extracts at 2-8°C, stock solution and working solutions at -20°C. Long-term stability in human plasma at QC-LOW and QC-HIGH concentrations stored at -20°C was evaluated for at least 104 days. The stability after 4 freeze/thaw cycles in human plasma was determined. One freeze/thaw cycle consisted of unassisted thawing at room temperature and subsequently freezing at -20°C for at least 12 hours straight. The acceptance criteria for the precision and accuracy for the human plasma QC samples and final extracts were ≤15% CV and ±15% bias, respectively, while for stock and working solutions these were ≤5% CV and ±5% bias, respectively.

2.8. Clinical application

This bioanalytical assay was developed to support paromomycin pharmacokinetic studies in visceral leishmaniasis patients. Human plasma K_2EDTA samples from visceral leishmaniasis patients were collected in a clinical trial conducted in Kacheliba Sub County Hospital, Kenya. Ethical approval was granted by all relevant institutional and national ethical review committees. Patients were treated with intramuscular injections of 20 mg/kg paromomycin q.d. for 14 days. Plasma samples were taken on day 1 and 14 prior to paromomycin treatment, and after 1, 2, 4/8 and 24 hours after administration. Written informed consent was obtained. At scheduled time points, a 2 mL blood sample was obtained via venipuncture. Blood samples were anticoagulated in K_2EDTA containing tubes and plasma was obtained by centrifugation at approximately 2,000 g at room temperature. Separated plasma was immediately (within 60 min of collection) stored at -20°C. The human plasma samples were eventually transported on dry-ice to the bioanalytical laboratory of The Netherlands Cancer Institute. The human plasma samples were further processed as described in section 2.4.

3. Results and discussion

3.1. Development

3.1.1. Sample preparation

Various sample preparation methods, including protein precipitation, were tested during the development of the bioanalytical assay. Protein precipitation is often performed using organic solvents e.g. ACN and methanol in combination with LC-MS/MS analysis. Paromomycin showed poor solubility in various organic solvent mixtures, therefore a polar protein precipitant agent was desired. Protein precipitation using TCA, a highly acidic and ionic chemical, showed an increase

in recovery and sensitivity, as well as a low background noise compared to other precipitants. Given the substantial improvements, TCA was chosen as protein precipitant. Systematically increasing the concentration of TCA in water, starting from 10% (w/v) to 20% (w/v), showed the highest precipitation potential around a concentration of 20% TCA in water (w/v). Dilution of the final extract resulted in an increase of retention through HFBA ion-pair mechanisms on the stationary phase of the column. Dilution of the final extract with water (1:1, v/v) was implemented to gain a constant retention time and to avoid solvent effects, yielding a TCA concentration of 4% (w/v) in the final extract.
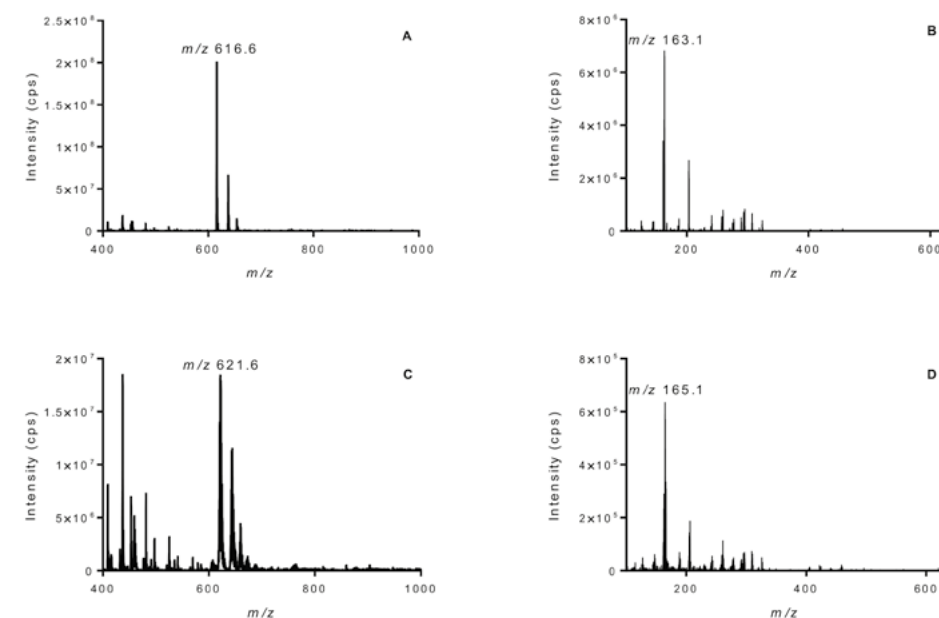

Figure 2: MS spectrum of paromomycin (A) and its product-ion spectrum (m/z 616.6), MS spectrum of D_5-paromomycin C) and its product-ion spectrum (m/z 621.6).

3.1.2. Chromatography and mass spectrometry

Previously reported methods for the quantification of paromomycin and other aminoglycosides have already indicated challenges regarding the LC-system. Aminoglycosides are highly polar, do not contain any hydrophobic groups, and exhibit a multiple ionic state, which results in poor retention using conventional reversed-phase methods. Ion-pair or HILIC are the most commonly applied methods to solve retention problems for aminoglycosides. We evaluated the use of a zwitterion-HILIC column, but paromomycin did not elute well resulting in broad peaks and poor peak shapes and thus poor sensitivity. Ion-pair chromatography using HFBA combined with the use of an aqueous C18 UPLC column improved analyte retention

and provided an acceptable peak shape. Subsequently, the modifier percentage (ACN) in the eluent was optimized and the minimal required amount of ion-pairing agent HFBA (3.5 mM) was established to obtain stable retention of the analyte with minimum matrix effects of the ion pairing reagent. Isocratic elution was desirable in order to prevent the conditioning of the column with the ion-pair reagent after each injection, which reduced the required run time substantially. After analysis of a batch of samples, the LC-MS/MS system was flushed using 0.1% formic acid in water-methanol (50:50, v/v) to prevent accumulation of HFBA. The LC system was equipped with an ESI interface operating in positive ion mode connected to an ultra-sensitive quadrupole linear ion trap (QTRAP 6500, Sciex) mass spectrometer. Single charged paromomycin [M+H]$^+$ with a Q3 mass transition at m/z 616.6 → 163.1 for paromomycin and m/z 621.6 → 165.1 for the D$_5$-paromomycin IS (Figure 2) were monitored. Considering the aim to develop a method with improved sensitivity, the bioanalytical range was determined by the lowest quantifiable concentration with an acceptable signal to noise ratio (5 ng/mL) and the corresponding ULOQ at which linearity of the calibration curve was not compromised (1000 ng/mL). Above 1000 ng/mL the linearity of the bioanalytical range was highly compromised. Representative chromatograms of double blank, blank, LLOQ and ULOQ samples are shown in Figure 3 for paromomycin and its internal standard.

3.2. Validation procedures

3.2.1. Calibration model

Calibration standards were analyzed in duplicate in three separate analytical runs. The reciprocal of the squared concentrations (1/x^2) was used as a weighting factor to obtain a constant bias over the validated concentration range. A linear fit with correlation coefficient (r^2) of ≥0.997 was obtained in three individual runs. The bioanalytical assay was linear over the range (5-1000 ng/mL) with accuracies of ≤5.7% for all calibration standards. The LLOQ was established at 5 ng/mL, exhibiting a minimum signal to noise ratio of 8:1.

3.2.2. Accuracy and precision

The assay performance data for paromomycin are summarized in Table 1. The performance at the QC-LOW, QC-MID and QC-HIGH levels were ±6.1% and ±8.3% for inter- and intra-assay accuracy, respectively, and ≤2.3% and ≤4.3% for inter- and intra-assay precision, respectively. At the LLOQ level the inter- and intra-assay accuracies were 15.1% and ±16.6%, respectively, while the inter-and intra-assay precisions were 1.4% and ≤3.6% respectively. The accuracy and precision data met the specified acceptance criteria.

3.2.3. Carry-over

Carry-over was determined by comparing the peak area present in the first double

blank sample following an ULOQ sample to the mean peak area of LLOQ samples in two-fold. The carry-over in three validation runs was ≤17.5%, which is within the acceptance criteria of ≤20%.

Table 1. Assay performance data for paromomycin. Accuracy and precisions were established in 3 analytical runs and each run contained 5 replicates per tested concentration.

Nominal paromomycin concentration (ng/mL)	Intra-run bias (%)	Inter-assay bias (%)	Intra-run precision (%)	Inter-assay precision (%)
5	12.5-16.6	15.1	2.3-3.6	1.4
15	0.7-4.0	2.0	1.4-4.0	1.1
300	3.5-5.6	4.6	1.3-4.3	a
800	3.1-8.3	6.1	2.0-2.8	2.3

a No significant additional variation was found due to the performance of the assay in different batches.

3.2.4. Specificity and selectivity

Selectivity in 6 individual human plasma batches was determined at the blank and LLOQ levels. The maximum interference co-eluting with paromomycin at the LLOQ level was 3.2% for paromomycin and there was no interference present at the retention time of the IS. The accuracy of paromomycin at the LLOQ level was also established for all six human plasma batches with a deviation of ≤13.2% compared to

the nominal concentration. Cross analyte/IS interference was determined. Paromomycin spiked at ULOQ level to human plasma did not show any interferences in the IS. The IS interference at the paromomycin mass transition shows 7.1-13.5% interference. These interferences were well within the acceptance criteria.

3.2.5. Matrix effect and recovery

Absolute matrix effect factors for both analyte and IS were calculated based on QC-LOW and QC-HIGH concentrations in matrix present and matrix absent samples. The IS-normalized matrix effect factor were 12.0% and 10.3% for QC-LOW and QC-HIGH levels, respectively (Table 2). The sample preparation recovery at QC-LOW and QC-HIGH concentrations varied between 100.1-109.3%, reflecting the recovery of paromomycin after the sample pre-treatment procedure.

3.2.6. Dilution integrity

Concentrations above the ULOQ were diluted 10, 50 and 100 times in a two-step dilution in five-fold. The intra-assay bias and precision for the 10 times dilution were 7.7% and 3.2% respectively, 0.5% and 5.1% respectively for the 50 times dilution, and -13.4% and 6.1% respectively for the 100 times dilution. Therefore, it can be concluded that samples with a concentration above the ULOQ can be diluted up to 100 times.
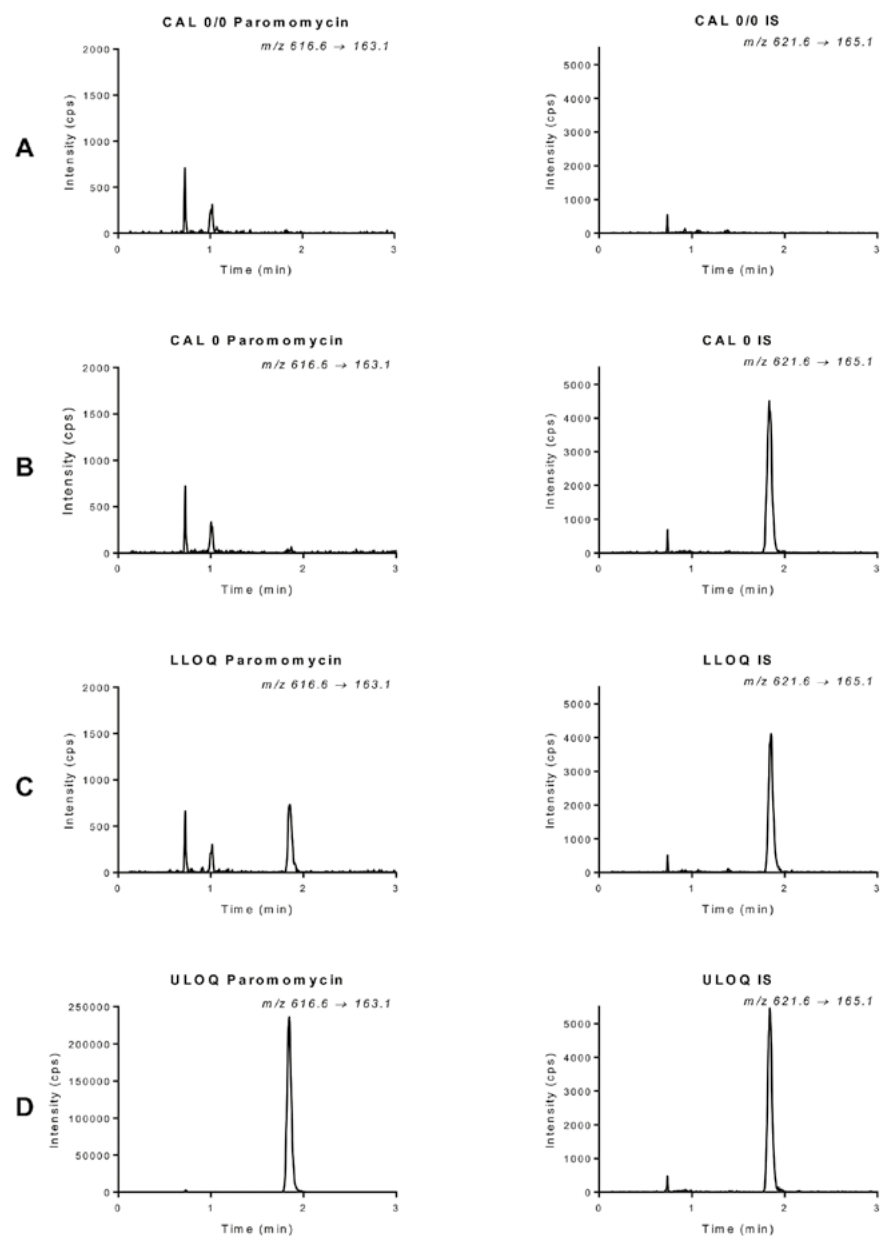
Figure 3. Representative MRM chromatograms of processed human plasma samples. A: double blank (CAL 0/0), B: blank (CAL 0, containing 111 ng/mL internal standard), C: LLOQ (5 ng/mL paromomycin and 111 ng/mL internal standard) and D: ULOQ (1000 ng/mL paromomycin and 111 ng/mL internal standard).

Table 2. Matrix factor and sample preparation recovery data for paromomycin.

Nominal paromomycin concentration (ng/mL)	Matrix Factor Analyte	Matrix Factor IS	IS-normalized Matrix Factor	Sample Preparation Recovery
15	1.02	0.91	1.12	109.3%
800	0.89	0.79	1.10	100.1%

3.2.7. Stability

The stability of paromomycin in human plasma was investigated under various conditions (Table 3). Stability was determined as a function of accuracy and precision for both QC-LOW and QC-HIGH concentrations. Paromomycin in human plasma stored for 6 and 24 hours at 2-8°C and room temperature were all within the criteria (±15%) and were considered stable (Table 3). Paromomycin in human plasma kept at 35°C was stable for a period of 6 hours, but not for 24 hours (bias QC-LOW -17.6%). The stability of final extracts was guaranteed for at least 44 days at 2-8°C. The stock solution was stable for at least 431 days and the working solutions for at least 60 days, both stored at -20°C in water.

Table 3. Stability data for paromomycin (n = 3 per quality control level) expressed in accuracy (bias %) and precision (coefficient of variation).

Conditions	Matrix	Nominal concentration (ng/mL)	Bias (%)	C.V. (%)
-20°C, 431d	Stock	100,000	2.5	4.9
-20°C, F/T 4 cycles	Human plasma	15.0	11.1	5.4
		800	12.2	3.1
35°C, 6h	Human plasma	15.0	-6.0	3.1
		800	1.0	5.8
35°C, 24h	Human plasma	15.0	-17.6	4.0
		800	-10.6	2.6
-20°C, 104 days	Human plasma	15.0	14.9	3.9
		800	0.7	3.2
RT, 6h	Human plasma	15.0	-2.7	4.3
		800	3.9	0.4
RT, 24h	Human plasma	15.0	1.8	6.4
		800	3.6	4.6
2-8°C, 24h	Human plasma	15.0	12.9	2.7
		800	7.4	1.4

Table 3. Stability data for paromomycin (n = 3 per quality control level) expressed in accuracy (bias %) and precision (coefficient of variation). (continued)

Conditions	Matrix	Nominal concentration (ng/mL)	Bias (%)	C.V. (%)
2-8°C, 44d	Final extract	15.0	11.6	1.4
		800	5.0	3.6

Abbreviations: C.V. = coefficient of variation; d = days; F/T = freeze/thaw cycles; h = hours; RT = room temperature between 20-25°C

3.3. Paromomycin glass adsorption

Only a few publications on the subject of aminoglycoside quantification address avoiding glassware due to possible adsorption of this class of compounds [10,22–25]. The adsorption issue was first assessed during the quantification of aminoglycosides using sodium pentanesulfonate ion-pair HPLC and fluorescent detection after post-column derivatization using o-phthalaldehyde reagent in 1978, mentioning the potential adsorption of aminoglycosides to glass [26]. This was described more extensively in radioimmunoassays for gentamycin and tobramycin, warning kit manufacturers of the possible impact to assay characteristics due to adsorption [27]. The proposed solution was to lower the pH of the environment, occupying the negatively charged silanol groups on the walls of the glass, avoiding positively charged aminoglycosides to bind the silanol groups. We confirmed that a final concentration of 4% TCA in water (v/v) prevented any adsorption issues to glass and allowed quantification of the LLOQ level. Alternatively, the use of polypropylene labware throughout the sample preparation and analysis is recommended.

3.4. Clinical application

This analytical assay was used to determine paromomycin plasma concentration in pharmacokinetic samples from visceral leishmaniasis patients treated with intramuscular paromomycin (20 mg/kg q.d. for 14 days). Paromomycin plasma concentration-time curves for 3 typical patients are shown in Figure 4. All trough samples after the first drug administration (t=0 h and t=24 h) were quantifiable and above 100 ng/mL, which is well above the LLOQ level. Previous pharmacokinetic studies failed to quantify these trough concentrations due to a lack of sensitivity of the bioanalytical assay [28,29]. Aminoglycoside pharmacokinetics are characterized by large variability between regions and populations; moreover, lower paromomycin mg/kg regimens have been licensed for the treatment of visceral leishmaniasis in India. The here presented assay enables the quantification of trough concentrations, also in patients that have been lower exposed than the patients in the current clinical application. Taking into account the demonstrated dilution integrity for concentrations above the ULOQ, this method is shown to be applicable for the quantification of paromomycin in clinical pharmacokinetic studies.
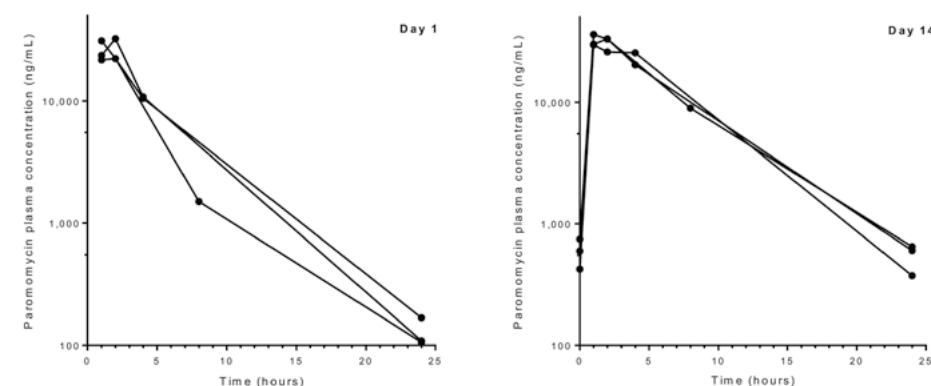

Figure 4. Concentration of paromomycin in human plasma versus time after paromomycin administration on day 1 and day 14 of the treatment in 3 patients.

4.   Conclusion

A fast and simple highly sensitive bioanalytical assay for the quantification of paromomycin in human K_2-EDTA plasma was developed and validated. The validated range of the assay is 5-1000 ng/mL using a stable isotope as the internal standard. This bioanalytical assay for paromomycin has a ten-fold lower limit of quantification compared to previously reported assays for paromomycin, while using an ion-pair LC system with simplified sample preparation. The assay setup consists of TCA protein precipitation as sample preparation, an isocratic ion-pair LC system connected to a QTRAP 6500 equipped with ESI in positive ion mode. Furthermore, the method maintained a high assay performance for the validated ranges in terms of linearity ($r^2 \geq 0.997$), accuracy and precision. Paromomycin was adsorbed by glass, lowering the sensitivity of the assay. Using a high concentration of TCA and/or the replacement of glass with polypropylene material solved the adsorption issue.

References

[1]   R. Chew, J.S. McCarthy, Paromomycin, Kucers Use Antibiot. A Clin. Rev. Antibacterial, Antifung. Antiparasit. Antivir. Drugs, Seventh Ed. (2017) 3149–3161. doi:10.1201/9781315152110.

[2]   G. Nahler, Committee for Veterinary Medicinal Products (CVMP), Dict. Pharm. Med. (2009) 32–32. doi:10.1007/978-3-211-89836-9_245.

[3]   C.N. Chunge, J. Owate, H.O. Pamba, L. Donno, Treatment of visceral leishmaniasis in Kenya by aminosidine alone or combined with sodium stibogluconate, Trans. R. Soc. Trop. Med. Hyg. 84 (1990) 221–225. doi:10.1016/0035-9203(90)90263-E.

[4]   R.N. Davidson, J. Seaman, D. Pryce, H.E. Sondorp, A. Moody, A.D.M. Bryceson, R.N. Davidson, J. Seaman, D. Pryce, H.E. Sondorp, A. Moody, A.D.M. Bryceson, R.N. Davidson, J. Seaman, D. Pryce, H.E. Sondorp, A. Moody, A.D.M. Bryceson, Epidemic Visceral Leishmaniasis in Sudan: A Randomized Trial of Aminosidine plus Sodium Stibogluconate versus Sodium Stibogluconate Alone, J. Infect. Dis. 168 (1993) 715–720. doi:10.1093/infdis/168.3.715.

[5]   C.P. Thakur, T.P. Kanyok, A.K. Pandey, G.P. Sinha, A.E. Zaniewski, H.H. Houlihan, P. Olliaro, A prospective randomized, comparative, open-label trial of the safety and efficacy of paromomycin (aminosidine) plus sodium stibogluconate versus sodium stibogluconate alone for the treatment of visceral leishmaniasis, Trans. R. Soc. Trop. Med. Hyg. 94 (2000) 429–431. doi:10.1016/S0035-9203(00)90130-5.

[6]   F. Farouk, H.M.E. Azzazy, W.M.A. Niessen, Challenges in the determination of aminoglycoside antibiotics, a review, Anal. Chim. Acta. 890 (2015) 21–43. doi:10.1016/j.aca.2015.06.038.

[7]   Y. Tao, D. Chen, H. Yu, L. Huang, Z. Liu, X. Cao, C. Yan, Y. Pan, Z. Liu, Z. Yuan, Simultaneous determination of 15 aminoglycoside(s) residues in animal derived foods by automated solid-phase extraction and liquid chromatography-tandem mass spectrometry, Food Chem. 135 (2012) 676–683. doi:10.1016/j.foodchem.2012.04.086.

[8]   M.J.S.K. Pinjari, R.S. Somani, R.M. Gilhotra, A rapid, sensitive and validated ultra performance liquid chromatography and tamdem mass spectrometry method for determination of paromomycin in mice plasma: application to pharmacokinetic study, Int. J. Pharm. Pharm. Sci. 9 (2017) 86. doi:10.22159/ijpps.2017v9i5.11024.

[9]   R. Oertel, V. Neumeister, W. Kirch, Hydrophilic interaction chromatography combined with tandem-mass spectrometry to determine six aminoglycosides in serum, J. Chromatogr. A. 1058 (2004) 197–201. doi:10.1016/j.chroma.2004.08.158.

[10]   C. Díez, D. Guillarme, A. Staub Spörri, E. Cognard, D. Ortelli, P. Edder, S. Rudaz, Aminoglycoside analysis in food of animal origin with a zwitterionic stationary phase and liquid chromatography-tandem mass spectrometry, Anal. Chim. Acta. 882 (2015) 127–139. doi:10.1016/j.aca.2015.03.050.

[11]   D.A. Bohm, C.S. Stachel, P. Gowik, Validation of a method for the determination of aminoglycosides in different matrices and species based on an in-house concept, Food Addit. Contam. - Part A Chem. Anal. Control. Expo. Risk Assess. 30 (2013) 1037–1043. doi:10.1080/19440049.2013.775709.

[12]   J. Lu, M. Cwik, T. Kanyok, Determination of paromomycin in human plasma and urine by reversed-phase high-performance liquid chromatography using 2,4-dinitrofluorobenzene derivatization, J. Chromatogr. B Biomed. Sci. Appl. 695 (1997) 329–335. doi:10.1016/S0378-4347(97)00192-8.

[13]   F.L. van Holthoon, M.L. Essers, P.J. Mulder, S.L. Stead, M. Caldow, H.M. Ashwin, M. Sharman, A generic method for the quantitative analysis of aminoglycosides (and spectinomycin) in animal tissue using methylated internal standards and liquid chromatography tandem mass spectrometry, Anal. Chim. Acta. 637 (2009) 135–143. doi:10.1016/j.aca.2008.09.026.

[14]   M.C. Savoy, P.M. Woo, P. Ulrich, A. Tarres, P. Mottier, A. Desmarchelier, Determination of 14 aminoglycosides by LC-MS/MS using molecularly imprinted polymer solid phase extraction for clean-up, Food Addit. Contam. - Part A Chem. Anal. Control. Expo. Risk Assess. 35 (2018) 674–685. doi:10.1080/19440049.2018.1433332.

[15]   S.J. Lehotay, K. Mastovska, A.R. Lightfield, A. Nuñez, T. Dutko, C. Ng, L. Bluhm, Rapid analysis of aminoglycoside antibiotics in bovine tissues using disposable pipette extraction and ultrahigh performance liquid chromatography-tandem mass spectrometry, J. Chromatogr. A. 1313 (2013) 103–112. doi:10.1016/j.chroma.2013.08.103.

[16]   A. Kaufmann, P. Butcher, K. Maden, Determination of aminoglycoside residues by liquid chromatography and tandem mass spectrometry in a variety of matrices, Anal. Chim. Acta. 711 (2012) 46–53. doi:10.1016/j.aca.2011.10.042.

[17]   W.R. Ravis, A. Llanos-Cuentas, N. Sosa, M. Kreishman-Deitrick, K.M. Kopydlowski, C. Nielsen, K.S. Smith, P.L. Smith, J.H. Ransom, Y.J. Lin, M. Grogl, Pharmacokinetics and absorption of paromomycin and gentamicin from topical creams used to treat cutaneous leishmaniasis, Antimicrob. Agents Chemother. 57 (2013) 4809–4815. doi:10.1128/AAC.00628-13.

[18]   K. Róna, G. Klausz, E. Keller, M. Szakay, P. Laczay, M. Shem-Tov, P. Székely-Körmöczy, Determination of paromomycin residues in turkey tissues by liquid chromatography/mass spectrometry, J. Chromatogr. B Anal. Technol. Biomed. Life Sci. 877 (2009) 3792–3798. doi:10.1016/j.jchromb.2009.09.018.

[19]   W.X. Zhu, J.Z. Yang, W. Wei, Y.F. Liu, S.S. Zhang, Simultaneous determination of 13 aminoglycoside residues in foods of animal origin by liquid chromatography-electrospray ionization tandem mass spectrometry with two consecutive solid-phase extraction steps, J. Chromatogr. A. 1207 (2008) 29–37. doi:10.1016/j.chroma.2008.08.033.

[20]   European Medicines Agency, Committee for Medicinal Products for Human Use. Guideline on bioanalytical method validation, 2012. doi:EMEA/CHMP/EWP/192217/2009.

[21]   Food and Drug Administration, Guidance for Industry Bioanalytical Method Validation Guidance for Industry Bioanalytical Method Validation Center for Veterinary Medicine (CVM) Contains Nonbinding Recommendations, 2013. http://www.fda.gov/Drugs/GuidanceComplianceRegulatoryInformation/Guidances/default.htm%0Ahttp://www.fda.gov/AnimalVeterinary/GuidanceComplianceEnforcement/GuidanceforIndustry/default.htm.

[22]   K. EL Hawari, Z. Daher, E. Verdon, M. AL Iskandarani, Impact of ion-pairs for the determination of multiclass antimicrobials residues in honey by LC-MS/MS, Food Addit. Contam. - Part A Chem. Anal. Control. Expo. Risk Assess. 34 (2017) 2131–2143. doi:10.1080/19440049.2017.1372641.

[23]   D.N. Heller, J.O. Peggins, C.B. Nochetto, M.L. Smith, O.A. Chiesa, K. Moulton, LC/MS/MS measurement of gentamicin in bovine plasma, urine, milk, and biopsy samples taken from kidneys of standing animals, J. Chromatogr. B Anal. Technol. Biomed. Life Sci. 821 (2005) 22–30. doi:10.1016/j.jchromb.2005.04.015.

[24]   P.A. Martos, F. Jayasundara, J. Dolbeer, W. Jin, L. Spilsbury, M. Mitchell, C. Varilla, B. Shurmer, Multiclass, multiresidue drug analysis, including aminoglycosides, in animal tissue using liquid chromatography coupled to tandem mass spectrometry, J. Agric. Food Chem. 58 (2010) 5932–5944. doi:10.1021/jf903838f.

[25]   A. Shen, J. Wei, J. Yan, G. Jin, J. Ding, B. Yang, Z. Guo, F. Zhang, X. Liang, Two-dimensional solid-phase extraction strategy for the selective enrichment of aminoglycosides in milk, J. Sep. Sci. 40 (2017) 1099–1106. doi:10.1002/jssc.201601086.

[26]   J.P. Anhalt, S.D. Brown, High-performance liquid-chromatography assay of aminoglycoside antibiotics in serum, Clin. Chem. 24 (1978) 1940–1947.

[27]   L. Josephson, P. Houle, M. Haggerty, Stability of dilute solutions of gentamicin and tobramycin, Clin. Chem. 25 (1979) 298–300.

[28]   T.P. Kanyok, A.D. Killian, K.A. Rodvold, L.H. Danziger, Pharmacokinetics of intramuscularly administered aminosidine in healthy subjects, Antimicrob. Agents Chemother. 41 (1997) 982–986. doi:10.1128/aac.41.5.982.

[29]   A.M. Musa, B. Younis, A. Fadlalla, C. Royce, M. Balasegaram, M. Wasunna, A. Hailu, T. Edwards, R. Omollo, M. Mudawi, G. Kokwaro, A. El-Hassan, E. Khalil, Paromomycin for the Treatment of Visceral Leishmaniasis in Sudan: A Randomized, Open-Label, Dose-Finding Study, PLoS Negl. Trop. Dis. 4 (2010) e855. doi:10.1371/journal.pntd.0000855.

2.1

Bioanalysis in Human Skin Tissue

3

Skin tissue sample collection, sample homogenization, and analyte extraction strategies for liquid chromatographic mass spectrometry quantification of pharmaceutical compounds

3.1

Ignace C. Roseboom
Hilde Rosing
Jos H. Beijnen
Thomas P.C. Dorlo

Abstract

Quantification of pharmaceutical compounds in skin tissue is challenging because of low expected concentrations, small typical sample volumes, and the hard nature of the skin structure itself. This review provides a comprehensive overview of sample collection, sample homogenization and analyte extraction methods that have been used to quantify pharmaceutical compounds in skin tissue, obtained from animals and humans, using liquid chromatography-mass spectrometry. For each step in the process of sample collection to sample extraction, methods are compared to discuss challenges and provide practical guidance. Furthermore, liquid chromatographic-mass spectrometry considerations regarding the quality and complexity of skin tissue sample measurements are discussed, with emphasis on analyte recovery and matrix effects. Given that the true recovery of analytes from skin tissue is difficult to assess, the extent of homogenization plays a crucial role in the accuracy of quantification. Chemical or enzymatic solubilization of skin tissue samples would therefore be preferable as homogenization method.

1. Introduction

Increased focus on target-site pharmacokinetics (PK) and pharmacodynamics (PD) in drug development has led to a growing interest and demand for bioanalytical drug quantification in tissues [1,2]. However, practical and ethical constraints, associated with the invasive sampling procedures required to obtain a sample, restrict its applicability. Establishing target-site PK/PD relationships for drugs is nevertheless important to assess and improve drug target strategies [3].

The aim of this review is to provide a comprehensive overview of general sampling methods and corresponding pre-treatment and extraction methods of skin tissue samples collected in *in vivo* studies for the quantification of small molecules through liquid chromatography coupled to mass spectrometry (LC-MS). The measurement of distribution of drugs from plasma into the skin has clinical importance e.g., in order to improve therapeutic strategies for skin infections. Uptake of drugs in the skin is dependent on the physicochemical properties of the drug and the route of administration used. Topical administration is effective for local treatment of skin-related diseases, e.g. anthralin cream and topical steroids for the treatment of psoriasis [4]. Systemic administration is e.g. used in the application of oral fluconazole for the treatment of fungal skin infections [5] or injection-based biologicals like adalimumab for the treatment of psoriasis [6].

The invasiveness of skin sampling techniques as well as the nature of the resulting skin samples has various implications for the bioanalytical procedures to extract, detect and quantify analytes in these samples. Tissue samples are typically only small in volume, which in turn requires a relatively low limit of quantification of the bioanalytical assay compared to plasma samples. Skin tissue is classified as 'hard' tissue, meaning that samples require more powerful sample preparation compared to tissue classified as 'soft' or 'tough' [2]. Moreover, releasing the analytes of interest from (sub)cellular compartments in these skin samples (stratum corneum, epidermis and dermis layers) requires rigorous sample pre-treatment methods, which at the same time cause the release of many other endogenous matrix components. Matrix effects, therefore, tend to be more pronounced in tissue samples compared to plasma samples [7]. Determining the true recovery of analytes from tissue samples is also more challenging compared to plasma samples [8]. Due to these factors, both ultra-sensitive bioanalytical methods, e.g. using liquid chromatography coupled to tandem mass spectrometry (LC-MS/MS), as well as proper sample preparation and extraction methods are of pivotal importance for the analysis of analytes in skin tissue samples.

As far as we know no other reviews have been published about sample preparation of skin tissue samples for the extraction and quantification of pharmaceutical compounds. This review further elaborates on bioanalytical considerations regarding the quality and complexity of tissue sample measurements.

3.1

2. Methodology

Quantification methods of analytes in skin tissue samples including sample collection methods, sample pre-treatment and extraction methods of the analytes were identified using a PubMed database search, restricted to the English language, using the following search terms for title and abstract contents: ((skin OR dermal) AND (liquid chromatography AND quantification AND mass spectrometry OR bioanalytical OR lcms OR lc-ms OR lc-ms/ms OR lcms ms OR lc-esi-ms/ms OR lc-esi-msms OR lc-apci-ms/ms OR lc apci ms ms)) NOT (DNA OR proteomics OR immunologic techniques OR peptides OR glycan OR permeation). If the title or abstract contained information suggesting that skin tissue was sampled from in vivo experiments or clinical trials and was used for the quantification of analytes via LC-MS/MS, the publication was included in this review. Both animal and human studies were included, except studies involving fish species because of significant differences in skin structure compared to mammals. Studies that focused on protein analysis in skin tissue were excluded since sample preparation is performed differently compared to small molecules. Given our focus on samples from *in* vivo studies, *in vitro* and *ex vivo* studies, such as permeation studies, were excluded from this analysis.

3. Results

The literature search resulted in 641 publications, of which 30 studies were identified as relevant and included in this review (search date 19 March 2020). Included studies are comprehensively summarized in Tables 1 through 3.

3.1. Skin tissue composition

The skin consists roughly of three different cellular layers, with each their own function and cellular composition (Figure 1). The outermost layer of the skin tissue, the epidermis is covered by the stratum corneum. The epidermis consists mainly (around 90%) of keratinocytes and is responsible for the protection against environmental hazards, like infections [9,10]. Underneath the epidermis lies the dermis, which is connected through fibers known as the basement membrane. The dermis is more complex than the epidermis as blood vessels, sweat glands, hair follicles and nerve endings are in the dermis and not in the epidermis, broadening the range of cell diversity. Underneath the dermis lies the hypodermis which consists of subcutaneous fat.
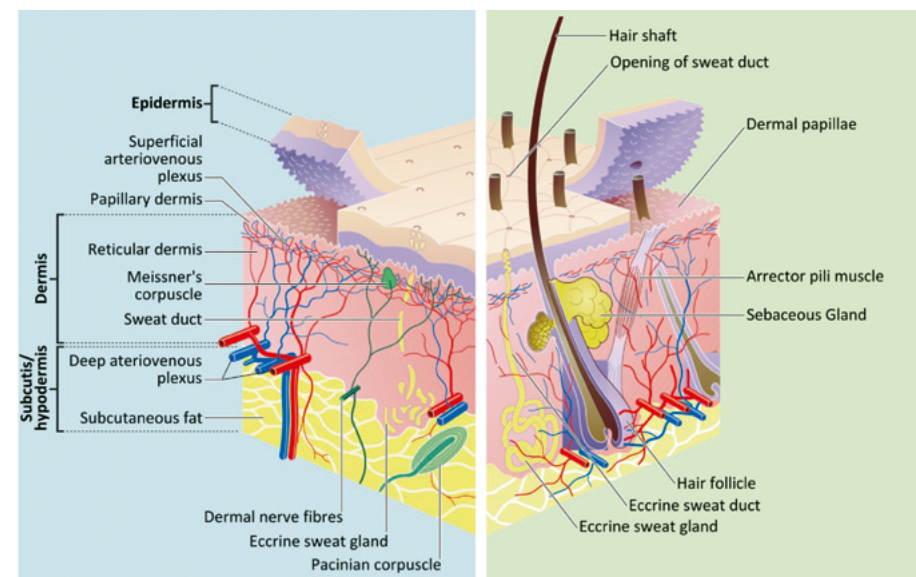
Figure 1: A cross-section of human skin tissue [11].

3.2. Sample collection methods

Skin tissue samples are typically obtained by three different methodologies with variable levels of invasiveness: tape stripping (section 3.2.1) can be considered less invasive, while skin punch biopsies (section 3.2.2) and shaving methods (section 3.2.3) are more invasive. Applying these different methodologies result in the isolation of different skin layers. For some applications the dermis and epidermis should be separated (section 3.2.4) before sample homogenization can take place to release the analytes from the biomatrix. Other methodologies to determine *in vivo* skin drug concentrations, such as microdialysis techniques, do not involve sampling of skin tissue and are out of the scope of this review.

3.2.1. Tape stripping method

Dermal tape stripping is performed using stripping tapes with a pre-specified surface area that peel off superficial layers of the skin of subjects by applying pressure (Figure 2). It is used for the identification or quantification of analytes in the stratum corneum. The stratum corneum is peeled away using a number of tapes [12,13]. The tapes are weighed prior to and after the stripping procedure to assess the amount of skin tissue adhering to each tape strip [14]. Commonly, the stratum corneum is stripped, while the dermis and epidermis remain. A typical amount of skin tissue obtained by skin-stripping tapes from washed skin is approximately 50 μg/cm², unwashed skin contains more debris which increases the typical mass per cm² [15–17]. Bioanalytical studies on tape strip samples were used for human skin [18–20] and porcine skin [21] to quantify 1,6-hexamethylene diisocyanate in relation to toxicity studies in the

skin, acetylaspartic acid and pyrrolidone carboxylic acid in cosmetics, and lidocaine local anesthetics. Obtaining layers of skin by dermal tape stripping is labor-intensive because the procedure needs to be done by hand using numerous tapes combined as a single sample. Analytes can be extracted from a stripping tape, e.g. by soaking the tapes in organic solvents followed by scraping the corneocytes from the tapes [20], or by more rigorous methods like bead homogenization of the tapes [18,19,21].
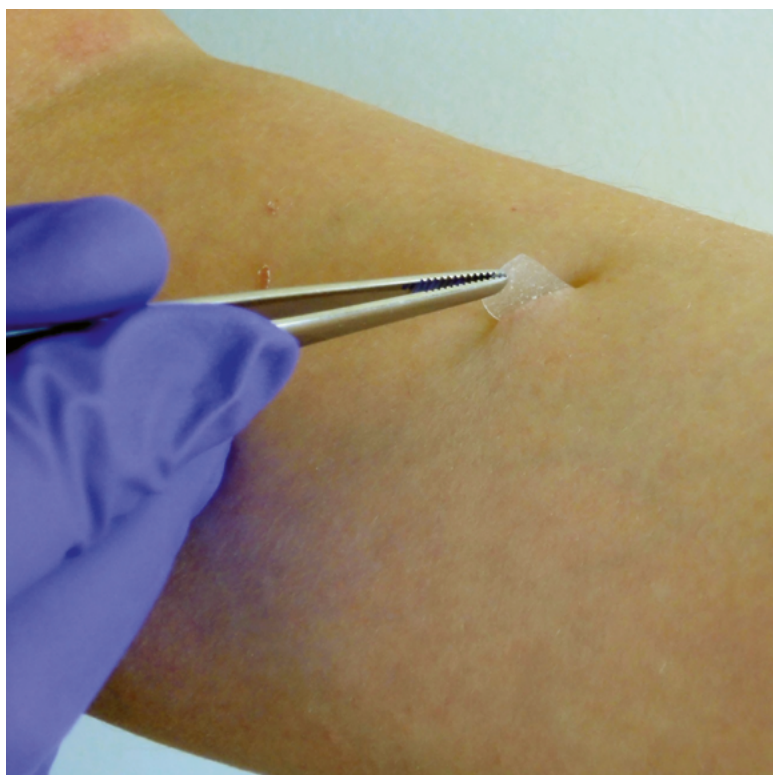

Figure 2: Peeling off the stratum corneum using the tape stripping method [22].

3.2.2. Skin punch biopsy

Various techniques have been applied to obtain a skin biopsy, which is usually obtained under local anesthesia. The skin punch biopsy is retrieved using a circular blade that ranges from 1 mm to 8 mm in diameter that is rotated by manual force though the skin layers until the hypodermis (fat layer) is reached and is retrieved by cutting through the subcutaneous fat layer (Figure 3) [23]. The skin punch biopsy is therefore cylindrical in shape. Typically, a 3 mm punch biopsy is used to obtain the biopsy, after which the resulting wound can be closed with a suture [23]. Smaller diameters often do not require suturing. Bioanalytical studies on skin punch biopsy samples were identified for human skin [24–26].
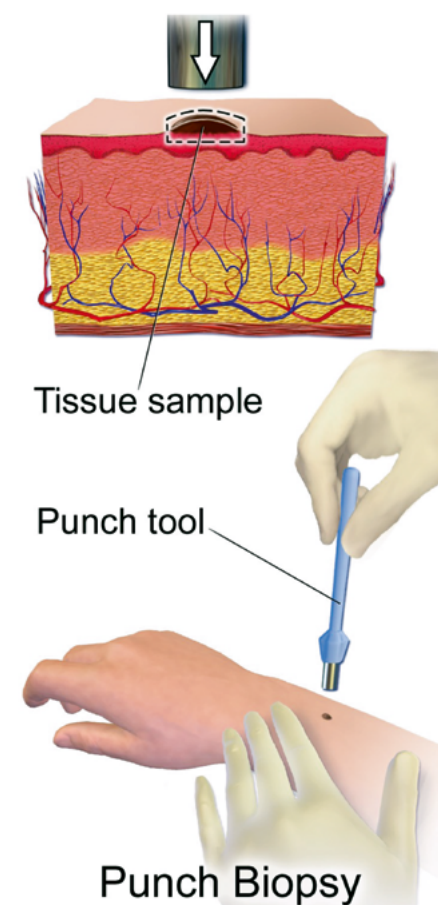

Figure 3: Skin punch biopsy method using a circular punch biopter [27].

3.2.3. Shaving methods

The shave biopsy technique is the most commonly used type of skin tissue sampling because of its simplicity [28]. Depending on the purpose, either a superficial shave biopsy or a saucerization biopsy can be used. Both methods shave the skin using a blade with a variable depth. Superficial shave biopsies yield the epidermis and the upper dermis, while saucerization biopsies yield a full-thickness biopsy, including dermis and possibly a fraction of subcutaneous fat [29]. Biopsies can be further categorized as incisional or excisional, for example removing a whole tumor is considered excisional, while removing a portion of the tumor is considered incisional. Such biopsies are usually taken with a scalpel and can be equally deep as skin punch biopsies, but lack the cylindrical shape[30]. Bioanalytical studies on shave biopsies were identified for both human [31–34] and animal skin [21,35–46].

3.2.4. Separation of dermis and epidermis

For some bioanalytical applications, there is an interest in the separation of the epidermis from the dermis after skin biopsy collection. This can be done by incubating the skin tissue for 1 hour in saline buffered water at 37°C [47]. Other methods involve incubation at 4°C with enzymatic solvents containing trypsin [48] or dispase [49] for 18 hours and incubating for 72 hours in 1 M NaCl and phenylmethylsulfonylfluoride (PMSF, a protease inhibitor) at 4°C [50]. After incubation, the epidermis and dermis are separated using forceps.

3.3. Sample homogenization methods

Homogenization of the tissue samples is necessary in order to release interstitial and intracellular analytes, prior to their extraction and quantification. Various methodologies for the homogenization of skin tissue have been described, aiming at a high level of cell disruption and a homogeneous suspension of cell constituents. The homogenization should ensure the transition of the skin tissue to a semisolid/suspension state [51] and preferably result in disruption of the cell structures. In total, 5 different homogenization methods were identified (Table 1), which are individually discussed below. Homogenization methods should preferably be amenable for high throughput and thus low in labor intensity and reliable, illustrated by low inter-sample variability.

3.3.1. Centrifugal precipitation

Precipitation is the simplest pre-treatment method with high throughput. A matrix is added to the skin and after mixing and centrifugation, the supernatant is used for analyte detection and quantification. Skin cell membranes are not disrupted by rotational force, which may lead to poor recovery of compounds that are mainly distributed intracellularly/interstitially and are thus not extracted in the precipitation matrix. The sample homogenization method has been used on mouse [35] skin biopsy samples using methanol/water (50/50, v/v) as matrix, the supernatant is then considered the skin tissue homogenate. Reproducibility might be dependent on the rotational force during centrifugation leading to variability in cell separation and analyte recovery [52].

3.3.2. Mechanical rotor-stator homogenization

Mincing of skin tissue is performed by using, for instance, a grater to cut skin tissue into a fine pulp. Rotational homogenization is a combination of mincing and pulverizing, showing similarities with bead homogenization (discussed later). A fast-rotating head shreds the skin tissue into smaller pieces using high-velocity rotational and collision forces. This homogenization procedure can be performed using a rotor-stator homogenizer or mixer, typically in a solvent such as blank plasma. Skin tissue

has also been homogenized using less specialized equipment, such as a cutter-mixer, a common kitchen appliance that has been used for bigger quantities of skin tissue samples. Animal skin tissue samples from pig [43,53], mouse [44], rabbit [41], rat [34,38,45], and chicken [46], as well as human [31,34] have all been homogenized using this method. The method of rotational homogenization is not always done high throughput since the speed depends on the size and thickness of the skin tissue and is performed using one sample at a time but it enables disruption of cell membranes by its high-velocity collisional force. In potential, a temperature-controlled environment will decrease variability in recovery given that the large acceleration energies might result in high uncontrolled local temperature differences, possibly affecting stability of the analyte.

3.3.3. Pulverization and grinding

Pulverization and grinding are more conventional homogenization methods and are performed using a tissue pulverizer or simply a mortar and pestle. The method has been applied to frozen human skin tissue samples from a full-thickness skin biopsy of which dermis and epidermis were separated from the stratum corneum [32]. A so-called Bessman tissue pulverizer makes use of a mortar and pestle, which fit tightly together to create a closed system. To increase performance, liquid nitrogen or dry ice can be added to the skin tissue sample in a tissue pulverizer and a hammer can be used to crush the frozen tissues into a powder-like form. Simple mortar and pestle methods can also efficiently break small frozen pieces of skin tissue to a powder form. This is performed simply with a pestle, grinding the frozen tissue into powdered form. Powdered skin tissue is suspended in solution for further analyte extraction. These methods are, however, highly labor-intensive and require extensive washing after each sample to prevent carryover and cross-contamination.

3.3.4. Bead homogenization

Bead homogenization is a combination of grinding and centrifugation. It is performed using stainless steel, zirconium or ceramic grinding balls, available in various sizes, in combination with a lysing solvent to disrupt the cells or plasma. Specialized cups and centrifuges are used in combination with these beads. Through high-velocity collision forces, the beads grind and disrupt the cell membranes, potentially resulting in the release of intracellular fluid. This methodology is commonly used for the homogenization of soft tissue samples. Although it is likely less effective for tough tissues, like skin, the method has been applied to human [24] as well as pig [21], mouse [40] and rat skin tissue [38]. This methodology can be considered versatile, as it can be applied to any type of skin tissue sample (tape stripped skin, full-thickness skin biopsy, and separated dermis and epidermis) and can be automated. The supernatant of the resulting homogeneous mixture is used for further extraction of the analyte. Bead homogenization is not labor-intensive and can be performed on multiple samples simultaneously.

Table 1: An overview of homogenization methods for skin tissue samples described in the selected studies.

Homogenization method	Homogenization specifications	Sampling method	Species	Analyte	Ref
Centrifugal precipitation					
	Centrifugation and supernatant extraction	Skin biopsy	Mouse	Digitoxigenin	[35]
	Cutting	Skin biopsy	Pig	Levamisole	[43]
				Clavulanic Acid	[53]
				Gefitinib	[44]
			Mouse	Capsaicin	[41]
		Stratum corneum tape stripping and skin biopsy	Rat	Avobenzone	[45]
Mechanical rotor-stator homogenization					
	Rotation by tissue tearer		Chicken	Ampicillin	[46]
			Human	Pegcantratinib	[31]
		Skin biopsy	Rat	Diclofenac	[38]
			Human and rat	Tigecycline	[34]
Pulverization and grinding					
	Mortar and pestle	Skin biopsy	Human	5-Methyltetrahydrofolate	[32]
	-	Skin biopsy	Pig	Lidocaine	[21]
		10 stripping tapes with stratum corneum		2,6-Dimethylaniline	
Bead homogenization					
	1.8- and 2.4-mm beads	Separation of dermis and epidermis by temperature incubation	Human	LEO 29102 Tofacitinib Ruxolitinib Tacrolimus	[24]
	0.9 – 2.0 mm beads	Skin biopsy	Rat	Diclofenac	[38]
Chemical/enzymatic solubilization					
	2 M ammonium hydroxide in 30% hydrogen peroxide	Separated dermis and epidermis using 1 M NaCl incubation	Human	Eumelanin and pheomelanin	[26]
	Collagenase in HEPES buffer	Skin biopsy	Rat	Diclofenac	[38]

3.3.5. Chemical and enzymatic solubilization

Chemical solubilization of skin tissue has been achieved using several techniques. Alkaline solvents can solubilize tissue structures due to hydrolysis mechanisms, while acidic solvents can lead to oxidation of the tissue structures [54]. Alkaline solubilization using 30% hydrogen peroxide in combination with 2 M ammonium hydroxide has been applied to human skin tissue [26]. Chemical tissue solubilization is typically performed under extremely high (e.g. ammonium hydroxide in hydrogen peroxide [26] or quaternary ammonium hydroxide compounds typically used in scintillation studies) or low pH (e.g. aqua regia) conditions, which means that the stability of analytes in these environments has to be assured. Enzymatic digestion using collagenase has also been used as a homogenization method and was performed on rat skin tissue [38]. Both chemical solubilization and enzymatic digestion of the tissue will, in theory, lead to a more complete release of intracellular and interstitial fluids than any of the other homogenization methods.

3.4. Analyte extraction methods

Extraction and purification of analytes can be performed by protein precipitation. This extraction procedure is conducted by dispersing homogenized skin tissue samples in precipitation agents, followed by centrifugation and separation of the supernatant and precipitant. The following analytes were extracted using this method: digitoxigenin [35], 4-n-butyl resorcinol [55], desmopressin acetate [33], gefitinib [44], avobenzone [45], 1,6-hexamethylene diisocyanate monomers and oligomers [18], pegcantratinib [31], acetylaspartic acid [19], tigecycline [34] and pyrrolidone carboxylic acid [20]. The solubility profile of the analyte determines the choice of sample collection homogenization precipitation agent. Filtration is often an addition to protein precipitation, separating filtrate from the rest of the homogenate in a semi-solid state. Solid particles will not pass the membrane of the filter and the filtrate is collected. Ultrafiltration employs semi-permeable membranes with specific molecular weight cut-offs, which can be used as an analyte extraction procedure [56,57] and can also be implemented for proteomic analysis [58]. Examples of analytes in skin tissue that were recovered after ultrafiltration were clavulanic acid [53] (using 30 kDa cut-off filters), 2,6-dimethylaniline [21] (using 10 kDa cut-off filters), ampicillin [46] (using 10 kDa cut-off filters). This extraction method was performed on full-thickness skin biopsies, homogenized by cutting, rotation by a tissue tearer and by bead homogenization methods. LLE or acid-base extraction methods have also been used to retrieve the following analytes from full-thickness skin biopsy homogenates and separated dermis and epidermis: capsaicin [41], levamisole [43], dexamethasone acetate [33], indomethacin [42] and diclofenac [38]. Centrifugal precipitation, cutting and bead homogenization were used as homogenization methods prior to LLE. SPE has been applied to skin tissue homogenates through (analyte-specific) ion-exchange mechanics, e.g. using a strong cation exchanger as stationary phase (levamisole [43] and lidocaine [21]) or a weak anion exchanger (eumelanin and pheomelanin[26]). SPE

3.1

is generally more labor-intensive compared to other analyte extractions; however, automated systems are available. Analyte selectivity and specificity are usually high due to the wide variety of sorbents that are available and various washing steps, producing relatively clean final extracts. SPE was used for different types of skin tissue samples; skin biopsies, and tape strips, either processed by mincing, cutting or bead homogenization [21,43]. An overview of analyte extraction methods of pre-treated skin tissue samples is provided (Table 2).

3.5. Matrix effects and recovery in skin tissue samples

The (sub-)cellular endogenous compounds released from the tissue cells during the homogenization procedures might give rise to increased matrix effects when using mass spectrometry detection. Matrix effects are typically more pronounced and challenging for tissue samples compared to plasma samples. Matrix effects and extraction recovery can be determined in multiple ways [2,7,59]. Sample homogenization and analyte extraction methods may influence the matrix effects and the recovery of the analytes of interest, and ultimately on the lower limit of quantification and/or reproducibility of the analytical method. Therefore, we have focused on reported matrix effects and recovery of analytes after skin tissue sample collection, homogenization, and extraction.

3.5.1. Matrix effects

Matrix effects are changes in the analytical signal that most often result from competition of analyte and undetected co-eluting factors from the sample matrix, causing ion suppression or enhancement compared to the analyte signal from non-biological matrices [7,60,61]. This theory is widely accepted, yet the origin and mechanisms are not fully understood [60–63]. Matrix effects are expressed as absolute matrix effect from the analyte peak area or as normalized IS matrix effects from the analyte/IS peak ratio. The skin tissue matrix consists of a diverse range of tissue constituents (in the solid and liquid phase), leading to a heterogeneous type of sample, in contrast to homogeneous plasma samples [7,9]. Increasing the complexity of the matrix may in theory increase matrix effects due to an increased diversity of endogenous substances in the sample, although this might be highly analyte- and tissue-dependent [64]. Absolute matrix effects of biological samples are likely to decrease when increasing the sample cleanup process steps such as extractions, as well as the separation power of the LC system. Reported absolute or IS-normalized matrix effects for the identified skin sample preparation methods appeared to be minimal (Table 3), showing no absolute or IS-normalized matrix effects for any of the reported homogenization/extraction methods or skin sources [21,31,34,35,38,41,45]. This IS-normalized matrix effect requires to be ≤15% CV in the validation of a bioanalytical assay according to the U.S. Food and Drug Administration (FDA) or European Medicines Agency (EMA) guidelines [65–67].

Table 2: Analyte extraction methods used in combination with different sample collection and homogenization methods for skin tissue samples.

Analyte extraction method	Sample collection method	Homogenization method	Species	Analyte	Ref
	Skin biopsy	Centrifugal precipitation	Mouse	Digitoxigenin	[35]
	Stratum corneum tape stripping, dermis and epidermis	-	Human	4-n-Butyl Resorcinol	[55]
	Skin tissue	-	Human	Desmopressin Acetate	[33]
		Cutting	Mouse	Gefitinib	[44]
	Stratum corneum tape stripping and skin biopsy	Rotation by tissue tearer	Rat	Avobenzone	[45]
Protein Precipitation	Tape stripped skin tissue	-	Human	1,6-Hexamethylene Diisocyanate	[18]
	Skin biopsy	Rotation by tissue tearer	Human	Pegcantratinib	[31]
			Human	Acetylaspartic Acid	[19]
	Tape stripped skin tissue	-	Human	Pyrrolidone Carboxylic Acid	[20]
	Skin biopsy	Rotation by tissue tearer	Human & rat	Tigecycline	[34]
		Cutting	Pig	Clavulanic acid	[53]
Ultrafiltration	Skin biopsy	Bead homogenization	Pig	2,6-Dimethylaniline	[21]
		Rotation by tissue tearer	Chicken	Ampicillin	[46]

Table 2: Analyte extraction methods used in combination with different sample collection and homogenization methods for skin tissue samples. (continued)

Analyte extraction method	Sample collection method	Homogenization method	Species	Analyte	Ref
	Skin biopsy	Centrifugal precipitation	Rabbit	Capsaicin Dihydrocapsaicin	[41]
		Cutting	Pig	Levamisole	[43]
		Centrifugal precipitation	Mouse	Indomethacin	[42]
LLE/Acid-Base extraction	Skin biopsy	Chemical/enzymatic solubilization, bead homogenization and rotation by tissue tearer	Rat	Diclofenac	[38]
	Skin biopsy	Cutting	Pig	Levamisole	[43]
SPE	Dermal stripping tapes	Bead homogenization	Pig	Lidocaine	[21]
	Epidermis	Chemical/enzymatic solubilization	Human	Eumelanin and pheomelanin	[26]

3.5.2. Recovery

Assessing the true recovery of analytes from tissue samples is challenging as pre-extraction spiking of the matrix is complicated, given that the analyte does not necessarily distribute to the intracellular/interstitial space as it would do in *in vivo* settings. Extraction recovery can be assessed by spiking tissue/plasma homogenates prior to extraction and compare this to post-extraction spiked matrix samples [8,65,67]. Establishing the overall recovery from plasma samples is less challenging compared to the overall recovery using tissue samples. Spiking analyte working solution to tissue homogenates pre-and post-extraction might give recovery from the extraction process but will not establish recovery during the homogenization process. The real concentration inside the tissue is unknown and the reproducibility of tissue sample treatment remains unidentified, which means true recovery cannot be determined. In pre-clinical studies, assessing true recovery could e.g. be done by administering a radiolabeled analyte [3,8]. None of the identified studies reported true recovery but rather established extraction recovery by spiking the skin tissue homogenates with analyte [18,21,26,31,34,35,38,41,42,44–46,53,65–67]. Centrifugal precipitation sample pre-treatment in combination with several extraction procedures resulted in the lowest extraction recovery (between 49.5 and 78.6%, Table 3), possibly due to a lack of tissue disruption and subsequent absence of matrix constituents in the supernatant. Adding analytes to non-homogenized samples for the determination of extraction recovery for a longer period could lead to diffusion into the tissue cells by unintentional incubation. If the tissue sample is not properly disrupted afterward this might result in an underestimation of extraction recovery. All the other homogenization methods led to extraction recoveries >78.2% (Table 3).

4. Discussion & conclusion

This review provides a comprehensive overview of general sampling methods and corresponding pre-treatment and analyte extraction methods for skin tissue samples collected in *in vivo* clinical and pre-clinical studies for the quantification of small molecules through liquid chromatography coupled to mass spectrometry (LC-MS).

Skin tissue samples are collected using invasive sampling methods such as punch or shaving biopsies, while tape stripping is a less invasive methodology. After collection, skin tissue samples require homogenization to disrupt the cell membranes of the skin tissue cells to release intracellular and interstitial constituents [51]. Different mechanical skin tissue homogenization methods have been applied, as well as chemical solubilization methods, e.g., using 30 % hydrogen peroxide in combination with 2 M ammonium hydroxide or enzymatic digestion methods using collagenase. Matrix effects and recovery experiments were conducted for skin tissue homogenization methods in combination with analyte extraction procedures.

3.1

In none of the studies, significant matrix effects were observed (C.V. >15%), neither in terms of IS-normalized or absolute analyte response (Table 3). This might indicate that endogenous constituents from the skin matrix generally have no substantial effect on the absolute analyte response in bioanalytical assays.

Extraction recovery was on the other hand not always optimal. Skin tissue centrifugal precipitation as a homogenization technique exhibited relatively low extraction recoveries compared to other homogenization methods (Table 3). This could be caused by the diffusion of the spiked analyte into the intact skin tissue matrix, which remains later unrecovered due to inefficient homogenization. This tissue partitioning is dependent on physical chemical properties, indicating that recovery may be highly analyte dependent. Additionally, LLE demonstrated consistently relatively low extraction recoveries as well. Given the low extraction recoveries, either centrifugal precipitation as homogenization or LLE as extraction, or a combination of both, are not recommended. No substantial difference in extraction recovery was found for the other homogenization methods and extraction methods.

Disruptiveness of the skin tissue homogenization technique appears defining for the extraction recovery but might also be pivotal for the homogenization efficiency and thus true recovery. While extraction recovery can be determined for the skin tissue matrix, true recovery (including homogenization recovery) is typically not possible to assess. It is therefore crucial that homogenization efficiency is evaluated as much as possible by alternative means, e.g., through visual inspection or by evaluating the recovery of a known endogenous marker in the tissue, such as the total amount of protein present after homogenization. However, except from the tigecycline study [34], no other study in our review reported on these aspects explicitly or mentioned the bias in trueness due to missing true recovery data. Chemical solubilization or enzymatic degradation homogenization methods may lead, theoretically, to the highest degree of homogenization or disruption of the tissue and would, therefore, be preferred in terms of homogenization efficiency. Although true recovery cannot be assessed, in theory these methodologies should result in a more complete release of compounds from the interstitial and intracellular space. However, stability of the analyte of interest under these conditions must be assured. Stability, matrix effects and extraction recovery need to be assessed, especially when chemical solubilizers (extreme high/low pH) or elevated incubation temperatures (collagenase) are used, which are necessary to completely homogenize or dissolve the skin tissue. In addition, the compatibility of these solubilizers with the subsequent extraction and chromatography methodologies need to be fully evaluated. Method development may, therefore, be more complex than for other sample preparation methods.

Table 3: Extraction recoveries and matrix effects established in the selected studies after applying different analyte extraction method and homogenization methods to skin tissue samples. Matrix factors are shown as % or numerical as the literature stated.

Extraction Method	Homogenization Method	Extraction Recovery	IS-Normalized Matrix Effect	Absolute Matrix Effect	Analyte	Ref
		70.7%–78.6%	-	90.5%–107%	Capsaicin	[41]
LLE	Centrifugal precipitation	63.1%–68.0%	-	91.2%–107.2%	Dihydrocapsaicin	[42]
		49.53%	-	-	Indomethacin	[38]
	Enzymatic digestion, bead homogenization and rotation by tissue tearer	64.5%–68.4%	0.90–1.10	0.97–1.02	Diclofenac	[21]
SPE	Bead homogenization	78.2%–98.0%	0.99–1.06	1.06–1.14	Lidocaine	[26]
	Chemical solubilization	79.3%	-	-	Eumelanin and pehomelanin	[35]
	Centrifugal precipitation	65.3%–79.5%	-	90.3%–104.1%	Digitoxigenin	[45]
		93.7%–106.5%	-	93.5%–110.4%	Avobenzone	[31]
Protein precipitation	Mincing/Cutting/Rotation by tissue tearer	86.4%–93.7%	0.91–1.02	0.92–1.05%	Pegcantratinib	[44]
		87.6%–100.9%	-	-	Gefitinib	[34]
		92.2%	-	94.5%–105.5%	Tigecycline	[18]
	-	106–116%	-	-	1,6-Hexamethylene Diisocyanate Mono/Oligomers	[53]
Ultrafiltration	Mincing/Cutting/Rotation by tissue tearer	95.5%–102.2%	-	-	Clavulanic acid	[46]
		93.0%	-	-	Ampicillin	

Given that true recovery of the analyte of interest is difficult to assess, emphasis should be given to the extent of homogenization during the development of sample preparation and extraction methods of skin tissue samples. Therefore, homogenization plays a crucial role in the accuracy of quantification if the true recovery cannot be evaluated. Chemical or enzymatic solubilization of skin tissue samples is preferable, because of the complete release of intracellular and extracellular components into the solubilization matrix. The inability to assess true recovery may lead to estimations of the pharmaceutical compound concentration in skin tissue instead of accurate quantifications. However, if the method is reproducible, it will be able to measure the relative distribution of drugs from plasma into the skin and this is of clinical importance to improve formulations or to optimize dosing strategies.

Funding

References

[1] M. Rizk, L. Zou, R. Savic, K. Dooley, Importance of Drug Pharmacokinetics at the Site of Action, Clin. Transl. Sci. 10 (2017) 133–142. https://doi.org/10.1111/cts.12448.

[2] Y.-J. Xue, H. Gao, Q.C. Ji, Z. Lam, X. Fang, Z. Lin, M. Hoffman, D. Schulz-Jander, N. Weng, Bioanalysis of drug in tissue: current status and challenges, Bioanalysis. 4 (2012) 2637–2653. https://doi.org/10.4155/bio.12.252.

[3] H. Neubert, S. Fountain, L. King, T. Clark, Y. Weng, D.M. O'Hara, W. Li, S. Leung, C. Ray, J. Palandra, M.F. Ocaña, J. Chen, C. Ji, M. Wang, K. Long, B. Gorovits, E. Fluhler, Tissue bioanalysis of biotherapeutics and drug targets to support PK/PD, Bioanalysis. 4 (2012) 2589–2604. https://doi.org/10.4155/bio.12.234.

[4] N.J. Lowe, R.E. Ashton, H. Koudsi, M. Verschoore, H. Schaefer, Anthralin for psoriasis: Short-contact anthralin therapy compared with topical steroid and conventional anthralin, J. Am. Acad. Dermatol. 10 (1984) 69–72. https://doi.org/10.1016/S0190-9622(84)80046-8.

[5] J.L. Lesher, Oral therapy of common superficial fungal infections of the skin, J. Am. Acad. Dermatol. 40 (1999) S31–S34. https://doi.org/10.1016/S0190-9622(99)70395-6.

[6] E.A. Alwawi, S.L. Mehlis, K.B. Gordon, Treating psoriasis with adalimumab, Ther. Clin. Risk Manag. 4 (2008) 345–351.

[7] S. Ho, Challenges of atypical matrix effects in tissue, Bioanalysis. 5 (2013) 2333–2335. https://doi.org/10.4155/bio.13.209.

[8] L. Yuan, L. Ma, L. Dillon, R.M. Fancher, H. Sun, M. Zhu, L. Lehman-McKeeman, A.-F. Aubry, Q.C. Ji, Investigation of the "true" extraction recovery of analytes from multiple types of tissues and its impact on tissue bioanalysis using two model compounds, Anal. Chim. Acta. 945 (2016) 57–66. https://doi.org/10.1016/j.aca.2016.09.039.

[9] B. Alberts, D. Bray, K. Hopkins, A. Johnson, J. Lewis, M. Raff, K. Roberts, P. And Walter, Essential Cell Biology, 3rd ed., New York, 2009.

[10] I. McColl, Rook's Textbook of Dermatology, Australas. J. Dermatol. 46 (2005) 206–206. https://doi.org/10.1111/j.1440-0960.2005.00184.x.

[11] M. M.Komorniczak, File: Skin_layers - Wikimedia Commons, (2012). https://commons.wikimedia.org/wiki/File:Skin_layers.svg (accessed August 29, 2019).

[12] C. Surber, F.P. Schwarb, E.W. Smith, Tape-stripping technique, J. Toxicol. Cutan. Ocul. Toxicol. 20 (2001) 461–474. https://doi.org/10.1081/CUS-120001870.

[13] N. V. Sheth, M.B. McKeough, S.L. Spruance, Measurement of the Stratum Corneum Drug Reservoir to Predict the Therapeutic Efficacy of Topical Iododeoxyuridine for Herpes Simplex Virus Infection, J. Invest. Dermatol. 89 (1987) 598–602. https://doi.org/10.1111/1523-1747.ep12461357.

[14] J.J. Escobar-Chavez, V. Merino-Sanjuán, M. López-Cervantes, Z. Urban-Morlan, E. Piñón-Segundo, D. Quintanar-Guerrero, A. Ganem-Quintanar, The Tape-Stripping Technique as a Method for Drug Quantification in Skin, J. Pharm. Pharm. Sci. 11 (2008) 104. https://doi.org/10.18433/J3201Z.

[15] H.-J. Weigmann, U. Lindemann, C. Antoniou, G.N. Tsikrikas, A.I. Stratigos, A. Katsambas, W. Sterry, J. Lademann, UV/VIS Absorbance Allows Rapid, Accurate, and Reproducible Mass Determination of Corneocytes Removed by Tape Stripping, Skin Pharmacol. Physiol. 16 (2003) 217–227. https://doi.org/10.1159/000070844.

[16] H.-J. Weigmann, J. Lademann, H. Meffert, H. Schaefer, W. Sterry, Determination of the Horny Layer Profile by Tape Stripping in Combination with Optical Spectroscopy in the Visible Range as a Prerequisite to Quantify Percutaneous Absorption, Skin Pharmacol. Physiol. 12 (1999) 34–45. https://doi.org/10.1159/000029844.

[17] E. Marttin, M.T.A. Neelissen-Subnel, F.H.N. De Haan, H.E. Boddé, A Critical Comparison of Methods to Quantify Stratum corneum Removed by Tape Stripping, Skin Pharmacol. Physiol. 9 (1996) 69–77. https://doi.org/10.1159/000211392.

[18] K.W. Fent, K. Jayaraj, L.M. Ball, L.A. Nylander-French, Quantitative monitoring of dermal

and inhalation exposure to 1,6-hexamethylene diisocyanate monomer and oligomers, J. Environ. Monit. 10 (2008) 500. https://doi.org/10.1039/b715605g.

[19]   L. Duracher, L. Visdal-Johnsen, A. Mavon, In vitro and in vivo dermal absorption assessment of acetyl aspartic acid: a compartmental study, Int. J. Cosmet. Sci. 37 (2015) 34–40. https://doi.org/10.1111/ics.12255.

[20]   M. Jung, J. Choi, S.-A. Lee, H. Kim, J. Hwang, E.H. Choi, Pyrrolidone carboxylic acid levels or caspase-14 expression in the corneocytes of lesional skin correlates with clinical severity, skin barrier function and lesional inflammation in atopic dermatitis, J. Dermatol. Sci. 76 (2014) 231–239. https://doi.org/10.1016/j.jdermsci.2014.09.004.

[21]   Q. Li, T. Magers, B. King, B.J. Engel, R. Bakhtiar, C. Green, R. Shoup, Measurement of lidocaine and 2,6-dimethylaniline in minipig plasma, skin, and dermal tapes using UHPLC with electrospray MS/MS, J. Chromatogr. B. 1087–1088 (2018) 158–172. https://doi.org/10.1016/j.jchromb.2018.04.030.

[22]   T. Sadowski, C. Klose, M.J. Gerl, A. Wójcik-Maciejewicz, R. Herzog, K. Simons, A. Reich, M.A. Surma, Large-scale human skin lipidomics by quantitative, high-throughput shotgun mass spectrometry, Sci. Rep. 7 (2017) 43761. https://doi.org/10.1038/srep43761.

[23]   Thomas J. Zuber, Punch Biopsy of the Skin - American Family Physician, Am. Fam. Physician. (2002) 1155–1158. http://www.aafp.org/afp/2002/0315/p1155.html.

[24]   I.S. Sørensen, C. Janfelt, M.M.B. Nielsen, R.W. Mortensen, N.Ø. Knudsen, A.H. Eriksson, A.J. Pedersen, K.T. Nielsen, Combination of MALDI-MSI and cassette dosing for evaluation of drug distribution in human skin explant, Anal. Bioanal. Chem. 409 (2017) 4993–5005. https://doi.org/10.1007/s00216-017-0443-2.

[25]   G. Szekely-Klepser, K. Wade, D. Woolson, R. Brown, S. Fountain, E. Kindt, A validated LC/MS/MS method for the quantification of pyrrole-2,3,5-tricarboxylic acid (PTCA), a eumelanin specific biomarker, in human skin punch biopsies, J. Chromatogr. B. 826 (2005) 31–40. https://doi.org/10.1016/j.jchromb.2005.08.002.

[26]   C.M. Lerche, P. Olsen, C.V. Nissen, P.A. Philipsen, H.C. Wulf, A novel LC-MS/MS method to quantify eumelanin and pheomelanin and their relation to UVR sensitivity – A study on human skin biopsies, Pigment Cell Melanoma Res. 32 (2019) 809–816. https://doi.org/10.1111/pcmr.12805.

[27]   BruceBlaus, File:Skin Punch Biopsy.png - Wikimedia Commons, (2017). https://commons.wikimedia.org/wiki/File:Skin_Punch_Biopsy.png (accessed July 4, 2019).

[28]   K.T. Tran, N.A. Wright, C.J. Cockerell, Biopsy of the pigmented lesion—When and how, J. Am. Acad. Dermatol. 59 (2008) 852–871. https://doi.org/10.1016/j.jaad.2008.05.027.

[29]   P.C. Ng, D.A. Barzilai, S.A. Ismail, R.L. Averitte, A.C. Gilliam, Evaluating invasive cutaneous melanoma: Is the initial biopsy representative of the final depth?, J. Am. Acad. Dermatol. 48 (2003) 420–424. https://doi.org/10.1067/mjd.2003.106.

[30]   H. Pickett, N. Air, F. Base, F. Medicine, M.O. Callaghan, F. Hospital, N. Air, F. Base, Shave and Punch Biopsy for Skin Lesions, (2011) 995–1002.

[31]   M. Zangarini, N. Rajan, M. Danilenko, P. Berry, S. Traversa, G.J. Veal, Development and validation of LC–MS/MS with in-source collision-induced dissociation for the quantification of pegcantratinib in human skin tumors, Bioanalysis. 9 (2017) 279–288. https://doi.org/10.4155/bio-2016-0199.

[32]   L.Z. Hasoun, S.W. Bailey, K.K. Outlaw, J.E. Ayling, Effect of serum folate status on total folate and 5-methyltetrahydrofolate in human skin, Am. J. Clin. Nutr. 98 (2013) 42–48. https://doi.org/10.3945/ajcn.112.057562.

[33]   M. Getie, R.H.. Neubert, LC–MS determination of desmopressin acetate in human skin samples, J. Pharm. Biomed. Anal. 35 (2004) 921–927. https://doi.org/10.1016/j.jpba.2004.02.009.

[34]   A. Ji Ji, J.P. Saunders, P. Amorusi, G. Stein, N.D. Wadgaonkar, K.P. O'Leary, M. Leal, E.N. Fluhler, Determination of tigecycline in human skin using a novel validated LC–MS/MS method, Bioanalysis. 2 (2010) 81–94. https://doi.org/10.4155/bio.09.159.

[35]   X. Feng, J. Turley, Z. Xie, S. V. Pierre, H. Koc, M.O. Khan, J. Hao, An LC–MS/MS method for the determination of digitoxigenin in skin samples and its application to skin permeation and metabolic stability studies, J. Pharm. Biomed. Anal. 138 (2017) 378–385. https://doi.org/10.1016/j.jpba.2016.12.029.

[36]   E.J. Park, M.S. Kim, Y.L. Choi, Y.-H. Shin, H.S. Lee, D.H. Na, Liquid chromatography–tandem mass spectrometry to determine the stability of collagen pentapeptide (KTTKS) in rat skin, J. Chromatogr. B. 905 (2012) 113–117. https://doi.org/10.1016/j.jchromb.2012.08.010.

[37]   L. Li, P. Ma, J. Wei, K. Qian, L. Tao, LC-ESI-MS method for the determination of dexamethasone acetate in skin of nude mouse, J. Chromatogr. B. 933 (2013) 44–49. https://doi.org/10.1016/j.jchromb.2013.06.024.

[38]   R. Nirogi, N.S.P. Padala, R.K. Boggavarapu, I. Kalaikadhiban, D.R. Ajjala, G. Bhyrapuneni, N.R. Muddana, Skin sample preparation by collagenase digestion for diclofenac quantification using LC–MS/MS after topical application, Bioanalysis. 8 (2016) 1251–1263. https://doi.org/10.4155/bio-2016-0031.

[39]   X.M.R. van Wijk, M.J. Vallen, E.M. van de Westerlo, A. Oosterhof, W. Hao, E.M. Versteeg, J. Raben, R.G. Wismans, T.F.C.M. Smetsers, H.B.P.M. Dijkman, J. Schalkwijk, T.H. van Kuppevelt, Extraction and structural analysis of glycosaminoglycans from formalin-fixed, paraffin-embedded tissues, Glycobiology. 22 (2012) 1666–1672. https://doi.org/10.1093/glycob/cws119.

[40]   J. Franco, C. Ferreira, T.J. Paschoal Sobreira, J.P. Sundberg, H. HogenEsch, Profiling of epidermal lipids in a mouse model of dermatitis: Identification of potential biomarkers, PLoS One. 13 (2018) e0196595. https://doi.org/10.1371/journal.pone.0196595.

[41]   D. Wang, F. Meng, L. Yu, L. Sun, L. Sun, J. Guo, A sensitive LC-MS/MS method for quantifying capsaicin and dihydrocapsaicin in rabbit plasma and tissue: application to a pharmacokinetic study, Biomed. Chromatogr. 29 (2015) 496–503. https://doi.org/10.1002/bmc.3302.

[42]   J. Ma, Y. Gao, Y. Sun, D. Ding, Q. Zhang, B. Sun, M. Wang, J. Sun, Z. He, Tissue distribution and dermal drug determination of indomethacin transdermal-absorption patches, Drug Deliv. Transl. Res. 7 (2017) 617–624. https://doi.org/10.1007/s13346-017-0392-5.

[43]   M. Cherlet, S. De Baere, S. Croubels, P. De Backer, Quantitative analysis of levamisole in porcine tissues by high-performance liquid chromatography combined with atmospheric pressure chemical ionization mass spectrometry, J. Chromatogr. B Biomed. Sci. Appl. 742 (2000) 283–293. https://doi.org/10.1016/S0378-4347(00)00171-7.

[44]   M. Zhao, C. Hartke, A. Jimeno, J. Li, P. He, Y. Zabelina, M. Hidalgo, S.D. Baker, Specific method for determination of gefitinib in human plasma, mouse plasma and tissues using high performance liquid chromatography coupled to tandem mass spectrometry, J. Chromatogr. B. 819 (2005) 73–80. https://doi.org/10.1016/j.jchromb.2005.01.027.

[45]   M.G. Kim, T.H. Kim, B.S. Shin, M.G. Kim, S.H. Seok, K.-B. Kim, J.B. Lee, H.G. Choi, Y.S. Lee, S.D. Yoo, A sensitive LC–ESI-MS/MS method for the quantification of avobenzone in rat plasma and skin layers: Application to a topical administration study, J. Chromatogr. B. 1003 (2015) 41–46. https://doi.org/10.1016/j.jchromb.2015.09.014.

[46]   K. Hamamoto, Y. Mizuno, LC-MS/MS measurement of ampicillin residue in chicken tissues at 2 days after in-feed administration, J. Vet. Med. Sci. 79 (2017) 474–478. https://doi.org/10.1292/jvms.15-0350.

[47]   M. Regnier, M. Prunieras, D. Woodley, Growth and Differentiation of Adult Human Epidermal Cells on Dermal Substrates, Front. Matrix Biol. 9 (1981) 4–35.

[48]   P.B. Medawar, Sheets of Pure Epidermal Epithelium from Human Skin, Nature. 148 (1941) 783–783. https://doi.org/10.1038/148783a0.

[49]   Y. KITANO, N. OKADA, Separation of the epidermal sheet by dispase, Br. J. Dermatol. 108 (1983) 555–560. https://doi.org/10.1111/j.1365-2133.1983.tb01056.x.

[50]   L.J. Scaletta, J.C. Occhino, D.K. MacCallum, J.H. Lillie, Isolation and immunologic identification of basement membrane zone antigens from human skin, Laboratory Investig.

39 (1978) 1–9.

[51]   C. Yu, L.H. Cohen, Not the Same Old Grind, Sample Prep. Perspect. LC-GC Eur. 17 (2004) 5.

[52]   C. DE DUVE, J. BERTHET, Reproducibility of Differential Centrifugation Experiments in Tissue Fractionation, Nature. 172 (1953) 1142–1142. https://doi.org/10.1038/1721142a0.

[53]   T. Reyns, S. De Boever, S. De Baere, P. De Backer, S. Croubels, Quantitative analysis of clavulanic acid in porcine tissues by liquid chromatography combined with electrospray ionization tandem mass spectrometry, Anal. Chim. Acta. 597 (2007) 282–289. https://doi.org/10.1016/j.aca.2007.06.056.

[54]   PerkinElmer, Application note: LSC Sample Preparation by Solubilization, (2008).

[55]   W. Wargniez, E. Jungman, S. Wilkinson, N. Seyler, S. Grégoire, Inter-laboratory skin distribution study of 4-n-butyl resorcinol: The importance of liquid chromatography/ mass spectrometry (HPLC–MS/MS) bioanalytical validation, J. Chromatogr. B. 1060 (2017) 416–423. https://doi.org/10.1016/j.jchromb.2017.05.026.

[56]   J. UEYAMA, K. KITAICHI, M. IWASE, K. TAKAGI, K. TAKAGI, T. HASEGAWA, Application of ultrafiltration method to measurement of catecholamines in plasma of human and rodents by high-performance liquid chromatography, J. Chromatogr. B. 798 (2003) 35–41. https://doi.org/10.1016/j.jchromb.2003.08.045.

[57]   F.-C. Cheng, J.-S. Kuo, L.-G. Chia, T.-H. Tsai, C.-F. Chen, Rapid measurement of the monoamine content in small volumes of rat plasma, J. Chromatogr. B Biomed. Sci. Appl. 654 (1994) 177–183. https://doi.org/10.1016/0378-4347(94)00002-6.

[58]   E. Chernokalskaya, S. Gutierrez, A.M. Pitt, J.T. Leonard, Ultrafiltration for proteomic sample preparation, Electrophoresis. 25 (2004) 2461–2468. https://doi.org/10.1002/elps.200405998.

[59]   F.L.S.T. Wenkui Li, Jie Zhang, Handbook of LC-MS bioanalysis : best practices, experimental protocols, and regulations, John Wiley & Sons, Inc., Hoboken, New Jersey, 2013.

[60]   P. Kebarle, L. Tang, From ions in solution to ions in the gas phase - the mechanism of electrospray mass spectrometry, Anal. Chem. 65 (1993) 972A-986A. https://doi.org/10.1021/ac00070a001.

[61]   B.K. Matuszewski, M.L. Constanzer, C.M. Chavez-Eng, Strategies for the Assessment of Matrix Effect in Quantitative Bioanalytical Methods Based on HPLC–MS/MS, Anal. Chem. 75 (2003) 3019–3030. https://doi.org/10.1021/ac020361s.

[62]   R. King, R. Bonfiglio, C. Fernandez-Metzler, C. Miller-Stein, T. Olah, Mechanistic investigation of ionization suppression in electrospray ionization, J. Am. Soc. Mass Spectrom. 11 (2000) 942–950. https://doi.org/10.1016/S1044-0305(00)00163-X.

[63]   A. Van Eeckhaut, K. Lanckmans, S. Sarre, I. Smolders, Y. Michotte, Validation of bioanalytical LC–MS/MS assays: Evaluation of matrix effects, J. Chromatogr. B. 877 (2009) 2198–2207. https://doi.org/10.1016/j.jchromb.2009.01.003.

[64]   W. Lv, Investigation of the effects of 24 bio-matrices on the LC–MS/MS analysis of morinidazole, Talanta. 80 (2010) 1406–1412. https://doi.org/10.1016/j.talanta.2009.09.043.

[65]   Food and Drug Administration, Guidance for Industry Bioanalytical Method Validation Guidance for Industry Bioanalytical Method Validation Center for Veterinary Medicine (CVM) Contains Nonbinding Recommendations, 2013.

[66]   European Medicines Agency, Committee for Medicinal Products for Human Use. Guideline on bioanalytical method validation, 2012. https://doi.org/EMEA/CHMP/EWP/192217/2009.

[67]   N. Kadian, K.S.R. Raju, M. Rashid, M.Y. Malik, I. Taneja, M. Wahajuddin, Comparative assessment of bioanalytical method validation guidelines for pharmaceutical industry, J. Pharm. Biomed. Anal. 126 (2016) 83–97. https://doi.org/10.1016/j.jpba.2016.03.052.

Development and validation of an HPLC-MS/MS method for the quantification of the anti-leishmanial drug miltefosine in human skin tissue

Ignace C. Roseboom
Bas Thijssen
Hilde Rosing
Fabiana Alves
Dinesh Mondal
Marcel B.M. Teunissen
Jos H. Beijnen
Thomas P.C. Dorlo

3.2

Abstract

Miltefosine is the only oral drug approved for the treatment of various clinical presentations of the neglected parasitic disease leishmaniasis. In cutaneous leishmaniasis and post-kala-azar dermal leishmaniasis, *Leishmania* parasites reside and multiply in the dermis of the skin. As miltefosine is orally administered and this drug is currently studied for the treatment of these skin-related types of leishmaniasis, there is an urgent need for an accurate assay to determine actual miltefosine levels in human skin tissue to further optimize treatment regimens through target-site pharmacokinetic studies. We describe here the development and validation of a sensitive method to quantify miltefosine in 4-mm human skin biopsies utilizing high-performance liquid chromatography coupled to tandem mass spectrometry. After the skin tissues were homogenized overnight by enzymatic digestion using collagenase A, the skin homogenates were further processed by protein precipitation and phenyl-bonded solid phase extraction. Final extracts were injected onto a Gemini C18 column using alkaline eluent for separation and elution. Detection was performed by positive ion electrospray ionization followed by a quadrupole – linear ion trap mass spectrometer, using deuterated miltefosine as an internal standard. The method was validated over a linear calibration range of 4 to 1000 ng/mL ($r^2 \geq 0.9996$) using miltefosine spiked digestion solution for calibration and quality control samples. Validation parameters were all within internationally accepted criteria, including intra- and inter-assay accuracies and precisions within ±15% and ≤15% (within ±20% and ≤20% at the lower limit of quantitation). There was no significant matrix effect of the human skin tissue matrix and the recovery for miltefosine, and internal standard were comparable. Miltefosine in human skin tissue homogenates was stable during the homogenization incubation (37°C, ±16 hours) and after a minimum of 10 days of storage at -20 °C after the homogenization process. With our assay we could successfully detect miltefosine in skin biopsies from patients with post-kala azar dermal leishmaniasis who were treated with this drug in Bangladesh.

1. Introduction

Miltefosine (hexadecylphosphocholine) (Figure 1) is the first FDA-approved oral drug for the treatment of various clinical phenotypes of the neglected tropical disease leishmaniasis [1]. While originally developed as an anti-cancer agent for the treatment of breast cancer and other solid tumours, miltefosine was ultimately found to be more potent as an antiprotozoal agent and has undergone further clinical development for the treatment of visceral leishmaniasis [2]. Besides visceral leishmaniasis, miltefosine is currently in use or undergoing further clinical development for the treatment of cutaneous leishmaniasis (CL) and post-kala-azar dermal leishmaniasis (PKDL), which are both caused by *Leishmania* parasite infections in the skin [3–8].

Previously published bioanalytical assays for the quantification of miltefosine were validated in blood-related bio-matrices like human plasma [9–11], human whole blood (volumetric absorptive microsampling and dried blood spots) [12,13], peripheral blood mononuclear cells [14] and rat and hamster plasma [10,15]. These assays and tools are pivotal to performing pharmacokinetic (PK) studies. Generally, PK studies in neglected tropical diseases have largely been lacking, although they are urgently needed to further optimize treatment regimens [16].

Target-site PK investigations are gaining popularity in clinical drug development as they provide useful insights about the actual concentration of a particular drug at the site of action of the drug, which help to determine how treatment regimens can be further optimized. This has led to an increasing interest in bioanalytical assays focussing on tissue bio-matrices, such as skin tissue [17–19]. For all types of leishmaniasis with dermal involvement, such as CL and PKDL, *Leishmania* parasites reside and multiply in the dermis of the skin. The efficacy of oral miltefosine for these clinical presentations of leishmaniasis will thus be critically dependent on the extent of drug penetration into the skin and the levels that can be maintained at this target-site. To our knowledge, no bioanalytical assay for the quantification of miltefosine in human skin tissue to enable skin PK studies in leishmaniasis, has been reported or published hitherto.

Developing bioanalytical methods in skin tissue is challenging. Skin tissue classifies as 'hard' tissue, requiring powerful sample preparation methods for homogenization [18]. Furthermore, the complete release of analytes into the matrix also requires extensive sample pre-treatment methods, with the risk of causing a higher matrix effect compared to plasma assays due to the release of endogenous matrix components, compromising the sensitivity of the assay [20]. Determination of the true recovery from (skin) tissues is challenging, and the accuracy of measurement deriving from non-dissolved analytes in the matrix is subject to the degree of destruction of tissue due to homogenization methods [19,21]. Chemical solubilization

3.2

or enzymatic digestion of (skin) tissue as a form of homogenization leads to the most accurate determination of analytes in the tissue since the complete sample is dissolved, provided that the analyte is stable during solubilization and sample pre-treatment [19]. However, these kinds of tissue solubilization methods have, to our knowledge, never been reported in the context of pharmaceutical bioanalytical assays on human skin tissue.

This study aimed to establish a sensitive and accurate method for the determination and quantification of miltefosine in human skin tissue, using healthy donor skin for the development. After development of this bioanalytical assay, including validation according to EMA and FDA guidelines [22,23], the clinical applicability of the developed assay was evaluated by measuring miltefosine concentrations in a selection of skin tissue samples originating from miltefosine-treated PKDL patients from Bangladesh, participating in a clinical pharmacokinetic study. To our knowledge, this is the first bioanalytical assay for the quantification of miltefosine in human skin tissue.

2. Materials and methods

2.1. Healthy human skin
Untreated control human skin tissue (n=2) was obtained as anonymized discarded tissue from corrective plastic surgery of the abdomen and breast. Punch biopsies of 4 mm diameter (40–60 biopsies per donor) were taken from normal-appearing skin and were immediately stored at -70°C until analysis. The biopsies were composed of only epidermis and dermis, as fatty tissue, if present, was removed. The study was carried out in agreement with the Dutch law (Medical Research Involving Human Subjects Act) and following the Declaration of Helsinki principles. According to the Dutch law, researchers are allowed to use anonymous human tissue without patient consent.

2.2. Chemicals
Miltefosine was purchased from Sigma-Aldrich (Zwijndrecht, the Netherlands) and its internal standard (d4-miltefosine) was purchased from Alsachim (Illkirch-Graffenstaden, France). Methanol, acetonitrile, and water (ULC grade) were bought from Biosolve Ltd (Valkenswaard, The Netherlands). Bovine serum albumin (BSA) fraction V and collagenase A were purchased from Roche (Woerden, the Netherlands). Triethylamine, ammonium acetate, ammonia 25% and acetic acid (glacial 100%) were supplied by Merck Chemicals B.V. (Amsterdam, the Netherlands), calcium chloride dihydrate and trisbase were from Sigma-Aldrich. Distilled water was acquired from B. Braun Medical (Melsungen, Germany), and phosphate-buffered saline (PBS) from Thermofischer (Breda, the Netherlands). Phenyl solid phase extraction cartridges were provided by Agilent (Amstelveen, the Netherlands).

2.3. Preparation of the digestion solution
A digestion solution was prepared as the blank matrix for the preparation of the calibration standards and quality control samples (see section 2.5). A 4% (g/v) BSA solution was made and diluted 1:1 (v/v) with 50 mM tris buffer (pH 7.5) to 2% BSA in 25 mM tris buffer (pH 7.5). Then, calcium chloride dihydrate was added to obtain a calcium chloride concentration of 5 mM and collagenase A to a concentration of 5 mg/mL. The mixture was mixed thoroughly at using a magnetic stirrer before use. The digestion solution was stored at -20°C.

2.4. Stock solutions and working solutions
Miltefosine stock solutions with a concentration of 1 mg/mL were made in methanol-water (1:1, v/v). Miltefosine stock solutions were separately made for calibration standards and quality control (QC) samples. The stock solutions were diluted in methanol-water (1:1, v/v) to obtain working solutions. A stock solution of internal standard (IS) was prepared in water at a concentration of 1 mg/mL. The working solution of the IS (WIS) was prepared by diluting the IS stock solution in methanol-water (1:1, v/v) to a final concentration of 4,000 ng/mL. Stock and working solutions were stored at -20°C.

2.5. Calibration standards, quality control samples
Calibration standards and quality control (QC) samples were prepared in the same way in batches in digestion solution before the start of the validation. Nine non-zero calibration standards were prepared by diluting the calibration standard working solutions 20 times in digestion solution (4, 10, 20, 50, 100, 200, 400, 800 and 1,000 ng/mL) and the same procedure was followed by diluting the QC sample working solutions 20 times in digestion solution to obtain QC samples at concentrations of 4, 12, 300 and 750 ng/mL (QC-LLOQ, QC-LOW, QC-MID, and QC-HIGH, respectively). Aliquots of 250 µL were stored at -20°C until analysis and were stable for at least 60 days (see section 3.2.7).

2.6. Tissue homogenization and sample preparation
After weighing a clean 1.5 mL reaction tube, one skin biopsy sample (average weight of a clinical full thickness skin tissue biopsy was 3.9 mg) was transferred to the tube and weighed again. A volume of 250 µL 100% PBS at room temperature was added to wash the skin tissue sample. After 30 min in a refrigerator (at 2-8°C), the reaction tube was vortexed, and the skin tissue was transferred using a polypropylene spatula to a clean 1.5 mL reaction tube containing 500 µL freshly prepared digestion solution. To the calibration standards (250 µL) and QC samples (250 µL), 25 µL of WIS (4,000 ng/mL) was added. To the skin tissue sample (500 µL), 50 µL of WIS (4,000 ng/mL) was added. Calibration standard, QC and skin tissue samples were incubated at 37°C overnight (≈16 hours) at 1,000 rpm in a thermomixer (VWR International BV, Amsterdam, the Netherlands). After incubation, the samples were vortex mixed 10 s. Prior to further

sample preparation, 275 µL of skin tissue sample homogenate was transferred to a clean 1.5 mL reaction tube. The remaining 275 µL was stored for re-analysis.

Protein precipitation was performed using 700 µL 2.5 M ammonium acetate (pH 4.5) and samples were centrifuged at 5°C for 5 minutes at 15,000 rpm. The phenyl-bonded solid phase extraction (SPE) cartridges were conditioned by adding 1 mL acetonitrile and 1 mL 2.5 M ammonium acetate (pH 4.5), then the total volume of the supernatant of the samples was added. The SPE cartridges were washed using 1 mL of water-methanol (1:1, v/v) and eluted using 1.5 mL 0.1% TEA in MeOH. The elution solvent was pipetted into glass autosampler vials before injection into the HPLC system.

2.7. LC equipment and conditions

The chromatographic system used was an UPLC LC-30AD pump with an inline degasser connected to a UPLC LC-30AMCP autosampler, set at 4°C and CTO-20AC column oven (Nexera X2 series, Shimadzu Corporation, Kyoto, Japan). Chromatographic separation was acquired using a Gemini C18 analytical column (Phenomenex, Torrance, CA, USA; 150 mm x 2.0 mm ID, 3.5 µm particles). The column temperature was kept at 30°C. The eluent consisted of 10 mM ammonium hydroxide in methanol-water (95:5, v/v), and was pumped through the analytical column at a flow rate of 0.3 mL/min. The purge and strong wash solvent used consisted of 0.1% formic acid in water-methanol (50:50, v/v). The chromatographic settings were replicated from previous assays developed by our research group on blood-related matrices using improved LC equipment [11–13,24].

2.8. MS equipment and conditions

Detection of miltefosine was performed using a QTRAP 6500 (Sciex, Framingham, MA, USA) quadrupole - linear ion trap MS equipped with a turbo ionspray interface operating in positive ion mode. The following settings were used: ion source voltage at 5500 V, ion source temperature at 750°C; ion source gas 1 at 30 psi (2.1 bar); ion source gas 2 at 35 psi (2.4 bar), curtain gas at 30 psi (2.1 bar) and collision gas at 10 psi (0.69 bar). Multiple reaction monitoring (MRM) mode was used to quantify miltefosine [M+H]$^+$ using the transition of m/z 408.231 → 125.046 and deuterated miltefosine (IS) with m/z 412.300 → 129.100 (Figure 1). Data acquisition and processing were performed with Analyst™ software (Sciex, version 1.6.2).

2.9. Validation procedures

The validation of the assay was performed based on the current EMA and FDA guidelines for the validation of bioanalytical assays in plasma, since no specific guidelines for bioanalytical assays in tissues are available [22,23]. The following validation parameters were established according to the FDA and EMA guidelines: calibration model, accuracy and precision, carry-over, selectivity (cross analyte/IS interferences), matrix effect, extraction recovery, dilution integrity, and stability under various conditions.
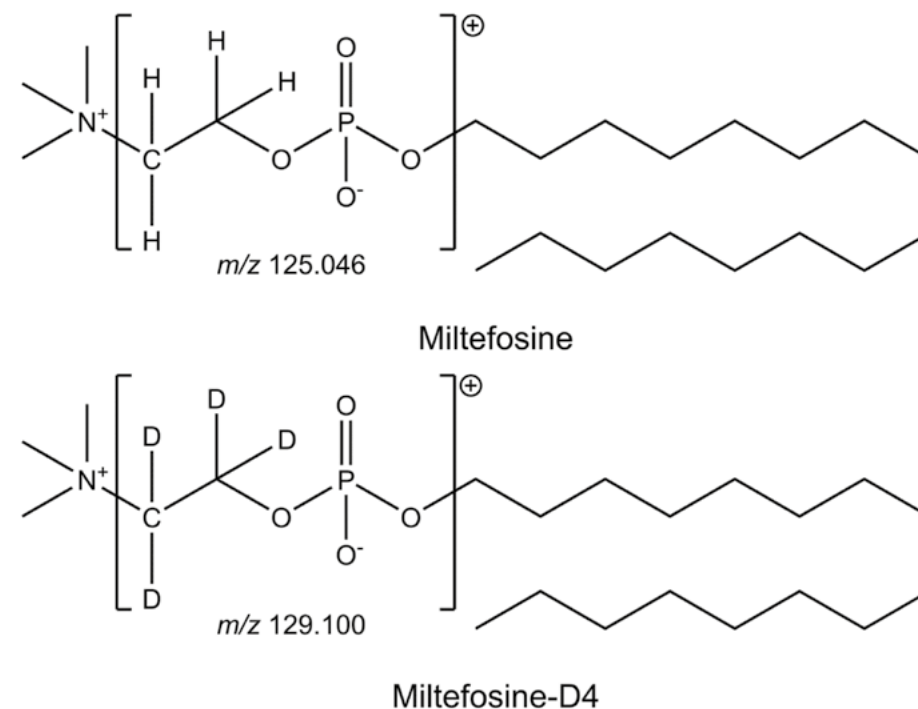

Figure 1: Chemical structures of miltefosine and miltefosine-D4 (IS), including fragmentation patterns in brackets and the mass-over-charge (m/z) of the monitored product ions.

2.10. Clinical application

This bioanalytical methodology was developed and validated to support skin target-site PK studies in various studies on miltefosine in the treatment of PKDL patients. Human skin biopsies were collected in the context of a clinical trial conducted in India and Bangladesh (CTRI/2017/04/008421), where an allometric dosing regimen of miltefosine was given for 21 days [25]. This trial was conducted following the Declaration of Helsinki principles and received ethical approval by all relevant local medical ethics committees. Full thickness skin tissue biopsy samples were collected in this trial on the last day of miltefosine treatment to account for maximal accumulation of miltefosine in the skin tissue. Skin tissue biopsies were stored and transported frozen at min -70 °C, after transport to Amsterdam, samples were kept frozen, likewise, at min -70 °C, until analysis. Before homogenization of the human skin tissue biopsies, the weight of each skin tissue biopsy was determined and from the measured concentration in ng/mL, the concentration of miltefosine in µg/g skin tissue was calculated for each individual human skin tissue sample. Miltefosine was also quantified in the washing step solution to assess the quality and relevance of the washing step during the development of the method. For this clinical application,

a selection of 5 skin biopsy samples were randomly selected from PKDL patients treated at the Surya Kanta Kala-Azar Research Centre, Mymensingh, Bangladesh.

3. Results and discussion

3.1. Development

3.1.1. Human skin tissue homogenization and sample preparation

Various mechanical homogenization approaches were tested as sample pre-treatments to homogenize human skin tissue biopsies, including bead homogenization, rotor-stator homogenization, and pulverization homogenization after freezing the human skin tissue with liquid nitrogen. These mechanical homogenization methods were, however, not able to fully homogenize skin tissue because intact pieces of skin tissue remained in solution after performing these techniques. Incomplete homogenization of tissues results in inaccurate quantification of the analyte because the analyte may still be bound to intact tissue and does not dissolve in the solution [19]. To overcome incomplete homogenization, a dissolution strategy was applied. Various dissolving methods were tested, including overnight incubation in 50% ammonia, 0.5 M quaternary ammonium hydroxide in toluene, 0.4 M quaternary ammonium hydroxide in water and enzymatic digestion. The 50% ammonia solution did not dissolve the skin tissue, whereas quaternary ammonium hydroxide did dissolve skin tissue fully, however, the chromatography of miltefosine was detoriated, and the responses were low due to severe matrix effects. These matrix effects had a significant effect on the sensitivity of the method. Enzymatic digestion using collagenase A fully dissolved skin tissue, except for the stratum corneum. This is not expected to affect the accuracy of measurements, since miltefosine penetration after oral administration into this keratinized layer of the skin with hardly any blood vessels is unlikely. Enzymatic digestion using collagenase A, unlike quaternary ammonium hydroxide homogenization, did not show significant matrix effects and the sensitivity was retained, so this homogenization method was eventually chosen.

The phenyl SPE sample preparation method has previously been described using plasma as a biological matrix [11]. A slight change was made to the sample clean-up. To enable protein precipitation, 2.5 M instead of 1 M ammonium acetate (pH 4.5) was used as the SPE loading solvent.
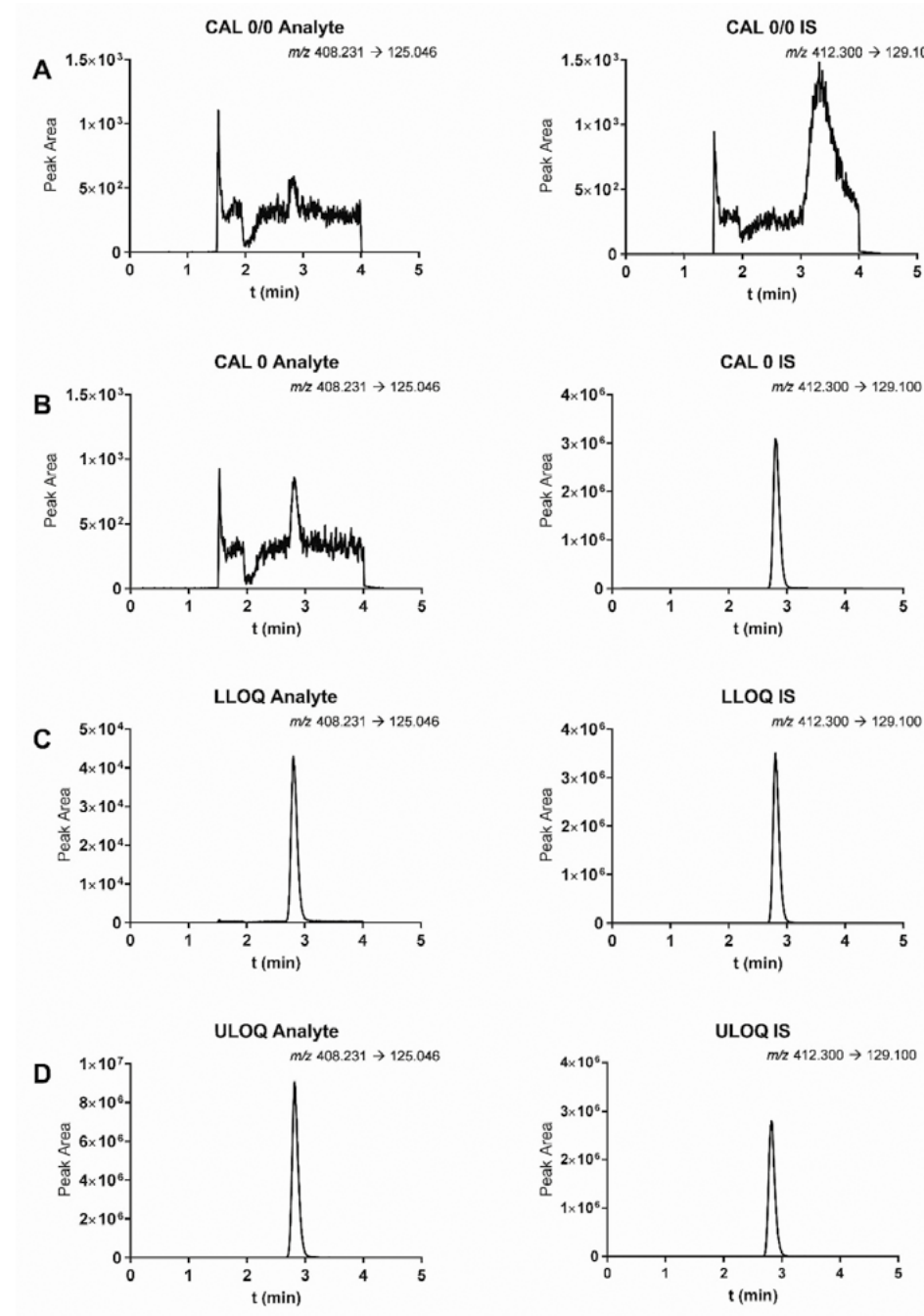

Figure 2: Representative MRM chromatograms showing the double blank (A), blank (B), LLOQ (4 ng/mL) (C) and ULOQ (1000 ng/mL) (D) of both miltefosine and IS samples in digestion solution.

3.2. Validation procedures

Human skin tissue samples are a rare bio-matrix and are difficult to acquire, therefore the final validation of the assay was performed in digestion solution. Additional tests (matrix effect, recovery and stability in skin biopsy homogenates) were performed to verify if this surrogate matrix could be used for the quantification of miltefosine in human skin biopsies, without making compromises in the accuracy and precision of the method.

3.2.1. Calibration model

Nine non-zero calibration standards ranging from 4-1,000 ng/mL were prepared in duplicate for each run in three separate validation runs. Linear regression was performed on the analyte peak area/IS peak area ratio versus nominal analyte concentration (x), weighted by a weighting factor of $1/x^2$. The deviations from the mean for each non-zero calibration standard should be within ±15% (±20% for the LLOQ) for a minimum of 75% of the non-zero standards. Correlation coefficient (r^2) of at least 0.9996 were obtained in three individual runs, along with back-calculated calibration standard concentrations within ±3.8% of the nominal concentration for all calibration standards. The minimum signal to noise ratio at the LLOQ concentration level of 4 ng/mL was 51:1. Representative MRM chromatograms are shown in Figure 2.

Table 1: Assay performance data for miltefosine. Accuracies and precisions were established in 3 analytical runs and each run contained 5 replicates per tested concentration.

Nominal miltefosine concentration (ng/mL)	Intra-assay (n = 15)		Inter-assay (n = 15)	
	Bias (%)	Precision (%)	Bias (%)	Precision (%)
4	-6.6 to -2.6	1.2 to 2.5	-4.6	1.9
12	-2.3 to -1.3	0.7 to 1.0	-1.8	0.3
300	-0.1 to 1.0	0.8 to 1.9	0.3	a
750	-0.0 to 0.7	0.8 to 1.0	0.2	a

a No substantial additional variation was found due to the performance of the assay in different runs.

3.2.2. Accuracy and precision

Intra-and inter-assay accuracy and precision were determined by measurements of five replicates of QC samples in three separate validation runs at the LLOQ (4 ng/mL), low (12 ng/mL), mid (300 ng/mL) and high (750 ng/mL) levels. The concentration of each sample was determined using the calibration standards and measured in the same batch. Accuracies were given as the bias from the nominal concentration and precision was calculated as the relative coefficient of variation (CV%). The intra-assay bias (%) is the bias of the mean measured concentration per analytical run as compared to the nominal concentration. The inter-assay bias (%) is the bias of the mean measured concentration in three analytical runs compared to the nominal concentration. The inter-run precision was calculated by performing a one-way ANOVA. The assay performance at the QC-LOW, QC-MID and QC-HIGH concentration levels was ±1.8% and ±2.3% for inter-and intra-assay accuracy, respectively, and ≤0.3% and ≤1.9% for inter-and intra-assay precision, respectively. At the LLOQ level, the inter-and intra-assay accuracies were 4.6% and ±6.6%, respectively, while the inter-and intra-assay precisions were 1.9% and ≤2.5% respectively. The acceptance criteria for both accuracy and precision values should be within ±15% and ≤15% (±20% and ≤20% at the LLOQ), respectively, and were therefore accepted. The inter-assay precision at QC-MID and QC-HIGH concentration levels could not be calculated as the between-assay mean square was less than the within-assay mean square, indicating that there is no substantial additional variation due to the performance of the assay between different runs. The assay performance data for miltefosine in digestion solution are summarized in Table 1.

3.2.3. Carry-over

Carry-over was evaluated by injecting two double blank samples after the upper limit of quantification (ULOQ, 1000 ng/mL) of the calibration standards. The peak areas at the retention times of the analyte and its internal standard detected in the double blank samples were compared to the mean area of the analyte and the IS in five QC-LLOQ samples. The carry-over was assessed in three separate validation runs. The peak areas in the double blank samples compared to the QC-LLOQ samples should be ≤20% for miltefosine and ≤5% for the IS. The analyte carry-over was ≤0.9% and for the IS no carry-over was observed. As a result, the carry-over fulfilled the acceptance criteria.

3.2.4. Cross-analyte/IS interference

Selectivity was evaluated in blank digestion solution without the use of blank (untreated control) skin biopsy homogenate. Matrix effects for the skin biopsy homogenate matrix were absent (see section 3.2.5), therefore using blank (i.e., untreated control) skin biopsy homogenates were not conditional for the evaluation of selectivity as the matrix did not affect the miltefosine chromatogram signals and blank digestion solution was used instead. Cross analyte/IS interferences were determined by spiking the analyte at the ULOQ concentration and separately the IS at the IS level. The interference of miltefosine with the IS should be ≤5% (peak area) and the interference of the IS with miltefosine should be ≤20% of the analyte peak area compared to the LLOQ samples. Miltefosine spiked at ULOQ level to digestion solution did not show any interference in the IS signal. The IS interference at the mass transition of miltefosine displayed a 1.2% interference, which was well within the acceptance criteria.

Table 2. Matrix factor and sample preparation recovery data for miltefosine and IS.

Nominal miltefosine concentration (ng/mL)	Matrix Factor Analyte	Matrix Factor IS	IS-normalized Matrix Factor	IS-normalized Matrix Factor C.V. (n=6)	Sample Preparation Recovery Analyte	Sample Preparation Recovery IS	IS-normalized Sample Preparation Recovery	IS-normalized Sample Preparation Recovery C.V. (n=3)
12	0.95	0.96	1.00	0.6%	73.3%	72.2%	101.5%	1.9%
750	0.94	0.94	1.00	0.8%	67.9%	68.6%	98.9%	1.1%

Abbreviation: C.V. = coefficient of variation

3.2.5. Matrix effect and extraction recovery

Matrix effect and recovery of the assay were determined through comparing samples prepared by spiking miltefosine before or after sample processing and homogenization at two QC levels (QC-LOW and QC-HIGH), using untreated control human skin tissue biopsy from a single individual. Matrix present samples were prepared in six-fold by spiking QC working solutions to a final extract resulting from fully processed blank skin biopsy samples. Matrix absent samples were prepared in three-fold by spiking QC working solutions to non-processed blank final extract matrix, 0.1% TEA in MeOH. Processed samples were prepared in three-fold by spiking QC working solutions to untreated control human skin tissue biopsies before tissue homogenization and sample pre-treatment, whereafter the standard sample treatment procedures, including homogenization of skin tissue, were performed as described in section 2.6.

The absolute matrix effect factor was calculated as the analyte or IS peak area ratio between matrix present and matrix absent samples at similar concentration levels. The mean absolute matrix factors for the analyte were 0.95 (ranging from 0.93-1.01) and 0.94 (ranging from 0.72-1.02) for QC-LOW and QC-HIGH concentration levels, respectively, indicating no significant absolute matrix factor interference by endogenous substances derived from homogenized skin tissue. Furthermore, the IS-normalized matrix effect factors, calculated as the ratio between the absolute matrix effect factor of miltefosine and IS, were 1.00 (ranging from 0.99-1.01) and 1.00 (ranging from 0.99-1.02) on average for QC-LOW and QC-HIGH levels, respectively. The IS-normalized matrix factor value is accepted, since the RSD is ≤0.8%, well within the acceptance criteria (≤15%).

The sample preparation recovery was calculated as the ratio between peak areas of the processed samples and matrix present samples for both analyte and IS. The analyte sample preparation recovery after the homogenization and sample pre-treatment procedure at QC-LOW and QC-HIGH concentration levels varied between 67.9 and 73.3%, with the IS sample preparation recovery varying between 68.6% and 72.2%. IS-normalized sample preparation recovery was calculated as the ratio between the sample preparation recovery of miltefosine and IS. The IS-normalized sample preparation recovery at the QC-LOW and QC-HIGH concentrations were 98.9% and 101.5%, respectively, showing no significant difference between the sample preparation recovery of analyte and IS, indicating that the IS corrected well for the lowered absolute sample preparation recovery of the analyte. The IS-normalized sample preparation recovery RSD is ≤1.9%. The matrix effect and sample preparation recovery data are summarized in Table 2.

3.2.6. Dilution integrity

Dilution integrity was determined by applying a ten-fold dilution of spiked digestion solution samples at a concentration of 5,000 ng/mL (5 times the ULOQ), performed in five-fold. The accuracy and precision were determined with acceptance criteria of ±15% bias and ≤15% CV%, respectively. The intra-assay bias and precision for the dilution were 1.0 and 1.2% respectively, thus the values were well within acceptance

criteria, leading to the conclusion that 10 times sample dilution does not alter the accuracy of the sample.

3.2.7. Stability

Short-term stability of miltefosine added to human skin tissue homogenates in digestion solution at QC-LOW and QC-HIGH levels was assessed up to 42 hours at 37°C and, in addition, up to 10 days at -20°C to allow storage of the digested skin sample prior to further sample preparation. Additionally, stability was assessed in final extracts at 2-8°C and was already established for both stock and working solutions at -20°C. Long-term stability in digestion solution at QC-LOW and QC-HIGH concentrations stored at -20°C was assessed for at least 60 days and the stability after 3 freeze/thaw cycles in digestion solution was determined. One freeze/thaw cycle included unassisted thawing at room temperature (±20°C) and subsequently freezing at -20°C for at least 12 consecutive hours. The acceptance criteria for the accuracy and precision for digestion solution, human skin tissue homogenates in digestion solution QC samples and final extracts were ±15% bias and ≤15% CV, respectively. Miltefosine present in human skin tissue homogenates in digestion solution and incubated up to 42 hours at 37°C or stored for 10 days at -20°C after digestion (in this case 16 hours incubation with collagenase A) appeared to be stable under these conditions as all measurements were within the criteria described above. Miltefosine in digestion solution stored at -20°C was stable for at least 3 freeze/thaw cycles and additionally for a minimum period of 60 days. The stability of final extracts was guaranteed for at least 60 days at 2-8°C. The stability data are summarized in Table 3.

Table 3. Stability data for miltefosine (n = 3 per quality control level) expressed by accuracy (bias %) and precision (coefficient of variation).

Matrix	Condition	Nominal Concentration (ng/mL)	Bias (%)	C.V. (%)
Digestion Solution	-20°C, F/T 3 cycles	12.0	1.4	1.3
		750	-1.6	0.9
Digestion Solution	-20°C, 60d	12.0	1.7	0.0
		750	-1.9	1.7
Human Skin Tissue Homogenate	-20°C, 10d	12.0	2.2	0.9
		750	-1.6	0.2
Human Skin Tissue Homogenate	37°C, 42h	12.0	2.2	1.2
		750	-0.4	1.3
Final extract	2-8°C, 60d	12.0	5.6	1.6
		750	1.1	0.4

Abbreviations: C.V. = coefficient of variation; d = days; F/T = freeze/thaw cycles; h = hours

3.3. Clinical application

The analytical method developed was used to determine miltefosine in a random selection of human skin tissue biopsies, originating from PKDL patients treated with miltefosine in Bangladesh. The assay performance was sufficiently sensitive as the presence of miltefosine could be quantified in all skin biopsies within the validated calibration range. Representative MRM chromatograms of one patient are shown in Figure 3 for both miltefosine and IS in the skin biopsy and washing step solution. Table 4 displays the miltefosine concentration in digestion solution (ng/mL), skin tissue (µg/g) and the washing step (ng/mL) at the end of treatment from 5 randomly selected individual PKDL patients treated at the Surya Kanta Kala Azar Research Centre, Mymensingh, Bangladesh. Skin biopsies were washed to avoid blood contamination of the skin biopsy concentrations. The high miltefosine concentrations in the washing step were expected and reflect the high miltefosine blood concentration at the time of sampling of the skin biopsy. The complete results from this target-site PK study in PKDL patients will be reported in more detail elsewhere.
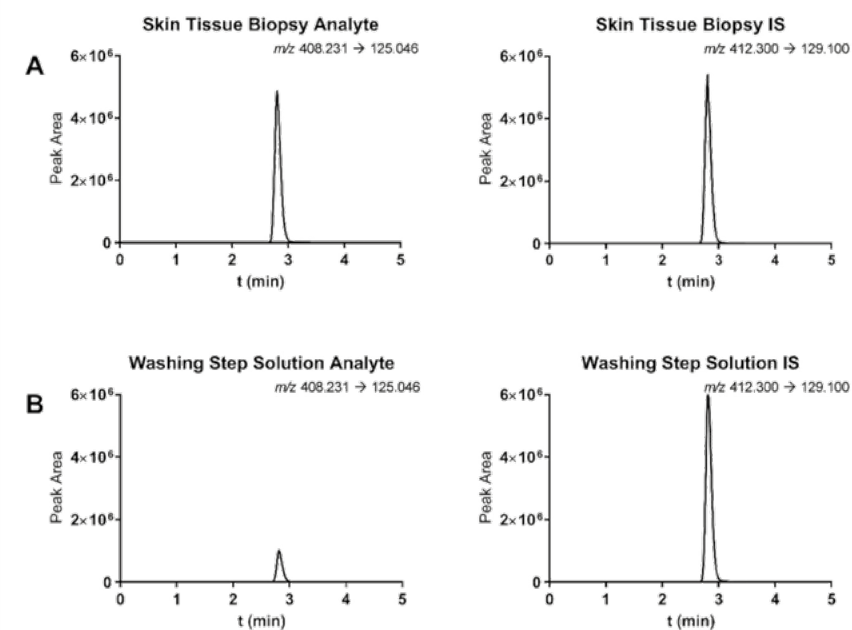

Figure 3: Representative MRM chromatograms of a clinical sample from a post kala-azar dermal leishmaniasis patient from Bangladesh, showing the skin biopsy (287 ng/mL or 51.6 µg/g) (A) and washing step (98.8 ng/mL) (B) chromatograms for both miltefosine and IS.

Table 4. Miltefosine skin tissue biopsy and washing step concentration data in 5 individual post kala-azar dermal leishmaniasis patients from Bangladesh at day 22 after receiving a 21-day miltefosine regimen.

Clinical Skin Biopsy #	Skin Biopsy Weight (mg)	Miltefosine Concentration in Digestion Solution (ng/mL)	Miltefosine Concentration in Skin Biopsy (µg/g)	Miltefosine Concentration in Washing Step Solution (ng/mL)
1	7.79	302	19.38	133
2	3.06	287	46.94	98.8
3	4.55	307	33.75	181
4	4.94	408	41.26	201
5	4.98	360	36.16	108

4. Conclusion

An accurate and sensitive bioanalytical assay was developed and validated for the quantification of miltefosine in 4-mm punch biopsies from human skin. Homogenization of skin tissue was necessary and was achieved after an overnight incubation with a digestion solution containing the enzyme collagenase A. Importantly, the presence of miltefosine could accurately be detected in this suspension of digested skin. Further sample preparation consisted of a salting out protein precipitation method using 2.5 M ammonium acetate (pH 4.5) to disrupt single cells originating from the tissue homogenization step followed by phenyl SPE using 0.1% triethylamine in methanol to elute miltefosine. The analytical setup consisted of an isocratic LC system connected to a QTRAP 65000 equipped with ESI in positive ion mode. The validated range of the assay is 4-1,000 ng/mL using a stable isotope labelled IS. Additionally, the method showed a high assay performance in the validated ranges concerning linearity (r^2 ≥0.9996), accuracy and precision, and miltefosine stability in skin tissue homogenates during the homogenization procedure and after 10 days of storage at -20°C. Subsequently, matrix effect and recovery experiments using untreated control human skin tissue biopsies indicated that there was no matrix effect of the human skin matrix on the performance of the assay and recovery was well corrected by the IS, meaning that a surrogate matrix of only digestion solution could be used as matrix for the preparation of calibration standards to accurately quantify miltefosine in human skin tissue homogenates. The bioanalytical assay was able to successfully detect and quantify miltefosine in human skin biopsies from patients with PKDL treated with oral administrated miltefosine in Bangladesh.

3.2

References

[1] Paladin Therapeutics, Impavido Package, Reference ID: 3473184, US Food Drug Adm. (2014).

[2] J. Engel, Miltefosine, the story of a successful partnership: disease endemic country - TDR - pharmaceutical industry (Zentaris), TDR News. (2002) 5. http://www.who.int/tdr/publications/documents/tdrnews-issue-68.pdf.

[3] S. Sundar, T.K. Jha, H. Sindermann, K. Junge, P. Bachmann, J. Berman, Oral miltefosine treatment in children with mild to moderate Indian visceral leishmaniasis, Pediatr. Infect. Dis. J. 22 (2003) 434–438. doi:10.1097/01.inf.0000066877.72624.cb.

[4] S. Sundar, T.K. Jha, C.P. Thakur, J. Engel, H. Sindermann, C. Fischer, K. Junge, A. Bryceson, J. Berman, Oral Miltefosine for Indian Visceral Leishmaniasis, N. Engl. J. Med. 347 (2002) 1739–1746. doi:10.1056/NEJMoa021556.

[5] J. Mbui, J. Olobo, R. Omollo, A. Solomos, A.E. Kip, G. Kirigi, P. Sagaki, R. Kimutai, L. Were, T. Omollo, T.W. Egondi, M. Wasunna, J. Alvar, T.P.C. Dorlo, F. Alves, Pharmacokinetics, Safety, and Efficacy of an Allometric Miltefosine Regimen for the Treatment of Visceral Leishmaniasis in Eastern African Children: An Open-label, Phase II Clinical Trial, Clin. Infect. Dis. 68 (2018) 1530–1538. doi:10.1093/cid/ciy747.

[6] J. Soto, J. Toledo, P. Gutierrez, R.S. Nicholls, J. Padilla, J. Engel, C. Fischer, A. Voss, J. Berman, Treatment of American Cutaneous Leishmaniasis with Miltefosine, an Oral Agent, Clin. Infect. Dis. 33 (2001) e57–e61. doi:10.1086/322689.

[7] S.L. Croft, G.H. Coombs, Leishmaniasis– current chemotherapy and recent advances in the search for novel drugs, Trends Parasitol. 19 (2003) 502–508. doi:10.1016/j.pt.2003.09.008.

[8] S. Burza, S.L. Croft, M. Boelaert, Leishmaniasis, Lancet. 392 (2018) 951–970. doi:10.1016/S0140-6736(18)31204-2.

[9] A.R. Godfrey, L. Jones, M. Davies, R. Townsend, Miltefosine: a novel internal standard approach to lysophospholipid quantitation using LC-MS/MS, Anal. Bioanal. Chem. 409 (2017) 2791–2800. doi:10.1007/s00216-017-0223-z.

[10] S. Jaiswal, A. Sharma, M. Shukla, J. Lal, LC-coupled ESI MS for quantification of miltefosine in human and hamster plasma, Bioanalysis. 8 (2016) 533–545. doi:10.4155/bio.16.7.

[11] T.P.C. Dorlo, M.J.X. Hillebrand, H. Rosing, T.A. Eggelte, P.J. de Vries, J.H. Beijnen, Development and validation of a quantitative assay for the measurement of miltefosine in human plasma by liquid chromatography–tandem mass spectrometry, J. Chromatogr. B. 865 (2008) 55–62. doi:10.1016/j.jchromb.2008.02.005.

[12] A.E. Kip, K.C. Kiers, H. Rosing, J.H.M. Schellens, J.H. Beijnen, T.P.C. Dorlo, Volumetric absorptive microsampling (VAMS) as an alternative to conventional dried blood spots in the quantification of miltefosine in dried blood samples, J. Pharm. Biomed. Anal. 135 (2017) 160–166. doi:10.1016/j.jpba.2016.12.012.

[13] A.E. Kip, H. Rosing, M.J.X. Hillebrand, S. Blesson, B. Mengesha, E. Diro, A. Hailu, J.H.M. Schellens, J.H. Beijnen, T.P.C. Dorlo, Validation and Clinical Evaluation of a Novel Method To Measure Miltefosine in Leishmaniasis Patients Using Dried Blood Spot Sample Collection, Antimicrob. Agents Chemother. 60 (2016) 2081–2089. doi:10.1128/AAC.02976-15.

[14] A.E. Kip, H. Rosing, M.J.X. Hillebrand, M.M. Castro, M.A. Gomez, J.H.M. Schellens, J.H. Beijnen, T.P.C. Dorlo, Quantification of miltefosine in peripheral blood mononuclear cells by high-performance liquid chromatography-tandem mass spectrometry, J. Chromatogr. B. 998–999 (2015) 57–62. doi:10.1016/j.jchromb.2015.06.017.

[15] G.R. Valicherla, P. Tripathi, S.K. Singh, A.A. Syed, M. Riyazuddin, A. Husain, D. Javia, K.S. Italiya, P.R. Mishra, J.R. Gayen, Pharmacokinetics and bioavailability assessment of Miltefosine in rats using high performance liquid chromatography tandem mass spectrometry, J. Chromatogr. B. 1031 (2016) 123–130. doi:10.1016/j.jchromb.2016.07.042.

[16] L. Verrest, T.P.C. Dorlo, Lack of Clinical Pharmacokinetic Studies to Optimize the Treatment of Neglected Tropical Diseases: A Systematic Review, Clin. Pharmacokinet. 56 (2017) 583–606. doi:10.1007/s40262-016-0467-3.

[17] M. Rizk, L. Zou, R. Savic, K. Dooley, Importance of Drug Pharmacokinetics at the Site of Action, Clin. Transl. Sci. 10 (2017) 133–142. doi:10.1111/cts.12448.

[18] Y.-J. Xue, H. Gao, Q.C. Ji, Z. Lam, X. Fang, Z. Lin, M. Hoffman, D. Schulz-Jander, N. Weng, Bioanalysis of drug in tissue: current status and challenges, Bioanalysis. 4 (2012) 2637–2653. doi:10.4155/bio.12.252.

[19] I.C. Roseboom, H. Rosing, J.H. Beijnen, T.P.C. Dorlo, Skin tissue sample collection, sample homogenization, and analyte extraction strategies for liquid chromatographic mass spectrometry quantification of pharmaceutical compounds, J. Pharm. Biomed. Anal. 191 (2020) 113590. doi:10.1016/j.jpba.2020.113590.

[20] S. Ho, Challenges of atypical matrix effects in tissue, Bioanalysis. 5 (2013) 2333–2335. doi:10.4155/bio.13.209.

[21] L. Yuan, L. Ma, L. Dillon, R.M. Fancher, H. Sun, M. Zhu, L. Lehman-McKeeman, A.-F. Aubry, Q.C. Ji, Investigation of the "true" extraction recovery of analytes from multiple types of tissues and its impact on tissue bioanalysis using two model compounds, Anal. Chim. Acta. 945 (2016) 57–66. doi:10.1016/j.aca.2016.09.039.

[22] European Medicines Agency, Committee for Medicinal Products for Human Use. Guideline on bioanalytical method validation, 2012. doi:EMEA/CHMP/EWP/192217/2009.

[23] Food and Drug Administration, Guidance for Industry Bioanalytical Method Validation Guidance for Industry Bioanalytical Method Validation Center for Veterinary Medicine (CVM) Contains Nonbinding Recommendations, 2013.

[24] A.E. Kip, H. Rosing, M.J.X. Hillebrand, M.M. Castro, M.A. Gomez, J.H.M. Schellens, J.H. Beijnen, T.P.C. Dorlo, Quantification of miltefosine in peripheral blood mononuclear cells by high-performance liquid chromatography-tandem mass spectrometry, J. Chromatogr. B. 998–999 (2015) 57–62. doi:10.1016/j.jchromb.2015.06.017.

[25] C.T.R. India, New treatment regimens for treatment of Post Kala Azar Dermal Leishmaniasis patients in India and Bangladesh region, New Delhi Database Publ. (India). Identifier CTRI/2017/04/008421. (2017) 7. http://ctri.nic.in/Clinicaltrials/pmaindet2.php?trialid=18509 (accessed February 26, 2021).

[26] Nordmark Biochemicals, SERVA Webinar, How to optimize your cell isolation with collagenase NB, (2015) 25. http://creschem.com/PDF/SERVA Webinar Collagenase_1.pdf (accessed February 26, 2021).

3.2

Development and validation of a high-performance liquid chromatography tandem mass spectrometry method for the quantification of the antiparasitic and antifungal drug amphotericin B in human skin tissue

Ignace C. Roseboom
Bas Thijssen
Hilde Rosing
Fabiana Alves
Shyam Sundar
Jos H. Beijnen
Thomas P.C. Dorlo

3.3

Abstract

Amphotericin B is an antifungal and antiparasitic drug used in first-line treatment of the parasitic neglected tropical disease leishmaniasis. Liposomal amphotericin B is currently studied for the treatment of cutaneous and post-kala-azar dermal leishmaniasis, where the dermis of the skin is infected with *Leishmania* parasites. For the optimization of known treatment regimens, accurate target-site concentrations of the drug are required. To date, no assay was available to assess human skin concentrations of amphotericin B. We here present a bioanalytical assay for the quantification of amphotericin B in 4-mm human skin biopsies. Human skin biopsies were homogenized by overnight digestion using collagenase A and were processed afterwards by simple protein precipitation using methanol. Separation and detection were achieved using a Gemini C18 column with slightly acidic chromatographic conditions and a quadrupole – linear ion trap mass spectrometer, respectively. The method was validated in digestion solution over a range of 10-2,000 ng/mL using natamycin as internal standard, with a correlation coefficient (r^2) of at least 0.9974. The assay performance, accuracy and precision, were acceptable over the validated range, using international (EMA and FDA) acceptance criteria. In the skin tissue extracts, amphotericin B ion enhancement was observed, however, the internal standard (IS) corrected for this effect hence calibration standards in digestion solvent could be used as a surrogate matrix for the quantification in skin tissue. Sample preparation recoveries were low (around 27%) because of degradation of amphotericin B during digestion and sample preparation processes, albeit highly reproducible, without compromising the accuracy and precision of the method. Using this assay, amphotericin B could be detected and quantified in skin biopsies originating from treated Indian post-kala-azar dermal leishmaniasis patients.

1. Introduction

Amphotericin B is a polyene antimycotic drug, targeting various fungal infections and is additionally used in the treatment of the parasitic neglected tropical disease leishmaniasis [1]. Because of its wide spectrum of action and low resistance potential, amphotericin B is a first-line treatment option for fungal and parasitic diseases [2,3]. Amphotericin B is a polyketide, formed naturally by polyketide biosynthesis. It was originally isolated from *Streptomyces nodosus* obtained from soil samples from the Orinoco river region in Venezuela, which is still used for its production [4,5]. To overcome the nephrotoxic potential of amphotericin B, a liposomal formulation of amphotericin B (AmBisome) was developed. While improving tolerability and decreasing severe toxicity associated with conventional amphotericin B, liposomal amphotericin B exhibits different pharmacokinetic characteristics and might be targeting macrophages which harbour *Leishmania* parasites during leishmaniasis. This liposomal formulation of amphotericin B was the first FDA approved drug for the treatment of visceral leishmaniasis, the most severe clinical phenotype of leishmaniasis [6].

A limited number of liquid chromatography coupled to tandem mass spectrometry (LC-MS/MS) assays were previously published for the quantification of amphotericin B in human plasma [7–11], minipig plasma [10], rat plasma [12], human urine and faeces [7,8], human cerebrospinal fluid [13] and rabbit cerebrospinal fluid [14]. Only a single LC-MS/MS assay for amphotericin B analysis in plasma has been reported in the context of the treatment of leishmaniasis [11].

There has been a growing interest in bioanalytical assays focusing on tissue bio-matrices, to enable target-site pharmacokinetic (PK) studies [15–17]. To better understand drug exposure-response relationships for the dermal clinical presentations of leishmaniasis, including cutaneous leishmaniasis (CL) and post-kala azar dermal leishmaniasis (PKDL), in which the *Leishmania* parasites reside and divide in the dermis of the skin, specific target-site pharmacokinetic (PK) studies are required to assess drug distribution at the site of the parasite infection [18]. This necessitates the development of accurate and precise bioanalytical assays for antileishmanial compounds in human skin matrix. The development of human skin tissue matrix bioanalytical methods compared to human blood matrices is challenging because skin tissue requires rigorous sample preparation to homogenize the biomatrix [17]. Endogenous interferences between plasma and skin tissue may differ as well as the sample preparation due to homogenization and the stability of analyte during homogenization steps, therefore surrogate matrix is recommended [15]. True recovery could not be distinguished in tissue matrices, however by completely dissolving skin tissue by chemical solubilization or enzymatic digestion and therefore the complete release of analyte from endogenous substances, the true recovery is approached

[15]. We previously developed and validated a sample preparation and bioanalytical method to enable quantification of another antileishmanial drug, miltefosine, in human skin biopsies using enzymatic digestion by collagenase A [18].

The aim of this study was to develop and validate an accurate assay with adequate sensitivity to quantify amphotericin B in human skin biopsy tissues. A skin tissue homogenization method using enzymatic digestion, which was previously described by our laboratory [18], was used as the basis for the sample preparation. The EMA and FDA guidelines for the validation of bioanalytical methods were followed during the validation of this assay [19,20]. The clinical applicability of the assay was evaluated using full thickness human skin biopsy tissue material collected in PKDL patients from India.

2. Materials and methods

2.1. Healthy human skin
Similar untreated control full thickness human skin tissue biopsies (4 mm diameter biopsies including stratum corneum, epidermis and dermis) from 4 patients were obtained as previously described [18]. This leftover surgery material was collected in the Amsterdam University Medical Centers in accordance with the Dutch Medical Research Involving Human Subjects Act, which allows researchers to use anonymous leftover human tissue without specific patient consent.

2.2. Chemicals
Amphotericin B European Pharmacopoeia reference standard and the internal standard natamycin were purchased from Sigma-Aldrich (Zwijndrecht, the Netherlands). Methanol, formic acid, and water (ULC grade) were obtained from Biosolve Ltd (Valkenswaard, The Netherlands). Bovine serum albumin (BSA) fraction V and collagenase A were purchased from Roche (Woerden, the Netherlands). Calcium chloride dihydrate and tromethamine (trisbase, tris buffer)) were from Sigma-Aldrich, phosphate-buffered saline (PBS) from Thermo Fischer Scientific (Breda, the Netherlands).

2.3. Preparation of the digestion solution
Digestion solution was prepared to be used as blank matrix for the preparation of the calibration standards and quality control (QC) samples as well as for the homogenization of skin tissue. A 5 mg/mL collagenase A 5 mM $CaCl_2$, 25 mM tris buffer (pH 7.5) and 2% BSA mixture was made as described previously [18]. In summary, a 4% BSA mixture was diluted 1:1 (v/v) with 50 mM tris buffer (pH 7.5) to a 2% BSA in 25 mM tris buffer (pH7.5) mixture. Afterwards, calcium chloride dihydrate (5 mM) and 5 mg/mL collagenase A were added to the buffer mixture. The digestion

solution was stored at -20°C for utmost 30 days, with no more than 2 freeze/thaw cycles, because of the decrease of enzymatic activity after freeze/thaw cycles [21].

2.4. Stock solutions and working solutions
Stock solutions with a concentration of 1 mg/mL amphotericin B and internal standard (IS) were separately prepared using dimethyl sulfoxide (DMSO) as solvent in amber-coloured reaction tubes. Amphotericin B stock solutions were independently prepared for calibration standards and QC samples. Working solutions of both amphotericin B and IS were prepared originating from diluted stock solutions using digestion solution. The final IS working solution (WIS) concentration was 10,000 ng/mL. The stock and working solutions were stored at -20°C.

2.5. Calibration standards, quality control samples
Prior to validation, calibration standards and QC samples were prepared by diluting their respective working solutions 20 times in digestion solution. Seven non-zero calibration standards were prepared at concentrations of 10, 20, 50, 100, 500, 1000, 2000 ng/mL. QC samples were categorized as the QC-LLOQ (lower limit of quantification), QC-LOW, QC-MID and QC-HIGH samples at respective concentrations of 10, 30, 150 and 1500 ng/mL. Calibration standards and QC samples were aliquoted in 50 µL volumes and were stored at -20°C prior to use.

2.6. Tissue homogenization and sample preparation
The masses (in mg) of individual clinical full thickness skin biopsies (including stratum corneum, epidermis, and dermis) were determined by weighing the clean amber 1.5 mL reaction tubes on an analytical balance first, transfer the samples using polypropylene spatulas, and determine the clinical skin tissue biopsies in the tubes. For the clinical full thickness skin biopsies, a washing step was employed to remove unwanted capillary blood, by the addition of a 100 µL volume of 100% PBS solution at room temperature to the samples, incubation for 30 minutes in a 2-8°C fridge and vortexing afterwards. After washing, full thickness skin biopsies were transferred to a clean amber 1.5 mL reaction tube using a clean polypropylene spatula. Digestion solution with a volume of 250 µL was added to the clinical skin biopsies together with 100 µL of WIS. Calibration standards and QC samples were prepared without skin tissue matrix (see section 2.5). Twenty µL of WIS was added to 50 µL aliquots of calibration standards and QC samples. All samples, including calibration standards, QC samples and clinical skin tissue samples, were vortexed thoroughly and incubated overnight (approximately 16 h) using a thermomixer (VWR International BV, Amsterdam, the Netherlands), while shaking at 1,000 rpm at a constant temperature of 37°C. All samples were vortex mixed afterwards for minimally 10 seconds after which 70 µL of the acquired skin tissue homogenate was transferred to clean amber 1.5 mL reaction tubes. The remainder of the skin tissue homogenate was stored at -70°C for potential re-analysis.

Sample preparation was performed by employing protein precipitation using 1000 µL of methanol and centrifugation at 15,000 rpm for 5 minutes at a temperature of 5°C. The supernatant was transferred to a clean 1.5 mL reaction tube and evaporated at 25°C in a turbovap demi-water bath to dryness in approximately 3 h. Afterwards, reconstitution was performed using 100 µL of methanol and vortex mixing until the precipitant was fully dissolved. The reconstituted samples were transferred to amber glass autosampler vials before injection into the UHPLC system.

2.7. LC equipment and conditions

For liquid chromatography an UHPLC Agilent 1290 system was used, including an online degasser, pumps, autosampler and column oven (Infinity II series, Agilent, Santa Clara, CA, USA). The autosampler was set at a temperature of 4°C and the column oven was set at a temperature of 30°C. Chromatographic separation was acquired using a Gemini C_{18} analytical column (Phenomenex, Torrance, CA, USA; 50 mm x 2.0 mm ID, 5 µm particles) and eluents consisting of 0.1 % formic acid (v/v) in water (A) and 0.1% formic acid (v/v) in methanol (B) with a flowrate of 0.4 mL/min. At first, the column was conditioned with 30% B for 0.45 minutes, then increased to 100% B at 0.5 minutes and remained so until 3.0 minutes. The organic phase was then decreased at 3.1 minutes to 30% B and conditioned until the end of analysis at 4.5 minutes. A preparation of 0.1% formic acid (v/v) in acetonitrile-isopropanol-methanol-water (25:25:25:25, v/v/v/v) was used as purge and strong wash solvents.

2.8. MS equipment and conditions

Amphotericin B detection was realized by tandem mass spectrometry using a quadrupole – linear ion trap MS (QTRAP6500, Sciex, Framingham, MA, USA) equipped with a turbo ionspray interface operated in positive mode. Amphotericin B [M+H]+ and the IS were measured in multiple reaction monitoring modus (MRM), employing a summation of transitions m/z 924.496 → 743.400 and m/z 906.461 → 743.382 for amphotericin B and m/z 666.340 → 503.200 for natamycin (IS) (Figure 1). The ion source settings used under the ion source temperature of 250°C were: 5500 V ion source voltage; 25 psi (1.72 bar) for both ion source gas 1 and 2; 30 psi (2.1 bar) curtain gas and 12 psi (0.83 bar) collision gas. Analyst™ software (Sciex, version 1.6.2) was used for the acquisition and processing of data.

2.9. Validation procedures

Validation of the bioanalytical assay was performed in line with the EMA and FDA guidelines for bioanalytical assays in plasma [19,20]. Established parameters in the validation of the assay included: calibration model, accuracy and precision, carry-over, selectivity (cross analyte/IS interferences), matrix effect, extraction recovery, dilution integrity, and stability under various conditions.
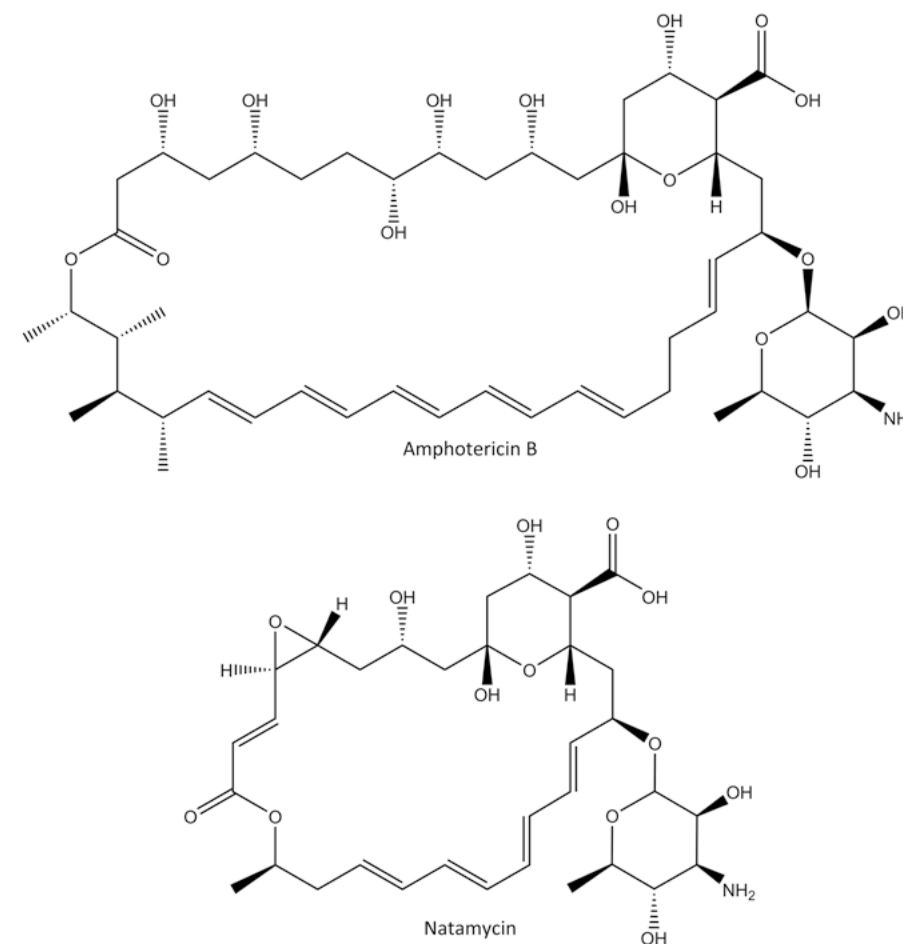

Figure 1: Chemical structures of amphotericin B and natamycin (IS).

2.9.1. Calibration model

Calibration samples were prepared in digestion solution, as explained in section 2.5, with a range of 10-2,000 ng/mL. The calibration model validation experiment samples were prepared in duplicate and performed in three separate validation runs. The ratio of the analyte peak area/IS peak area on the y-axis and the nominal amphotericin B concentration on the x-axis with weighing factor $1/x^2$ was used in the determination of the linear regression of the assay. According to the EMA and FDA guidelines, the deviations for each non-zero calibration samples in the calibration model should be within ±15% for at least 75% of the non-zero calibration samples, except for the LLOQ (±20%).

2.9.2. Accuracy and precision

The assay performance, expressed as the inter-/intra-assay accuracy and precision, was assessed using QC samples at the QC-LLOQ (10 ng/mL), QC-LOW (30 ng/mL), QC-MID (150 ng/mL) and QC-HIGH (1500 ng/mL) concentration levels in five-fold, during three separate validation runs. The concentrations were determined by the peak area/IS peak area ratio in the calibration model (see section 2.9.1). Accuracies were obtained by determination of bias of the mean measured concentrations compared to the nominal concentrations distinguishing the intra-assay accuracy (%), measured per analytical run, and the inter-assay (%) measured in all three validation runs. Precisions were expressed as the relative coefficient of variation (%CV) and inter-run precision was determined by a one-way ANOVA. Inter/intra-assay bias and coefficients of variation should be within ±15% and ≤15% (±20% and ≤20% at the LLOQ), respectively.

2.9.3. Carry-over

Carry-over was assessed during the calibration model validation experiments (section 2.9.1), in three separate validation runs. Injections of two separate double blank samples after the ULOQ calibration standard were performed, whereas the mean peak areas of amphotericin B and IS of five QC-LLOQ samples were compared to the peak areas in the two separate double blanks.

2.9.4. Cross-analyte/IS interference

Selectivity by determining cross analyte/IS interferences were obtained by spiking exclusively amphotericin B at the ULOQ concentration and in separate samples exclusively natamycin (IS) at the IS concentration level in digestion solution. The interferences of amphotericin B peak areas crossing over in the IS peak area must be ≤5% and the interference of the IS in the amphotericin B peak must be ≤20% of peak area at the LLOQ concentration level.

2.9.5. Matrix effect and extraction recovery

Untreated control human skin tissue biopsies from a single batch (one individual) were used in the determination of the matrix effect and recovery of the assay. Amphotericin B was spiked before or after sample processing and homogenization at the QC-LOW and QC-HIGH concentration levels, with three different categories of prepared samples for the determination of matrix effects and recovery: matrix present, matrix absent, and processed samples. Matrix absent and processed samples were prepared in triplicate for each QC concentration level by spiking QC working solutions to the final extract matrix, methanol, or spiking QC working solutions to untreated control skin tissue in digestion solution prior to sample treatment, respectively. Matrix present samples were prepared in six-fold per concentration level, spiking QC working solutions in final extracts of non-spiked sample prepared untreated skin tissue homogenates. Processed samples and the non-spiked untreated skin tissue homogenates were prepared according to section 2.6.

Absolute matrix effect, IS-normalized and sample preparation recovery were calculated using the samples described above, all at equal QC concentration levels. The ratio of amphotericin B or IS peak areas between matrix present and matrix absent samples was expressed as the absolute matrix effect, the direct consequence of endogenous interferences of the matrix to the intensity of the analyte signal detection. The ratio of amphotericin B and IS absolute matrix effect factors was described as the IS-normalized matrix factor. The ratio of processed and matrix present samples for amphotericin B or IS was evaluated as the sample preparation recovery. The EMA and FDA guidelines acceptance criteria for matrix effects were RSD's (%) within ≤15%.

2.9.6. Dilution integrity

A concentration of 20,000 ng/mL spiked digestion solution, 5 times the ULOQ concentration, was diluted ten-fold in digestion solution, performed in five-fold to assess the integrity of the dilution steps. The acceptance criteria values were ±15% for intra-assay accuracy and ≤15% for intra-assay precision.

2.9.7. Stability

Stability of amphotericin B in digestion solution, untreated control human skin tissue homogenates and final extracts was determined by measurement of QC samples at the QC-LOW (30 ng/mL) and QC-HIGH (1,500 ng/mL) concentration levels in triplicate in the calibration model, using freshly spiked calibration samples (see section 2.5). The bias (%) and CV (%) from the nominal concentration were calculated. Stock solution and working solution stabilities acceptance criteria should be within ±5% bias, whereas acceptance criteria values for long-term, short-term, and final extract stability need to be ±15% bias and ≤15% CV% for the accuracy and precision, respectively. Short term stability in untreated control human skin tissue homogenates stored at -70°C for 3 days after undergoing digestion incubation of 16 hours was determined as well as digestion incubation stability of amphotericin B during the homogenization process in digestion solution. Long-term stability in digestion solution stored 30 days at -20°C was assessed, as well as stock and working solutions at the same temperature for 14 and 33 days, respectively. Subsequently, stability was assessed in final extracts at 2-8°C for at least 2 days. Furthermore, the amphotericin B stability was determined at the QC-LOW and QC-HIGH concentration level by a comparison between samples after digestion incubation versus samples absent of the digestion incubation. The loss of amphotericin B during this homogenization process was reported.

2.10. Clinical application

The goal for development and validation of the bioanalytical assay was to support clinical PK studies in Bangladesh and India on the treatment of PKDL patients assessing skin target site exposure to antileishmanial drugs (CTRI/2017/04/008421). Till date there is absence of data on the distribution and exposure of systematically

administered amphotericin B in *Leishmania* infected skin tissue. The trial was performed with ethical approval by all relevant local medical ethics committees. The amphotericin B regimen had a total duration of 15 days, with liposomal amphotericin B intravenous infusions on days 1, 4, 8, 11, and 15 (5 x 4 mg/kg IV, total dose of 20 mg/kg) [22]. The human skin biopsies were sampled on day 15, following the last infusion. Skin tissue biopsies were stored (at -20 °C or -70 °C) before transporting the samples at -80°C (on dry ice) to Amsterdam, where they were stored at - 70°C. As described in section 2.6, clinical skin tissue biopsy masses (in mg) were determined before sample preparation. The concentration amphotericin B was determined in ng/mL and was converted to the unit of measurement µg/g amphotericin B in skin biopsy using the masses of the clinical skin biopsy. To show the clinical application of the assay, amphotericin B concentrations in 5 randomly selected clinical skin biopsies from PKDL patients treated at the Kala-Azar Medical Research Center, Muzaffarpur, the field site of the Institute of Medical Sciences, Banaras Hindu University, Varanasi, India, were measured.

3. Results and discussion

3.1. Development
The development and optimization of human skin tissue homogenization techniques for bioanalytical purposes were described in more depth previously [15,18]. While quaternary ammonium hydroxide fully homogenized skin tissue after overnight incubation at 50°C, amphotericin B was not stable under these conditions leading to complete degradation. Enzymatic digestion using collagenase A incubation overnight at 37°C did not lead to complete degradation (stability shown in section 3.2.7), while still fully homogenizing homogenizing the human skin tissue sample and was therefore selected as preferred homogenization technique for the analysis of amphotericin B.

Simple methanol protein precipitation was subsequently implemented for a fast and easy sample clean-up method of the digested sample, using only 1/5th of the homogenized sample volume (50 out of 250 µL). Due to unavailability of a stable isotope labelled analyte, two chemical analogues were evaluated as internal standard, which were amphotericin B methyl ester and natamycin. Amphotericin B methyl ester showed slight cross analyte interferences to amphotericin B in the LC-MS/MS obtained chromatograms, this was shown in a CAL0 sample (IS spiked to blank sample) chromatogram. The signal was at the limit of detection and did not directly affect the sensitivity. However, amphotericin B was also converted into amphotericin B methyl ester and was displayed after spiking a sample with upper limit of quantification (ULOQ) concentration amphotericin B (with the IS absent) and monitoring the amphotericin B and IS chromatograms. The relative peak height of

amphotericin B methyl ester after spiking the amphotericin B ULOQ concentration in comparison to the spiked IS sample height was about 5%. The hypothesis is that a slight esterification reaction occurred at the carboxylic acid region of amphotericin B in combination with methanol. Amphotericin B methyl ester was considered not reliable enough for use as internal standard although the effects of the interferences were relatively low. The use of natamycin as IS did not demonstrate any cross analyte/IS interferences and was therefore selected as internal standard. Slight tailing occurred for both amphotericin B and natamycin, especially at higher concentrations (as seen in Figure 2, LLOQ vs ULOQ). One of the possible explanations is that both amphotericin B and IS are slightly cationic, indicating silica bonding at higher concentrations due to saturation of C18 tails in the relatively small LC column (5 cm).

Skin amphotericin B concentrations were expected to be low, particularly compared to plasma concentrations and therefore efforts were made to maximize sensitivity of the skin tissue assay. Efforts were made to optimize MS and sample preparation procedures. Amphotericin B was subjected to Q1 in-source fragmentation parallel to the increase of the source temperature. Degradation of the parent ion [M+H]+ m/z 924.5 to m/z 906.5 in Q1 was apparent when increasing the source temperature from 250°C to 400°C, with an inverse proportional increase in the signal of m/z 906.5. Both parent and Q1 in-source fragment ions share the same fragmentation pattern with m/z 924.496 → 743.400 and m/z 906.461 → 743.382 as the most sensitive transitions. The 18 Da loss in source indicates the loss of water from the parent molecule. Summing of both transitions showed an increase in peak height without a proportional increase in noise, which had a positive impact on the signal to noise ratio. Decreasing source temperature and summing up parent ions increased the relative sensitivity by 4.3-fold. To further improve sensitivity, supernatant of the protein precipitation procedure was evaporated at room temperature (25°C) and reconstituted in 100 µL methanol. Despite evaporation and reconstitution had a minor negative impact on the stability of amphotericin B, overall, the sensitivity was improved due to this concentrating step by another 1.66-fold and the decreased recovery therefore considered acceptable.

3.2. Validation procedures
The development and validation of the bioanalytical assay was performed in digestion solution, because of the scarcity and invasiveness associated with acquiring the biological matrix. Validation experiments such as matrix effect, recovery and stability were therefore performed in human skin tissue homogenates to verify and ensure that digestion solution could be used as a surrogate matrix for skin tissue homogenates.

3.2.1. Calibration model
The calibration model was determined by calculating concentrations, the linear fit and signal-to-noise ratio at the LLOQ concentration level. The bias of all back-

calculated concentrations of the calibration model were within ±9.3%, including a correlation coefficient (r^2) value for the linear fit of at least 0.9974, along with the LLOQ signal-to-noise ratio of at least 5.6, all in three individual validation runs. Representative MRM Chromatograms of the double blank, blank, LLOQ and ULOQ are displayed in Figure 2.

3.2.2. Accuracy and precision

The assay performance was established in digestion solution, summarized in Table 1. All acceptance criteria were met, including inter/intra assay accuracies at the QC-LOW, QC-MID, and QC-HIGH concentration levels of ±8.8% and ±10.4%, respectively, and inter/intra assay precisions of ≤2.5% and ≤5.0%, respectively. The inter/intra assay accuracies at the QC-LLOW concentration level were demonstrated at 7.6% and ±11.4%, respectively, whereas the inter/intra assay precisions were 2.6% and ≤12.3%, respectively.

Table 1: Assay performance data for amphotericin B. Accuracies and precisions were established in 3 analytical runs and each run contained 5 replicates per tested concentration.

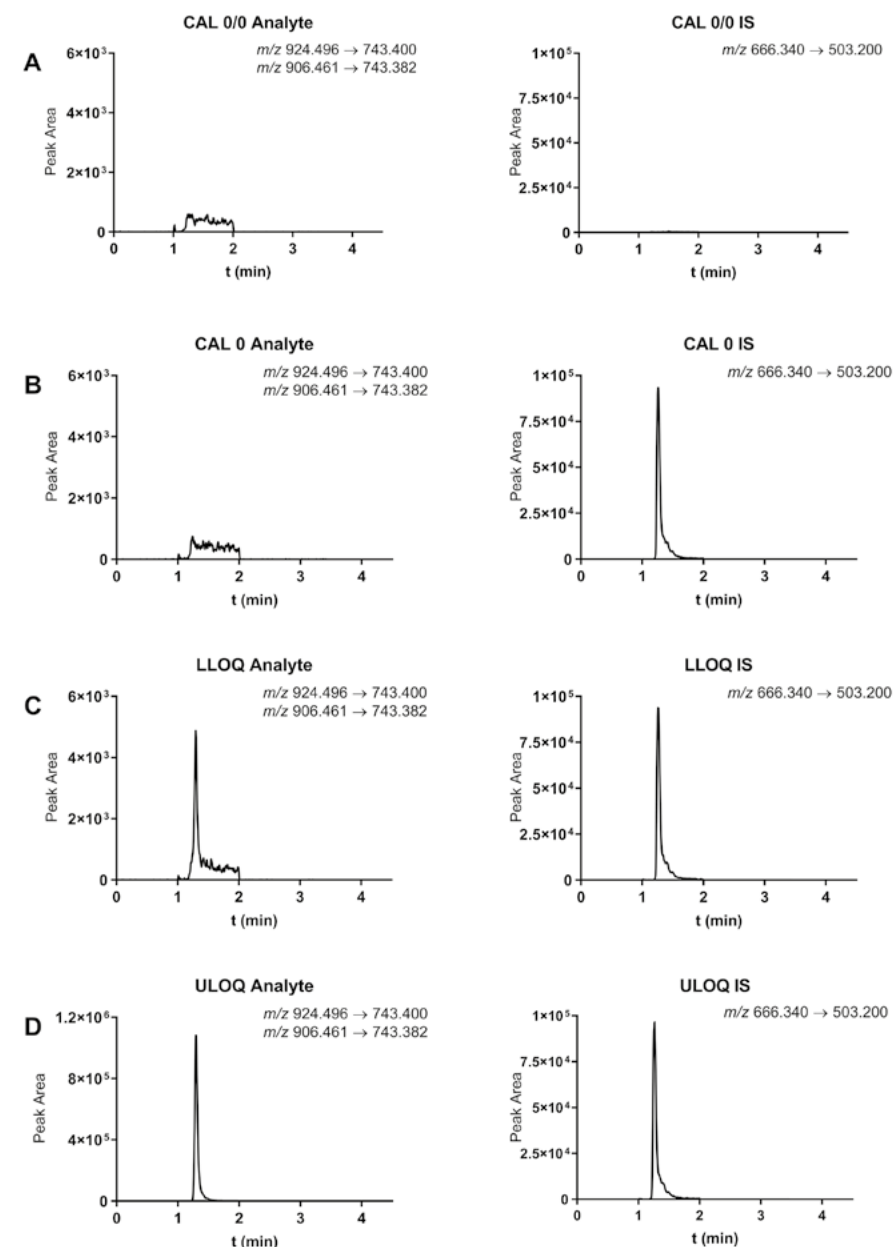| Nominal amphotericin B concentration (ng/mL)	Intra-assay (n = 15)		Inter-assay (n = 15)	
	Bias (%)	Precision (%)	Bias (%)	Precision (%)
10	±11.4	≤12.3	7.6	2.6
30	±3.3	≤5.0	-1.2	0.8
150	±3.5	≤4.2	0.1	2.5
1500	±10.4	≤2.8	8.8	0.9

Figure 2: Representative MRM chromatograms showing the double blank (A), blank (B), LLOQ (10 ng/mL) (C) and ULOQ (2000 ng/mL) (D) of amphotericin B and natamycin IS samples in digestion solution.

3.2.3. Carry-over

Carry-over was assessed in two separate double blank samples after the ULOQ calibration standards, performed in three separate validation runs. Amphotericin B peak area carry-over was observed to be ≤14.5% in the double blanks after ULOQ, well within the acceptance criteria value of ≤20%. Furthermore, no detectable carry-over was observed for the peak areas of the IS, with acceptance criteria of ≤5%.

3.2.4. Cross-analyte/IS interference

The interferences of amphotericin B peak transitions in the IS peak area transitions were determined. Subsequently, both amphotericin B and IS peak area interferences were not observed under the tested conditions.

3.2.5. Matrix effect and extraction recovery

The matrix effect and recovery experiments were performed as described in section 2.9.5. Matrix factor determinations include the use of six different batches of matrix, whereas the matrix factor determination described included a single batch of skin tissue matrix. This is a limitation of the matrix effect determination, however the EMA stated that hard to obtain matrices are exempted and less than six different batches may be used [19]. The average absolute matrix factors for amphotericin B were 1.39 and 1.26 at QC-LOW and QC-HIGH concentration levels, respectively, potentially implying ion enhancement by endogenous substances derived from homogenized skin tissue. Average IS-normalized factors were 1.10 and 1.15 for QC-LOW and QC-HIGH levels, respectively, with an RSD of ≤2.3%. The IS-normalized matrix factor was slightly higher than 1, possible affecting accuracy/sensitivity of the assay, however, since the bias was within the acceptable bias ranges (0.85-1.15), according to FDA and EMA guidelines, this deviation was deemed acceptable. Sample preparation recovery of amphotericin B was evaluated after the homogenization and sample pre-treatment procedures at QC-LOW and QC-HIGH concentration levels and varied between 27.8% and 27.5%. The sample preparation recovery of the IS varied between 45.2% and 51.4% at the analyte QC-LOW and QC-HIGH concentration levels. The sample preparation recovery was relatively low, especially for amphotericin B but very reproducible (RSD ≤5.0%). Amphotericin B was not stable during the digestion incubation, probably due to the increased temperature (37°C for 16 hours). Amphotericin B recoveries of 63.5% and 58.1% for the QC-LOW and QC-HIGH, respectively, were observed after digestion and without the concentration step (evaporation to dryness) executed. IS recoveries showed no significant changes during solely digestion incubation conditions, with recoveries of 96.8% and 103.1% on QC-LOW and QC-HIGH concentration levels respectively. This might, partially, explain the differences in sample preparation recovery between amphotericin B and IS. An additional loss in recovery of both analyte and IS was caused by the drying and reconstitution process during sample preparation, resulting in the total sample pre-treatment recoveries described above. All data is summarized in Table 2.

Table 2: Matrix factor (n = 6) and sample preparation recovery (n = 3) data for amphotericin B and natamycin (IS) in digestion solution.

Nominal Amphotericin B Concentration (ng/mL)	Matrix Factor Analyte	Matrix Factor IS	IS-normalized Matrix Factor	Enzymatic digestion (16h, 37 °C) Recovery Analyte	Enzymatic digestion (16h, 37 °C) Recovery IS	Total Sample Preparation Recovery Analyte	Total Sample Preparation Recovery IS	IS-normalized Sample Preparation Recovery
30	1.39	1.26	1.10	63.5%	96.8%	27.8%	45.2%	61.5%
	(C.V. = 4.5%)	(C.V. = 4.0%)	(C.V. = 3.2%)	(C.V. = 2.0%)	(C.V. = 2.6%)	(C.V. = 5.0%)	(C.V. = 6.3%)	(C.V. = 5.8%)
1,500	1.42	1.24	1.15	58.1%	103.1%	27.5%	51.4%	53.5%
	(C.V. = 2.0%)	(C.V. = 3.2%)	(C.V. = 2.3%)	(C.V. = 7.4%)	(C.V. = 9.8%)	(C.V. = 4.5%)	(C.V. = 2.1%)	(C.V. = 4.8%)

Abbreviation: C.V. = coefficient of variation

3.2.6. Dilution integrity

Assessment of samples diluted ten times was performed. The intra-assay accuracy and intra-assay precision were met with values of 1.0 and 1.5%, respectively. To conclude, a ten-fold dilution may be performed without compromising the accuracy and precision of the measurements.

Table 3: Stability data for amphotericin B (n = 3 per quality control level) expressed by accuracy (bias %) and precision (coefficient of variation).

Matrix	Condition	Amphotericin B Nominal Concentration (ng/mL)	Bias (%)	C.V. (%)
Digestion Solution	-20°C, 30d	30.0	13.9	4.3
		1500	10.4	1.9
Human Skin Tissue Homogenate	-70°C, 3d	30.0	-8.2	2.2
		1500	0.7	3.0
Final extract digestion solution (n=2)	2-8°C, 2d	30.0	1.8	5.3
		1500	13.7	1.2
Working Solution	-20°C, 33d	30.0	-3.1	3.4
		1500	2.5	1.6
Stock Solution	-20°C, 14d	1.000.000	-4.9	0.7

Abbreviations: C.V. = coefficient of variation; d = days; F/T = freeze/thaw cycles; h = hours

3.2.7. Stability

Stability assessment was performed in various conditions. Stability in untreated control human skin tissue homogenates stored at -70°C for 3 days , in digestion solution stored 30 days at -20°C, stock and working solutions at the same temperature for 14 and 33 days, respectively, and finally in final extracts at 2-8°C for at least 2 days met the acceptance criteria according to the EMA and FDA guidelines, included in Table 3. The stability of amphotericin B in digestion solution during the enzymatic digestion incubation period was also determined and compared to homogenized QC-LOW and QC-HIGH samples, reported as a loss of analyte in percentages. The loss of amphotericin B during incubation process at the QC-LOW and QC-HIGH concentration levels were 34.6% and 44.2%, respectively. Instability of amphotericin B during enzymatic digestion incubation could be caused by prolonged elevated temperatures (37°C) along with exposure to light due to photosensitivity and partly explains low recoveries during the recovery experiments described in section 3.2.5.

3.3. Clinical application

Determination of amphotericin B concentrations in clinical human skin biopsies from PKDL patients receiving liposomal amphotericin B treatment at the Kala-Azar Medical Research Center, Muzaffarpur, the field site of the Institute of Medical Sciences, Banaras Hindu University, Varanasi, India, was performed using this bioanalytical assay after its validation. The assay proved to have adequate accurate and precise performance (see section 3.2.2) and was sensitive enough to quantify all clinical skin biopsy samples within the validated calibration range. A representative MRM chromatogram of a clinical sample is depicted in Figure 3. Quantification results of five individual patients are displayed in Table 4. Pharmacokinetic results from this clinical target-site PK study will be reported in more detail elsewhere.
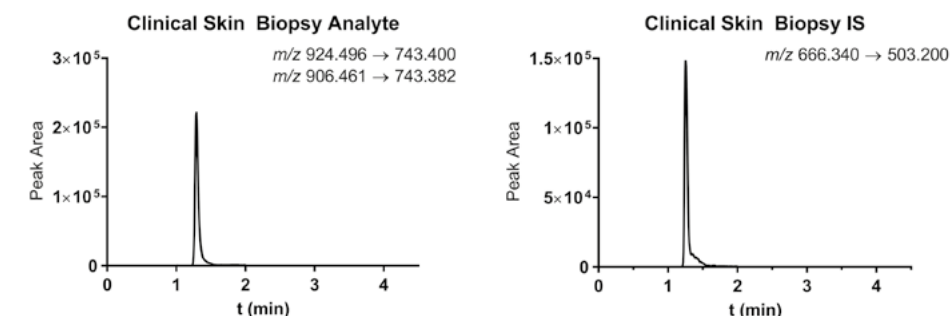

Figure 3: Representative MRM chromatograms of an Indian clinical patient sample suffering from post kala-azar dermal leishmaniasis, showing the clinical skin biopsy peak shape with a concentration of 401 ng/mL in human skin tissue homogenate or 8.34 µg/g human skin tissue.

Table 4: Amphotericin B skin tissue biopsy concentration data in 5 individual post kala-azar dermal leishmaniasis patients from India at day 15 after receiving a 15-day amphotericin B regimen.

Clinical Skin Biopsy #	Skin Biopsy Weight (mg)	Amphotericin B Concentration in Digestion Solution (ng/mL)	Amphotericin B Concentration in Skin Biopsy (µg/g)
1	12.02	401	8.34
2	3.54	184	10.40
3	1.69	45.2	6.68
4	1.73	34.7	5.01
5	9.47	239	6.31

4. Conclusion

A relatively easy, accurate and sensitive bioanalytical assay was developed and subsequently validated for the determination and quantification of amphotericin B in human skin punch biopsies. Enzymatic digestion homogenization was applied using collagenase A and overnight incubation , which allowed for accurate quantification of amphotericin B in human skin tissue, using a chemical analogue, natamycin, as its internal standard. Amphotericin B was extracted from the digestion solution by using simple methanol protein precipitation. The supernatant was evaporated at 25°C and reconstituted to final extract using methanol. LC separation was achieved using gradient elution on a C_{18} column and sensitive detection was established using a QTRAP 6500 operated in positive ion mode. The bioanalytical assay was validated for a range of 10-2,000 ng/mL using a chemical analogue, natamycin, as internal standard, displaying a linear fit with a correlation coefficient (r^2) of minimally 0.9974. Furthermore, accuracy and precision values were well within acceptance criteria and stability of amphotericin B in human skin tissue homogenates was evaluated after 3 days at -70°C. The identified absolute matrix effects for amphotericin B were adequately corrected for by the internal standard, indicating that digestion solution can be used as a surrogate matrix for human skin tissue quantification without compromising accuracy of amphotericin B quantifications in clinical skin biopsies. The bioanalytical assay was able to accurately quantify amphotericin B in clinical skin biopsies from PKDL patients from India treated with liposomal amphotericin B .

References

[1] World Health Organization, Control of the leishmaniases., World Health Organ. Tech. Rep. Ser. (2010) xii–xiii, 1–186.

[2] G. Medoff, G.S. Kobayashi, Strategies in the Treatment of Systemic Fungal Infections, N. Engl. J. Med. 302 (1980) 145–155. https://doi.org/10.1056/NEJM198001173020304.

[3] Y.-L. Chang, S.-J. Yu, J. Heitman, M. Wellington, Y.-L. Chen, New facets of antifungal therapy, Virulence. 8 (2017) 222–236. https://doi.org/10.1080/21505594.2016.1257457.

[4] R. Donovick, W. Gold, J.F. Agano, H.A. Stout, Amphotericins A and B, antifungal antibiotics produced by a streptomycete. I. In vitro studies., Antibiot. Annu. 3 (n.d.) 579–86.

[5] D.J. D, W. Gold, P.J. F, J. Vandeputte, Amphotericin b, its production, and its salts, US Pat. Appl. 2908611. (1959).

[6] A. Meyerhoff, U.S. Food and Drug Administration approval of AmBisome (liposomal amphotericin B) for treatment of visceral leishmaniasis., Clin. Infect. Dis. 28 (1999) 42–8; discussion 49-51. https://doi.org/10.1086/515085.

[7] J.W. Lee, M.E. Petersen, P. Lin, D. Dressler, I. Bekersky, Quantitation of Free and Total Amphotericin B in Human Biologic Matrices by a Liquid Chromatography Tandem Mass Spectrometric Method, Ther. Drug Monit. 23 (2001) 268–276. https://doi.org/10.1097/00007691-200106000-00015.

[8] I. Bekersky, R.M. Fielding, D.E. Dressler, J.W. Lee, D.N. Buell, T.J. Walsh, Pharmacokinetics, Excretion, and Mass Balance of Liposomal Amphotericin B (AmBisome) and Amphotericin B Deoxycholate in Humans, Antimicrob. Agents Chemother. 46 (2002) 828–833. https://doi.org/10.1128/AAC.46.3.828-833.2002.

[9] N.M. Deshpande, M.G. Gangrade, M.B. Kekare, V. V. Vaidya, Determination of free and liposomal Amphotericin B in human plasma by liquid chromatography–mass spectroscopy with solid phase extraction and protein precipitation techniques, J. Chromatogr. B. 878 (2010) 315–326. https://doi.org/10.1016/j.jchromb.2009.11.036.

[10] W. Qin, H. Tao, Y. Chen, Z. Chen, N. Wu, Sensitive, Accurate and Simple Liquid Chromatography-Tandem Mass Spectrometric Method for the Quantitation of Amphotericin B in Human or Minipig Plasma, J. Chromatogr. Sci. 50 (2012) 636–643. https://doi.org/10.1093/chromsci/bms049.

[11] A.E. Kip, S. Blesson, F. Alves, M. Wasunna, R. Kimutai, P. Menza, B. Mengesha, J.H. Beijnen, A. Hailu, E. Diro, T.P.C. Dorlo, Low antileishmanial drug exposure in HIV-positive visceral leishmaniasis patients on antiretrovirals: an Ethiopian cohort study, J. Antimicrob. Chemother. 76 (2021) 1258–1268. https://doi.org/10.1093/jac/dkab013.

[12] C. Su, H. Yang, H. Sun, J.P. Fawcett, D. Sun, J. Gu, Bioanalysis of free and liposomal Amphotericin B in rat plasma using solid phase extraction and protein precipitation followed by LC-MS/MS, J. Pharm. Biomed. Anal. 158 (2018) 288–293. https://doi.org/10.1016/j.jpba.2018.06.014.

[13] X. Xiong, S. Zhai, F. Liu, Determination of Amphotericin B in Human Cerebrospinal Fluid by LC–MS–MS, Chromatographia. 70 (2009) 329–332. https://doi.org/10.1365/s10337-009-1112-1.

[14] M. Fang, T.M. Lü, A. De Ma, L. Wang, G.L. Li, A.Z. Qiu, Z.Y. Pan, Y.Y. Wang, X.J. Liu, Comparative Pharmacokinetics of Continuous and Conventional Intrathecal Amphotericin B in Rabbits, Antimicrob. Agents Chemother. 56 (2012) 5253–5257. https://doi.org/10.1128/AAC.00304-12.

[15] I.C. Roseboom, H. Rosing, J.H. Beijnen, T.P.C. Dorlo, Skin tissue sample collection, sample homogenization, and analyte extraction strategies for liquid chromatographic mass spectrometry quantification of pharmaceutical compounds, J. Pharm. Biomed. Anal. 191 (2020) 113590. https://doi.org/10.1016/j.jpba.2020.113590.

[16] M. Rizk, L. Zou, R. Savic, K. Dooley, Importance of Drug Pharmacokinetics at the Site of Action, Clin. Transl. Sci. 10 (2017) 133–142. https://doi.org/10.1111/cts.12448.

3.3

[17]   Y.-J. Xue, H. Gao, Q.C. Ji, Z. Lam, X. Fang, Z. Lin, M. Hoffman, D. Schulz-Jander, N. Weng, Bioanalysis of drug in tissue: current status and challenges, Bioanalysis. 4 (2012) 2637–2653. https://doi.org/10.4155/bio.12.252.

[18]   I.C. Roseboom, B. Thijssen, H. Rosing, F. Alves, D. Mondal, M.B.M. Teunissen, J.H. Beijnen, T.P.C. Dorlo, Development and validation of an HPLC-MS/MS method for the quantification of the anti-leishmanial drug miltefosine in human skin tissue, J. Pharm. Biomed. Anal. (2021) 114402. https://doi.org/10.1016/j.jpba.2021.114402.

[19]   European Medicines Agency, Committee for Medicinal Products for Human Use. Guideline on bioanalytical method validation, 2012. https://doi.org/EMEA/CHMP/EWP/192217/2009.

[20]   Food and Drug Administration, Guidance for Industry Bioanalytical Method Validation Guidance for Industry Bioanalytical Method Validation Center for Veterinary Medicine (CVM) Contains Nonbinding Recommendations, 2013.

[21]   F. Israel-Roming, G. Luta, D. Balan, E. Gherghina, C.P. Cornea, F. Matei, Time and Temperature Stability of Collagenase Produced by Bacillus licheniformis, Agric. Agric. Sci. Procedia. 6 (2015) 579–584. https://doi.org/10.1016/j.aaspro.2015.08.091.

[22]   C.T.R. India, New treatment regimens for treatment of Post Kala Azar Dermal Leishmaniasis patients in India and Bangladesh region, New Delhi Database Publ. (India). Identifier CTRI/2017/04/008421. (2017) 7.

3.3

3.3

Development and validation of an ultra-high performance liquid chromatography coupled to tandem mass spectrometry method for the quantification of the antileishmanial drug paromomycin in human skin tissue

3.4

Ignace C. Roseboom
Bas Thijssen
Hilde Rosing
Fabiana Alves
Brima Younis
Ahmed M. Musa
Jos H. Beijnen
Thomas P.C. Dorlo

Abstract

Bioanalytical assay development and validation procedures were performed to quantify antiprotozoal drug paromomycin in human skin tissue by ultra-high performance liquid chromatography coupled to tandem mass spectrometry. Paromomycin, an aminoglycoside drug, is administered intra-muscularly and used in the treatment of multiple clinical presentations of the neglected tropical disease leishmaniasis. It is currently studied in the treatment of post-kala-azar dermal leishmaniasis, a disease where the *Leishmania* parasites divide and reside in the skin. We present a target-site bioanalytical method to accurately quantify paromomycin in human skin tissue, with the clinical purpose of quantifying paromomycin in skin biopsies from post-kala-azar dermal leishmaniasis patients originating from Sudan. Enzymatic digestion using collagenase A incubated at 37°C overnight was employed as homogenization method to produce skin tissue homogenates. Further sample preparation was performed by protein precipitation using trichloroacetic acid and a dilution step. Final extracts were injected onto a C18 analytical column, and isocratic heptafluorobutyric acid ion-pair separation and elution were employed. The chromatography system was coupled to a triple quadrupole mass spectrometer for detection. The method was validated in digestion solution over a linear range from 5 to 1000 ng/mL ($r^2 \geq 0.9967$) with the assay performance of accuracy and precision within acceptable criteria values as stated by the EMA guidelines. Furthermore, matrix effects were observed in human skin tissue and were corrected by the multiple deuterated paromomycin internal standard. No substantial IS-normalized matrix effect was detected along with relatively high sample preparation recovery. Consequently, digestion solution matrix serving as the preparation of calibration standards can be used as surrogate matrix for human skin tissue, which is convenient given the limited availability of control matrix. Finally, paromomycin was accurately quantified in skin of post-kala-azar dermal leishmaniasis patients originating from clinical trials in Sudan.

1. Introduction

Paromomycin (aminosidine) is a broad spectrum aminoglycoside antibiotic, derived from *Streptomyces rimosus* var. *paromomycinus* [1]. It has antiprotozoal activity and is considered an effective oral agent for the treatment of intestinal infections like amebiasis, giardiasis, and dientamoebiasis [2]. Intramuscular paromomycin is one of the few available effective treatment options against the neglected tropical parasitical disease leishmaniasis [3,4]. Intramuscular paromomycin is considered highly efficacious and cost-effective against visceral leishmaniasis both in mono- as well as combination therapy [5–9], while for cutaneous leishmaniasis a topical formulation of paromomycin has been evaluated [10,11]. The use of a combination therapy including intramuscular paromomycin for the cutaneous disease post-kala-azar dermal leishmaniasis (PKDL) is currently being investigated in clinical trials [12].

Target-site pharmacokinetic (PK) studies have gained more prominence recently in clinical studies, accompanied by an increased interest in the development of bioanalytical assays focusing on biological tissue matrices [13–15]. In both PKDL and cutaneous leishmaniasis, *Leishmania* parasites reside and multiply in the dermis of the skin. Little is known about the actual distribution of antileishmanial drugs in skin of patients after systemic treatment [16], while target-site PK data are urgently required to further optimize and rationalize therapy. Previously, we developed and validated the first bioanalytical method to quantify the antileishmanial drug miltefosine in skin biopsy tissue of PKDL patients [17].

Developing chromatography-based bioanalytical assays for aminoglycosides remains challenging, because of poor retention to conventional reversed phase (RP) liquid chromatography (LC) columns, due to their hydrophilicity and poly-ionic charge [18]. Only a few LC-based quantification methods of paromomycin in human biological matrices have been described in literature: in human plasma [19–21], serum [22] or urine [19]. Bioanalytical paromomycin assays for biological tissues were described previously solely for animal tissues in the food industry for the purpose of residue analysis , none of these included skin tissue as bioanalytical matrix [23–27].

The aim of this study was to develop a novel method with sufficient sensitivity to quantify paromomycin in human skin tissue biopsies. The validation of the method was based on the EMA guidelines [28]. Applicability of the developed methodology in clinical skin target-site pharmacokinetic studies was evaluated based on clinical skin biopsies from PKDL patients treated in Sudan.

3.4

2. Materials and methods

2.1. Untreated human skin

Untreated control skin tissue bio-matrix was collected from leftover surgery material from anonymous patients in the Amsterdam University Medical Centers and was used in the development and validation of the assay. Leftover human tissue without specific patient consent was collected in line with the Dutch Medical Research Involving Human Subjects Act. Punch biopsies (4 mm) were taken using a circular blade, collecting the stratum corneum, dermis, epidermis until the subcutaneous layer is reached. The untreated control human skin biopsies were stored at -70°C until use.

2.2. Chemicals

Paromomycin sulphate and the internal standard (IS) consisting of multiple deuterated paromomycin acetic acid were purchased from Toronto Research Chemicals (North York, Ontario, Canada). The deuterium-label in the deuterated paromomycin IS varied between 0 (D0) and 7 (D7) deuterium atoms, with the following distribution: D0 0.13 %; D1 0.53 %; D2 2.47 %; D3 8.77 %; D4 18.13 %; D5 22.23 %; D6 20.60 %; D7 13.62 % according to the certificate of analysis. Acetonitrile, formic acid, methanol, and water (ULC grade) were bought from Biosolve Ltd (Valkenswaard, The Netherlands). Trichloroacetic acid (TCA) (99.5 %) was supplied by Merck Chemicals B.V. (Amsterdam, the Netherlands), heptafluorobutyric acid (HFBA) solution (0.5 M), calcium chloride dihydrate ($CaCl_2 \cdot 2H_2O$), and tris base were from Sigma-Aldrich (Zwijndrecht, the Netherlands). Bovine serum albumin (BSA) fraction V and collagenase A were purchased from Roche (Woerden, the Netherlands). Phosphate-buffered saline (PBS) was from Thermofischer (Breda, the Netherlands).

2.3. Preparation of the digestion solution

Preparation of digestion solution was performed by dissolving 5 mg/mL collagenase A in a buffer containing 2% BSA, 5 mM $CaCl_2$ and 25 mM tris buffer (pH 7.5). The digestion solution was stored at -20°C. Collagenase A is known to have decreased enzymatic activity following multiple freeze/thaw (F/T) cycles [29] and was therefore not used after more than 2 F/T cycles to homogenize human skin tissue.

2.4. Stock solutions and working solutions

Stock solutions of both paromomycin and IS were prepared in water with concentrations of 0.1 mg/mL (free base) and 1 mg/mL (prepared using the multi deuterated paromomycin reference standard, see section 2.2), respectively. Dilutions of paromomycin stock solution in water resulted in working solutions for calibration standards and quality control (QC) samples, both made from separately prepared paromomycin stock solutions. IS stock solution was diluted in water to a working solution of IS (WIS) concentration of 111 ng/mL D5-paromomycin, the most abundant isotope of the IS reference standard (see section 2.2). Stock and working solution were stored at -20°C.

2.5. Calibration standards, quality control samples

Dilution of working solution for calibration standards and QC samples (see section 2.4) was performed in digestion solution, by diluting the working solutions 20 times to their corresponding concentration levels. For the calibration samples, seven non-zero samples with concentrations of 5, 10, 25, 50, 100, 500, and 1000 ng/mL were prepared and for QC samples, concentrations of 5, 15, 300, and 800 ng/mL corresponding to abbreviations QC-LLOQ, QC-LOW, QC-MID, and QC-HIGH, respectively, were made. Calibration standards and QC samples were aliquoted to 50 µL volumes and stored at -20°C.

2.6. Tissue homogenization and sample preparation

Clinical full thickness skin biopsy masses (ranged from 0.835 to 8.619 mg) were determined by weighing patient samples in clean 1.5 mL reaction tubes at the analytical balance, after tarring the reaction tubes individually. A washing step followed to remove external endogenous substances from the clinical skin biopsy. Clinical skin biopsies were washed by addition of 200 µL PBS, vortex mixing and incubation for 30 min in the fridge at 2-8°C. Afterwards, the washing samples were vortexed mixed, and the patient skin biopsy samples were transferred using a polypropylene spatula to clean 1.5 mL reaction tubes. Subsequently 250 µL of digestion solution and 50 µL WIS were added to the patient samples. An increase of five times the volumes prepared for calibration-and QC samples because of poor enzymatic capabilities in low volumes using 5 mg/mL collagenase A. Stated in section 2.5, both calibration-and QC samples were prepared in the absence of skin tissue matrix. Due to the absence of skin matrix in calibration-and QC samples , WIS with a volume of 10 µL was added to 50 µL aliquoted calibration standards and QC samples. All samples were vortex mixed extensively and, subsequently, incubated overnight (≈ 16 hours) at 37°C with a rotation speed of 1,000 rpm in a thermomixer (VWR International BC, Amsterdam, the Netherlands). After overnight incubation the stratum corneum remain undissolved however the solution is clear. Subsequently, 60 µL of the clinical skin biopsy homogenates were transferred to clean 1.5 mL reaction tubes. The remainder of the clinical skin biopsy homogenate (240 µL) was stored at -70°C for re-analysis purposes.

Protein precipitation was performed by adding 40 µL 20% TCA in water (w/v) to the samples and centrifugation at 5°C for 5 minutes at 15,000 rpm. The supernatant was transferred to a clean 1.5 mL reaction tube and mixed with 150 µL water to dilute the acidity of the samples. After vortex mixing, the samples were transferred to polypropylene autosampler vials before injection into the UHPLC system.

2.7. LC equipment and conditions

Separation by liquid chromatography was performed using an UHPLC Agilent model 1290 (Infinity II series, Agilent, Santa Clara, CA, USA). The system included

an inline degasser, pumps, autosampler set at 4°C and column oven set at 40°C. Chromatographic separation by isocratic elution was performed using a HSS T3 analytical column (Waters, Milford, MA, USA; 150 mm x 2.1 mm ID, 1.8 μm particles) and 5 mM HFBA in water - acetonitrile (7:3, v/v) mixture (overall 3.5 mM HFBA in the mixture) mobile phase, at a flow rate of 0.4 mL/min for 3 minutes, as described in our earlier work [21]. A mixture of 0.1% (v/v) formic acid in acetonitrile-isopropanol-methanol-water (25:25:25:25, v/v/v/v) was used as purge and strong wash solvent.

2.8. MS equipment and conditions

Tandem mass spectrometry was used for the detection of paromomycin, using a triple quadrupole – linear ion trap system (QTRAP 6500 (Sciex, Framingham, MA, USA)) operated in positive ion mode. Paromomycin and IS were quantified in multiple reaction monitoring (MRM) mode, using transitions m/z 616.6 → 163.1 (Figure 1) and the deuterated paromomycin (IS) with m/z 621.6 → 165.1. Ion source settings were a temperature set at 500°C, ion source voltage at 5500 V, ion source gasses 1 and 2 set at 60 psi (4.1 bar) and 40 psi (2.8 bar) respectively, a curtain gas setting as 25 psi (1.7 bar) and collision gas at 10 psi (0.69 bar). Processing and acquisition of data were performed using Analyst™ software (Sciex, version 1.6.2).

2.9. Validation procedures

The assay is validated including validation parameters: calibration model, accuracy and precision, carry-over, selectivity (cross analyte/IS interferences), matrix effect, extraction recovery, dilution integrity, and stability under various conditions. The validation procedures performed were described by the EMA guidelines for the validation of bioanalytical assays in plasma [28].

2.10. Clinical application

The bioanalytical assay was developed and validated aiming to support target-site PK studies in skin of PKDL patients treated at the Prof. Elhassan Centre for Tropical Medicine, Doka, Gedaref, Sudan, with intramuscular paromomycin as part of a larger clinical trial (DNDi-MILT COMB-02-PKDL) coordinated by Drugs for Neglected Diseases initiative. The trial received ethical approval from all relevant national and local medical ethics committees. Patients were treated with daily intramuscular injections of paromomycin (20 mg/kg/d) for 14 days and skin biopsies were collected on the last day of administration [12]. Thereafter, the clinical skin biopsies were transported to Amsterdam frozen on dry ice (temperature of -80°C) and were subsequently stored at -70°C. The determination of clinical skin biopsy masses was done as described in section 2.6. The concentrations of clinical skin biopsies were measured in ng/mL and were converted to μg/g concentrations of paromomycin in skin using the determined mass of individual clinical skin biopsy masses. To demonstrate the clinical applicability of the validated assay, a selection of 5 PKDL patient samples were processed and paromomycin concentrations were determined.
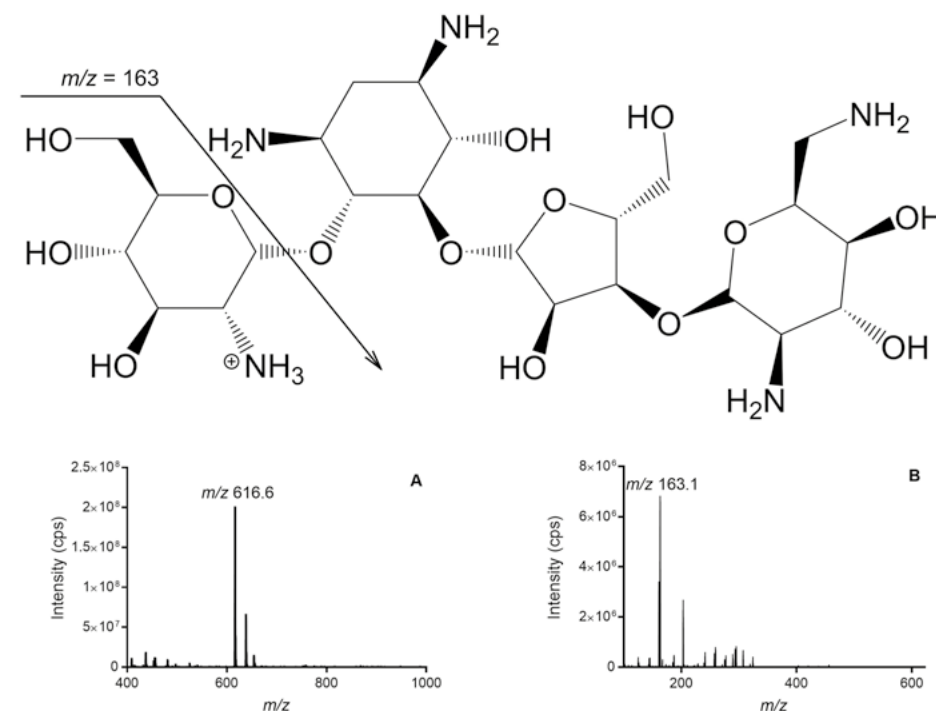
Figure 1: Chemical structure and MS spectrum of paromomycin (A) and its proposed product ion (m/z 163) (B).

3. Results and discussion

3.1. Development

The development and evaluation of human skin tissue homogenization techniques for bioanalytical purposes was described in more depth previously [15,17,30]. During development, the use of quaternary ammonium hydroxide was evaluated to dissolve skin tissue due to its strong solubility properties. The human skin tissues were fully dissolved after overnight incubation at 50°C, however, paromomycin was not stable under these conditions, mainly because of the high temperature for an extensive period. Around 28% of paromomycin was retrieved in the digestion solution after these incubation conditions compared to non-digested matrix absent samples in digestion solution, thus around 72% of paromomycin underwent degradation. The homogenization method of choice is an enzymatic digestion using collagenase A and overnight incubation at 37°C, because paromomycin was more stable under these milder thermic conditions, retrieving around 76% in digestion solution compared to non-homogenized samples in digestion solution. Enzymatic digestion of human skin tissue with a collagenase A concentration of 5 mg/mL was achieved using ≥250 μL digestion solution. QC samples with volumes of 250 μL were quantified against 50 μL

calibration samples to investigate the option of using 5 times lower volumes of WIS, calibration-and QC samples during measurement of clinical samples. Variability of sample volumes with proportionally volumes of WIS did not display errors, therefore clinical skin tissue samples with volumes ≥250 µL could be adequately quantified using calibration samples with a volume of 50 µL.

Protein precipitation sample preparation of human plasma using TCA and chromatography using HFBA as ion-pair reagent were tested similar to our previously published bioanalytical assay of paromomycin in human plasma [21]. The endogenous composition of human plasma, however, differs from human skin tissue homogenates and digestion solution. During the sample preparation procedure using digestion solution to gain final extracts of 4% TCA, the peak shape started to broaden after multiple injections. The problem was solved by 1:1 (v/v) dilution of the final extracts with water to lower the TCA concentration to 2% in the final extract (w/v). The peak shape and retention time of paromomycin returned to normal afterwards. The buffer capacity of digestion solution compared to human plasma may had influence on the competition between the highly acidic TCA versus the ion pair reagent HFBA. Sensitivity of 5 ng/mL in digestion solution was achieved and proved to be sufficient for our application after quantifying paromomycin in a selection of five randomly selected clinical human skin biopsies originating from a PKDL clinical trial.

3.2. Validation procedures
The validation procedures were executed in digestion solution. To verify the use of digestion solution as surrogate matrix for the quantification of paromomycin in human skin biopsies, additional validation experiments (matrix effect, recovery, and stability in skin biopsy homogenates) were performed in human skin tissue homogenates. Untreated human skin tissue, opposed to human plasma, is a rare bio-matrix and is challenging to acquire, thus a surrogate matrix was tested during the validation.

3.2.1. Calibration model
The calibration standards were prepared in a range of 5 – 1000 ng/mL as described in section 2.5. For each validation run, a duplicate set of calibration standards was prepared. The calibration model validation experiment was performed in three separate runs. Linearity of the calibration model was calculated using linear regression with a weighting factor of $1/x^2$ on the analyte/IS ratio against the nominal analyte concentration (x). Correlation coefficient (r^2) of 0.9967 or better were obtained. A deviation of the mean for non-zero calibration standards should be ±15% (±20% for the LLOQ) for a minimum of 75% of the non-zero calibration samples, according to EMA guidelines. The back-calculated calibration concentrations were ±9.3%, furthermore displaying a minimum signal to noise ratio at the LLOQ level of 7.2. Double blank, blank, LLOQ and upper limit of quantification (ULOQ) MRM chromatograms are shown in Figure 2.
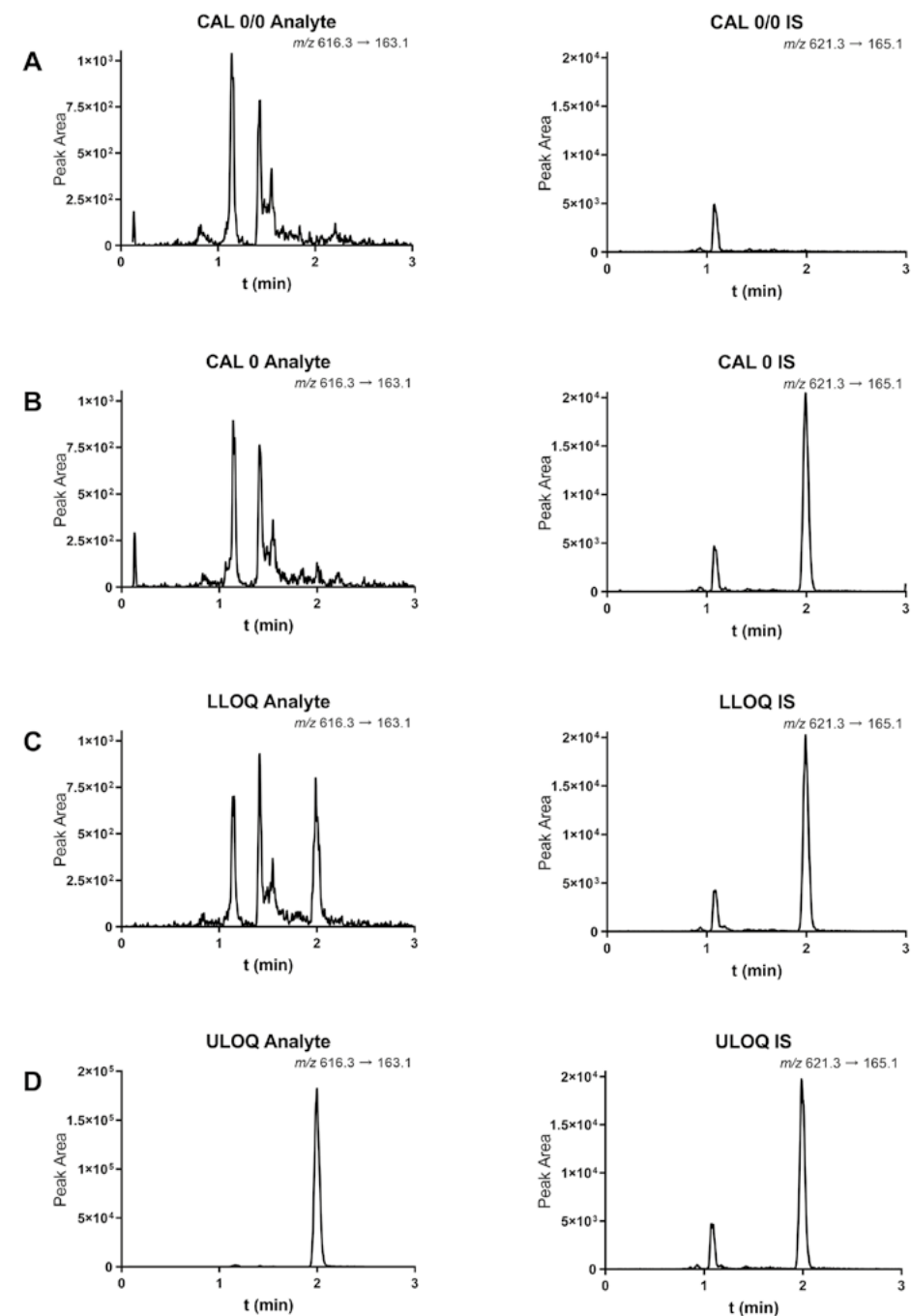

Figure 2: Representative MRM chromatograms showing the double blank (A), blank (B), LLOQ (5 ng/mL) (C) and ULOQ (1,000 ng/mL) (D) of paromomycin and IS samples in digestion solution.

3.2.2. Accuracy and precision

The assay performance was determined using five replicates of QC samples at the QC-LLOQ (5 ng/mL), QC-LOW (15 ng/mL), QC-MID (300 ng/mL) and QC-HIGH (800 ng/mL) concentration levels in three separate validation runs. The calibration model (see section 3.2.1) was used to determine the concentrations at each QC concentration level. The deviation or bias (%) from the nominal concentration is the accuracy of the assay, with the intra-assay accuracy measured per validation run and the inter-assay calculated from the three validation runs. The relative coefficient of variance (%CV) was used for the calculation of precision, performing a one-way ANOVA using the CV% at each nominal concentration level for the inter-run precision. The accuracies at the QC-LOW, QC-MID and QC-HIGH concentration levels were ±6.0% and ±7.5% for the inter-assay and intra-assay respectively, and ≤4.4% and ≤7.4% for the inter-run and intra-run precisions respectively. Accuracies at the QC-LLOQ concentration level were calculated at 16.1% and ±17.0% for the inter-assay and intra-assay respectively, the intra-assay precision was ≤7.2%. The inter-assay precision could not be calculated with one-way ANOVA, the mean square between groups was less than the mean square within groups, concluding that there is no significant additional variation due to differences in performance between assays. Acceptance of the assay performance, according to the EMA guidelines, were ±15% and ≤15% (±20% and ≤20% at the LLOQ), respectively, and all results met these criteria. The assay performance data is summarized in Table 1.

Table 1: Assay performance data for paromomycin. Accuracies and precisions were established by performing 3 analytical runs with each run containing 5 replicates of the tested concentrations.

Nominal paromomycin concentration (ng/mL)	Measured paromomycin concentration (ng/mL)	Intra-assay (n = 15)		Inter-assay (n = 15)	
		Bias (%)	Precision (%)	Bias (%)	Precision (%)
5	5.8 (±0.4)	±17.0	≤7.2	16.1	NA[a]
15	15.9 (±0.6)	±7.5	≤5.1	6.0	NA[a]
300	312 (±7.8)	±6.5	≤2.5	4.1	1.9
800	811 (±46.8)	±6.2	≤7.4	1.8	4.4

[a] No substantial additional variation was found due to the performance of the assay in different runs.

3.2.3. Carry-over

Carry-over of the analytical assay determined by the validated calibration model, was assessed in three separate validation runs. Paromomycin and IS peak areas at the retention times in two individual double blank samples after injection of the ULOQ calibration standard (1000 ng/mL) were compared to the peak areas in 5 QC-LLOQ samples. Paromomycin and IS calculated carry-over values were ≤9.9% and ≤0.7%, respectively, with acceptance criteria values of ≤20% for paromomycin and ≤5% for

the IS, and all results met these criteria and therefore the carry-over was found to be acceptable.

3.2.4. Cross-analyte/IS interference

The analyte interference was assessed by measuring paromomycin at the ULOQ concentration level (1000 ng/mL) without spiking IS to determine paromomycin in the IS transition, with an acceptance value of ≤5% of the IS peak area. IS interference was determined in IS spiked blank samples to detect IS in the paromomycin transition, with an acceptance value of ≤20% at the LLOQ level peak area. No cross-analyte/IS interferences were observed in both transitions. Conclusively, the deuterated mixture of IS (see section 2.2.) transition did not interfere with the analyte transition.

3.2.5. Matrix effect and extraction recovery

Matrix effect and recovery validation experiments were performed using single individual untreated control human skin biopsies at the paromomycin QC-LOW and QC-HIGH concentration levels. Preparation of matrix present samples includes the spiking final extract matrix with both paromomycin and IS after receiving the full sample preparation of untreated control human skin biopsies (≈ 15 mg) double blanks, as described in section 2.6, executed in six-fold. Processed samples are skin tissue biopsy samples in digestion solution at the QC-LOW and QC-HIGH concentrations, including WIS, that received full sample preparation. Matrix absent samples consists of a composition of final extract matrix absent of bio-matrix, spiked with paromomycin and IS at the exact theoretical concentrations of QC-LOW and QC-HIGH final extract concentrations. Matrix absent samples and processed samples were both performed in three-fold.

Variants of ratios between the three matrix effect and recovery samples are calculated to determine absolute matrix factors, IS-normalized matrix factors or recovery parameters, using the absolute measured peak areas. Absolute matrix factors are calculated as the paromomycin and IS peak ratios of matrix present and matrix absent samples, at their corresponding QC concentration levels. IS-normalized is the ratio of the absolute matrix factors of both paromomycin and IS. Recovery is calculated through the ratio of processed samples and matrix present samples. There is no EMA criterium for recovery, whereas the acceptance criteria for matrix effects were RSD's (%) within ≤15%, to limit variance of absolute peak areas.

Paromomycin and IS absolute matrix factors at both QC-LOW and QC-HIGH concentration levels were 0.59, indicating ion suppression due to endogenous substances originating from human skin tissue. However, the IS corrected adequately for this, leading to mean IS-normalized matrix factors of 1.10 and 0.99 at the QC-LOW and QC-HIGH paromomycin concentration levels, respectively, with an RSD of ≤6.1%. Paromomycin recovery values were 98.9% and 101.6% and IS recovery values

of 92.5% and 100.3% at the QC-LOW and QC-HIGH paromomycin concentration levels respectively. Matrix effect and recovery data are displayed in Table 2.

Table 2: Matrix factor (n = 6) and sample preparation recovery (n = 3) data for paromomycin and IS.

Nominal paromomycin Concentration (ng/mL)	Matrix Factor Analyte	Matrix Factor IS	IS-normalized Matrix Factor	Total Sample Preparation Recovery Analyte	Total Sample Preparation Recovery IS	IS-normalized Sample Preparation Recovery
15	0.59 (C.V. = 11.4%)	0.54 (C.V. = 7.2%)	1.10 (C.V. = 6.1%)	98.9% (C.V. = 11.3%)	92.5% (C.V. = 10.1%)	106.9%
800	0.59 (C.V. = 1.8%)	0.59 (C.V. = 6.2%)	0.99 (C.V. = 4.7%)	101.6% (C.V. = 7.0%)	100.3% (C.V. = 2.0%)	101.3%

Abbreviation: C.V. = coefficient of variation

3.2.6. Dilution integrity
Paromomycin with a concentration of 10,000 ng/mL (10 times the ULOQ concentration level) was diluted in digestion solution with a dilution factor of 20 to a concentration of 500 ng/mL. This was performed in five-fold to determine the performance of dilution. Accuracy and precision were calculated based on the nominal concentration of 500 ng/mL, with acceptance criteria values of ±15% for accuracy and ≤15% for precision. With an intra-assay accuracy of 2.9% and precision of 1.8%, the accuracy and precision were within acceptance criteria and a ten-fold dilution does not compromise the assay performance.

Table 3: Stability data for paromomycin (n = 3 per quality control level) expressed by accuracy (bias %) and precision (coefficient of variation).

Matrix	Condition	Nominal Concentration (ng/mL)	Measured Concentration (ng/mL)	Bias (%)	C.V. (%)
Digestion Solution	-20°C, 271d	15.0	15.5 (±0.8)	3.1	5.4
		800	746 (±75)	-6.8	10.1
Freeze/Thaw = 3	-20°C, F/T3	15.0	14.7 (±0.6)	-2.2	3.8
		800	801 (±12)	0.1	1.5
Human Skin Tissue Homogenate	-70°C, 19d	15.0	14.0 (±0.4)	-6.9	2.9
		800	707 (±13)	-11.7	1.8
Final extract	2-8°C, 23d	15.0	14.3 (±0.4)	-4.7	3.0
		800	783 (±24)	-2.1	3.0

Abbreviations: ᵃ = not stable; C.V. = coefficient of variation; d = days; F/T = freeze/thaw cycles.

3.2.7. Stability
Stability was determined by measuring QC-LOW and QC-HIGH samples in triplicate and assess the bias (%) and CV (%) from the nominal concentrations, with acceptance criteria values of ±15% bias and ≤15% CV%. The stability in stock and working solutions were assessed previously [21]. Stability of paromomycin was determined in untreated control human skin tissue (≈ 15 mg) homogenates stored at -70°C for 19 days, digestion solution stored for 271 days at -20°C, 3 F/T cycle stability and in final extracts for 23 days at 2-8°C. The acceptance criteria were met, and data are presented in Table 3.

3.3. Clinical application
A random selection of 5 PKDL patient skin biopsy samples collected in Sudan were analyzed using the validated bioanalytical method. The measured concentrations (ng/mL) of the clinical skin tissue biopsy homogenates were converted to concentrations of paromomycin in skin tissue (µg/g). Chromatograms and concentrations are shown in Figure 3 and Table 4, respectively. The median (range) paromomycin concentration in these patient skin samples was 14.13 (5.16 – 28.28) µg/g. In depth PK analysis from the clinical target-site PK study will be reported in detail elsewhere.
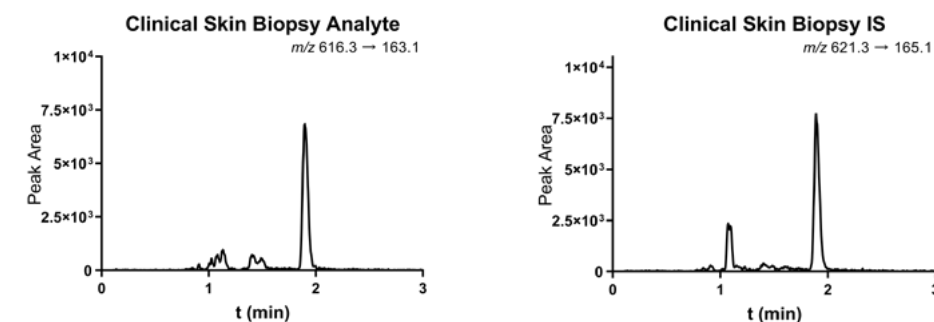

Figure 3: Representative MRM chromatograms of a Sudanese post kala-azar dermal leishmaniasis patient in treatment with a duration of 14 days (20 mg/kg/d paromomycin), showing the clinical skin biopsy peak shape with a concentration of 44.7 ng/mL or 5.16 µg/g.

Table 3: Paromomycin skin tissue biopsy concentration data in 5 individual post kala-azar dermal leishmaniasis patients from Sudan at day 14 after receiving a 14-day paromomycin regimen.

Clinical Skin Biopsy #	Skin Biopsy Weight (mg)	Paromomycin Concentration in Digestion Solution (ng/mL)	Paromomycin Concentration in Skin Biopsy (μg/g)
1*	2.166	44.7	5.16
2	3.591	203	14.13
3	2.428	105	10.81
4	1.273	144	28.28
5	2.481	187	18.84

* = as shown in Figure 3.

4. Conclusion

Paromomycin quantification in 4-mm human skin punch biopsies using LC-MS/MS was successfully developed and validated employing an accurate and sensitive bioanalytical assay within approved EMA acceptance criteria. Skin tissue biopsies were first subjected to overnight enzymatic digestion to homogenize the tissues, following simple protein precipitation with TCA for the extraction of paromomycin and the deuterated IS. Ion-pair UPLC chromatography was employed for the separation of paromomycin, using ion-pair reagent HFBA in an isocratic setup, connected to a triple quadrupole MS system for detection. The method was validated over a range from 5 to 1000 ng/mL, displaying adequate assay performance. The sensitivity of 5 ng/mL was achieved despite retrieving around 76% of paromomycin during collagenase A enzymatic digestion incubation conditions. The IS adequately corrected for the matrix effects affecting paromomycin response, allowing accurate quantification of paromomycin in human skin tissue using digestion solution as surrogate matrix, accomplishing an IS-normalized recovery of 100%. Paromomycin was stable for at least 19 days at -70°C in human skin tissue homogenates. Finally, the bioanalytical was successfully applied to quantify paromomycin in clinical skin biopsies from PKDL patients treated with intramuscular paromomycin in Sudan.

3.4

References

[1]   R.N. Davidson, M. den Boer, K. Ritmeijer, Paromomycin, Trans. R. Soc. Trop. Med. Hyg. 103 (2009) 653–660. https://doi.org/10.1016/j.trstmh.2008.09.008.

[2]   S. Sundar, J. Chakravarty, Paromomycin in the treatment of leishmaniasis, Expert Opin. Investig. Drugs. 17 (2008) 787–794. https://doi.org/10.1517/13543784.17.5.787.

[3]   S.L. Croft, P. Olliaro, Leishmaniasis chemotherapy—challenges and opportunities, Clin. Microbiol. Infect. 17 (2011) 1478–1483. https://doi.org/10.1111/j.1469-0691.2011.03630.x.

[4]   S. Sundar, T.K. Jha, C.P. Thakur, P.K. Sinha, S.K. Bhattacharya, Injectable Paromomycin for Visceral Leishmaniasis in India, N. Engl. J. Med. 356 (2007) 2571–2581. https://doi.org/10.1056/NEJMoa066536.

[5]   K.M. Jamil, R. Haque, R. Rahman, M.A. Faiz, A.T.M.R.H. Bhuiyan, A. Kumar, S.M. Hassan, H. Kelly, P. Dhalaria, S. Kochhar, P. Desjeux, M.A.A. Bhuiyan, M.M. Khan, R.S. Ghosh, Effectiveness Study of Paromomycin IM Injection (PMIM) for the Treatment of Visceral Leishmaniasis (VL) in Bangladesh, PLoS Negl. Trop. Dis. 9 (2015) e0004118. https://doi.org/10.1371/journal.pntd.0004118.

[6]   A.M. Musa, B. Younis, A. Fadlalla, C. Royce, M. Balasegaram, M. Wasunna, A. Hailu, T. Edwards, R. Omollo, M. Mudawi, G. Kokwaro, A. El-Hassan, E. Khalil, Paromomycin for the treatment of visceral leishmaniasis in Sudan: a randomized, open-label, dose-finding study., PLoS Negl. Trop. Dis. 4 (2010) e855. https://doi.org/10.1371/journal.pntd.0000855.

[7]   Y. Melaku, S.M. Collin, K. Keus, F. Gatluak, K. Ritmeijer, R.N. Davidson, Treatment of kala-azar in southern Sudan using a 17-day regimen of sodium stibogluconate combined with paromomycin: a retrospective comparison with 30-day sodium stibogluconate monotherapy., Am. J. Trop. Med. Hyg. 77 (2007) 89–94. http://www.ncbi.nlm.nih.gov/pubmed/17620635.

[8]   R. Kimutai, A.M. Musa, S. Njoroge, R. Omollo, F. Alves, A. Hailu, E.A.G. Khalil, E. Diro, P. Soipei, B. Musa, K. Salman, K. Ritmeijer, F. Chappuis, J. Rashid, R. Mohammed, A. Jameneh, E. Makonnen, J. Olobo, L. Okello, P. Sagaki, N. Strub, S. Ellis, J. Alvar, M. Balasegaram, E. Alirol, M. Wasunna, Safety and Effectiveness of Sodium Stibogluconate and Paromomycin Combination for the Treatment of Visceral Leishmaniasis in Eastern Africa: Results from a Pharmacovigilance Programme., Clin. Drug Investig. 37 (2017) 259–272. https://doi.org/10.1007/s40261-016-0481-0.

[9]   S. Sundar, P.K. Sinha, M. Rai, D.K. Verma, K. Nawin, S. Alam, J. Chakravarty, M. Vaillant, N. Verma, K. Pandey, P. Kumari, C.S. Lal, R. Arora, B. Sharma, S. Ellis, N. Strub-Wourgaft, M. Balasegaram, P. Olliaro, P. Das, F. Modabber, Comparison of short-course multidrug treatment with standard therapy for visceral leishmaniasis in India: an open-label, non-inferiority, randomised controlled trial., Lancet (London, England). 377 (2011) 477–86. https://doi.org/10.1016/S0140-6736(10)62050-8.

[10]   A. Asilian, T. Jalayer, M. Nilforooshzadeh, R.L. Ghassemi, R. Peto, S. Wayling, P. Olliaro, F. Modabber, Treatment of cutaneous leishmaniasis with aminosidine (paromomycin) ointment: Double-blind, randomized trial in the Islamic Republic of Iran, Bull. World Health Organ. 81 (2003) 353–359. https://doi.org/10.1590/S0042-96862003000500009.

[11]   N. Sosa, J.M. Pascale, A.I. Jiménez, J.A. Norwood, M. Kreishman-Detrick, P.J. Weina, K. Lawrence, W.F. McCarthy, R.C. Adams, C. Scott, J. Ransom, D. Tang, M. Grogl, Topical paromomycin for New World cutaneous leishmaniasis., PLoS Negl. Trop. Dis. 13 (2019) e0007253. https://doi.org/10.1371/journal.pntd.0007253.

[12]   NCT03399955, Short Course Regimens for Treatment of PKDL (Sudan), 2018.

[13]   M. Rizk, L. Zou, R. Savic, K. Dooley, Importance of Drug Pharmacokinetics at the Site of Action, Clin. Transl. Sci. 10 (2017) 133–142. https://doi.org/10.1111/cts.12448.

[14]   Y.-J. Xue, H. Gao, Q.C. Ji, Z. Lam, X. Fang, Z. Lin, M. Hoffman, D. Schulz-Jander, N. Weng, Bioanalysis of drug in tissue: current status and challenges, Bioanalysis. 4 (2012) 2637–2653. https://doi.org/10.4155/bio.12.252.

[15]   I.C. Roseboom, H. Rosing, J.H. Beijnen, T.P.C. Dorlo, Skin tissue sample collection, sample homogenization, and analyte extraction strategies for liquid chromatographic mass

[16]   A.E. Kip, J.H.M. Schellens, J.H. Beijnen, T.P.C. Dorlo, Clinical Pharmacokinetics of Systemically Administered Antileishmanial Drugs, Clin. Pharmacokinet. 57 (2018) 151–176. https://doi.org/10.1007/s40262-017-0570-0.

[17]   I.C. Roseboom, B. Thijssen, H. Rosing, F. Alves, D. Mondal, M.B.M. Teunissen, J.H. Beijnen, T.P.C. Dorlo, Development and validation of an HPLC-MS/MS method for the quantification of the anti-leishmanial drug miltefosine in human skin tissue, J. Pharm. Biomed. Anal. (2021) 114402. https://doi.org/10.1016/j.jpba.2021.114402.

[18]   F. Farouk, H.M.E. Azzazy, W.M.A. Niessen, Challenges in the determination of aminoglycoside antibiotics, a review, Anal. Chim. Acta. 890 (2015) 21–43. https://doi.org/10.1016/j.aca.2015.06.038.

[19]   J. Lu, M. Cwik, T. Kanyok, Determination of paromomycin in human plasma and urine by reversed-phase high-performance liquid chromatography using 2,4-dinitrofluorobenzene derivatization, J. Chromatogr. B Biomed. Sci. Appl. 695 (1997) 329–335. https://doi.org/10.1016/S0378-4347(97)00192-8.

[20]   W.R. Ravis, A. Llanos-Cuentas, N. Sosa, M. Kreishman-Deitrick, K.M. Kopydlowski, C. Nielsen, K.S. Smith, P.L. Smith, J.H. Ransom, Y.J. Lin, M. Grogl, Pharmacokinetics and absorption of paromomycin and gentamicin from topical creams used to treat cutaneous leishmaniasis, Antimicrob. Agents Chemother. 57 (2013) 4809–4815. https://doi.org/10.1128/AAC.00628-13.

[21]   I.C. Roseboom, B. Thijssen, H. Rosing, J. Mbui, J.H. Beijnen, T.P.C. Dorlo, Highly sensitive UPLC-MS/MS method for the quantification of paromomycin in human plasma, J. Pharm. Biomed. Anal. 185 (2020) 113245. https://doi.org/10.1016/j.jpba.2020.113245.

[22]   R. Oertel, V. Neumeister, W. Kirch, Hydrophilic interaction chromatography combined with tandem-mass spectrometry to determine six aminoglycosides in serum, J. Chromatogr. A. 1058 (2004) 197–201. https://doi.org/10.1016/j.chroma.2004.08.158.

[23]   W.X. Zhu, J.Z. Yang, W. Wei, Y.F. Liu, S.S. Zhang, Simultaneous determination of 13 aminoglycoside residues in foods of animal origin by liquid chromatography-electrospray ionization tandem mass spectrometry with two consecutive solid-phase extraction steps, J. Chromatogr. A. 1207 (2008) 29–37. https://doi.org/10.1016/j.chroma.2008.08.033.

[24]   K. Róna, G. Klausz, E. Keller, M. Szakay, P. Laczay, M. Shem-Tov, P. Székely-Körmöczy, Determination of paromomycin residues in turkey tissues by liquid chromatography/mass spectrometry, J. Chromatogr. B Anal. Technol. Biomed. Life Sci. 877 (2009) 3792–3798. https://doi.org/10.1016/j.jchromb.2009.09.018.

[25]   A. Kaufmann, P. Butcher, K. Maden, Determination of aminoglycoside residues by liquid chromatography and tandem mass spectrometry in a variety of matrices, Anal. Chim. Acta. 711 (2012) 46–53. https://doi.org/10.1016/j.aca.2011.10.042.

[26]   S.J. Lehotay, K. Mastovska, A.R. Lightfield, A. Nuñez, T. Dutko, C. Ng, L. Bluhm, Rapid analysis of aminoglycoside antibiotics in bovine tissues using disposable pipette extraction and ultrahigh performance liquid chromatography-tandem mass spectrometry, J. Chromatogr. A. 1313 (2013) 103–112. https://doi.org/10.1016/j.chroma.2013.08.103.

[27]   D.A. Bohm, C.S. Stachel, P. Gowik, Validation of a method for the determination of aminoglycosides in different matrices and species based on an in-house concept, Food Addit. Contam. - Part A Chem. Anal. Control. Expo. Risk Assess. 30 (2013) 1037–1043. https://doi.org/10.1080/19440049.2013.775709.

[28]   European Medicines Agency, Committee for Medicinal Products for Human Use. Guideline on bioanalytical method validation, 2012. https://doi.org/EMEA/CHMP/EWP/192217/2009.

[29]   F. Israel-Roming, G. Luta, D. Balan, E. Gherghina, C.P. Cornea, F. Matei, Time and Temperature Stability of Collagenase Produced by Bacillus licheniformis, Agric. Agric. Sci. Procedia. 6 (2015) 579–584. https://doi.org/10.1016/j.aaspro.2015.08.091.

[30]   I.C. Roseboom, B. Thijssen, H. Rosing, F. Alves, S. Sundar, J.H. Beijnen, T.P.C. Dorlo, Development and validation of a high-performance liquid chromatography tandem mass spectrometry method for the quantification of the antiparasitic and antifungal drug amphotericin B in human skin tissue, J. Chromatogr. B. 1206 (2022) 123354. https://doi.org/10.1016/j.jchromb.2022.123354.

spectrometry quantification of pharmaceutical compounds, J. Pharm. Biomed. Anal. 191 (2020) 113590. https://doi.org/10.1016/j.jpba.2020.113590.

3.4

Pharma-cokinetics in Human Skin Tissue

4

Skin pharmacokinetics of miltefosine in the treatment of post kala-azar dermal leishmaniasis

Semra Palić
Ignace C. Roseboom
Shyam Sundar
Dinesh Mondal
Pradeep Das
Krishna Pandey
Sheeraz Raja
Suman Rijal
Abdullah Hamadeh
Paul R.V. Malik
Jos H. Beijnen
Alwin D.R. Huitema
Erik Sjögren
Fabiana Alves
Thomas P.C. Dorlo

4.1

Abstract

Post-kala-azar dermal leishmaniasis (PKDL) is a dermal complication of visceral leishmaniasis (VL). Effective treatments for PKDL are lacking and skin distribution of antileishmanial compounds is unknown in human. The present study evaluated the skin distribution of miltefosine in PKDL patients, to better understand of target-site pharmacokinetics in PKDL.

Fifty-three PKDL patients were treated with Ambisome® (liposomal amphotericin B) (20mg/kg) plus miltefosine by allometric dosing for 21 days. Miltefosine concentrations were measured in plasma on days 7, 14, 21, 29, while a punch skin biopsy was taken on day 22. A physiologically based PK (PBPK) model of miltefosine skin penetration was developed.

Following the allometric weight-based dosing regimen, skin concentrations on day 22 were on median 43.73 **µg/g (IQR: 60.65 – 21.94 µg/g)** and in plasma 33.29 µg/ml (IQR: 25.9 – 42.58 µg/ml). The median concentration ratio of skin to plasma was 1.19 (IQR: 0.79 – 1.9). Approximately 90% of PKDL patients had exposure in the skin above a suggested PK target associated with in vitro activity (EC90 of 10.6 mg/L). Simulations showed that residence time of miltefosine in the skin is nearly twice longer compared to blood plasma, estimated by mean residence time at 604 hours versus 266 hours respectively.

The present study provides the first accurate measurements of miltefosine penetration in the skin, estimating to which extent the parasite-loaded macrophages in the skin are exposed to miltefosine. As such, combined with parasitological and clinical data, this is a promising start for future optimization of miltefosine in treatment of PKDL

1. Introduction

Leishmaniasis is an infectious disease caused by the protozoan parasite *Leishmania*, transmitted by sand flies. By primarily affecting the poorest populations, leishmaniasis remains one of the most neglected tropical diseases [1]. The most common clinical presentation of the disease, which affects up to 2 million people per year, is cutaneous leishmaniasis (CL), leading to skin ulcers and lesions at the site of infection [2]. The most severe form of leishmaniasis is visceral leishmaniasis (VL) or kala azar [3]. VL affects internal organs and is lethal within months without adequate treatment. In addition, some patients who were previously treated for VL develop post kala-azar dermal leishmaniasis (PKDL) months or years after treatment. Clinical manifestation of PKDL include skin rash in form of macular, nodular or mixed lesions [4,5]. In South Asia, PKDL develops in 5 – 10 % of VL treated patients within an average of 2 years after VL treatment and with predominance of the macular form [4]. As *Leishmania* parasites reside in the skin, sand flies feeding on PKDL patients may become infected and further transmit the parasite. Therefore, patients with chronic PKDL serve as reservoirs for VL transmission, and all patients should be treated.

Miltefosine is the first and still only oral agent available in treatment of leishmaniasis. It is an alkylphosphocholine compound, consisting of long-chain alcohols in phosphocholine esters [6]. Due to its chemical structure, with its long hydrophobic tail, miltefosine has a high affinity for lipid rafts, and is able to incorporate in the lipid bilayers of cell membranes, without disrupting the membrane itself [7,8]. With respect to pharmacokinetics (PK), miltefosine is slowly absorbed from the gastrointestinal tract, with reported saturable absorption in both preclinical and clinical studies [9,10]. In addition, plasma clearance is low, with elimination half-lives estimated at 7 and ~30 days [6]. Due to these PK properties, miltefosine accumulates in plasma until the end of treatment [11,12].

Treatment regimens with miltefosine have been established for CL and VL. In South Asia, current recommended treatment for PKDL is miltefosine for long period of 12 weeks, while recent studies have also shown the efficacy of Ambisome for the treatment of PKDL. Long treatment duration of 12 weeks together with poor tolerability may hinder treatment compliance. In addition, women of childbearing age require 8 months of contraception (during treatment and 5 months after treatment) due to miltefosine teratogenicity. Shorter treatment durations are therefore needed, urging for adequate evidence-based treatment for PKDL. Due to a lack of studies investigating exposure-response relationships for miltefosine in the treatment of PKDL, it remains challenging to further optimize and rationalize treatment. The main burden of parasite biomass in PKDL is located in the dermis of the skin, however, no investigations have been performed on target-site exposure in the skin of any of the currently used antileishmanial drugs in the treatment of any

type of dermal leishmaniasis [13]. Such PK studies are pivotal to further optimize and rationalize treatment regimens for the various different clinical presentations of leishmaniasis. In the present study, we aimed to provide the first data on miltefosine exposure in skin tissue from PKDL patients treated with miltefosine, as a proxy of target-site exposure at the site of the parasite infection. Furthermore, we used a physiologically based PK (PBPK) modelling approach to further elucidate miltefosine PK in both skin and plasma after oral administration as a framework for target-site tissue predictions.

2. Patients and Methods

2.1. Clinical studies and patient cohorts

2.1.1. PKDL study

The clinical data originated from a non-comparative, open label, randomized phase II trial, which was conducted to assess the safety and efficacy of Ambisome monotherapy (total dose of 20 mg/kg) and Ambisome (20 mg/kg) in combination with miltefosine (allometric dosing) in treatment of PKDL patients from Bangladesh (study site of the International Centre for Diarrhoeal Disease Research) and India (study sites of Rajendra Memorial Research Institute of Medical Sciences, Patna and Kala Azar Medical Research Centre, Muzzafarpur, both in Bihar state), which will be reported in another manuscript. In the combination arm, oral miltefosine daily dose was divided in two administrations (with food) according to a previously determined allometric dose for a duration of 21 days. Allometric dosing algorithm increases mg/kg dose for patients with body weight < 30 kg [10,14], while there is no difference no difference between the allometric scale and conventional dose of 2.5 mg/kg/day for patients > 30 kg. Enrolment criteria included patients with confirmed PKDL by clinical presentation and demonstration of parasites by microscopy skin smear or qPCR, with a documented stable or progressive disease lasting longer than 4 months. The age inclusion criteria ranged from 6 to 60 years of age, and written informed consent from patients, or patient's parent or guardian for children younger than 18 years was obtained before the treatment initiation. Patients who had a prior treatment for PKDL in the last two years were not included in this study. The study further excluded pregnant and lactating women, women of childbearing potential did not accept to take effective contraception for the duration of treatment and 5 months thereafter, patients with contaminant infection such as tuberculosis or HIV, and severe underlying disease such as cardiac, renal or hepatic diseases, as well as individuals who presented severe malnutrition. Miltefosine plasma samples were collected on day 7, day 14, day 21, and day 29 after treatment onset correspondent to scheduled study visits on days 8, 15, 22 and 30, as well as at three months during the follow up period. In addition, on day 22 (approximately 24 hours after the last dose

on day 21) a punch biopsy of the skin was taken from all patients randomized to the Ambisome/miltefosine treatment group.

2.1.2. CL study

Prior PK data from a study in CL patients were used to enable the development of the miltefosine PBPK model, as the PK data from the PKDL trial lacked plasma samples to accurately estimate drug absorption. Thirty-one Dutch military personnel who were infected with CL (*Leishmania major*) and were otherwise systemically healthy were included in the present analysis. A population PK analysis of this trial has been previously reported [15]. Plasma samples were obtained at 2, 4, and 6 hours post first dose on the first day of treatment, then weekly during the treatment on an outpatient basis, as well as during 5 months of follow up [15].

2.2. Quantification of miltefosine concentrations

2.2.1. In plasma

Miltefosine was quantified in plasma by liquid chromatography coupled to tandem mass spectrometry (LC-MS/MS) in both studies, previously validated with the lowest limit of quantification (LLOQ) of 4 ng/ml and 10 ng/ml for the CL and PKDL studies, respectively [16]. Samples from the PKDL study were measured at the bioanalytical laboratory of Lambda Therapeutic Research, in Ahmedabad, India Samples from the CL study were measured at the bioanalytical laboratory of the Antoni van Leeuwenhoek hospital / Netherlands Cancer Institute in Amsterdam.

2.2.2. In skin

Collected biopsies were stored at -70 °C and transported on dry ice to the bioanalytical laboratory. Detailed bioanalytical assay development and validation will be reported in a separate publication (manuscript in draft). In short, the assay employed chemical skin tissue digestion, followed by solid phase extraction (SPE) and quantification using LC-MS/MS, similar to the miltefosine plasma PK methodology. Prior to digestion, the skin tissue was washed using 250 µL cold phosphate buffer saline (PBS). This was followed by skin tissue transfer from the washing buffer. The washing buffer was diluted 1:1 (vol/vol) with 4% bovine serum albumin (BSA). Following the washing step, skin tissue was transferred to a clean reaction tube containing 500 µL digestion buffer [2% BSA in 5 mM $CaCl_2$ 25 mM Tris (pH 7.5) and 5 mg/mL collagenase A]. A volume of 50 µL miltefosine-d4 stable isotope internal standard (IS) was added. Subsequently, the skin tissue was incubated overnight at 37°C, using a thermos shaker. After incubation, 275 µL homogenized human skin tissue, including IS, was extracted using phenyl-bonded SPE cartridges. Seven hundred microliter 2.5 M ammonium acetate (pH 4.5) was added to homogenized skin tissue and centrifuged at 5°C for 5 minutes at 23,100 g, before adding the supernatant to the SPE cartridge. For the SPE cartridge, 1 mL ACN conditioning solvent and subsequently 1 mL 2.5 M ammonium

acetate (pH 4.5) activation solvent was added before transferring the supernatant of human skin tissue mixture. The SPE cartridge was then washed with 1 mL water/MeOH (1:1, vol/vol) and eluted using 1.5 mL 0.1% TEA in MeOH. The elution solvent was transferred to glass autosampler vials. The LC-MS/MS instruments were modernized relative to the Dorlo et al. method, employing a UPLC LC-30AD pump with an inline degasser connected to a UPLC LC-30AMCP autosampler, set at 4 °C and CTO-20AC column oven (Nexera X2 series, Shimadzu Corporation, Kyoto, Japan). The validated concentration range for a standardized skin biopsy sample weight of 15 mg, was 4 – 1000 ng/ml, converted into µg/g miltefosine in skin biopsy using the mass of each individual human skin tissue sample. Mass/charge transitions at m/z 408.5 to 125.1 and at 412.6 to 129.2, were monitored for miltefosine and miltefosine-d4, respectively. The relative error was ±2.3% for the concentrations above LLOQ and ±6.6% at LLOQ level. The coefficient of variation in terms of method precision was <1.9% for the concentrations above LLOQ, and <2.5% at LLOQ level.

2.3. PBPK Model development

This work applied middle-out strategies to facilitate PBPK model development. As such, firstly the PBPK model was developed based on the databases containing drug-specific, system-specific parameters, in vitro and preclinical data regarding miltefosine PK. Next, clinical data was used to optimize the model parameters.

2.3.1. Software

PBPK modeling was performed using the Open System Pharmacology Suite including the modeling software PK-Sim® and MoBi® (Open Systems Pharmacology Suite 9.0, https://www.open-systems-pharmacology.org). Graphical evaluation and statistical analyses were performed in R and R Studio (version 3.6.3 and 3.4.3) [17].

2.3.2. Miltefosine PBPK model building

At start, the miltefosine drug model was built using drug physicochemical properties. The model was informed by available data regarding the processes of absorption, distribution, metabolism and elimination (ADME). The literature was reviewed through the PubMed database to collect drug-specific parameter values. In case of multiple values identified for a parameter, either a range of values was tested on the model, or when that was not possible, each value was tested for its ability to result in a simulation that adequately fitted the observed data. Parameters were identified by minimization of the residuals between observed data and corresponding simulation output adopting the optimization functionality and the Levenberg-Marquardt algorithm included in PK-Sim®.

Secondly, a full body PBPK model was built for miltefosine adopting the generic model for small molecules within the software PK-Sim. This is a full body PBPK model accommodating 15 different organs with rich information regarding the

volumes, blood flow rates, metabolism etc [18]. Each of these organs further consists of compartments representing the plasma, interstitial and intracellular space. At start, the miltefosine drug model was informed by available data regarding drug physicochemical properties and the processes of absorption, distribution, metabolism and elimination (ADME). The literature was reviewed through the PubMed database to collect drug-specific parameter values. In case of multiple values identified for a parameter, either a range of values was used as input in the model and tested for its ability to result in a simulation that adequately fitted the observed data. To further improve model performance drug-related parameters were further optimized towards PK data from two clinical studies of miltefosine PK in CL and PKDL patients. Parameters were identified by minimization of the residuals between observed data and corresponding simulation output adopting the optimization functionality and the Levenberg-Marquardt algorithm included in PK-Sim®. On basis of the pooled data of miltefosine concentrations in plasma, distribution and elimination were parametrized by optimizing parameters such as lipophilicity, specific intestinal permeability (transcellular) and specific drug clearance (normalized to the enzyme concentration of 1 mmol/l). In addition, since miltefosine has a long hydrophobic chain, it was expected to be incorporated into the cell membrane, and subsequently enter the cell. This unspecific binding was accommodated in the model by including an unspecific binding partner located at the cell membranes. MoBi was then employed to facilitate simulation output representative for clinical reference skin concentration measurements by creating an observer to trace the concentration of the drug sequestered in the cell membrane, while conserving drug mass balance within the original PBPK model. Membrane binding of miltefosine was explicitly represented by the cell membrane accumulation factor, determined by the equilibrium constant K_d, and the dissociation constant k_{off}. In physiological terms, this factor represents all lipid membranes to which miltefosine binds. In this respect, K_d, and the relative expression of the cell membrane binding partner was optimized in the skin based on the measured miltefosine concentrations in patient biopsies, and then subsequently fixed for the other organs. As this membrane binding is applicable for all organs, the same structure is assumed, thus the estimated corresponding relative expression are scaled by the volumes of organs, plasma compartments and blood flow rates. The mass transfer of the drug from plasma into each organ is then determined by the K_d, volumes of the compartments and the concentration of drug

2.4 Simulations

A number of simulations were performed based on the virtual patient populations representative of the patient cohorts of the included clinical data. For each of simulations, the dosing regimen of miltefosine corresponding to the clinical study was used. For this purpose, virtual populations of individuals were created utilizing the in-built population algorithm in PK-Sim and based on the population characteristics stated in the respective publication. System-dependent parameters,

4.1

such as age, weight, height, organ weights, blood flow rates, tissue composition, etc., were varied by the implemented algorithm in PK-Sim [19]. Simulations of miltefosine in plasma and the skin were used for the final parameter identification step. At last, the optimized PBPK model was used to simulate PK profiles of miltefosine in the spleen and liver.

3. Results

3.1. Patients and data
In total, PK data of 52 patients was available from the PKDL study. The details of patient demographics, as well as the dosing of miltefosine are provided in Table 1. A total of 273 miltefosine plasma concentrations, and 52 skin biopsies were available for this analysis.

3.2. Observed skin penetration of miltefosine and comparison with exposure in plasma
The miltefosine concentrations that were measured in the collected skin biopsies, represent a combination of intracellular and interstitial concentrations, since extracellular miltefosine and dermal blood were washed off during the sample preparation. Observed miltefosine concentrations in the skin and plasma are presented in Figure 1.

Miltefosine concentrations in the skin on day 22 were on median 43.73 **µg/g (IQR: 60.65 – 21.94 µg/g) while median concentrations in plasma at the same time point were 33.29** µg/ml (IQR: 25.9 – 42.58 µg/ml). High interindividual variability (IIV) in concentrations of miltefosine was observed for both skin and plasma (coefficient of variation (CV)% of 65.9 and 39.5%, respectively). The median concentration ratio of skin to plasma was 1.19 (IQR: 0.79 – 1.9). In total 17 patients had a ratio of skin to plasma < 1, while 35 had this ratio >1. Individual plasma and skin miltefosine concentrations showed a moderate degree of correlation with a correlation coefficient of 0.53.

3.3. Miltefosine PBPK model and simulations
Summary of the model parameters utilized in the drug model are given in Table 2. Simulated PK parameters are given in Table 3. Identified parameters are in line with previous reports [20] and are summarized in Table 4. Skin concentrations were used to estimate parameters of the cell membrane binding partner (Table 4). The developed model adequately predicted typical miltefosine concentrations in the two compartments for which observations were available, i.e., plasma and skin. Accumulation of the drug in the skin exceeded concentrations in plasma, as illustrated in Figure 2, which is in line with higher median observations of miltefosine in the skin than inred patients' plasma. The model-based simulations indicated that

the residence time of miltefosine in the skin is nearly twice as long compared to residence time in blood plasma, as estimated by mean residence time (MRT) for the skin at 604 hours compared to 266 hours in plasma. The established PBPK model can be used to derive predicted exposure of other tissues of interests, which should be validated further (Figure 3). Simulated PK parameters for the spleen and liver are further summarized in the Table 3. Lastly, the PK target for miltefosine in VL has been previously been suggested as the time the miltefosine concentration is above the in vitro susceptibility EC_{90} value of 10.6 mg/L [12]. Present data show that 90% of PKDL patients had exposure in the skin above this target value. Typical time > EC_{90} in the skin as simulated by the PBPK model was 52 days (from day 2 till day 54). Evaluation of this target was not performed in any PKDL study till now, while could be appropriate since it is same parasite causing different disease manifestations.

Table 1: Patient demographics and the dosing of miltefosine for the clinical studies included in the PBPK model development

Parameter	Median value (interquartile range)
	PKDL study
	Bangladesh
Total number of patients	14
Age (years)	27 (15 – 38)
Weight (kg)	44 (39 -53)
Height (cm)	160 (153 – 164)
Dose (mg/kg/day)	2.27 (1.89 – 2.60)
	India
Total number of patients	38
Age (years)	22 (15 – 33)
Weight (kg)	47 (41 -53)
Height (cm)	153 (147 -161)
Dose (mg/kg/day)	2.16 (1.87 – 2.39)

Table 2: Summary of miltefosine drug model parameters used in simulations

Parameter	Value	Unit
Physiochemical parameter		
Molecular weight	407.58	g/mol
Fu (plasma)	0.03	
pKa (acid)	2	
pKa (base)	7.2	
Aqueous diffusion coefficient	$2.9 * 10^{-4}$	cm²/min
Solubility (at reference pH)	2.5 (7.2)	mg/ml

Fu (plasma): fraction unbound in plasma, pKa: acid dissociation constant
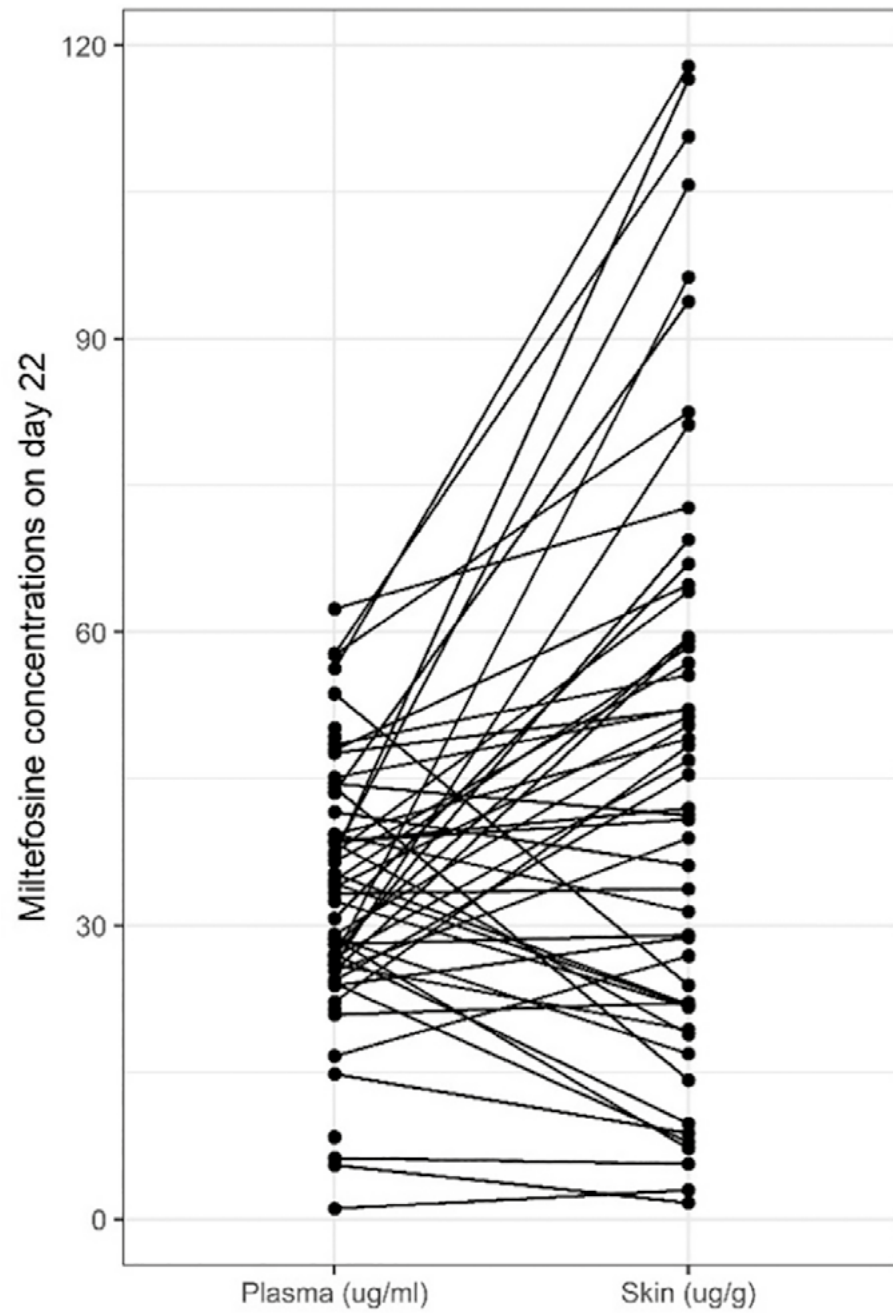
4.1

Figure 1: Observed miltefosine concentrations in plasma and skin after 21-day treatment with an allometric weight-based dosing regimen. Individual patient measurements for both plasma and skin are paired by individual lines
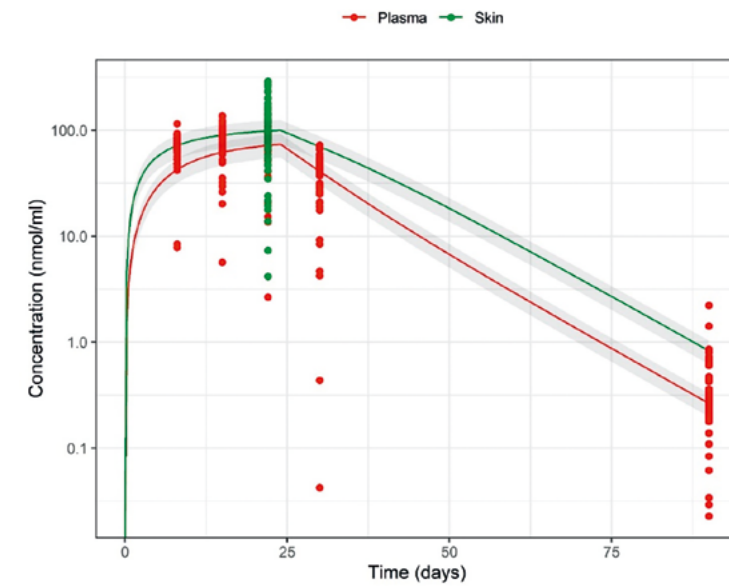

Figure 2: Observed and simulated miltefosine concentrations in plasma and skin tissues. Red dots represent observed concentrations in plasma while red line represents model simulation of miltefosine in plasma. Green dots represent observed miltefosine concentrations in the skin while the green line illustrates the simulated skin concentration based on the PBPK model. Shaded areas indicate 95% CI of the mean.
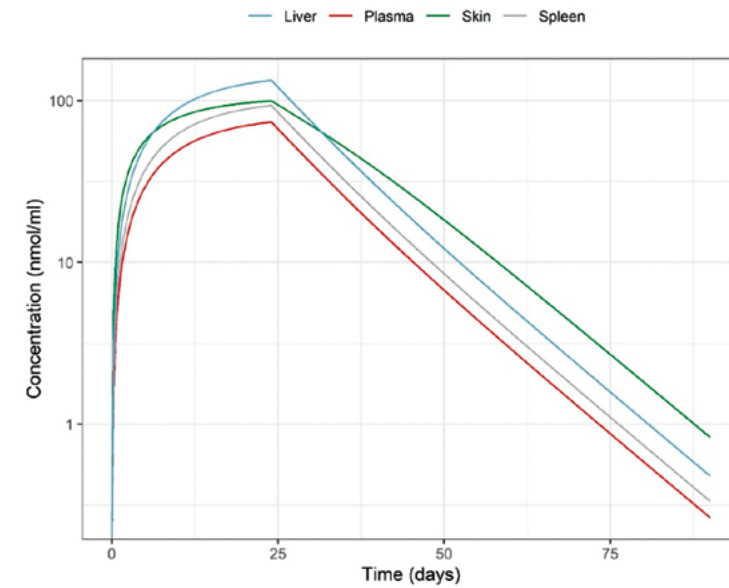

Figure 3: Model based simulations of miltefosine pharmacokinetics in various organs following allometric weight-based dosing regimen in duration of 21 days. Blue line (liver), red line (plasma), green line (skin), gray line (spleen).

Table 3: Simulated pharmacokinetic parameters of miltefosine following the dosing regimen utilized in the clinical studies

Global PK analyses		
Parameter	**Value**	**Unit**
Vss (plasma)	690	**ml/kg**
Vd (plasma)	788	**ml/kg**
Vss (phys-chem)	633	**ml/kg**
Total plasma clearance	0.04	**ml/min/kg**
Plasma PK		
C_max	74	**µmol/l**
t_max	576	**h**
AUC_tEnd	2.8×10^6	**µmol*min/l**
Elimination Half-Life	210	**h**
MRT	266	**h**
Vss (plasma)/F	691	**ml/kg**
Skin PK		
C_max	100	**µmol/l**
t_max	576	**h**
AUC_tEnd	4.8×10^6	**µmol*min/l**
Elimination Half-Life	211	**h**
MRT	604	**h**
Spleen PK		
C_max	93	**µmol/l**
t_max	576	**h**
AUC_tEnd	3.6×10^6	**µmol*min/l**
Elimination Half-Life	210	**h**
MRT	265	**h**
Vss (plasma)/F	545	**ml/kg**
Liver PK		
C_max	133	**µmol/l**
t_max	576	**h**
AUC_tEnd	5.1×10^6	**µmol*min/l**
Elimination Half-Life	210	**h**
MRT	265	**h**
Vss (plasma)/F	**381**	**ml/kg**

Vss: volume at steady state, C_max: maximum (compartment) concentration, t_max: the time take to reach C_max, AUC_tEnd: area under the concentration time curve until the end of treatment, MRT: mean residence time

Table 4: Optimized model parameters of the full PBPK model based on the clinical observations of miltefosine in skin and plasma

Optimized Parameter	Value	Unit
Physiochemistry		
Lipophilicity	3	log
Specific intestinal permeability	1.5	cm/min
CLspec*	3.17 *10-3	1/min
Cell membrane binding partner		
K_d	1	mmol/l
k_{off}	101.8	1/min
Reference concentration	56.95	mmol/l

*Specific clearance normalized to the enzyme concentration of 1 mmol/l. K_d: equilibrium constant, k_{off}: dissociation constant

4. Discussion

The present study quantified miltefosine exposure in the skin following an allometric weight-based dosing regimen of 21 days in PKDL patients treated with a combination of Ambisome and miltefosine therapy. Several dosing regimens have previously been evaluated for miltefosine in the treatment of VL, such as the conventional linear weight-based dosing (2.5 mg/kg/daily for 28 days) or an allometric weight-based dosing (up to 3.9 mg/kg/day for 28 days), while for PKDL considerably longer 12 weeks of miltefosine treatment was previously suggested. This study provides the first evidence of miltefosine skin exposure and target-site PK in PKDL, which together with parasitological and clinical response to treatment will be of crucial value for future optimization and rationalization of miltefosine treatment in PKDL.

Miltefosine concentrations in the skin were highly variable between patients, which has also been observed for miltefosine in plasma in various previous studies [10–12]. In having available only, a single time point measurement of skin concentrations, empirical PK modeling could not be applied to further characterize skin PK of miltefosine. Therefore, we applied more advanced methods of PBPK modeling utilizing drug-specific and system-specific information to further predict skin PK. Furthermore, this approach allowed us to characterize target-site PK (e.g. MRT), parameters that could otherwise not be derived from a single observation.

Results of PK target achievement in the skin are in line with previous evaluations of the allometric weight-based dosing regimen in plasma [10,12], suggesting that this dosing regimen achieves sufficient target exposure of the parasites in skin tissue, also after 21 days. Since the target was defined based on the concentration of miltefosine required to induce intracellular susceptibility of *Leishmania donovani*,

it could be assumed that such exposure is sufficient for killing of the same parasite localized within the dermis. In the present study, 90% of the patients reached this target. However, due to the invasive nature of the biopsy sampling, which limited the number of samples which could be collected (only one per patient), this study was limited for a longitudinal individual patient evaluation in target exposure attainment over time. It remains to be assessed in future studies, whether reaching this target exposure in skin is associated with parasitological and clinical response to treatment.

We also developed a PBPK model of miltefosine, further used to simulate concentrations in the organs known to be affected by *Leishmania* parasites. With the here collected skin concentrations along with pooled data of plasma concentrations, we were able to inform the PBPK model and introduce a cell membrane binding partner which represents the membrane binding capacity. It can be anticipated that this cell membrane binding property is not tissue-specific. Mechanisms of miltefosine binding to the membrane is similar for all cell types, thus the extent of membrane binding is related to the number of cells in any compartment. Nonetheless, in having limited data to validate this model, further simulated exposures in spleen and liver should be interpreted with caution. The PBPK model-based predicted concentration-time curve in the skin suggested that typical target attainment ($T>EC_{90}$) after this 21-day regimen is twice higher (52 days) than previously reported $T>EC_{90}$ values in plasma of VL patients treated for 28 days (~24-27 days) [10,12].

In conclusion, in this study we showed that miltefosine penetrates to a large extent into the skin after oral administration and that skin concentrations are potentially high enough to exert activity on the dermal parasites in PKDL. Bridging the gap in knowledge of miltefosine disposition in human skin, the present study provides a promising start for future optimization of miltefosine in the treatment of PKDL. The PBPK model enabled the prediction of miltefosine concentrations in various other organ tissues, such as spleen and liver affected in VL, which would be unfeasible to sample in clinical trials. In future studies, such predictions and extrapolations from the developed model might be valuable to characterize miltefosine exposure and parasite killing response in respective organs or tissues.

References

[1]   J. Alvar, I.D. Vélez, C. Bern, M. Herrero, P. Desjeux, J. Cano, J. Jannin, M. de Boer, Leishmaniasis worldwide and global estimates of its incidence, PLoS One. (2012). https://doi.org/10.1371/journal.pone.0035671.

[2]   D.P. Eiras, L.A. Kirkman, H.W. Murray, Cutaneous Leishmaniasis: Current Treatment Practices in the USA for Returning Travelers., Curr. Treat. Options Infect. Dis. 7 (2015) 52–62. https://doi.org/10.1007/s40506-015-0038-4.

[3]   R. Arenas, E. Torres-Guerrero, M.R. Quintanilla-Cedillo, J. Ruiz-Esmenjaud, Leishmaniasis: A review, F1000Research. 6 (2017). https://doi.org/10.12688/f1000research.11120.1.

[4]   E.E. Zijlstra, A.M. Musa, E.A.G. Khalil, I.M. El Hassan, A.M. El-Hassan, Post-kala-azar dermal leishmaniasis, Lancet Infect. Dis. 3 (2003) 87–98. https://doi.org/10.1016/S1473-3099(03)00517-6.

[5]   A. Ismail, E.A.G. Khalil, A.M. Musa, I.M. EL Hassan, M.E. Ibrahim, T.G. Theander, A.M. EL Hassan, The pathogenesis of post kala-azar dermal leishmaniasis from the field to the molecule: Does ultraviolet light (UVB) radiation play a role?, Med. Hypotheses. 66 (2006) 993–999. https://doi.org/10.1016/j.mehy.2005.03.035.

[6]   T.P.C. Dorlo, M. Balasegaram, J.H. Beijnen, P.J. de Vries, Miltefosine: a review of its pharmacology and therapeutic efficacy in the treatment of leishmaniasis, J. Antimicrob. Chemother. 67 (2012) 2576–2597. https://doi.org/10.1093/jac/dks275.

[7]   W. Baumer, P. Wlaz, G. Jennings, C. Rundfeldt, The putative lipid raft modulator miltefosine displays immunomodulatory action in T-cell dependent dermal inflammation models, Eur J Pharmacol. 628 (2010) 226–232. https://doi.org/10.1016/j.ejphar.2009.11.018.

[8]   A.K. Mukherjee, G. Gupta, A. Adhikari, S. Majumder, S. Kar Mahapatra, S. Bhattacharyya Majumdar, S. Majumdar, Miltefosine triggers a strong proinflammatory cytokine response during visceral leishmaniasis: role of TLR4 and TLR9, Int Immunopharmacol. 12 (2012) 565–572. https://doi.org/10.1016/j.intimp.2012.02.002.

[9]   C. Ménez, M. Buyse, R. Farinotti, G. Barratt, Inward Translocation of the Phospholipid Analogue Miltefosine across Caco-2 Cell Membranes Exhibits Characteristics of a Carrier-mediated Process, Lipids. 42 (2007) 229–240. https://doi.org/10.1007/s11745-007-3026-8.

[10]   S. Palić, A.E. Kip, J.H. Beijnen, J. Mbui, A. Musa, A. Solomos, M. Wasunna, J. Olobo, F. Alves, T.P.C. Dorlo, Characterizing the non-linear pharmacokinetics of miltefosine in paediatric visceral leishmaniasis patients from Eastern Africa, J. Antimicrob. Chemother. (2020). https://doi.org/10.1093/jac/dkaa314.

[11]   T.P.C. Dorlo, A.D.R. Huitema, J.H. Beijnen, P.J. de Vries, Optimal dosing of miltefosine in children and adults with visceral leishmaniasis., Antimicrob. Agents Chemother. 56 (2012) 3864–72. https://doi.org/10.1128/AAC.00292-12.

[12]   T.P.C. Dorlo, A.E. Kip, B.M. Younis, S.J. Ellis, F. Alves, J.H. Beijnen, S. Njenga, G. Kirigi, A. Hailu, J. Olobo, A.M. Musa, M. Balasegaram, M. Wasunna, M.O. Karlsson, E.A.G. Khalil, Visceral leishmaniasis relapse hazard is linked to reduced miltefosine exposure in patients from Eastern Africa: a population pharmacokinetic/pharmacodynamic study, J. Antimicrob. Chemother. 72 (2017) 3131–3140. https://doi.org/10.1093/jac/dkx283.

[13]   I.C. Roseboom, H. Rosing, J.H. Beijnen, T.P.C. Dorlo, Skin tissue sample collection, sample homogenization, and analyte extraction strategies for liquid chromatographic mass spectrometry quantification of pharmaceutical compounds, J. Pharm. Biomed. Anal. 191 (2020). https://doi.org/10.1016/j.jpba.2020.113590.

[14]   J. Mbui, J. Olobo, R. Omollo, A. Solomos, A.E. Kip, G. Kirigi, P. Sagaki, R. Kimutai, L. Were, T. Omollo, T.W. Egondi, M. Wasunna, J. Alvar, T.P.C. Dorlo, F. Alves, Pharmacokinetics, safety and efficacy of an allometric miltefosine regimen for the treatment of visceral leishmaniasis in Eastern African children: an open-label, phase-II clinical trial, Clin. Infect. Dis. (2018).

[15]   T.P.C. Dorlo, P.P.A.M. Van Thiel, A.D.R. Huitema, R.J. Keizer, H.J.C. De Vries, J.H. Beijnen,

4.1

P.J. De Vries, Pharmacokinetics of miltefosine in old world cutaneous leishmaniasis patients, Antimicrob. Agents Chemother. 52 (2008) 2855–2860. https://doi.org/10.1128/AAC.00014-08.

[16]   T.P.C. Dorlo, M.J.X. Hillebrand, H. Rosing, T.A. Eggelte, P.J. de Vries, J.H. Beijnen, Development and validation of a quantitative assay for the measurement of miltefosine in human plasma by liquid chromatography–tandem mass spectrometry, J. Chromatogr. B. 865 (2008) 55–62. https://doi.org/10.1016/J.JCHROMB.2008.02.005.

[17]   R Core Team (2015). R: A language and environment for statistical computing. R Foundation for Statistical Computing, Vienna, Austria., (n.d.).

[18]   S. Willmann, J. Lippert, M. Sevestre, J. Solodenko, F. Fois, W. Schmitt, PK-Sim®: A physiologically based pharmacokinetic "whole-body" model, Drug Discov. Today BIOSILICO. 1 (2003) 121–124. https://doi.org/10.1016/s1478-5382(03)02342-4.

[19]   S. Willmann, K. Höhn, A. Edginton, M. Sevestre, J. Solodenko, W. Weiss, J. Lippert, W. Schmitt, Development of a physiology-based whole-body population model for assessing the influence of individual variability on the pharmacokinetics of drugs, J. Pharmacokinet. Pharmacodyn. 34 (2007) 401–431. https://doi.org/10.1007/s10928-007-9053-5.

[20]   Miltefosine | C21H46NO4P - PubChem, (n.d.).

4.1

4.1

Semi-mechanistic PK modelling of liposomal amphotericin B - mononuclear phagocyte system interactions in plasma and skin tissue of post kala-azar dermal leishmaniasis patients

4.2

Wan-Yu Chu
Ignace C. Roseboom
Shyam Sundar
Dinesh Mondal
Pradeep Das
Krishna Pandey
Alwin D.R. Huitema
Fabiana Alves
Thomas P.C. Dorlo

Abstract

Leishmaniasis is clinically characterized by a large production of macrophages where *Leishmania* parasites reside and replicate. The efficacy and safety of shortened liposomal amphotericin B (Ambisome®; LAmB) regimens for post kala-azar dermal leishmaniasis (PKDL) is under investigation on the Indian subcontinent. Mononuclear phagocyte system (MPS) generally plays a pivotal role in the disposition of liposomal drugs; however, the pharmacokinetics (PK) of LAmB in leishmaniasis patients, who present large production of macrophages, remain unclear. This study aimed to characterize the PK of LAmB in plasma and skin tissue of PKDL patients and to investigate the effects of PKDL disease status on the PK of LAmB.

The PK data originated from PKDL patients in Bangladesh and India, given five doses of LAmB 4 mg/kg (a total of 20 mg/kg) intravenously over 15 days. Total amphotericin B concentrations in plasma and skin were analyzed. Plasma samples were collected after the first and the last LAmB administration. One skin biopsy was taken either at the end of the last LAmB infusion or at 1 week after the last LAmB infusion. Population PK analysis was performed using nonlinear mixed effects modelling (NONMEM).

PK data from 60 patients were analyzed. Saturable distribution of LAmB, most likely as a consequence of MPS phagocytosis, was described by a model with maximal binding capacity function, representing drug accumulation in MPS. The maximal drug accumulation in MPS (B_{max}) is a composition of physiological B_{max} and disease B_{max}, where the disease fraction increased by 36% in patients with a 10-fold higher baseline parasite burden. Median amphotericin B concentration in skin was 7.11 µg/g (IQR 4.72-10.5) and 4.51 µg/g (IQR 2.28-6.05) at end and at 1 week after the last LAmB infusion, respectively. Estimated drug elimination half-life in skin was over 40-fold longer compared to plasma (346 hour in skin versus 8 hours in plasma).

PK of LAmB in plasma and skin were elucidated in leishmaniasis patients for the first time. The present model suggested LAmB follows non-linear PK characteristics of liposome disposition due to saturation of MPS uptake. Maximal LAmB accumulation in MPS increased with baseline parasite load suggesting an effect of disease-driven macrophages burden. LAmB presented a prolonged residence time in the skin tissue, indicating discrepancy between skin and plasma PK. This result highlights the importance of target site PK studies in PKDL patients and other dermal forms of leishmaniasis.

1. Introduction

Leishmaniasis is a neglected parasitic tropical disease, clinically characterized by a large production of macrophages in which *Leishmania* parasites reside and replicate [1]. Post kala-azar dermal leishmaniasis (PKDL) is a dermal complication following a primary episode of visceral leishmaniasis (VL) caused by *Leishmania donovani* [2]. The clinical manifestations of PKDL include macular, maculopapular, and nodular lesions, which are thought to serve as reservoirs of *Leishmania* parasites and perpetuate parasite transmission [3]. Therefore, PKDL is considered a public health problem posing a threat to the inter-epidemic periods of VL [4]. One of the obstacles in the management of PKDL is a lack of knowledge on the optimal treatment regimen and duration, complicated by geographical variation in clinical symptoms and apparent therapeutic response.

Liposomal amphotericin B (LAmB), under the trade name AmBisome®, is a unilamellar liposomal formulation of amphotericin B used as antifungal and antileishmanial treatment [5,6]. Recent studies of LAmB as mono- and combination therapy in the treatment of PKDL showed promising results on the Indian subcontinent (ISC) [7–9]. However, a major drawback of these potential regimens is the lengthy treatment period, requiring long hospitalization with the risk of poor patient compliance. Therefore, the efficacy and safety of shortened LAmB regimens in PKDL is currently under investigation on the ISC [10].

The outstanding activity of LAmB in the treatment of leishmaniasis can be attributed to several features of liposomal formulation. First, liposomes naturally target cells of the mononuclear phagocyte system (MPS), particularly macrophages, where the *Leishmania* parasites reside [11,12]. Therefore, in leishmaniasis, the liposomal fraction of LAmB has been regarded as the active moiety instead of the free drug fraction [13]. In addition, the liposomal formulation prolongs the drugs residence time in plasma and reduces nephrotoxicity. Compared with conventional amphotericin B, LAmB presented a 10-fold higher plasma exposure while markedly reduced the excretion of unchanged drug in the urine and feces [14].

The phagocytosis of liposomes by macrophages involves opsonization and a range of binding receptors, including scavenger receptors, mannose receptors, complement receptors, etc. [11]. Potential saturation and activation of receptors lead to complex pharmacokinetics (PK) of liposomal drugs [12,15]. In previous PK studies of LAmB, the increase in drug exposure was found exceeding dose proportionality, demonstrating a nonlinear dosage relationship [16,17]. Additionally, increasing LAmB exposure after repeated doses, has been observed in patients with invasive fungal disease, most likely attributed to saturable macrophage uptake [18,19].

The PK properties of LAmB in leishmaniasis patients, who exhibit a massive increase in macrophage burden compared to other infectious pathophysiologies, remain unclear. While it is known that the MPS generally plays a crucial role in the disposition of liposomal drugs, the influence of leishmaniasis pathophysiology on the PK of LAmB has not been characterized. Moreover, for PKDL which manifests as skin lesions, target site exposure of LAmB in the skin has never been investigated. A better understanding of both systemic PK of LAmB in PKDL patients and target site exposure in the skin of a shortened LAmB regimen currently under investigation, is pivotal to further optimize the treatment regimen of LAmB for PKDL.

The first aim of this study was to characterize plasma PK of LAmB in PKDL patients using a semi-mechanistic population modelling approach. Furthermore, the effect of disease status on the PK of LAmB were investigated. The second aim of this study was to describe the PK of LAmB in skin tissue of PKDL patients to improve the understanding of the relationship between plasma and skin target site PK in PKDL patients.

2. Methods

2.1. Clinical trial and patients

A non-comparative, open label, randomized phase II clinical trial was conducted in Bangladesh and India to assess the safety and efficacy of two short course treatment modalities, LAmB monotherapy and a combination of LAmB plus miltefosine, for PKDL treatment in ISC. The trial was registered with the clinical trial registry in India under the reference number CTRI/2017/04/008421. Characterizing PK of LAmB in plasma and skin was one of the secondary objectives of this trial. A total of three study sites were included in this trial, one in Bangladesh (International Centre for Diarrhoeal Disease Research (ICMR Institute), Bangladesh), and two in India (Rajendra Memorial Research Institute of Medical Sciences at Patna, Bihar, India; Kala Azar Medical Research Centre, Muzzafarpur, India).

In this study, PKDL patients were randomly allocated to LAmB monotherapy arm and LAmB plus miltefosine combination therapy arm. In both arms, LAmB was given intravenously at a total dose of 20 mg/kg divided over 15 days (5 x 4 mg/kg at day 1, 4, 8, 11 and 15). In the combination therapy arm, miltefosine (Impavido®, Paladin Labs, Montreal, Canada) was given orally twice daily using the allometric daily dose regimen for 21 days. Eligible patients were hospitalized during the administration of LAmB. The miltefosine treatment started at the same time as LAmB treatment and continued until completion of 21 days on an out-patient basis.

2.2. Sampling schedule

Plasma and full thickness skin biopsy (3 mm Ø) samples were collected for the PK assessments in a sub-set of 30 patients per arm. Blood plasma samples were collected after the first dose (day 1, at the end of infusion, and at 2, 4, 8, and 22 hours after the end of infusion) and after the last dose (day 15, at prior to infusion, at the end of infusion and at 2, 6, and 22 hours after the end of infusion). An additional single plasma sample was collected on day 22 for patients in the combination arm, and on day 30 for patients in the monotherapy arm. One skin biopsy was taken on day 15 approximating to the end of last LAmB infusion for patients allocated in the monotherapy arm, and on day 22 (1 week after the last LAmB infusion), coinciding with the last day of miltefosine co-treatment, for patients allocated in the combination therapy arm.

Clinical presentation of PKDL lesions and parasitological examinations were assessed before the start of treatment, on day 30 at the end of treatment phase, and at 3-months, 12-months, and 24-months follow-up visits. Parasite loads in plasma and skin were measured by quantitative real-time PCR (qRT-PCR). PKDL lesions were quantified by an established scoring system, in which the distribution of the lesions is plotted on a manikin as was designed in Bangladesh and the severity is assessed by counting the number of affected squares [20].

2.3. Bioanalysis

Total amphotericin B concentrations, including free, tissue-bound, protein-bound, and liposomal amphotericin B, in plasma and skin were analyzed. Measuring total amphotericin B level is justified by the fact that the liposomal fraction of amphotericin B, suggesting the active component in the treatment of leishmaniasis, represents the largest fraction (>95%) of the drug in blood circulation after administration [19]. Bioanalysis to quantify amphotericin B in human plasma and human skin tissue included in the study was performed using liquid chromatography coupled to tandem mass spectrometry (LC-MS/MS), including natamycin as internal standard. Human plasma samples were measured at the bioanalytical laboratory of Lambda Therapeutic Research in Ahmedabad, India, whereas human skin tissue samples were measured at bioanalytical laboratory of the Antoni van Leeuwenhoek hospital / Netherlands Cancer Institute in Amsterdam, the Netherlands.

2.3.1. Human plasma bioanalysis

Human plasma bioanalysis calibration standards and quality control samples were prepared in human K2EDTA plasma with a validated range of 0.50 µg/mL – 100.05 µg/mL. Human plasma samples were stored at -65°C prior to measurement. Sample aliquots of 50 µL human plasma were prepared by adding 100 µL internal standard before applying protein precipitation by addition of 750 µL 2 mM ammonium formate (pH 3.0) in water/methanol (2:8, v/v) followed by centrifugation at ≤10°C for 10 minutes. The supernatant was injected into the LC-MS/MS system afterwards.

LC-MS/MS apparatus employed were Acquity BSM and SM (Waters Corporation, Milford, USA) LC systems and TSQ Quantum Ultra (Thermo Fisher Scientific, Waltham, USA). Separation was accomplished using an Eclipse XDB C8 (Agilent, Santa Clara, USA; 150 mm x 4.6 mm; 5 µm particles) analytical column in combination with 2 mM ammonium formate (pH 3.0) in water and methanol employed as the mobile phase. Detection and quantification were performed by using mas/charge transitions m/z 924.420 → 743.320 for amphotericin B and m/z 666.200 → 503.300 for natamycin. The performance of the validated assay using the relative error was ±10.3% and ±9.0% at the LLOQ and above LLOQ concentration levels, respectively, whereas the coefficient of variation was ≤6.4% and ≤7.5% at the LLOQ and above LLOQ concentration levels, respectively.

2.3.2. Human skin bioanalysis

Human skin biopsies were collected and stored at -70°C pending analysis. Details on the development and validation of the bioanalytical assay in human skin tissue were previous described by our laboratory [21]. Validated range of the assay was 10 ng/mL – 2000 ng/mL combined with calibration standards and quality control samples in digestion solution (2% BSA in 5 mM CaCl2 25 mM Tris (pH 7.5) and 5 mg/mL collagenase A). Skin tissue samples were washed using phosphate buffered saline (PBS) followed by transfer of the washed skin tissue to clean amber 1.5 mL reaction tubes. Homogenization of skin tissue was performed by addition of 250 µL digestion solution and 100 µL internal standard in digestion solution, prior to incubation at 37°C in a thermomixer for 16 hours (overnight) at 1000 rpm. Clinical skin homogenates were transferred to clean amber 1.5 reaction tubes aliquots with a volume of 70 µL. Further sample preparation was performed by protein precipitation, adding 1000 µL methanol to skin tissue homogenates and centrifugation for 5 minutes at 5°C. Supernatant was transferred to clean 1.5 mL reaction tubes and evaporated to dryness at 25°C in a turbovap. The samples were reconstituted by addition of 100 µL methanol and vortex shaking before injection to the LC-MS/MS system. LC-MS/MS apparatus used were UHPLC 1290 series (Infinity II, Agilent, Santa Clara, USA) LC system and a QTRAP6500 (Sciex, Framingham, USA) for detection. Separation was performed using a Gemini C18 analytical column (Phenomenex, Torrance, USA; 150 mm x 2.0 mm; 3.5 µm particles) in combination with 0.1% formic acid in water and 0.1% formic acid in methanol mobile phase. Detection and quantification were performed using mass/charge transition employing a summation of transitions m/z 924.496 → 743.400 and m/z 906.461 → 743.382 for amphotericin B and m/z 666.340 →503.200 for natamycin. Human skin tissue samples were converted from ng/mL to µg/g amphotericin B in skin tissue. The performance of the assay using the relative error was ±11.4% at the LLOQ level and ±10.4% above the LLOQ concentration levels, whereas the coefficient of variation was ≤12.3% and ≤5.0% at the LLOQ and above the LLOQ concentration levels, respectively.

2.4. Population pharmacokinetic analysis

2.4.1. Structural model development

One to three compartment models with linear elimination from the central compartment were evaluated as structural models for LAmB. Given that liposomal drugs exhibit non-linear kinetics as a result of phagocytosis by MPS, particularly by macrophages, the saturable disposition of LAmB was presumed [22]. Therefore, a two-compartment model with linear elimination from the central compartment and saturable distribution towards the MPS compartment was tested. The saturable distribution was described by a maximal binding capacity (B_{max}) function as shown in equation 1:

$$\frac{dA(MPS)}{dt} = k_{in} * A_{Central} * \left(1 - \frac{A_{MPS}}{B_{max}}\right) - k_{out} * A_{MPS} \qquad (1)$$

In this function, B_{max} represents the maximal drug uptake by MPS. k_{in} represents uptake rate when MPS compartment is empty and k_{out} describes subsequent release by the MPS compartment. By applying B_{max} function, the extent of drug distribution is regulated by drug accumulation in the MPS compartment.

The status of leishmaniasis could affect macrophage burden and macrophage activity. As B_{max} was assumed to be related to MPS uptake capacity, the influence of PKDL disease status on B_{max} was further investigated. PKDL disease status was informed by PKDL lesion score and parasite load in skin.

Interindividual variability (IIV) in PK parameters was estimated with an exponential variance model using equation 2:

$$P_i = P_{pop} * exp(\eta_i) \qquad (2)$$

Where P_i is the individual parameter estimate for individual i, P_{pop} is the typical population parameter estimate, and η_i is assumed to be normally distributed with mean 0 and variance w^2.

Residual unexplained variability in plasma and skin were estimated using separate error models as equation 3:

$$C_{obs.ij} = C_{pred,ij} * \left(1 + \varepsilon_{p,ij}\right) \qquad (3)$$

Where $C_{obs.ij}$ represents the observed concentration for individual i at observation j, $C_{pred,ij}$ represents the individual predicted concentration, and $\varepsilon_{p,ij}$ is the proportional error that normally distributed with mean 0 and variance σ^2.

4.2

2.4.2. Covariate Analysis

Following structural model development, potential effects of body size, age, geological region, nutritional status (informed by BMI), as well as the interaction effects such as treatment-arm related differences in PK parameter estimates were evaluated. The impact of body size on clearance (CL) and volume of distribution (V_d) was tested by allometric scaling using body weight (WT) as a descriptor, with fixed exponents of 0.75 on all clearances and 1 on all volumes of distribution [23].

2.4.3. Skin pharmacokinetic analysis

Graphical analysis was performed to visualize the relationship between maximum plasma concentrations (C_{max}) and skin concentrations collected at the end of the last LAmB infusion. The skin concentrations were also included in the population pharmacokinetic model. A skin compartment was added to the developed population model as an effect compartment without mass transfer, following equation 4, where the transfer rate from plasma to skin and the elimination rate from skin tissue are represented by first-order rate constants $k_{in\,(skin)}$ and $k_{out\,(skin)}$, respectively.

$$\frac{dA(Skin)}{dt} = k_{in\,(skin)} * C_{plasma} - k_{out\,(skin)} * C_{skin} \qquad (4)$$

2.4.4. Software and model evaluation

Population PK analysis was performed with nonlinear mixed-effects modelling program NONMEM (version 7.5; ICON Development Solutions, Ellicott City, MD), aided by Perl-speaks-NONMEM (PsN, version 5.0) and Pirana (version 2.9.9) for run deployment [24,25]. Model parameters were estimated using the first-order conditional estimation with interaction (FOCE-I) method implemented in NONMEM.

Model adequacy was guided by statistical and graphical methods as well as physiological plausibility. The change in objective function value (OFV), which equals to minus two the log-likelihood, was used to define statistical significance between hierarchical models (Chi-square distribution with 1 degree of freedom [df]). A decrease in OFV of ≥ 3.84, representing a p-value of < 0.05, was consider statistically significant in this study. Individual Bayesian parameters were obtained using the POSTHOC option of NONMEM. R (version 4.0) and Xpose (version 4) were used for performing goodness-of-fit plots to assist graphical evaluation. Visual predictive check (VPC) and sampling importance resampling (SIR) were performed to assess the predictive performance and the parameter precision with 95% confidence interval (CI) for the final model [26,27].

3. Results

3.1. Patients and sampling

In total, 10 patients from Bangladesh and 50 patients from India were included in the PK analysis and were equally allocated into LAmB monotherapy arm (n=30) and LAmB plus miltefosine combination arm (n=30).

Table 1. Patient demographics

| Parameter	Bangladesh (n=10)	India (n=50)
	n (%)	
Treatment arm		
Liposomal amphotericin B	5 (50.0%)	25 (50.0%)
Liposomal amphotericin B + Miltefosine	5 (50.0%)	25 (50.0%)
Sex		
Female	7 (70.0%)	25 (50.0%)
Male	3 (30.0%)	25 (50.0%)
	Median [Min, Max]	
Age (years)	28.0 [10.0, 45.0]	22.0 [10.0, 58.0]
Weight (kg)	47.0 [33.0, 62.0]	45.5 [26.0, 69.0]
BMI (kg/m²)	17.1 [14.5, 19.3]	19.3 [16.1, 27.6]
Parasite loads in skin (1/ug DNA)	124 [2.57, 9080]	[a]87900 [776, 66800000]
Lesion (squares)	*93.5 [3.00, 317]*	*187 [5.00, 472]*

a. *Missing data n=26*

4.2
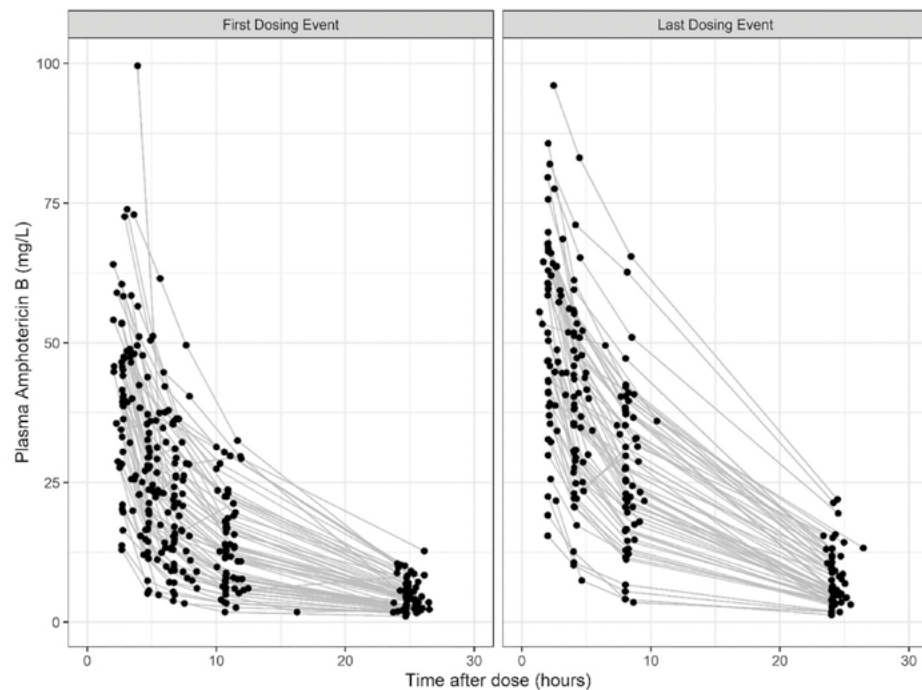
Figure 1: Plasma observed time-concentration data. Blood plasma samples were collected at the first dose (day 1) and at the last dose (day 15). Drug exposures were generally higher at the last dosing event.

Demographics and baseline characteristics of the population can be found in Table 1. A total of 657 plasma amphotericin B concentrations collected at the first and the last LAmB dosing event were analyzed, 65 samples were below the lower limit of quantitation (LLOQ) of 0.5 mg/L. Below LLOQ data was imputed as LLOQ/2, and a fix additive residual error component of LLOQ/2 was included. Skin amphotericin B concentrations were available in 30 patients from the LAmB monotherapy arm where skin samples were taken at the end of last LAmB infusion on day 15, and in 25 patients from the combination arm where skin samples were taken at 6 to 10 days after the last LAmB administration. A total of 4 skin measurements considered unreliable were excluded. Observed plasma and skin concentrations over time are shown in Figure 1 and 2, respectively.
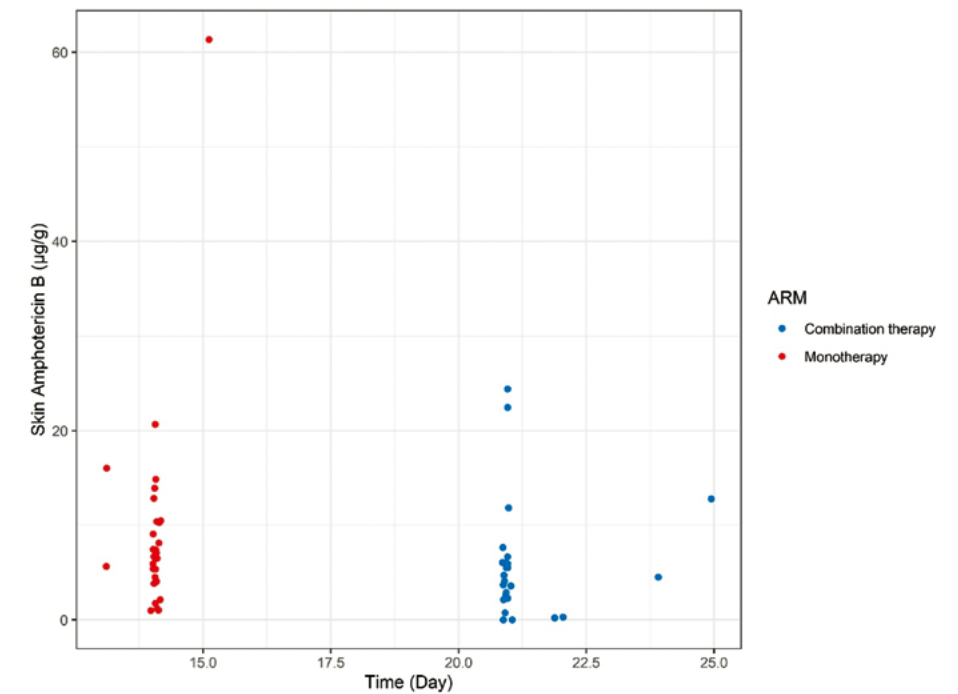

Figure 2: Skin observed time-concentration data. One skin sample was collected at the end of last LAmB infusion for patients allocated in the monotherapy arm (red), and at 1 week after the last infusion for patients allocated in the combination therapy arm (blue). One (erroneous) observation of 360 µg/g was removed from the plot.

3.2. Plasma pharmacokinetic analysis

The final structure of the model is depicted in Figure 3 and the final parameter estimates with corresponding SIR-derived 95% CI are shown in Table 2.
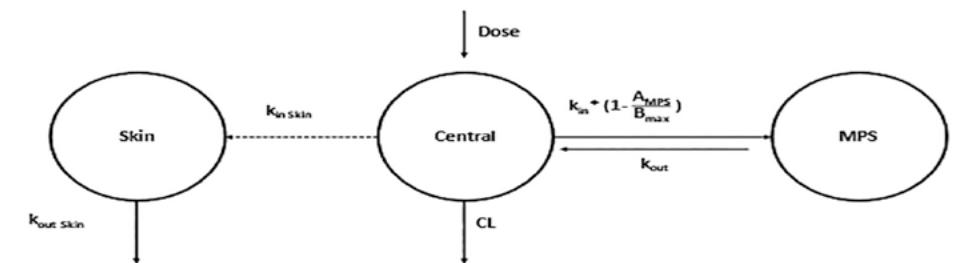
4.2

Figure 3: Final model structure. CL, drug clearance from the central compartment; B_{max}, the maximal drug accumulation in the peripheral compartment; A_{MPS}, drug amount in the MPS compartment; k_{in}, first-order rate constant of distribution to MPS compartment when the compartment is empty; k_{out}, first-order rate constant of release from MPS compartment. $k_{in\,(skin)}$, first-order rate constant of distribution from plasma to skin; $k_{out\,(skin)}$, first-order rate constant of elimination from skin tissue.

Table 2. Final parameter estimates

Parameter	Unit	Estimates (CI)	IIV (CV%)
CL	L/h/70kg	0.4 ± 0.04	44.4
V_d	L/70kg	4.66 ± 0.22	27.4
k_{in}	1/h	0.6 ± 0.12	74.8
k_{out}	1/h	0.016 ± 0.002	81.7
$B_{max\ physiology}$	mg	42.4 ± 6.12	-
$B_{max\ disease}$	mg	$B_{max\ physiology}$. 0.36 (log10(Parasite load* Lesion Score)-log10(3000))	46.2
$k_{in\ (skin)}$	1/h	0.004 ± 0.002	-
$k_{out\ (skin)}$	1/h	0.002 ± 0.003	-
Residual variability plasma concentration	Propotional (%)	21.5	-
	Additive (mg/L)	0.25 (Fixed)	
Residual variability skin concentration	Propotional (%)	64.7	-

CL, drug clearance from the central compartment; V_d, volumn of distribution of the central compartment; B_{max}, the maximal drug accumulation in the MPS compartment; k_{in}, first-order rate constant of distribution to MPS compartment when the compartment is empty; k_{out}, first-order rate constant of release from MPS compartment; $k_{in\ (skin)}$, first-order rate constant of distribution from plasma to skin; $k_{out\ (skin)}$, first-order rate constant of elimination from skin tissue.

3.2.1. Structural model development

Plasma observed time-concentration profile (Figure 1) underlined potential non-linear kinetics of LAmB. Drug exposure in plasma was generally higher at the last dosing event compared to the first dosing event. Moreover, trough concentration ratio between first and last dosing event was below 1.2 showing no evidence of drug accumulation. One to three compartmental models with linear elimination were tried, but over-predicted observations of the first dosing event and under-predicted observations of the last dosing event.

The model described saturable distribution using B_{max} function was therefore used and provided adequate description of the data. CL and Vd of the central compartment were 0.4 ± 0.04 L/h and 4.66 ± 0.22 L for a weight of 70 kg, respectively. k_{in} and k_{out} were estimated at 0.6 ± 0.121/h and 0.016 ± 0.002 1/h, respectively. The model parameter estimates suggested that a majority of LAmB was distributed to the MPS compartment, highlighting that LAmB follows the non-linear PK characteristics of liposome disposition, likely driven by saturation of macrophage uptake.

Parasite qPCR was missing in 26 patients. Based on the available data, a positive trend between skin parasite load and lesion score measured before the start of treatment was seen in graphical examination (Suppl). Therefore, initial total parasite burden, informed by multiplying skin parasite load (parasites/µgDNA) by lesion score (squares), was used as an indicator of initial disease status, and was plotted against B_{max} as shown in Figure 4.
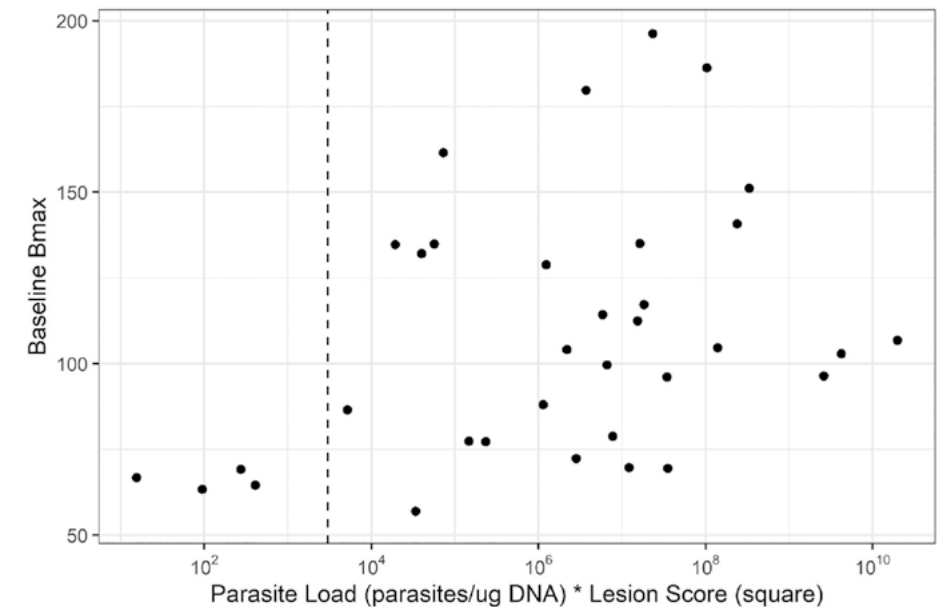

Figure 4: Total parasite number before treatment versus baseline Bmax. The dashed line represents the observed threshold of parasite number, which approximates 3000 parasites.

B_{max} was discovered to be low and stable when the total parasite number was below a threshold of around 3000 and started to increase with higher parasite numbers. Since macrophages are essential cells providing functional immunity despite the absence of disease, a physiological B_{max} value was considered. Therefore, total B_{max} level was denoted as a combination of physiological B_{max} ($B_{max\ physiology}$) and disease related B_{max} ($B_{max\ disease}$) as equation 5, in which $B_{max\ disease}$ is informed by initial parasite load and lesion score using equation 6.

$$B_{max} = B_{max\ physiology} + B_{max\ disease} \quad (5)$$

$$B_{max\ disease} = B_{max\ physiology} * \theta_{parasite} * (\log_{10}(Parasite\ load * Lesion\ Score) - (\log_{10}(3000))) \quad (6)$$

For patients missing parasite qPCR data, an estimated baseline parasite load of $3.98*10^6$ was used. Including initial parasite number as a covariate on $B_{max\ disease}$

4.2

significantly improved model fit with a 9.95-unit OFV drop. $B_{max\ physiology}$ was estimated at 42.4 ± 6.12 mg, representing baseline B_{max} level for patients with parasite amount below the defined threshold of 3000. For patients with parasite burden above threshold, a 10-fold increase in parasite amount resulted in a 36% increase in $B_{max\ disease}$ ($\theta_{parasite}$ = 0.36 ± 0.05).

3.2.2. Covariate analysis

WT was included as a covariate on CL and V_d of the central compartment with a fixed exponent allometric scaling approach, which improved model goodness-of-fit. Effects of age, geographical region, BMI on PK parameters could not be identified. No difference in PK parameters was found between the mono- and combination therapy treatment arms, suggesting no relevant drug interaction of LAmB and miltefosine.

3.3. Skin pharmacokinetic analysis

Drug accumulation in skin tissue was compared to systemic exposure (Figure 2). The median skin amphotericin B concentration at end of the last LAmB infusion (day 15) was 7.11 µg/g, showing a wide range from 1 to 360 µg/g. The median skin concentration at 1 week after the last LAmB infusion (day 22) was 4.51 µg/g, with 2/55 patients below detectable concentrations. On day 15, after the last LAmB infusion, a positive trend between C_{max} in plasma and skin tissue drug concentration was observed (Figure 5). To facilitate the comparison of skin amphotericin B concentrations to plasma values as well as *in vitro* literature values, the density of skin tissue was assumed to be 1 g/mL [28]. In total, 93% of skin observations were above the highest reported *in vitro* IC50 value against intracellular *Leishmania donovani* amastigotes (0.09-0.36 mg/L) [29].

Given the potential correlation between plasma and skin LAmB exposure as suggested by graphical evaluation (Figure 5), the skin was implemented as an effect compartment of the central plasma compartment in the model. As skin LAmB observations were measured at the end of last LAmB infusion for patients in the monotherapy arm, while at 6-10 days after the last LAmB infusion for patients in the combination arm, the accumulation phase and elimination phase of LAmB in skin were able to be captured. The estimated rate of distribution from plasma to skin tissue was 0.004 ± 0.002 1/h, and the drug elimination half-life in the skin was 346 hours. The elimination half-life in the skin was more than 40-fold longer than in plasma, indicating a much longer residence time of the drug at the target site in skin tissue compared to plasma.
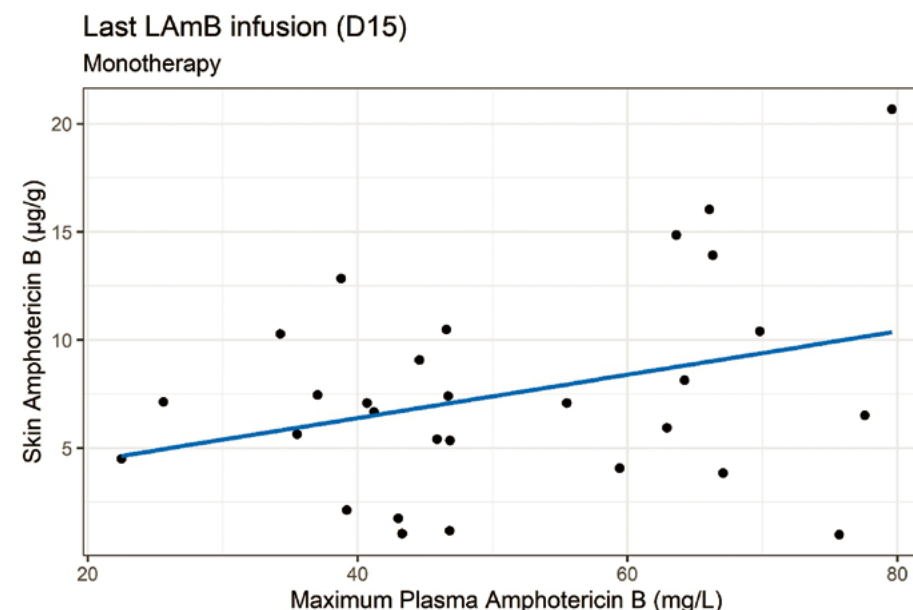

Figure 5: Maximum plasma concentrations versus skin concentrations observed after the last LAmB infusion. All patients were from the monotherapy arm.

3.4 Model Evaluation

The final model provided an adequate description of the plasma and the skin data. Goodness-of-fit plots (Figure 6), including observed verse population- and individual-predicted concentration plots and the conditional weighted residuals verse population-predicted concentration and time plots, did not reveal considerable trends or bias in plasma and skin predictions. In the VPC (Figure 7), the simulations adequately captured plasma observations at the first and the last dosing event.
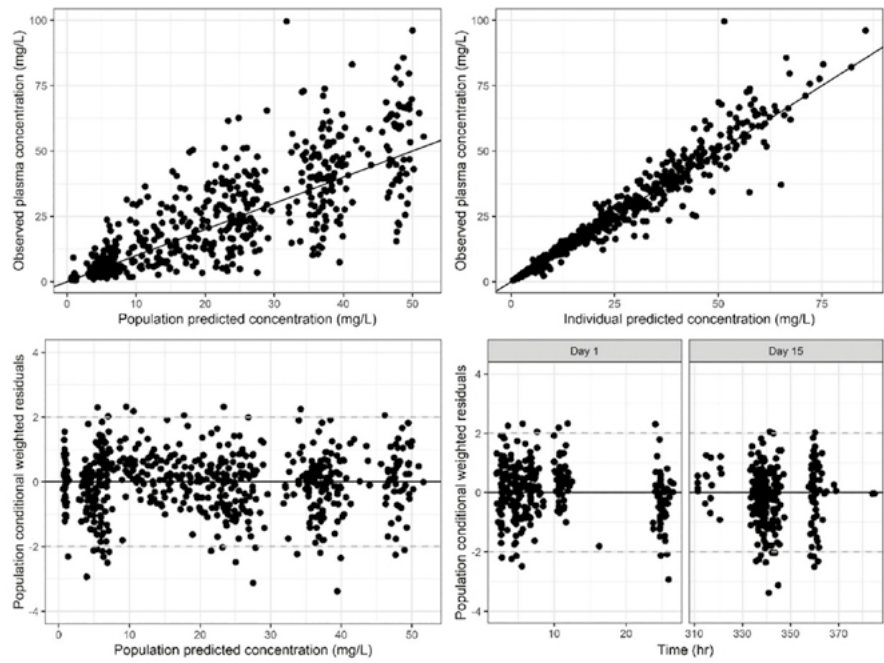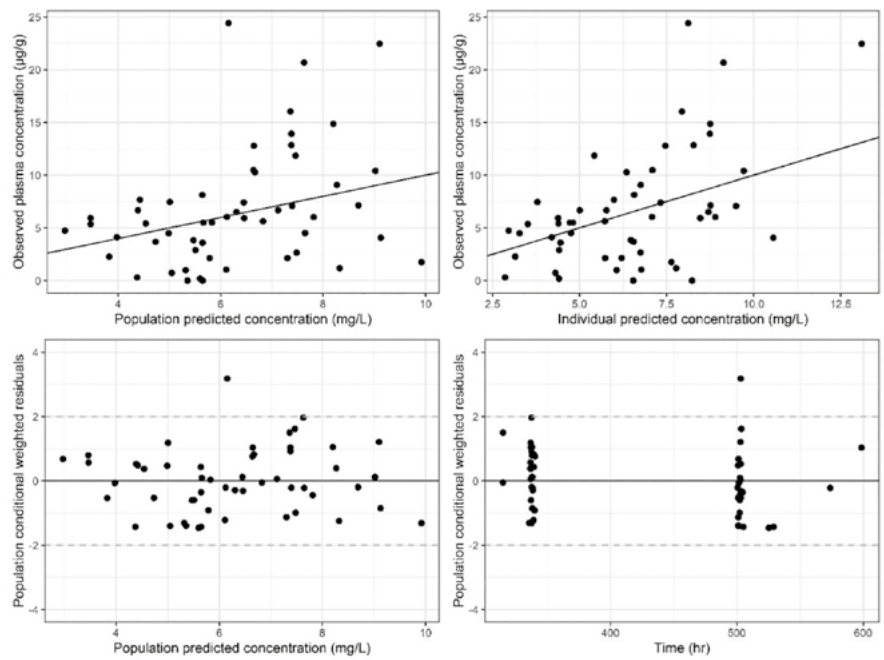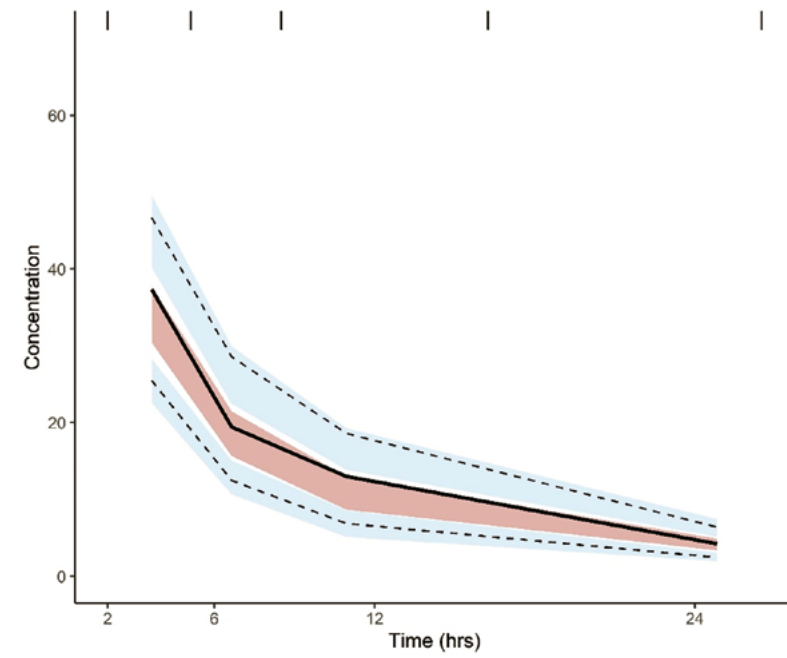
4.2

Figure 6A: Plasma GOF

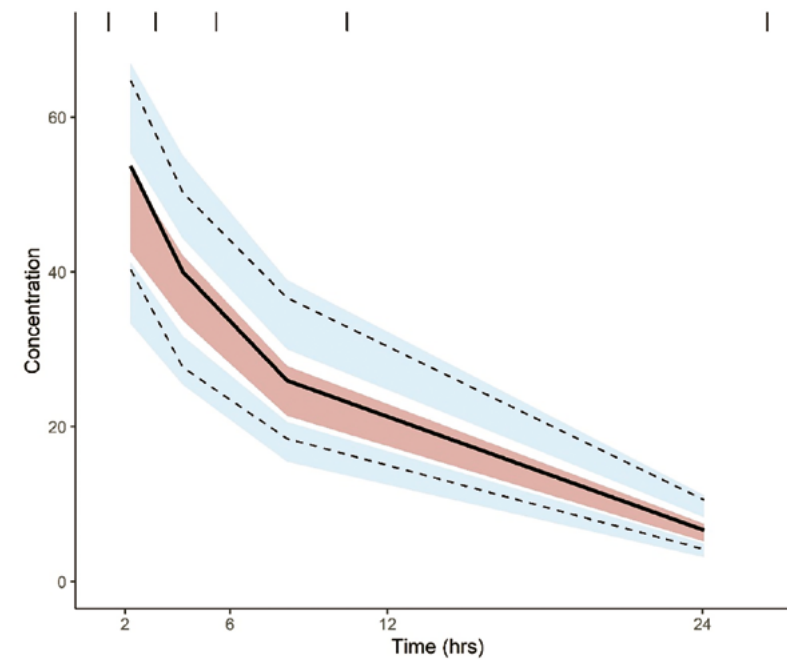Figure 7A: VPC First dosing event

Figure 6B: Skin GOF

Figure 7B: VPC Last dosing event

4. Discussion

For the first time, PK of LAmB in plasma and skin was elucidated in PKDL patients. The present study suggested LAmB follows the non-linear PK characteristics of liposome disposition, driven by potential saturation of macrophage phagocytosis. A maximal binding capacity (B_{max}) function was applied, where B_{max} is assumed to represent the maximal drug accumulation in MPS, particularly in macrophages. The level of B_{max} was associated with initial parasite number, underlining the influence of disease status on macrophage activity. A positive relationship between LAmB exposure in plasma and the skin target site was observed. Nevertheless, the residence time of LAmB in the skin was much longer than in plasma, indicating a unique PK profile of LAmB in skin tissue.

The non-linear PK characteristics of LAmB in plasma were confirmed by this study, highlighting a saturation of drug distribution. The non-linearity in LAmB PK has been proposed in previous population PK studies; however, previous studies only empirically explained this by either a decrease in V_d or CL at the end of treatment [18,19]. In this study, B_{max} function was used to describe the saturable distribution of LAmB towards the MPS compartment. Since the liposomal form of LAmB is the predominant fraction (96-99%) of the drug systemically, the B_{max} function most likely reflects the uptake of liposomes by macrophages [30].

Liposomes are naturally targeted by macrophage phagocytosis [11]. The mechanism of phagocytosis involves a high affinity saturable and a low affinity non-saturable binding system [31]. Besides, opsonins(plasma proteins that bind to liposomes) can enhance or diminish the rate and extent of phagocytosis [32]. Accordingly, saturable plasma clearance has been suggested a typical characteristic of liposomes, and the activity of macrophages plays an important role in defining the disposition liposomes [12]. Based on the features of liposomes, the saturable distribution of LAmB found in this study suggests a result of drug uptake by macrophages. Therefore, the B_{max} parameter in the model was assumed an indicator of the maximal capacity for drug accumulation in macrophages, which regulated the distribution of LAmB within a dosing event and between multiple dosing events. The estimated rate of distribution to the peripheral compartment (k_{in}) was 10-fold greater than the rate of systemic elimination, supporting the vital role of macrophages in the distribution of LAmB. In most patients, accumulation of LAmB in macrophages reached a plateau 2-4 hours after the end of drug infusion followed by a slow-release back into the systemic circulation. Before the start of the last LAmB administration, remaining drug accumulation capacity in macrophages was less than 50% of the maximal drug accumulation capacity at baseline, leading to higher drug exposure in plasma after repeating doses.

Leishmania is an intracellular parasite of macrophages, therefore LAmB acts as an efficient drug to target the intramacrophageal site of infection [13]. In this study, a higher initial parasite count was found to increase B_{max}, indicating an impact of PKDL disease severity on the maximal drug accumulation in macrophages. Patients with a 10-fold higher initial total parasite load in the skin, informed by multiplying parasite load by lesion score, were found to accumulate 36% more LAmB in macrophages. The pathogenesis of all sorts of leishmaniasis includes activation of macrophages and shifts between macrophage phenotypes [33,34]. Therefore, the possible correlation between the quantity of *Leishmania* parasites and the activity of macrophages was elucidated. Apart from disease-influenced B_{max}, a physiological B_{max} level was found, suggesting relatively low activated macrophages for patients with low baseline parasite count. As macrophages are essential for immunology, the physiological B_{max} might represent the baseline macrophages activity in the absence of disease. Drug treatment is expected to lead to parasite elimination (Supp2), which could subsequently lower the level and activity of the parasitized macrophage burden. Changes in the state of the macrophage could alter its phagocytic ability resulting in dynamic B_{max}. Potential time-related changes in PK will be explored in our future study.

The PK of LAmB in the skin target site where the *Leishmania* parasite in PKDL are located was previously unknown. Recently, a bioanalysical method for the quantification of amphotericin B in human skin tissue was developed and validated by our group, which finally enabled skin PK studies in leishmaniasis [21]. In this study, two sampling schedules were applied for skin data. For patients in the monotherapy arm, one skin biopsy was taken at the end of the last LAmB infusion (day 15), and the median concentration was 7.11 μg/g. For patients in the combination arm, one skin biopsy was taken a week after the last LAmB infusion (day 22), and the median concentration was 4.1 μg/g. Almost all patients exhibited skin concentrations that were above the in vitro IC_{50} value against intracellular *Leishmania donovani* amastigotes, suggesting adequate target site exposure attainment [29]. As shown in Figure 5, higher plasm concentration tended to relate to higher skin concentrations on day 15 at the end of the last LAmB infusion. The distribution half-life of LAmB to skin tissue was around 7 days, indicating a slow accumulation process in the skin tissue. Moreover, the terminal half-life in the skin was around 14 days, which was much longer than the in half-life of 8 hours in plasma. The discrepancy between skin and plasma residence time suggested LAmB presents an extended exposure period in skin, which may not be comparable to plasma. As skin is the target site of PKDL, a prolonged effective treatment duration than current knowledge could be expected.

4.2

5. Conclusion

This study semi-mechanistically characterized the PK of LAmB in plasma and skin tissue in a population of PKDL patients and highlighted potential interactions between liposomes, MPS (specific macrophages), and *Leishmania* parasites. The plasma PK of LAmB suggested follows the non-linear PK characteristics of liposome disposition which was regulated by the maximal drug accumulation in MPS. Maximal LAmB accumulation in macrophages varied between patients as a consequence of baseline disease status. A much longer residence time of LAmB in the skin than in plasma was identified, indicating that drug exposure at the skin target site cannot be simply informed by PK in plasma. This result emphasizes the importance of target site PK studies in PKDL patients and other dermal forms of leishmaniasis.

References

[1] Centers for Disease Control and Prevention (CDC) -Leishmaniasis, (2021). https://www.cdc.gov/parasites/leishmaniasis/index.html.

[2] E.E. Zijlstra, A.M. Musa, E.A.G. Khalil, I.M. El Hassan, A.M. El-Hassan, Post-kala-azar dermal leishmaniasis, Lancet Infect. Dis. 3 (2003) 87–98. https://doi.org/10.1016/S1473-3099(03)00517-6.

[3] P. Kumar, M. Chatterjee, N. Das, Post kala-azar dermal leishmaniasis: Clinical features and differential diagnosis, in: Indian J. Dermatol., Indian J Dermatol, 2021: pp. 24–33. https://doi.org/10.4103/ijd.IJD_602_20.

[4] M.R. Gedda, B. Singh, D. Kumar, A.K. Singh, P. Madhukar, S. Upadhyay, O.P. Singh, S. Sundar, Post kala-azar dermal leishmaniasis: A threat to elimination program, PLoS Negl. Trop. Dis. 14 (2020) 1–25. https://doi.org/10.1371/journal.pntd.0008221.

[5] N.R.H. Stone, T. Bicanic, R. Salim, W. Hope, Liposomal Amphotericin B (AmBisome®): A Review of the Pharmacokinetics, Pharmacodynamics, Clinical Experience and Future Directions, Drugs. 76 (2016) 485–500. https://doi.org/10.1007/s40265-016-0538-7.

[6] L.D. Saravolatz, C. Bern, J. Adler-Moore, J. Berenguer, M. Boelaert, M. den Boer, R.N. Davidson, C. Figueras, L. Gradoni, D.A. Kafetzis, K. Ritmeijer, E. Rosenthal, C. Royce, R. Russo, S. Sundar, J. Alvar, Liposomal Amphotericin B for the Treatment of Visceral Leishmaniasis, Clin. Infect. Dis. 43 (2006) 917–924. https://doi.org/10.1086/507530.

[7] V. Ramesh, K.K. Dixit, N. Sharma, R. Singh, P. Salotra, Assessing the Efficacy and Safety of Liposomal Amphotericin B and Miltefosine in Combination for Treatment of Post Kala-Azar Dermal Leishmaniasis, J. Infect. Dis. 221 (2020) 608–617. https://doi.org/10.1093/infdis/jiz486.

[8] V. Ramesh, K. Avishek, V. Sharma, P. Salotra, Combination therapy with Amphotericin-B and miltefosine for post-kala-azar dermal leishmaniasis: A preliminary report, Acta Derm. Venereol. 94 (2014) 242–243. https://doi.org/10.2340/00015555-1582.

[9] U. Marking, M. den Boer, A.K. Das, E.M. Ahmed, V. Rollason, B.N. Ahmed, R.N. Davidson, K. Ritmeijer, Hypokalaemia-Induced Rhabdomyolysis after Treatment of Post-Kala-azar Dermal Leishmaniasis (PKDL) with High-Dose AmBisome in Bangladesh-A Case Report, PLoS Negl. Trop. Dis. 8 (2014) e2864. https://doi.org/10.1371/journal.pntd.0002864.

[10] C.T.R. India, New treatment regimens for treatment of Post Kala Azar Dermal Leishmaniasis patients in India and Bangladesh region, New Delhi Database Publ. (India). Identifier CTRI/2017/04/008421. (2017) 7. https://doi.org/10.1002/CENTRAL/CN-01894602.

[11] C. Kelly, C. Jefferies, S.-A. Cryan, Targeted liposomal drug delivery to monocytes and macrophages, J. Drug Deliv. 2011 (2011) 1–11. https://doi.org/10.1155/2011/727241.

[12] H. Harashima, H. Kiwada, Liposomal targeting and drug delivery: kinetic consideration, Adv. Drug Deliv. Rev. 19 (1996) 425–444. https://doi.org/10.1016/0169-409X(96)00012-9.

[13] S. Sundar, J. Chakravarty, Liposomal Amphotericin B and Leishmaniasis: Dose and Response, J. Glob. Infect. Dis. 2 (2010) 159. https://doi.org/10.4103/0974-777X.62886.

[14] I. Bekersky, R.M. Fielding, D.E. Dressler, J.W. Lee, D.N. Buell, T.J. Walsh, Pharmacokinetics, excretion, and mass balance of liposomal amphotericin B (AmBisome) and amphotericin B deoxycholate in humans, Antimicrob. Agents Chemother. 46 (2002) 828–833. https://doi.org/10.1128/AAC.46.3.828-833.2002.

[15] T.M. Allen, C.B. Hansen, D.E.L. de Menezes, Pharmacokinetics of long-circulating liposomes, Adv. Drug Deliv. Rev. 16 (1995) 267–284. https://doi.org/10.1016/0169-409X(95)00029-7.

[16] T.J. Walsh, J.L. Goodman, P. Pappas, I. Bekersky, D.N. Buell, M. Roden, J. Barrett, E.J. Anaissie, Safety, tolerance, and pharmacokinetics of high-dose liposomal amphotericin B (AmBisome) in patients infected with Aspergillus species and other filamentous fungi: Maximum tolerated dose study, Antimicrob. Agents Chemother. 45 (2001) 3487–3496.

4.2

https://doi.org/10.1128/AAC.45.12.3487-3496.2001.

[17]   T.J. Walsh, V. Yeldandi, M. McEvoy, C. Gonzalez, S. Chanock, A. Freifeld, N.I. Seibel, P.O. Whitcomb, P. Jarosinski, G. Boswell, I. Bekersky, A. Alak, D. Buell, J. Barret, W. Wilson, Safety, tolerance, and pharmacokinetics of a small unilamellar liposomal formulation of amphotericin B (AmBisome) in neutropenic patients, Antimicrob. Agents Chemother. 42 (1998) 2391–2398. https://doi.org/10.1128/aac.42.9.2391.

[18]   G. Würthwein, C. Young, C. Lanvers-Kaminsky, G. Hempel, M.N. Trame, R. Schwerdtfeger, H. Ostermann, W.J. Heinz, O.A. Cornely, H. Kolve, J. Boos, G. Silling, A.H. Groll, Population pharmacokinetics of liposomal amphotericin B and caspofungin in allogeneic hematopoietic stem cell recipients, Antimicrob. Agents Chemother. 56 (2012) 536–543. https://doi.org/10.1128/AAC.00265-11.

[19]   J.M. Lestner, A.H. Groll, G. Aljayyoussi, N.L. Seibel, A. Shad, C. Gonzalez, L. V. Wood, P.F. Jarosinski, T.J. Walsh, W.W. Hope, Population pharmacokinetics of liposomal amphotericin B in immunocompromised children, Antimicrob. Agents Chemother. 60 (2016) 7340–7346. https://doi.org/10.1128/AAC.01427-16.

[20]   D. Mondal, M.G. Hasnain, M.S. Hossain, D. Ghosh, P. Ghosh, H. Hossain, J. Baker, R. Nath, R. Haque, G. Matlashewski, S. Hamano, Study on the safety and efficacy of miltefosine for the treatment of children and adolescents with post-kala-azar dermal leishmaniasis in Bangladesh, and an association of serum vitamin E and exposure to arsenic with post-kala-azar dermal leishmaniasis: A, BMJ Open. 6 (2016) e010050. https://doi.org/10.1136/bmjopen-2015-010050.

[21]   I.C. Roseboom, B. Thijssen, H. Rosing, F. Alves, S. Sundar, J.H. Beijnen, T.P.C. Dorlo, Development and validation of a high-performance liquid chromatography tandem mass spectrometry method for the quantification of the antiparasitic and antifungal drug amphotericin B in human skin tissue, J. Chromatogr. B. Analyt. Technol. Biomed. Life Sci. 1206 (2022) 123354. https://doi.org/10.1016/J.JCHROMB.2022.123354.

[22]   H. Harashima, C. Yamane, Y. Kume, H. Kiwada, Kinetic analysis of AUC-dependent saturable clearance of liposomes: mathematical description of AUC dependency, J. Pharmacokinet. Biopharm. 21 (1993) 299–308. https://doi.org/10.1007/BF01059781.

[23]   G.B. West, J.H. Brown, B.J. Enquist, A general model for the origin of allometric scaling laws in biology, Science (80-.). 276 (1997) 122–126. https://doi.org/10.1126/science.276.5309.122.

[24]   L. Lindbom, J. Ribbing, E.N. Jonsson, Perl-speaks-NONMEM (PsN)--a Perl module for NONMEM related programming, Comput. Methods Programs Biomed. 75 (2004) 85–94. https://doi.org/10.1016/J.CMPB.2003.11.003.

[25]   R.J. Keizer, M. van Benten, J.H. Beijnen, J.H.M. Schellens, A.D.R. Huitema, Piraña and PCluster: A modeling environment and cluster infrastructure for NONMEM, Comput. Methods Programs Biomed. 101 (2011) 72–79. https://doi.org/10.1016/j.cmpb.2010.04.018.

[26]   M. Bergstrand, A.C. Hooker, J.E. Wallin, M.O. Karlsson, Prediction-Corrected Visual Predictive Checks for Diagnosing Nonlinear Mixed-Effects Models, AAPS J. 13 (2011) 143. https://doi.org/10.1208/S12248-011-9255-Z.

[27]   A.G. Dosne, M. Bergstrand, M.O. Karlsson, An automated sampling importance resampling procedure for estimating parameter uncertainty, J. Pharmacokinet. Pharmacodyn. 44 (2017) 509–520. https://doi.org/10.1007/s10928-017-9542-0.

[28]   J.A. Johnson, R.M. Fusaro, The role of the skin in carbohydrate metabolism, Adv. Metab. Disord. 60 (1972) 1–55. https://doi.org/10.1016/B978-0-12-027306-5.50006-1.

[29]   M. Vermeersch, R.I. Da Luz, K. Toté, J.P. Timmermans, P. Cos, L. Maes, In vitro susceptibilities of Leishmania donovani promastigote and amastigote stages to antileishmanial reference drugs: practical relevance of stage-specific differences, Antimicrob. Agents Chemother. 53 (2009) 3855–3859. https://doi.org/10.1128/AAC.00548-09.

[30]   I. Bekersky, R.M. Fielding, D.E. Dressler, J.W. Lee, D.N. Buell, T.J. Walsh, Plasma protein binding of amphotericin B and pharmacokinetics of bound versus unbound amphotericin

B after administration of intravenous liposomal amphotericin B (AmBisome) and amphotericin B deoxycholate, Antimicrob. Agents Chemother. 46 (2002) 834–840. https://doi.org/10.1128/AAC.46.3.834-840.2002.

[31]   T. Ishida, H. Harashima, H. Kiwada, Liposome Clearance, Biosci. Rep. 22 (2002) 197–224. https://doi.org/10.1023/A:1020134521778.

[32]   X. Yan, G.L. Scherphof, J.A.A.M. Kamps, Liposome opsonization, J. Liposome Res. 15 (2005) 109–139. https://doi.org/10.1081/LPR-64971.

[33]   E.E. Zijlstra, The immunology of post-kala-azar dermal leishmaniasis (PKDL), Parasites and Vectors. 9 (2016). https://doi.org/10.1186/s13071-016-1721-0.

[34]   D. Mukhopadhyay, S. Mukherjee, S. Roy, J.E. Dalton, S. Kundu, A. Sarkar, N.K. Das, P.M. Kaye, M. Chatterjee, M2 Polarization of Monocytes-Macrophages Is a Hallmark of Indian Post Kala-Azar Dermal Leishmaniasis, PLoS Negl. Trop. Dis. 9 (2015). https://doi.org/10.1371/JOURNAL.PNTD.0004145.

4.2

Supplementary

Supp1. Baseline skin parasite load verse lesion score
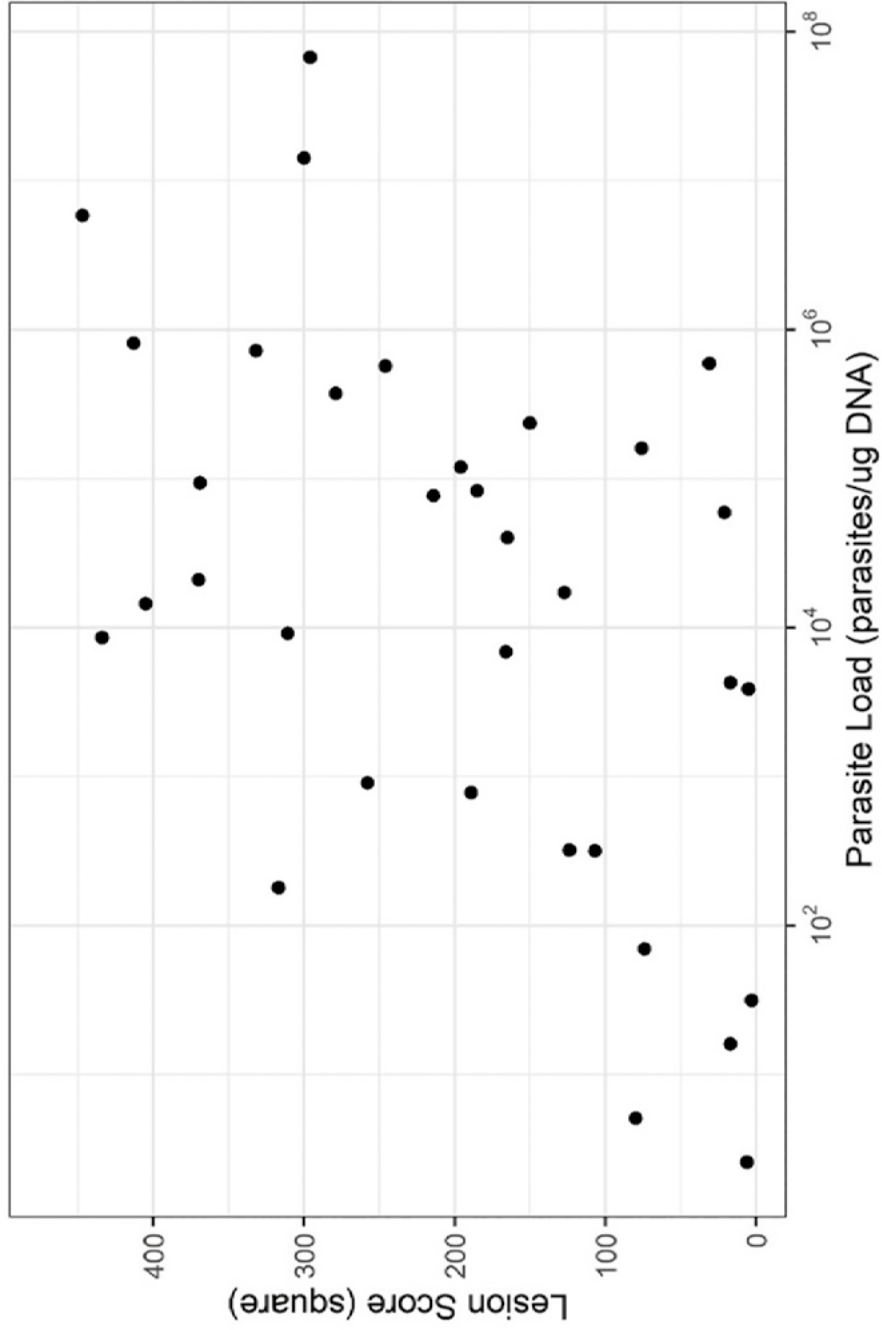
Supp2. Skin parasite load over treatment period

4.2
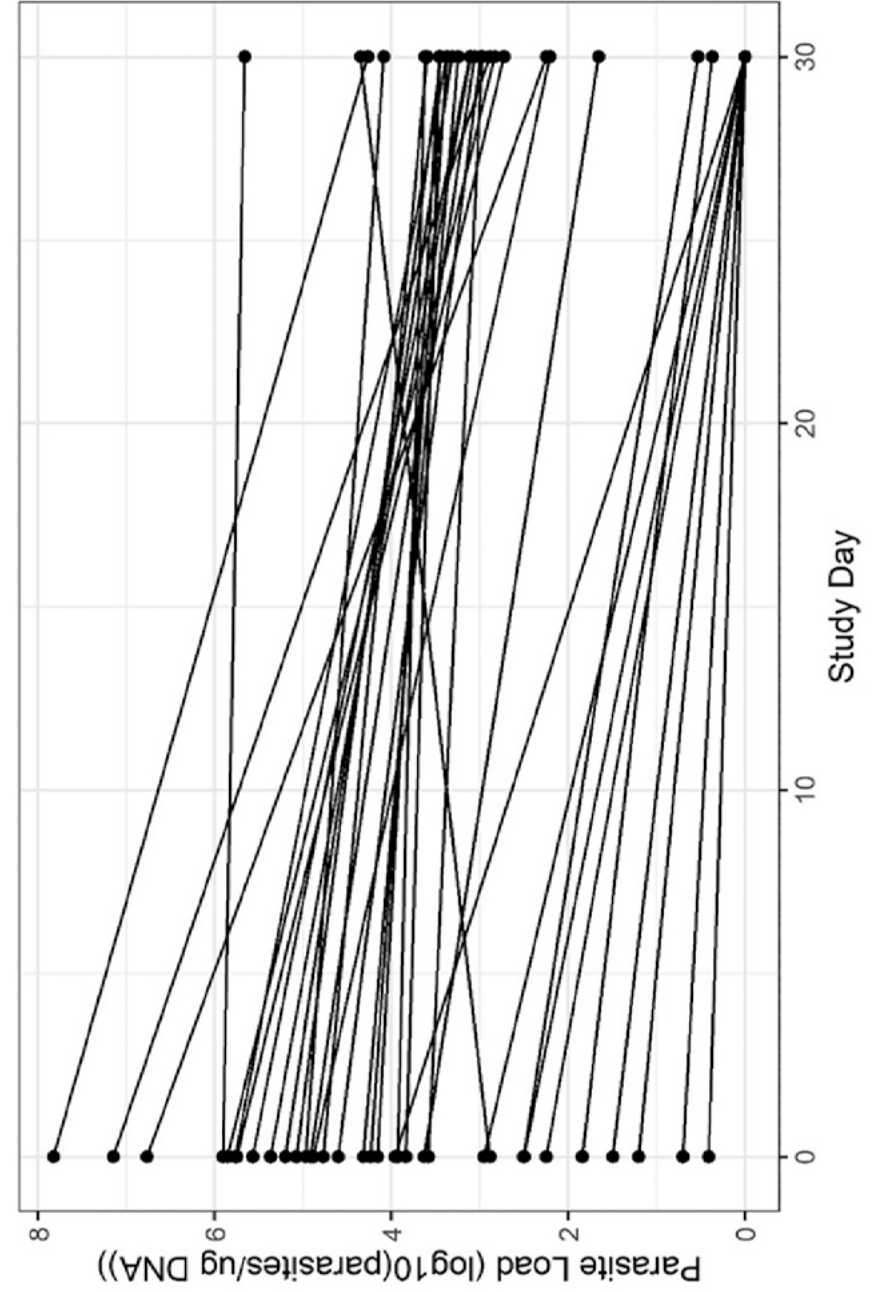
Conclusion & Perspectives

5

In the past few years substantial progress has been made in the optimization of current antileishmanial treatment regimens. Development of dedicated bioanalytical assays enabled important clinical pharmacokinetic (PK) studies in affected patient populations, including pediatrics, which led to changes in the recommended dose regimens. Currently, clinical trials are ongoing to find optimal dosing regimens for old and novel compounds to treat both visceral and dermal (cutaneous and post-kala-azar dermal) leishmaniasis, through shortened combination treatment regimens. Bioanalytical assays are pivotal and needed to enable clinical PK studies of these novel regimens, to assess adequacy of drug exposure and drug-drug interactions and to establish pharmacokinetic-pharmacodynamic (PKPD) relationships.

Leishmania parasites divide and reside in the dermis of the skin after a bite of a *Leishmania* infected sandfly. Current antileishmanial drug measurements are performed in blood matrices to assist PK studies and to provide estimates of drug exposure. This study setup was common in PK studies and provided the best alternative to target site PK studies. Particularly, little is known about the drug exposure of the parasite at the site of infection in the skin of patients with cutaneous leishmaniasis (CL) and post-kala-azar dermal leishmaniasis (PKDL), which limits interpretation of established PKPD relationships. Therefore, there is an urgent need to develop bioanalytical assays focused on the target site where the parasite is located, to assess drug exposure of the intracellular parasite within tissue after systemic administration of antileishmanial drugs. This thesis focuses mainly on developing and implementing target site bioanalytical systems for the quantification of antileishmanial agents and the target site clinical PK outcomes generated by these developed bioanalytical assays.

Conclusions

The need for increased sensitivity for quantification of paromomycin in human plasma

Bioanalytical assays for the quantification of paromomycin in human plasma were limited by a low sensitivity, leading to lower limits of quantification of ≥50 ng/mL [1–3]. Due to geographical variability in paromomycin pharmacokinetics during drug treatment, plasma concentrations in patients from various regions are highly variable as well [4]. Although paromomycin plasma concentration levels are initially high after the first hour of intramuscular administration, paromomycin is rapidly excreted renally [5]. Consequently, many PK data points during the clearance phase were below the limit of quantitation, which compromised an accurate estimation of paromomycin clearance.

Developing a more sensitive quantification method was achieved to overcome this problem by using simple protein precipitation, a stable isotope labelled internal

standard and ultra-high performance liquid chromatography [6], described in **chapter 2.1**. The method holds an advantage over previously developed bioanalytical methods in terms of increased sensitivity, lower sampling volume to 50 µL, improving assay performance and assay robustness by including a paromomycin stable isotope labelled internal standard, a short and fast sample preparation method, and state of the art chromatographic setup. The developed assay incorporated a lower limit of quantification (LLOQ) of 5 ng/mL and was at least 10 times more sensitive than previous published methods in human plasma (LLOQ of ≥ 50 ng/mL) [1–3]. The assay performance was excellent in terms of accuracy (±8.3%) and precision (≤4.3%). This method enabled the quantification of all the paromomycin plasma concentrations from visceral leishmaniasis (VL) patient treated with a combination of paromomycin (20 mg/kg intramuscular injections for 14 days) plus miltefosine originating from Eastern Africa in clinical trials.

Accordingly, new PK insights were unveiled with the help of the developed highly sensitive bioanalytical assay. Clearance and subsequent overall drug exposure parameters could be estimated more reliably and displayed non-linear characteristics during the course of treatment. Clearance appeared dependent on the level of neutropenia of patients. There were no geographical differences in paromomycin pharmacokinetics found in this particular study that could explain potential geographical differences in efficacy. Further clinical trial outcomes have yet to be published.

Introducing a novel skin tissue digestion method for target site bio-analytical quantification of antileishmanial drugs

Old and novel treatments for patients suffering from CL and PKDL are investigated in clinical trials to improve dosing regimens by combined and shortened treatment regimens. *Leishmania* parasites divide and reside in the dermis of the skin for the dermal leishmaniasis clinical phenotypes. PKPD studies were previously performed using blood (plasma, serum, or whole blood) matrices to relate to efficacy data without taking into account the fraction of drug actually penetrating into the skin after systemic administration. Therefore, it is important to exploit antileishmanial PK data from the skin tissue during treatment for better understanding antileishmanial drug skin penetration and exposure to *Leishmania* parasites. The absence of a suitable skin tissue homogenization method hampered the bioanalytical development of antileishmanial drug quantification in skin tissue. Achieving a homogenization method for 'hard' tissues such as skin is particularly challenging as described in more detail in **chapter 3.1**.

Full homogenization of skin tissue was achieved following pilot experiments on untreated human skin tissue biopsies. Mechanical homogenization did not fully homogenize skin tissue and was as well labour intensive. Chemical homogenization

5

or solubilization was achieved using a highly alkaline solvent, quaternary ammonium hydroxide, incubated at 50°C overnight and did fully homogenize skin tissue. Stability of antileishmanial drugs during incubation, however, was low and unacceptable, particularly for paromomycin and amphotericin B, as described in **chapter 3.1**.

A novel skin tissue homogenization method by enzymatic digestion using the enzyme collagenase A was developed, which was compatible with further sample preparation techniques like protein precipitation and solid phase extraction, described in detail in **chapters 3.2**, **3.3**, and **3.4**. Human skin tissue biopsies are reduced to single cell suspensions during collagenase A incubation. Collagen is the main extracellular structural protein in the skin. By cleaving peptide bonds in collagen proteins, skin tissue loses its extracellular structure and cells that were attached to collagen proteins start to disperse in the solution. Intracellular components were released by disrupting cell membranes using protein precipitation methods, including highly acidic, organic, or high salt concentrated precipitation solutions. By neutralizing pH and decreasing incubation temperature to 37°C, the stability of antileishmanial drugs amphotericin B, paromomycin, and miltefosine during sample incubation was found to be adequate and subsequent bioanalytical assays with sufficient sensitivity could be achieved. Drug quantification in clinical skin tissue biopsy samples originating from PKDL patients were conducted. In conclusion, a novel homogenization method using collagenase A enzymatic digestion for human skin tissue target site bioanalysis was achieved that further enabled the development of bioanalytical methods for the quantification of small molecules in human skin tissue samples.

Distribution of amphotericin B and miltefosine in human skin

Skin tissue concentrations and exposure of antileishmanial drugs amphotericin B and miltefosine could at first be approximated using models that described systemic exposure in plasma. Skin tissue concentration data was absent and unknown because bioanalytical methods lacked skin target site analysis for the quantification of antileishmanial drugs, as mentioned above. After development, validation of bioanalytical methods for amphotericin B (**chapter 3.3**) and miltefosine (**chapter 3.2**), target site exposure could be quantified in skin tissue samples from PKDL, demonstrating penetration of these drugs in skin, to the best of our knowledge for the first time.

Exposure of miltefosine in human skin tissue of PKDL patients in India and Bangladesh after allometric weight-based oral dosing regimen of 21 days was described in **chapter 4.1**. Skin biopsy concentrations at the end of treatment, at the time of maximal accumulation, were compared to plasma concentrations. Miltefosine target site skin concentrations indicated an increased disposition in skin compared to plasma concentrations at the same time point, albeit with a high level of inter-individual variability. Because only a single skin concentration was available per

patient, PK modeling was limited and a semi-mechanistic PBPK model utilizing drug-specific and system-specific information was developed to further characterize the determinants of tissue distribution of miltefosine.

Characterization of amphotericin B pharmacokinetics in human skin tissue of PKDL patients in India and Bangladesh after a dosing regimen of 20 mg/kg intravenous liposomal amphotericin B for 15 days was described in **chapter 4.2**. Amphotericin B distributed in skin tissue and a semi-mechanistic PK model describing the uptake and opsonization of the amphotericin B-containing liposomes by macrophages. Plasma and skin tissue concentrations were compared, demonstrating distinct differences in drug elimination between the two sites of distribution. Estimated drug elimination half-life in skin was over 40-fold longer compared to plasma, indicating a longer residence time of amphotericin B in skin tissue compared to plasma.

Future perspectives

Bioanalytical multiplex assays for the quantification of antileishmanial drugs

The validated bioanalytical assays described in detail in **chapters 2**, **3.2**, **3.3**, and **3.4** were assays quantifying a single particular antileishmanial drug, either amphotericin B [7], miltefosine [8], or paromomycin [6]. These bioanalytical assays were developed for clinical trials in Kenya, India and Bangladesh [9], and Sudan [10] to support the PK studies investigating the use of shortened combination treatment regimens in various endemic regions. The outcome of the specified clinical trials, with respect to combination therapy regimens paromomycin-miltefosine and amphotericin B-miltefosine, could lead to new treatment protocols to treat VL, PKDL and CL. The favored therapy regimen would encourage bioanalytical development regarding multiplex assays. As described in **chapter 1**, developing such a multiplex assay is challenging because of wide differences in chemical properties of these antileishmanial drugs, each with their respective conceivable problems in terms of sample preparation, separation, and detection as well as stability [11]. Nonetheless, developing multiplex assays does have its advantages. The efficiency of the bioanalytical assay would increase because less resources (eluents, organic solvents, labware) are used as well as the bioanalytical assay data acquisition process would become faster, translating to lowering both laboratory costs and time. There is also the advantage of lowering sampling volumes needed to conduct a bioanalytical assay. Lowering sampling volumes in turn lowers the volumes of blood drawn in clinical settings, because less blood volume is necessary to perform the assays. Conclusively, combining single analyte assays to multiplex assays increases efficiency and saves costs by lowering the number of necessary lab-resources and data processing time as well as lowering the burden on patients by requiring smaller volumes of blood.

5

This could prove useful in future clinical measurements.

Exploring the true recovery of antileishmanial drugs in human skin tissue to improve accuracy

During the development and validation of bioanalytical assays to quantify antileishmanial drugs in human skin tissues, described in **chapters 3.2**, **3.3**, and **3.4**, validation extraction recovery experiments were performed. The experiments described the recovery of the sample preparation method after collagenase A enzymatic digestion of human skin tissue to homogenize/dissolve skin tissue [8]. As mentioned in **chapter 3.1**, the true recovery of analytes from skin tissue is impossible to assess based on human clinical samples [12]. The assessment of true recovery in bioanalytical assays of tissue samples is important to be able to generate and report accurate drug concentrations.

The true recovery of analytes is a combination of the sample preparation recovery and recovery from the tissue after the homogenization step, defined by spiking analytes pre-homogenization in matrix. Homogenous matrices, mainly bodily fluids, pre-homogenization spiking need not to be done because the matrices itself are homogenous. By spiking these homogeneous matrices with analyte, performing simple vortex mixing is enough to retain a homogeneous mixture. For non-homogeneous samples like tissues, the analytes cannot be spiked pre-homogenization. In **chapters 3.2**, **3.3**, and **3.4** the extraction (sample preparation) recovery is described. The determination of true recovery and true concentration from skin tissues cannot be conducted because the distribution of analyte intracellularly in skin would not be comparable to clinically administered drug treatment regimens. **Chapter 3.1** describes methods for the solubilization of skin tissue (chemical solubilization or enzymatic digestion) which approximates the closest to complete homogenization [12]. Mechanical homogenization methods were not advised due to the risk of incomplete homogenization of skin tissue, thereby failing to release analytes from the endogenous mixture of substances fully. While chemical solubilization and enzymatic digestion lead to homogeneous samples for further sample processing, the true recovery from the original clinical samples cannot be assessed. Therefore, the real concentration inside the tissue is unknown and the reproducibility of tissue sample treatment remains unidentified. The unknown bias may contribute to errors in further PK studies.

Radio-labelled antileishmanial drugs experiments may contribute to establish true recovery. Quantification of drugs before homogenization of human skin tissue can be performed using radio-labelled analytes for drug administration combined with scintillation counting measurements after tissue sampling [13,14]. The scintillation counting concentration assessment could then be compared to the quantification of analytes described in **chapters 3.2**, **3.3**, and **3.4** to determine potential loss of

analyte due to the homogenization process. These experiments could also be setup in pre-clinical animal studies [15], although differences in composition of skin tissue between species should be taken into account in this translational approach. Should the scintillation detector be adequately sensitive and radioactive signals of analytes sufficiently high, administering a microdose of radio-labelled antileishmanial drugs in humans could potentially remove these pre-clinical studies to assess the true recovery in human skin tissue directly. State-of-the-art mass spectrometry methods like accelerator mass spectrometry (AMS) could also be implemented in future true recovery studies in case of a low scintillation detection sensitivity.

Target site bioanalytical and pharmacokinetic studies for patients suffering from leishmaniasis

Target site bioanalytical and PK studies in PKDL patients were performed in **chapters 3.2, 3.3, 3.4, 4.1, and 4.2**. These studies investigated human skin tissue from patients suffering from dermal leishmaniasis. Furthermore, concentrations of miltefosine in peripheral blood mononuclear cells were previously assessed by Kip *et al*., indirectly providing miltefosine intracellular exposure data as a potential proxy for the tissue macrophages and monocytes in which intracellular *Leishmania* parasites reside [16]. Bioanalytical methods in peripheral blood mononuclear cells have not yet been developed and validated for paromomycin and amphotericin B (or other antileishmanial drugs) and could help provide insight into the target site drug exposure of *Leishmania* parasites for all leishmaniasis clinical phenotypes. For VL, no bioanalytical assay using VL sampling matrix (spleen, liver, and bone marrow) was developed for amphotericin B, paromomycin, and miltefosine hitherto, apart from miltefosine in peripheral blood mononuclear cells [16]. Therefore, no distribution data and exposure-response relationships with the waning parasite load in e.g. liver, spleen, and bone marrow in humans have been evaluated. Bioanalytical assay development could be performed on biopsy material taken from patients after the last drug administration, however tissue aspirates originating from spleen, liver, or bone marrow are highly invasive and not regularly performed unless there is suspicion of treatment failure or relapse [17,18]. Nevertheless, these highly invasive sampling matrices could also be obtained making use of mouse or hamster cutaneous leishmaniasis infection models, as another potential for translational research.

Bioanalysis in resource-poor settings

Leishmaniasis is a typical disease of the poor and malnourished, endemic in the poorest regions of the world. In Eastern Africa, clinical trials for clinical phenotypes VL or PKDL are hard to perform because of several reasons. The people living in remote regions usually live in environments where infrastructure standards are low and hospitals are far remote. Drug treatment, which currently still requires hospitalization, is therefore highly challenging in these settings. In clinical trials on leishmaniasis, blood sampling, (intravenous) drug administration and the

requirement for extensive hospitalization to treat VL remain problematic. As for the antileishmanial drugs described in this thesis; liposomal amphotericin B is administered intravenously and has low stability in high temperature settings and paromomycin is administered intramuscularly, both requiring hospitalization. Miltefosine, however, is administered orally by capsules and is highly stable under high temperature settings and has the potential to be administered on an outpatient basis, at least for part of the treatment.

Sampling of blood in clinical trials is problematic in leishmaniasis patients, because of severe anemia caused by the prolonged suppression of bone marrow during *Leishmania* infection [19] and because of the remoteness of the clinical trial infrastructure, where often a cold-chain logistics are difficult to establish. Kip *et al*. developed and validated bioanalytical assays to tackle these challenges using dried blood spots on filter paper [20] and volumetric absorptive microsampling [21] methods for miltefosine quantification. This was enabled by the stability of miltefosine in high temperature conditions and stability in both absorption materials. The stability under these conditions should be tested for other antileishmanial drugs, amphotericin B, paromomycin, but also pentamidine and future antileishmanial drugs. As opposed to miltefosine, amphotericin B and paromomycin are less stable at higher temperatures, which could possibly be a limiting factor in the transport and storage of dried blood spots and other microsampling tools.

The possibility of using these sampling methods instead of venous sampling, which requires a primary health center infrastructure, would possibly increase the number of patients that could be recruited in clinical trials also in more remote parts of the leishmaniasis endemic regions, creating new possibilities for better study design and a better representation of 'real-world' patients in clinical trials. Cutting the cold chain transport of frozen blood samples from poor remote regions would increase the practicality and decrease the costs of the clinical trials performed.

Concluding remarks

In conclusion, this thesis described the most current progress of bioanalytical and PK studies for the antileishmanial drugs amphotericin B, miltefosine, and paromomycin in VL and PKDL patients. By applying state of the art bioanalytical tools, our research goal was to create new bioanalytical assays for the quantification of the three antileishmanial drugs in a complex and unique sampling matrix, human skin tissue, for currently practiced PKDL clinical trials as well as improving the performance of assays to quantify paromomycin in VL patients' plasma by increasing sensitivity by lowering the LLOQ of the assays. Increasing the sensitivity of the paromomycin bioanalytical assay provided new insights into non-linear PK characteristics of this

drug during the treatment course as well as a variability in clearance. Combination drug treatment regimen improvements are to be further investigated. Increasing clinical trial accessibility of remote regions and developing sensitive multiplex assays will improve the efficiency of these investigations. Furthermore, a novel human skin tissue homogenization method was developed using collagenase A enzymatic digestion. This enabled the development of sensitive bioanalytical assays to quantify amphotericin B, miltefosine and paromomycin in human skin tissue. PK analysis was performed in human skin tissue for the first time for both amphotericin B and miltefosine, showing accumulation of both antileishmanial drugs in skin tissue compared to plasma. Target site bioanalytical methods are convenient tools to support future target site PK studies in clinical trials for development and improvement of current drug treatment regimens including amphotericin B, miltefosine, and paromomycin in patients suffering from leishmaniasis. Target site bioanalytical matrices are to be expanded to spleen, liver, and peripheral blood mononuclear cells for future studies to investigate exposure of antileishmanial drugs in non-dermal leishmaniasis patients as well. Increasing accuracy and reproducibility for future studies can be achieved by exploring true recovery of clinical samples to investigate the performance of collagenase A enzymatic digestion, either in human or preclinical animal studies. Conclusively, new study designs were unlocked for improvement of antileishmanial drug regimen due to the achievement of developing and validating target site skin tissue bioanalytical assays forming its fundamental supporting role.

5

References

[1] W.R. Ravis, A. Llanos-Cuentas, N. Sosa, M. Kreishman-Deitrick, K.M. Kopydlowski, C. Nielsen, K.S. Smith, P.L. Smith, J.H. Ransom, Y.J. Lin, M. Grogl, Pharmacokinetics and absorption of paromomycin and gentamicin from topical creams used to treat cutaneous leishmaniasis, Antimicrob. Agents Chemother. 57 (2013) 4809–4815. https://doi.org/10.1128/AAC.00628-13.

[2] R. Oertel, V. Neumeister, W. Kirch, Hydrophilic interaction chromatography combined with tandem-mass spectrometry to determine six aminoglycosides in serum, J. Chromatogr. A. 1058 (2004) 197–201. https://doi.org/10.1016/j.chroma.2004.08.158.

[3] J. Lu, M. Cwik, T. Kanyok, Determination of paromomycin in human plasma and urine by reversed-phase high-performance liquid chromatography using 2,4-dinitrofluorobenzene derivatization, J. Chromatogr. B Biomed. Sci. Appl. 695 (1997) 329–335. https://doi.org/10.1016/S0378-4347(97)00192-8.

[4] L. Verrest, M. Wasunna, G. Kokwaro, R. Aman, A.M. Musa, E.A.G. Khalil, M. Mudawi, B.M. Younis, A. Hailu, Z. Hurissa, W. Hailu, S. Tesfaye, E. Makonnen, Y. Mekonnen, A.D.R. Huitema, J.H. Beijnen, S.A. Kshirsagar, J. Chakravarty, M. Rai, S. Sundar, F. Alves, T.P.C. Dorlo, Geographical Variability in Paromomycin Pharmacokinetics Does Not Explain Efficacy Differences between Eastern African and Indian Visceral Leishmaniasis Patients, Clin. Pharmacokinet. 60 (2021) 1463–1473. https://doi.org/10.1007/s40262-021-01036-8.

[5] A.S. of H.-S. Pharmacists, Paromomycin Monograph for Professionals - Drugs.com, (n.d.). https://www.drugs.com/monograph/paromomycin.html (accessed February 21, 2022).

[6] I.C. Roseboom, B. Thijssen, H. Rosing, J. Mbui, J.H. Beijnen, T.P.C. Dorlo, Highly sensitive UPLC-MS/MS method for the quantification of paromomycin in human plasma, J. Pharm. Biomed. Anal. 185 (2020) 113245. https://doi.org/10.1016/j.jpba.2020.113245.

[7] I.C. Roseboom, B. Thijssen, H. Rosing, F. Alves, S. Sundar, J.H. Beijnen, T.P.C. Dorlo, Development and validation of a high-performance liquid chromatography tandem mass spectrometry method for the quantification of the antiparasitic and antifungal drug amphotericin B in human skin tissue, J. Chromatogr. B. 1206 (2022) 123354. https://doi.org/10.1016/j.jchromb.2022.123354.

[8] I.C. Roseboom, B. Thijssen, H. Rosing, F. Alves, D. Mondal, M.B.M. Teunissen, J.H. Beijnen, T.P.C. Dorlo, Development and validation of an HPLC-MS/MS method for the quantification of the anti-leishmanial drug miltefosine in human skin tissue, J. Pharm. Biomed. Anal. (2021) 114402. https://doi.org/10.1016/j.jpba.2021.114402.

[9] C.T.R. India, New treatment regimens for treatment of Post Kala Azar Dermal Leishmaniasis patients in India and Bangladesh region, New Delhi Database Publ. (India). Identifier CTRI/2017/04/008421. (2017) 7.

[10] NCT03399955, Short Course Regimens for Treatment of PKDL (Sudan), 2018.

[11] DrugBank Online | Database for Drug and Drug Target Info, (n.d.). https://go.drugbank.com/ (accessed May 16, 2022).

[12] I.C. Roseboom, H. Rosing, J.H. Beijnen, T.P.C. Dorlo, Skin tissue sample collection, sample homogenization, and analyte extraction strategies for liquid chromatographic mass spectrometry quantification of pharmaceutical compounds, J. Pharm. Biomed. Anal. 191 (2020) 113590. https://doi.org/10.1016/j.jpba.2020.113590.

[13] H. Neubert, S. Fountain, L. King, T. Clark, Y. Weng, D.M. O'Hara, W. Li, S. Leung, C. Ray, J. Palandra, M.F. Ocaña, J. Chen, C. Ji, M. Wang, K. Long, B. Gorovits, E. Fluhler, Tissue bioanalysis of biotherapeutics and drug targets to support PK/PD, Bioanalysis. 4 (2012) 2589–2604. https://doi.org/10.4155/bio.12.234.

[14] L. Yuan, L. Ma, L. Dillon, R.M. Fancher, H. Sun, M. Zhu, L. Lehman-McKeeman, A.-F. Aubry, Q.C. Ji, Investigation of the "true" extraction recovery of analytes from multiple types of tissues and its impact on tissue bioanalysis using two model compounds, Anal. Chim. Acta. 945 (2016) 57–66. https://doi.org/10.1016/j.aca.2016.09.039.

[15] E.N. Loria-Cervera, F.J. Andrade-Narvaez, Animal models for the study of leishmaniasis immunology, Rev. Inst. Med. Trop. Sao Paulo. 56 (2014) 1–11. https://doi.org/10.1590/S0036-46652014000100001.

[16] A.E. Kip, H. Rosing, M.J.X. Hillebrand, M.M. Castro, M.A. Gomez, J.H.M. Schellens, J.H. Beijnen, T.P.C. Dorlo, Quantification of miltefosine in peripheral blood mononuclear cells by high-performance liquid chromatography-tandem mass spectrometry, J. Chromatogr. B. 998–999 (2015) 57–62. https://doi.org/10.1016/j.jchromb.2015.06.017.

[17] R. Artan, A. Yilmaz, M. Akçam, N.H. Aksoy, Liver biopsy in the diagnosis of visceral leishmaniasis, J. Gastroenterol. Hepatol. 21 (2006) 299–302. https://doi.org/10.1111/j.1440-1746.2006.04172.x.

[18] B.L. Herwaldt, Leishmaniasis., Lancet (London, England). 354 (1999) 1191–9. https://doi.org/10.1016/S0140-6736(98)10178-2.

[19] N. Varma, S. Naseem, Hematologic Changes in Visceral Leishmaniasis/Kala Azar, Indian J. Hematol. Blood Transfus. 26 (2010) 78–82. https://doi.org/10.1007/s12288-010-0027-1.

[20] A.E. Kip, H. Rosing, M.J.X. Hillebrand, S. Blesson, B. Mengesha, E. Diro, A. Hailu, J.H.M. Schellens, J.H. Beijnen, T.P.C. Dorlo, Validation and Clinical Evaluation of a Novel Method To Measure Miltefosine in Leishmaniasis Patients Using Dried Blood Spot Sample Collection, Antimicrob. Agents Chemother. 60 (2016) 2081–2089. https://doi.org/10.1128/AAC.02976-15.

[21] A.E. Kip, K.C. Kiers, H. Rosing, J.H.M. Schellens, J.H. Beijnen, T.P.C. Dorlo, Volumetric absorptive microsampling (VAMS) as an alternative to conventional dried blood spots in the quantification of miltefosine in dried blood samples, J. Pharm. Biomed. Anal. 135 (2017) 160–166. https://doi.org/10.1016/j.jpba.2016.12.012.

5

Appendix

Summary

This thesis focuses on bioanalytical method development and validation of antileishmanial drugs amphotericin B, miltefosine, and paromomycin in human plasma and human skin tissue followed by clinical target site pharmacokinetic outcomes induced by these developed bioanalytical methods.

Chapter 1 gives a comprehensive overview of published validated bioanalytical assays for the quantification of antileishmanial drugs amphotericin B, miltefosine, paromomycin, pentamidine, and pentavalent antimonials in human matrices. Each antileishmanial drug was discussed regarding their applicability of the assay for leishmaniasis clinical trials as well as providing their relevance for PK studies with emphasis on the choice of matrix, calibration range, sample volume, sample preparation, choice of internal standards, separation, and detection. Suggestions were made regarding future bioanalytical development of the antileishmanial drugs to improve and aid the implementation of these methods in future clinical trials. There were no multiplex assays developed and published hitherto, only single analyte analysis assays were able to quantify antileishmanial drugs. Clinical trials showed an improvement in treatment efficacy because of combination drug regimens. Striving to develop multiplex assays aiming to combine these antileishmanial drugs into one assay is cost effective, lowers laboratory labour, decreases the use of chemicals, and speeds up the acquisition of bioanalytical data. Moving towards target site bioanalytical assays combined with target site pharmacokinetic studies in clinical trials provide more information on the distribution and exposure of antileishmanial drugs and can be used as a tool for better understanding of underlying mechanisms. The use of microsampling strategies in remote regions and the development of bioanalytical assays using matrix from microsamples could be the solution to a challenging cold chain logistics and storage as well as decreasing the invasive sampling techniques for patients.

Chapter 2 describes the development and validation of the bioanalytical assay for the quantification of the antileishmanial drug paromomycin in human plasma using ion-pair ultra-high performance liquid chromatography-tandem mass spectrometry (UHPLC-MS/MS). The method was fully validated following the U.S. Food and Drug Administration (FDA) and European Medicines Agency (EMA) guidelines for human plasma matrix and was the first to use a stable isotope labelled internal standard (SILIS) deuterated paromomycin for the quantification of paromomycin. Volatile ion-pair additive heptafluorobutyric acid was used with a reversed phase column, because paromomycin was too hydrophilic to gain retention. This method was linear, accurate, and precise as well as showing no significant IS-normalized matrix effects. Paromomycin adsorbs to glass containers at low concentrations, and therefore acidic conditions were used throughout the assay, in combination with polypropylene tubes

and autosampler vials. The assay was successfully applied in a pharmacokinetic study in visceral leishmaniasis patients from Eastern Africa.

Chapter 3 focusses on human skin tissue target site bioanalytical methods for the quantification of miltefosine, amphotericin B and paromomycin. Full validations were performed according to the EMA guidelines. Before further elaboration of these bioanalytical methods, **chapter 3.1** described the challenges of skin tissue bioanalysis for the quantification of pharmaceutical compounds. A comprehensive overview was provided of sample collection, sample homogenization and analyte extraction methods that have been used to quantify pharmaceutical compounds in skin tissue, obtained from animals and humans, using liquid chromatography-mass spectrometry. For each step in the process of sample collection to sample extraction, methods are compared to discuss challenges and provide practical guidance. Furthermore, LC-MS considerations regarding the quality and complexity of skin tissue sample measurements are discussed, with emphasis on analyte recovery and matrix effects. Given that the true recovery of analytes from skin tissue is difficult to assess, the extent of homogenization plays a crucial role in the accuracy of quantification. A suggestion was made for chemical solubilization or enzymatic digestion of skin tissue samples, as they would be preferable as a homogenization method in sample processing steps before analyte extraction. **Chapter 3.2** outlines the target site bioanalytical development and validation for the quantification of miltefosine in human skin tissue using LC-MS/MS. To homogenize human skin tissue before extraction of miltefosine, enzymatic digestion was implemented using collagenase A and overnight (±16 hours) incubation at a constant temperature of 37°C. Digestion solution was used as a surrogate matrix for calibration and quality control (QC) samples instead of skin tissue homogenates to quantify miltefosine in human skin tissue samples. The skin tissue did not have any significant matrix effect on the surrogate matrix. The method was found to be accurate, precise, and linear over the validated range, using a deuterated SILIS. The assay was successfully applied to skin biopsy samples from patients with post-kala azar dermal leishmaniasis who were treated with miltefosine in Bangladesh. **Chapter 3.3** concentrates on the target site bioanalytical development and validation for the quantification of the antiparasitic and antifungal drug amphotericin B in human skin tissue using LC-MS/MS. Homogenization of human skin tissue samples was performed using a digestion solution containing collagenase A, followed by overnight incubation at 37°C. Digestion solution was used as a surrogate matrix for calibrations and QC samples. Natamycin, a chemical analogue, was used as internal standard (IS), and although the recovery of amphotericin B after overnight enzymatic digestion was relatively low (around 27%), the IS corrected appropriately without significant IS-normalized matrix factors. Using this assay, amphotericin B could be detected and quantified in skin biopsies originating from treated Indian post-kala-azar dermal leishmaniasis patients. Finally, **chapter 3.4** gets into detail about target site bioanalytical development and

validation for the quantification of the paromomycin in human skin tissue using ion-pair UHPLC-MS/MS. The human skin tissue digestion process was performed using collagenase A overnight incubation at 37°C, using digestion solution as a surrogate matrix for the preparation of calibration and QC samples. Paromomycin peak area signal was accurately corrected using a deuterated SILIS, showing no significant IS-normalized matrix factor. The bioanalytical method was considered linear, accurate and precise following the EMA guidelines. Finally, paromomycin was accurately quantified in the skin of post-kala-azar dermal leishmaniasis patients originating from clinical trials in Sudan.

Conclusively, **chapter 4** elaborates further on the processing of human skin tissue data acquired by the bioanalytical assays in clinical trials, displaying the development of pharmacokinetic modeling to investigate exposure-response relationships of antileishmanial drugs in the treatment of patients. **Chapter 4.1** describes the comparison between plasma and skin tissue miltefosine concentrations at the end of an allometric dosed treatment of 21 days in India and Bangladesh. The median concentration ratio of skin and plasma was 1.19, showing a significant accumulation of miltefosine in the skin. The exposure of killing the parasites was reached in >90% of the patients. By developing a semi-mechanistic PBPK model utilizing drug-specific and system-specific information, predictions to describe spleen and liver miltefosine distributions using a limited miltefosine skin tissue concentration dataset were accomplished. **Chapter 4.2** illustrates amphotericin B pharmacokinetics in human skin tissue of Indian and Bangladeshi patients, after receiving a 15-day 20 mg/kg intravenously dosing regimen. Plasma and skin tissue amphotericin B concentrations were compared and described using a semi-mechanistic PK model, demonstrating distinct differences in drug elimination between the two sites of distribution. Estimated drug elimination half-life in skin was over 40- fold longer compared to plasma, indicating a longer residence time of amphotericin B in skin tissue compared to plasma.

Nederlandse samenvatting

Dit proefschrift spitst zich toe op de ontwikkeling en validatie van bioanalytische methoden om antileishmaniale middelen (amfotericine B, miltefosine en paromomycine) in humaan bloedplasma en huid te kwantificeren, waarna klinische farmacokinetisch onderzoek op lokaal doelwit weefsel (huid) werd uitgevoerd.

Hoofdstuk 1 geeft een uitgebreid overzicht van gepubliceerde en gevalideerde bioanalytische assays, voor het kwantificeren van antileishmaniale middelen (amfotericine B, miltefosine, paromomycine, pentamidine en pentavalent antimoon) in humane matrices. Elk van de antileishmaniale middelen werd besproken aan de hand van de praktische toepasbaarheid in klinisch onderzoek. De relevantie in pk-onderzoek werd gecorreleerd aan de matrix keuze, kalibratie bereik, monster volume, opwerk methoden, interne standaard keuzes, scheiding en detectie. Verder werden er adviezen gegeven met betrekking tot de opzet voor de verbetering van nieuw bioanalytisch onderzoek van deze antileishmaniale middelen, met het oog op de toepasbaarheid in toekomstig klinisch onderzoek. Er was geen assay ontwikkeld, gevalideerd of gepubliceerd waarbij meerdere antileishmaniale middelen tegelijkertijd werd gekwantificeerd, slechts assays voor het kwantificeren van een enkel middel. Klinisch onderzoek toonde aan dat het combineren van meerdere antileishmaniale middelen bij de behandeling een verbeterde werkzaamheid had. Door het combineren van meerdere bioanalytische assays in één assay komen voordelen als lagere kosten, minder laboratorium werk, verlaging van het aantal gebruikte chemicaliën en een versneld acquisitie proces tevoorschijn. Klinisch onderzoek profiteert van data waarbij onderliggende mechanismen uitgelegd kunnen worden aan de hand van de daadwerkelijke distributie en blootstelling van antileishmaniale middelen. Dit door data te genereren in de combinatie met bioanalytische assays en farmacokinetische studies in medicinaal lokaal doelwit weefsel. Ook werd het mogelijke gebruik van microsampling strategieën in afgelegen regionen besproken, waarbij de ontwikkeling van bioanalytische methoden op de microsampling monsters van cruciaal belang is om koud transport en opslag en invasieve manier van bloedprikken op te lossen.

Hoofdstuk 2 bevat de ontwikkeling en validatie van de paromomycin kwantificatie bioanalytische methode in humaan bloedplasma, gebruikmakend van ion-paar ultra-high performance vloeistofchromatografie gekoppeld aan massaspectrometrie (UHPLC-MS/MS). Deze methode was, met succes, gevalideerd volgens de richtlijnen van het voedsel en waren autoriteit van de VS (FDA) en van het Europees medicijn bureau (EMA), toepasbaar op humane bloedplasma matrix. Het daarbij ook de eerste publicatie met het gebruik van stabiele isotoop gelabelde interne standaard (SILIS) bij het kwantificeren van paromomycine. Een vluchtig ion-paar additief, vijfvoudig fluor boterzuur, in combinatie met een reversed-phase analytische kolom

werd in gebruik genomen, omdat paromomycine te hydrofiel bleek te zijn voor een acceptabele retentie op een reversed-phase analytische kolom. De methode bleek lineair, accuraat en precies, en liet geen significant IS-genormaliseerde matrix factor zien. Zure condities in combinatie met polypropyleen autosampler flacons werden door de hele methode gebruikt, omdat paromomycine de neiging heeft bij lage concentraties te adsorberen aan glas. Verder werd de assay succesvol gebruikt in een klinische studie, waarbij paromomycine werd gekwantificeerd in Oost-Afrikaanse patiënten die gediagnosticeerd waren met viscerale leishmaniasis.

Hoofdstuk 3 focust zich op bioanalytische methoden voor het kwantificeren van miltefosine, amfotericine B en paromomycine in humaan huid als lokaal doelwit weefsel. Volledige validatie procedures werden uitgevoerd volgens de EMA-regelgeving. Voordat dit in detail besproken wordt, beschreef **hoofdstuk 3.1** de uitdagingen van de bioanalyse van huidweefsel op de kwantificatie van farmaceutische producten. Hierbij werd een uitvoerig overzicht weergegeven van het verzamelen, de homogeniteit en de extractie methode van huidweefsel in publicaties die de kwantificatie van farmaceutische producten in huid, van zowel dieren als mens, beschreven met behulp van vloeistofchromatografie en massaspectrometrie (LC-MS). Elke stap in de gegeven publicaties, van het verzamelen tot en met extractie van product, wordt met elkaar vergeleken om de valkuilen uit te leggen en om praktische richtlijnen weer te geven. Ook wordt de kwaliteit en complexiteit van huidweefsel metingen besproken aan de hand van recovery en matrix effecten. De juistheid van de correcte recovery is moeilijk te weerleggen en is onderhevig aan de mate van homogeniteit. Hierbij werden chemische oplosbaarheid en enzymatische digestie methoden geadviseerd alvorens het analiet werd geëxtraheerd. **Hoofdstuk 3.2** gaat verder in op de bioanalytische ontwikkeling en validatie van de methode om miltefosine in humaan huid te kwantificeren, gebruikmakend van LC-MS/MS. Enzymatische digestie door middel van overnacht (±16 uur) incubatie op 37°C in een collagenase A oplossing werd gebruikt als homogenisatie methode voor humaan huidweefsel, voordat miltefosine werd geëxtraheerd. De digestie oplossing werd gebruikt als surrogaat matrix voor de assay in plaats van humaan huidweefsel homogenaat, om miltefosine in humaan huidweefsel monsters te kwantificeren. Huidweefsel had geen significant matrix effect op de surrogaat matrix. De methode, gebruikmakend van een gedeutereerde SILIS, was accuraat, precies en lineair in het gevalideerde bereik. De assay werd succesvol toegepast op huidbiopten van PKDL-patiënten afkomstig uit Bangladesh. Deze patiënten werden behandeld met miltefosine. **Hoofdstuk 3.3** focust zich op de bioanalytische ontwikkeling en validatie van de methode om amfotericine B in humaan huid te kwantificeren met behulp van LC-MS/MS. Huidweefsel werd gehomogeniseerd door een enzymatische digestie methode, collagenase A overnacht incubatie. Hierbij werd digestie middel gebruikt als surrogaat matrix voor kalibratie en QC-standaarden. Natamycine werd gebruikt als chemisch analoge interne standaard (IS) van amfotericine B. De recovery van

amfotericin B was laag (rond de 27%), maar werd correct gecorrigeerd door de IS zonder enig significante IS-genormaliseerde matrix factor. De assay was in staat om amfotericine B in alle met amfotericine B behandelde Indiase PKDL-patiënten huid monsters te detecteren en kwantificeren. Tot slot gaat **hoofdstuk 3.4** verder in op de bioanalytische ontwikkeling en validatie van de methode om paromomycine in huidweefsel te kwantificeren met behulp van ion-paar UHPLC-MS/MS. Huidweefsel werd gehomogeniseerd met behulp van collagenase A overnacht incubatie op 37°C. Het digestie middel werd gebruikt als surrogaat matrix voor kalibratie en QC-standaarden. Het paromomycine signaal werd accuraat gecorrigeerd door middel van een gedeutereerde SILIS en liet geen significant IS-genormaliseerde matrix factor zien. De bioanalytische assay was, volgens de EMA-richtlijnen, accuraat, precies en lineair. Uiteindelijke werd ook paromomycine met succes gekwantificeerd in huidbiopten van PKDL-patiënten uit Sudan, die behandeld werden met paromomycine.

Tenslotte gaat **hoofdstuk 4** verder op de verkregen huidweefsel concentratie data, met behulp van de bioanalytische assays. De blootstelling van antileishmaniale middelen tijdens de behandeling van patiënten werd weergegeven in de farmacokinetische modellen, waarbij de ontwikkeling daarvan werd beschreven. **Hoofdstuk 4.1** vergelijkt plasma en huidweefsel miltefosine concentraties aan het einde van de 21-daagse, allometrisch gedoseerde behandeling in India en Bangladesh. De mediaan van de concentratie ratio's van huid versus plasma was 1.19 en toont daarmee een significante accumulatie van miltefosine in huidweefsel aan tijdens de behandeling. De beoogde blootstelling om parasieten te doden, werd bij >90% van de patiënten bereikt. Een semi-mechanistisch PBPK-model werd ontwikkeld, gebruikmakend van medicijn-specifieke en systeem-specifieke informatie. Deze kon miltefosine verdeling in de milt en lever voorspellen, aan de hand van een gelimiteerde miltefosine huidweefsel/ plasma concentratie dataset. **Hoofdstuk 4.2** illustreert de farmacokinetiek van amfotericine B in huid van Indiase en Bengalese leishmaniasis patiënten, na een 20 mg/kg intraveneuze, 15-daagse behandeling met amfotericine B. De amfotericine B plasma en huidweefsel concentraties werden met elkaar vergeleken en beschreven met behulp van een semi-mechanistisch PK-model. Deze liet een significant verschil zien van de klaring van amfotericine B uit elke van de blootgestelde locaties. De geschatte halfwaardetijd in huid 40 maal langer is dan die van plasma en betekent een langere verblijftijd van amfotericine B in huidweefsel ten opzichte van plasma.

A

List of publications

Publications

N.E. Aronson, **I.C. Roseboom**, M. Digby, C. Bravos, D. Selig, A. Farmer, P.-P. AM van Thiel, T. Dorlo. 1662. Pushing the Dose: Miltefosine Treatment for a Supersized American with Cutaneous Leishmaniasis

Open Forum Infect. Dis. 6 (2019) S608–S608.

I.C. Roseboom, B. Thijssen, H. Rosing, J. Mbui, J.H. Beijnen, T.P.C. Dorlo. Highly sensitive UPLC-MS/MS method for the quantification of paromomycin in human plasma

J. Pharm. Biomed. Anal. 185 (2020) 113245.

I.C. Roseboom, H. Rosing, J.H. Beijnen, T.P.C. Dorlo. Skin tissue sample collection, sample homogenization, and analyte extraction strategies for liquid chromatographic mass spectrometry quantification of pharmaceutical compounds

J. Pharm. Biomed. Anal. 191 (2020) 113590.

A. Contejean, X. Ayral, T.P.C. Dorlo, **I.C. Roseboom**, H. Yera, I. Gana, L. Chouchana, E. Canouï, P. Buffet, C. Charlier. Relapsing leishmanial arthritis: report of a tricky localization and evidence of miltefosine diffusion in synovial fluid

J. Antimicrob. Chemother. 76 (2021) 2740–2741.

I.C. Roseboom, B. Thijssen, H. Rosing, F. Alves, D. Mondal, M.B.M. Teunissen, J.H. Beijnen, T.P.C. Dorlo. Development and validation of an HPLC-MS/MS method for the quantification of the anti-leishmanial drug miltefosine in human skin tissue

J. Pharm. Biomed. Anal. 207 (2021) 114402.

I.C. Roseboom, B. Thijssen, H. Rosing, F. Alves, S. Sundar, J.H. Beijnen, T.P.C. Dorlo. Development and validation of a high-performance liquid chromatography tandem mass spectrometry method for the quantification of the antiparasitic and antifungal drug amphotericin B in human skin tissue

J. Chromatogr. B. 1206 (2022) 123354.

I.C. Roseboom, B. Thijssen, H. Rosing, F, Alves, B.M. Younis, A.M. Musac, J.H. Beijnen, T.P.C. Dorlo. Development and validation of an ultra-high performance liquid chromatography coupled to tandem mass spectrometry method for the quantification of the antileishmanial drug paromomycin in human skin tissue

J. Chromatogr. B. 1211 (2022) 123494

I.C. Roseboom, H. Rosing, J.H. Beijnen, T.P.C. Dorlo. Bioanalytical methods for pharmacokinetic studies of antileishmanial drugs

Biomed. Chromatogr. (2022) e5519

Conference proceeding

I.C. Roseboom, B. Thijssen, H. Rosing, J.H. Beijnen, T.P.C. Dorlo. Novel methods to quantify miltefosine, paromomycin and amphotericin B in skin biopsies from post-kala-azar dermal leishmaniasis patients

2022 WorldLeish 7th edition.

Author Affiliations

Ahmed M. Musac   Institute of Endemic Diseases, University of Khartoum, Sudan

Bas Thijssen   Department of Pharmacy & Pharmacology, Antoni van Leeuwenhoek Hospital, the Netherlands Cancer Institute, Amsterdam, the Netherlands

Brima M. Younis   Institute of Endemic Diseases, University of Khartoum, Sudan

Dinesh Mondal   International Centre for Diarrhoeal Disease Research, Bangladesh (icddr,b), Dhaka, Bangladesh

Fabiana Alves   Drugs for Neglected Diseases initiative, Geneva, Switzerland

Hilde Rosing   Department of Pharmacy & Pharmacology, Antoni van Leeuwenhoek Hospital, the Netherlands Cancer Institute, Amsterdam, the Netherlands

Jane Mbui   Centre for Clinical Research, Kenya Medical Research Institute, Nairobi, Kenya

Jos H. Beijnen   Department of Pharmacy & Pharmacology, Antoni van Leeuwenhoek Hospital, the Netherlands Cancer Institute, Amsterdam, the Netherlands

Department of Pharmaceutical Sciences, Faculty of Science, Utrecht University, Utrecht, the Netherlands

Marcel B.M. Teunissen   Department of Dermatology, Amsterdam University Medical Centers, location AMC, University of Amsterdam, The Netherlands

Shyam Sundar   Institute of Medical Sciences, Banaras Hindu University, Varanasi, Uttar Pradesh, India

Thomas P.C. Dorlo   Department of Pharmacy & Pharmacology, Antoni van Leeuwenhoek Hospital, the Netherlands Cancer Institute, Amsterdam, the Netherlands

Department of Pharmacy, Uppsala University, Uppsala, Sweden

Dankwoord

Dit was het dan. Na 5 jaar in het bioanalytisch laboratorium van de apotheek in het AvL sta ik hier met mijn proefschrift in handen. Binnengekomen als een broekie voor een masterstage en geïnspireerd geraakt door de OIO's plus de uitnodigende omgeving om zelf onderzoek te verrichten. Hier sta ik dan na 4 jaar onderzoekend labwerk gedaan te hebben, op het punt het instituut te verlaten. Dat doe ik met een traantje. Een beetje alsof je het uitmaakt met je eerste vriendinnetje ('het ligt niet aan jou, het ligt aan mij. Laten we vrienden blijven…'). De eerste baan na mijn studie, het voelt onwerkelijk allemaal.

Allereerst wil ik de **patiënten** uit meerdere klinische trials bedanken. De mensen uit Bangladesh, India, Kenia, Ethiopië en Sudan die aan leishmania lijden, hebben ondanks het verschrikkelijke ziektebeeld hun bloed en/of huid gegeven aan de wetenschap. Dit offer werd gedaan om de behandeling van de ziekte te verbeteren. Ook de **dokters** en **verpleging** ter plaatse hebben hieraan bijgedragen, waarvoor ik eveneens diep respect heb.

Jos, ik ben je ontzettend dankbaar voor de vele adviezen, het nuttige commentaar bij alle manuscripten en verbeteringen tijdens mijn promotieonderzoek. Ook in de laatste fase van mijn onderzoek, waarin ik aangaf de opleiding tot klinisch chemicus te willen doen, heb je mij ontzettend geholpen de door het AMC opgelegde deadline te halen en jouw hand in het vuur voor mij te steken. Ik ben dankbaar voor een promotor als jij. Mijn waardering is groot.

Thomas, het was mij een waar genoegen jou als copromotor te hebben. Ik heb diep respect voor jouw onvermoeibare inzet in het onderzoek naar de behandeling van leishmania, een echte inspiratiebron voor velen. Je nam altijd de tijd om uitgebreid naar mijn stukken te kijken, hebt vele inhoudelijke discussies gevoerd met mij in de wekelijkse dinsdagochtend meetings en was er altijd voor mij bij de vele vragen die ik had. Dankjewel dat ik mocht bijdragen aan jouw prachtige project, een mooi stukje wereldverbetering.

Hilde, mijn promotieonderzoek is eigenlijk bij jou begonnen. Je nam mij aan als stagiair tijdens mijn master voor een erg interessant onderzoek naar de kwantificatie van monoklonale antistoffen. Daarmee is het balletje gaat rollen en mocht ik de daaropvolgende 4 jaren onderzoek doen in jouw laboratorium. Ik kon altijd jouw kantoor binnenlopen voor advies, je hebt ontzettend meegedacht aan de ontwikkeling van de assays en stond altijd klaar voor mij. Dankjewel voor de prettige samenwerking deze 5 jaar.

Bas, mijn steun en toeverlaat in het lab, de labcoach. Zonder jou was het niet gelukt.

Ik kon altijd bij jou aankloppen voor elk probleem en daar had je vaak een oplossing voor. Naast alle inhoudelijke zaken was je ook altijd in voor een lach en praatje. Ik kon mij geen fijner persoon wensen om mee samen te werken. Ik dank je hartelijk voor alles dat je hebt betekend.

Geachte leden van de **leescommissie**. Hartelijk dank voor het lezen en beoordelen van het proefschrift.

Abadi, mijn eerste labcoach tijdens de stageperiode, maar stiekem ook tijdens het hele onderzoek. Je hebt mij ontzettend geholpen met de hands-on bediening van elk apparaat, waarvan de Shimadzu, Agilent en QTRAP in het bijzonder. Ik had uiteindelijk geen aantekening boekje meer nodig. We hebben ontzettend leuke tijden gekend, met daarbij ontzettend veel buikpijn van het lachen. Hierbij bedank ik ook alle **analisten** en **studieleiders** van het bioanalytisch laboratorium, voor de warme tijden, leuke koffiepauzes en het hartelijke onthaal. Ik heb mij onderdeel van jullie hechte team gevoeld.

Alle **lab OIO's**, van de oude garde tot de nieuwe, hartelijk dank voor de fijne gesprekken, gevraagde of ongevraagde adviezen en het volhouden met mij op het lab. Zonder jullie was het was het labwerk niet hetzelfde geweest. Daarbij wil ik ook alle **OIO's** van H3 bedanken voor de leuke tijden, OIO weekenden, illegale ski-reis, vele lunches en borrels (met borrelmama **Marit**). Het blijft knap dat jullie mij niet zat waren na de vele flauwe grapjes (of wel maar dat is dan nooit uitgesproken).

De **golf-OIO's**, **Karen** (**Krautie**), **Jona** (**GN #2**), **Marinda** (**Esmee**), **Maarten** voor de vele rondjes golf bij de Hoge Dijk. Echt een top idee om ons GVB te gaan halen en vele euro's aan balletjes het diepe gras in te verdwijnen of het water in te slaan, met vele frustraties van dien. Misschien worden we ooit nog eens goed (ik denk het niet).

Alle **kamergenoten** van de afgelopen jaren (**H3.009**). For the non-Dutch speakers, what started as the weirdo room, became a room full of laughter and inappropriate jokes. Thank you for the good times. Thank you, **Wendy**, for we knew each other shortly, but you had a great impact on the thesis. **Lisa** voor alles. Goede gesprekken, adviezen, lachen; je bent een heel fijn persoon! **Maud**, ook al hebben wij niet lang op dezelfde kamer gezeten, je hebt een fijne indruk op mij gemaakt met vele leuke conversaties. Dank jullie wel allemaal.

Mijn **Paranimfen** (paranymphomaniacs), **Niels** en **Semra**, dankjewel voor alle leuke tijden. **Niels** (**GN #3**), ik heb er echt nieuwe vrienden bij met jou en **Lotte**. Ik heb ontzettend veel met je gelachen, we konden elkaar altijd vinden in het lab en ik ga de flauwe grappen missen (samen met de grote automatische capper). **Semra**, **Bosnian Queen**. Thank you for all the good times, the silly laughter, complaining about stuff,

spontaneous dirty jokes and for being my friend. You both made the working place a place of enjoyment.

Ook mijn oude huisgenoten van **Fredje T**, jullie hebben onbedoeld zo ontzettend veel van mijn promotieonderzoek moeten aanhoren. **Dimanche**, zonder jullie is mijn leven een stuk minder leuk. Door jullie heb ik mijn hoofd vele malen leeg kunnen maken met een schroevendraaier. En niet te vergeten al mijn vrienden (plus partners) uit de **D&T**.

Pap en **mam**, **Hans** en **Nicole**, dank jullie wel voor de onvoorwaardelijke steun en liefde. Ik kon altijd mijn ei bij jullie kwijt, ook al was ik niet de makkelijkste. Dat ik hier nu sta in mijn leven, wie had dat gedacht vele jaren geleden op de middelbare school. **Marnix** en **Irma**, dank jullie wel voor de vele discussies en steunbetuigingen. **Lala**, **Azer**, **Qam**, **Ali**, **Xander**, dank jullie wel voor de steun, al was het soms moeilijk te behappen wat ik allemaal uitspookte. Çox sağol dəyərli ailəm.

De laatste alinea is voor jou, **Shams**, mijn zonnetje, mənim həyatım. Je hebt mij ontzettend doen groeien de afgelopen jaren. Ik weet echt niet waar ik zonder jou geweest zou zijn, zonder jou had ik dit nooit kunnen doen. We hebben samen gelachen, gehuild en het beste in elkaar naar boven gebracht. De laatste tijden waren roerig, we hebben een marathon gesprint (op volle snelheid). Dat typeert ons enorm. Ik houd onvoorwaardelijk van jou. Ik kijk uit naar het pad dat wij bewandelen samen met onze lieve dochter **Leyla**.

Curriculum Vitae

Ignace Charles Roseboom was born on June 11th, 1992 in Almere, the Netherlands. After graduating from high school in 2011 at OSG de Meergronden in Almere, he went on to study Pharmaceutical Sciences at the Vrije Universiteit Amsterdam. After obtaining his Bachelor of Science in 2016, he proceeded to obtain his Master of Science in Chemistry (Analytical track) at the Vrije Universiteit Amsterdam and Universiteit van Amsterdam in 2018. As part of his Masters' program, he performed an independent research project. He carried out this project at the bioanalytical laboratory of the pharmacy at the MC Slotervaart under supervision of dr. Hilde Rosing, where he investigated the possibility to quantify the therapeutic monoclonal antibody Nivolumab in human plasma by liquid chromatography coupled to iontrap mass spectrometry. In 2018 he started his PhD research at the Department of Pharmacy & Pharmacology of the Netherlands Cancer Institute – Antoni van Leeuwenhoek under supervision of prof. dr. Jos Beijnen and dr. Thomas Dorlo, which is described in this thesis.

A